PB87-232641

SENSITIVITY ANALYSIS FOR APPLICATION OF INHALATION EXPOSURE METHODOLOGY (IEM) TO STUDIES OF HAZARDOUS WASTE MANAGEMENT FACILITIES

Oak Ridge National Laboratory
Oak Ridge, TN

Aug 87

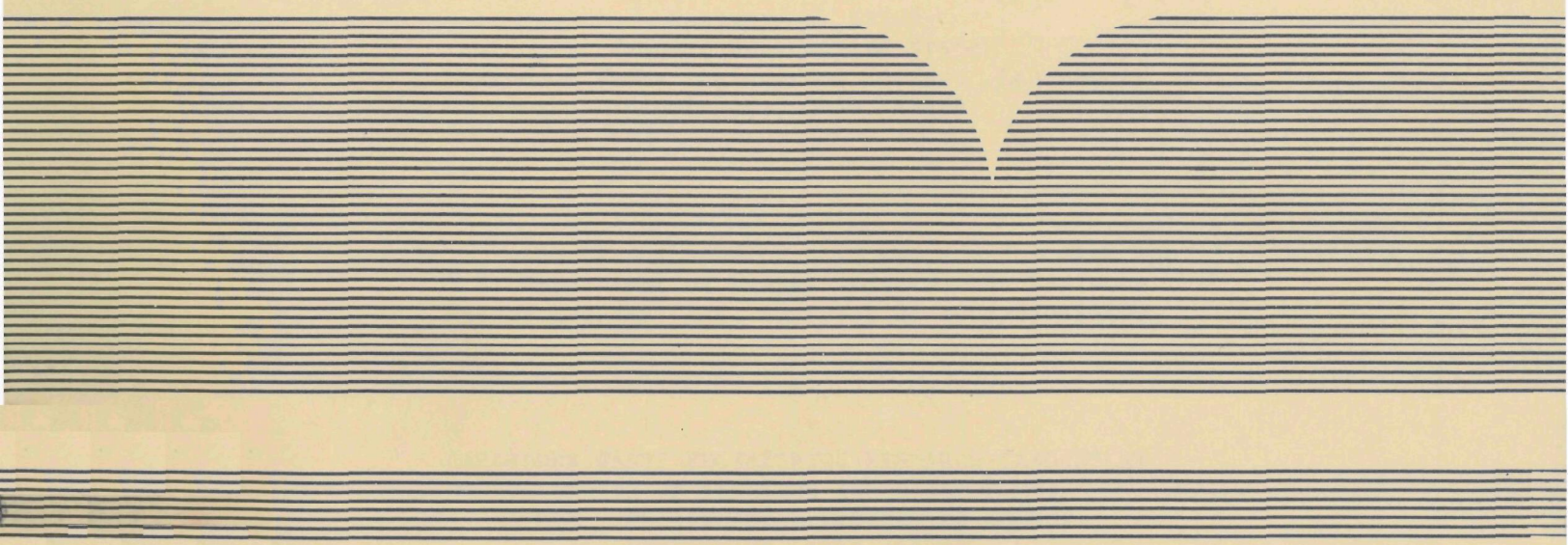

U.S. DEPARTMENT OF COMMERCE
National Technical Information Service
NTIS®

PB87-232641

EPA/600/2-87/071
August 1987

SENSITIVITY ANALYSIS FOR APPLICATION OF THE INHALATION EXPOSURE METHODOLOGY (IEM) TO STUDIES OF HAZARDOUS WASTE MANAGEMENT FACILITIES

by

F. R. O'Donnell
Health and Safety Research Division

and

C. C. Gilmore
Energy Division
Oak Ridge National Laboratory
Oak Ridge, Tennessee 37830

IAG No. DW14930265-01-1

Project Officer

Benjamin L. Blaney
Thermal Destruction Branch
Hazardous Waste Engineering Research Laboratory
Cincinnati, Ohio 45268

This research was conducted in cooperation with the U.S. Department of Energy under Martin Marietta Energy Systems, Inc. contract DE-AC05-840R21400

HAZARDOUS WASTE ENGINEERING RESEARCH LABORATORY
OFFICE OF RESEARCH AND DEVELOPMENT
U.S. ENVIRONMENTAL PROTECTION AGENCY
CINCINNATI, OHIO 45268

TECHNICAL REPORT DATA (Please read Instructions on the reverse before completing)		
1. REPORT NO. EPA/600/2-87/071	2.	3. RECIPIENT'S ACCESSION NO. PB87 232641/AS
4. TITLE AND SUBTITLE Sensitivity Analysis for Application of Inhalation Exposure Methodology (IEM) to Studies of Hazardous Waste Management Facilities		5. REPORT DATE August 1987 6. PERFORMING ORGANIZATION CODE
7. AUTHOR(S) F. R. O'Donnell and C. C. Gilmore		8. PERFORMING ORGANIZATION REPORT NO
9. PERFORMING ORGANIZATION NAME AND ADDRESS Oak Ridge National Laboratory P.O. Box X Oak Ridge, Tennessee 37830		10. PROGRAM ELEMENT NO. 11. CONTRACT/GRANT NO DW14930265-01-1
12. SPONSORING AGENCY NAME AND ADDRESS Hazardous Waste Engineering Research Laboratory Office of Research and Development U.S. Environmental Protection Agency Cincinnati, Ohio 45268		13. TYPE OF REPORT AND PERIOD COVERED 1/1/84 - 12/31/84 14. SPONSORING AGENCY CODE EPA/12/600
15. SUPPLEMENTARY NOTES		

16. ABSTRACT

The Inhalation Exposure Methodology (IEM) is an integrated system of computer programs that simulates the atmospheric transport of and the resulting human exposures to pollutants released from one or more sources at an industrial complex. This study was undertaken to determine the sensitivity of IEM predictions of pollution concentrations and population exposures to (1) variations of selected, user-supplied source, meteorological, climatological, and pollutant parameter values and (2) use of the three available source modeling options to represent emission sources found at hazardous waste management facilities (HWMFs). These sources include incinerators and associated structures, storage, and treatment tanks, drum stacks, process buildings, surface impoundments, waste piles, and land treatment areas.

17. KEY WORDS AND DOCUMENT ANALYSIS		
a. DESCRIPTORS	b. IDENTIFIERS/OPEN ENDED TERMS	c. COSATI Field Group
18. DISTRIBUTION STATEMENT RELEASE TO PUBLIC	19. SECURITY CLASS (This Report) UNCLASSIFIED	21. NO. OF PAGES
	20. SECURITY CLASS (This page) UNCLASSIFIED	22. PRICE

EPA Form 2220-1 (Rev. 4-77) PREVIOUS EDITION IS OBSOLETE

NOTICE

This document has been reviewed in accordance with U.S. Environmental Protection Agency policy and approved for publication. Mention of trade names or commercial products does not constitute endorsement or recommendation for use.

FOREWORD

Today's rapidly developing and changing technologies and industrial products and practices frequently carry with them increased generation of solid and hazardous wastes. These materials, if improperly dealt with, can threaten both public health and the environment. Abandoned waste sites and accidental releases of toxic and hazardous substances to the environment also have important environmental and public health implications. The Hazardous Waste Engineering Research Laboratory assists in providing an authoritative and defensible engineering basis for assessing and solving these problems. Its products support the policies, programs and regulations of the Environmental Protection Agency, the permitting and other responsibilities of state and local governments and the needs of both large and small businesses in handling their wastes responsibly and economically.

This report discusses the sensitivity of predictions made by the Inhalation Exposure Methodology (IEM) to the more important, user-controlled input parameters and modeling options that are applicable to low-level emission sources found at hazardous waste management facilities. It is intended to provide additional information on the use of IEM to staff and contractors of EPA interested in modeling releases of pollutants from industrial complexes and in estimating associated population exposures. For further information, please contact the Alternative Technologies Division of the Hazardous Waste Engineering Research Laboratory.

Thomas R. Hauser, Director
Hazardous Waste Engineering Research Laboratory

ABSTRACT

The Inhalation Exposure Methodology (IEM) is an integrated system of computer programs that simulates the atmospheric transport of and the resulting human exposures to pollutants released from one or more sources at an industrial complex. This study was undertaken to determine the sensitivity of IEM predictions of pollutant concentrations and population exposures to (1) variations of selected, user-supplied source, climatological, and pollutant parameter values and (2) use of the three available source modeling options to represent emission sources found at hazardous waste management facilities (HWMFs). These sources include incinerators and associated structures, storage and treatment tanks, drum stacks, process buildings, surface impoundments, landfills, waste piles, and land treatment areas.

This report was submitted by the Oak Ridge National Laboratory in partial fulfillment of IAG No. DW14930265-01-1 under sponsorship of the U.S. Environmental Protection Agency. This report covers the period January 1, 1984, to December 31, 1984, and work was completed in January 1986.

CONTENTS

FIGURES

TABLES

ACKNOWLEDGEMENTS

It is a pleasure to acknowledge the assistance of Dr. Benjamin L. Blaney, Dr. David E. Layland, and Dr. William B. Peterson of the U.S. Environmental Protection Agency and of Dr. Brian D. Murphy and Dr. Frank C. Kornegay of the Oak Ridge National Laboratory. Their comments and insights during the review of this document were most helpful.

SECTION 1

INTRODUCTION

BACKGROUND

The Inhalation Exposure Methodology (IEM) is an integrated system of computer programs that simulates the atmospheric transport of and the resulting human exposures to pollutants released from one or more sources at an industrial complex.[1] The IEM uses a Gaussian-plume atmospheric dispersion model to calculate annual-average, sector-averaged, centerline, ground-level, air concentrations of released pollutants at user-selected receptor points. It uses these concentrations to calculate average concentrations over each sector segment of a user-specified polar grid. Finally, it multiplies the sector-segment-averaged concentrations and their corresponding sector-segment populations to give estimates of human exposures to the released pollutants. Although applicable to a variety of problems, the IEM was developed as a tool for estimating pollutant concentrations and associated human exposures in the vicinity of hazardous waste management facilities (HWMFs).

An interactive version of the IEM system has been installed, for use by contractors and staff of the U. S. Environmental Protection Agency, on the IBM system at the National Computer Center, Research Triangle Park, North Carolina.[1] This version provides automatic access to and linkage of on-line (1) meteorological data, (2) population data, (3) a slightly modified version (called ISCLTM) of the long-term version of the Industrial Source Complex (ISCLT) Dispersion Model,* and (4) a concentration-exposure estimation program (CONEX). Persons wishing to use this version of the IEM should contact their Project Officers to arrange access to the IBM system and the IEM programs and data files. These persons also should consult the IEM user's guide[1] and its addendum,[2] and the ISCLT user's guide[3] and revisions.[4]

Whenever a computer simulation of reality, such as the IEM, is used to predict the impacts of an activity, concern arises about the accuracy (validity) of the predictions. This accuracy is dependent on both the accuracy of the computing algorithms (how well the model calculations match reality) and the certainty of the values assigned to the required input

* The calculations performed by the ISCLTM are identical to those performed by the ISCLT; the only differences between the two codes are in sections that control the flow of input and output data.

parameters (although the best available values are used, they may be approximations or may be selected from a range of possible values). Ideally, the accuracy of the predictions could be determined by comparing the predictions to environmental measurements taken under conditions similar to those used to make the predictions. Unfortunately, such comparisons require a large observational data base. In the case of the IEM, the data base should contain measured annual-average, ground-level air concentrations of and corresponding exposures to gaseous and particulate pollutants released from a variety of sources under a variety of meteorological conditions. Such a data base is difficult and expensive to obtain and, to our knowledge, does not exist. Therefore, we did not attempt to validate IEM predictions in this study. However, some general comments can be made concerning the accuracy of the IEM algorithms.

Previous studies indicate that Gaussian plume models, such as the ISCLTM, give reasonably accurate, but often slightly high, predictions of annual-average, centerline, ground-level, air concentrations of pollutants released from various sources under well-behaved meteorological conditions over flat terrain.[5] For example, most predicted concentrations at receptor points located within 10 km of the sources were between 0.5 and 2 times the measured concentrations.[6-10] Predicted concentrations at receptor points located between 10 and 150 km from the sources were between 0.25 and 4 times the measured concentrations.[11-16] (The use of a simple Gaussian plume model to predict concentrations beyond 50 km from the source usually is not recommended.)[17] Heron, et al.[18] used the ISCLT to study particulates released from a steel processing complex located in "relatively" flat terrain and found predicted concentrations to be between 0.7 and 1.3 (mean = 0.9) times concentrations measured at six sampling stations, after correcting for background. For releases under complex meteorological conditions (e.g., sea breezes) or over complex terrain, predicted concentrations were found to be between 0.1 and 10 times the measured concentrations.[19-21] (If complex meteorological and terrain conditions are present, the use of models other than simple Gaussian plume models should be considered.)[17] The presence of structures near release points or other conditions that cause turbulence also affect predictions adversely. Use of the building wake effects and stack-tip downwash algorithms available in the ISCLTM dispersion model should improve the agreement between predicted and measured values when such structures or conditions are present, but the wake effects algorithm tends to underpredict concentrations in the building wake region.[22]

The accuracy of the sector-segment-averaged concentrations calculated by CONEX (see Sect. 3) is approximately the same as the accuracy of the concentrations calculated by ISCLTM. However, the accuracies of the procedures used in the IEM to estimate the number of persons residing in the sector segments and to estimate human exposures are unknown. As discussed in Section 3, the IEM results are similar to those obtained using the Human Exposure Model (HEM).[23]

PURPOSE AND STRUCTURE OF THIS REPORT

This study was undertaken to illustrate the sensitivity of IEM predictions to (1) variations of selected, user-supplied source, meteorological, climatological, and pollutant parameter values and (2) use of the three available source modeling options to represent emission sources found at hazardous waste management facilities (HWMFs). These sources include incinerators and associated structures, storage and treatment tanks, drum stacks, process buildings, surface impoundments, landfills, waste piles, and land treatment areas. Several sources may be found at one HWMF.

Table 1 is a summary of source dimensions found at several HWMFs.[24,25] The area covered by these sources ranges from very small (essentially a point) to very large (up to 400 x 10^6 m^2). The height at which these sources release pollutants generally is low (between ground level and 20 m); even the incinerator stacks have low release heights (i.e., <30 m). Modeling the sources found at a HWMF could present problems because they may be located close together, be near buildings and structures that could influence pollutant dispersion, and have ill-defined pollutant release rates. In some cases, source-specific pollutant release rates may be unavailable, thus forcing the modeler to represent several sources as a single source.

The remainder of this section contains a brief overview of the IEM system. Section 2 is a summary of our findings. Section 3 contains descriptions and discussions of the IEM algorithms for calculating sector-segment concentrations and populations, and exposures. The methods used to conduct the sensitivity analysis of the atmospheric dispersion algorithms are discussed in Section 4. The effects of varying meteorological, source, and pollutant parameter values and of using different receptor layouts are discussed in Section 5. This discussion complements the work of Eldridge and Gschwandtner.[26] Finally, the effects on predictions due to using the three source representation options (point, area, and volume) to model typical HWMF sources are demonstrated in Section 6. Many of the results of the sensitivity analysis runs are presented in the Appendixes as normalized concentration profiles, plots of X/Q [$(\mu g/m^3)/(g/s)$] as a function of downwind distance. A glossary and a list of symbols and acronyms are given also.

GENERAL OVERVIEW OF THE IEM*

The IEM consists of four groups of computer programs called MET, POP, ISCLTM, and CONEX. Each group consists of one or more computational and one or more EXEC programs (Fig. 1). The EXEC programs control the flow of the IEM because they contain the programming needed to access system-stored data files and programs, to direct the user in preparation of problem-specific input data files for the main programs, to submit the programs and data files to the IBM operating system, and to process program outputs.

* The reader should consult reference 1 for details of the IEM and reference 2 for a discussion of procedures for manually creating and editing input data files.

Table 1. Typical source dimensions at HWMFs

Type	Area, m^2	Release height, m
Surface impoundments	20 - 75 x 10^3 <1900>[a]	0
Land treatment areas	4000 - 4 x 10^8 <3.3 x 10^6>	0
Landfills	930 - 9.3 x 10^7 <6500>	0
Waste piles	30 - 4 x 10^5 <280>	<3.1>
Process buildings	75 - 300 <150>	3 - 18 <9.4>
Drum stacks	~1300	~6.1
Storage tanks	50 - 1400 <320>	2 - 10 <6.7>
Incinerator structures	125 - 315 <220>	4 - 20 <12>
Incinerator stacks		9 - 27 <22>

[a]Mean values are enclosed by < >.

Sources:

The MITRE Corporation, Air Emission Control Practices at Hazardous Waste Management Facilities, Working Paper WP-83-W00048 (1983).

B. L. Blaney, U.S. Environmental Protection Agency, Cincinnati, OH, Personal Communication, 1984.

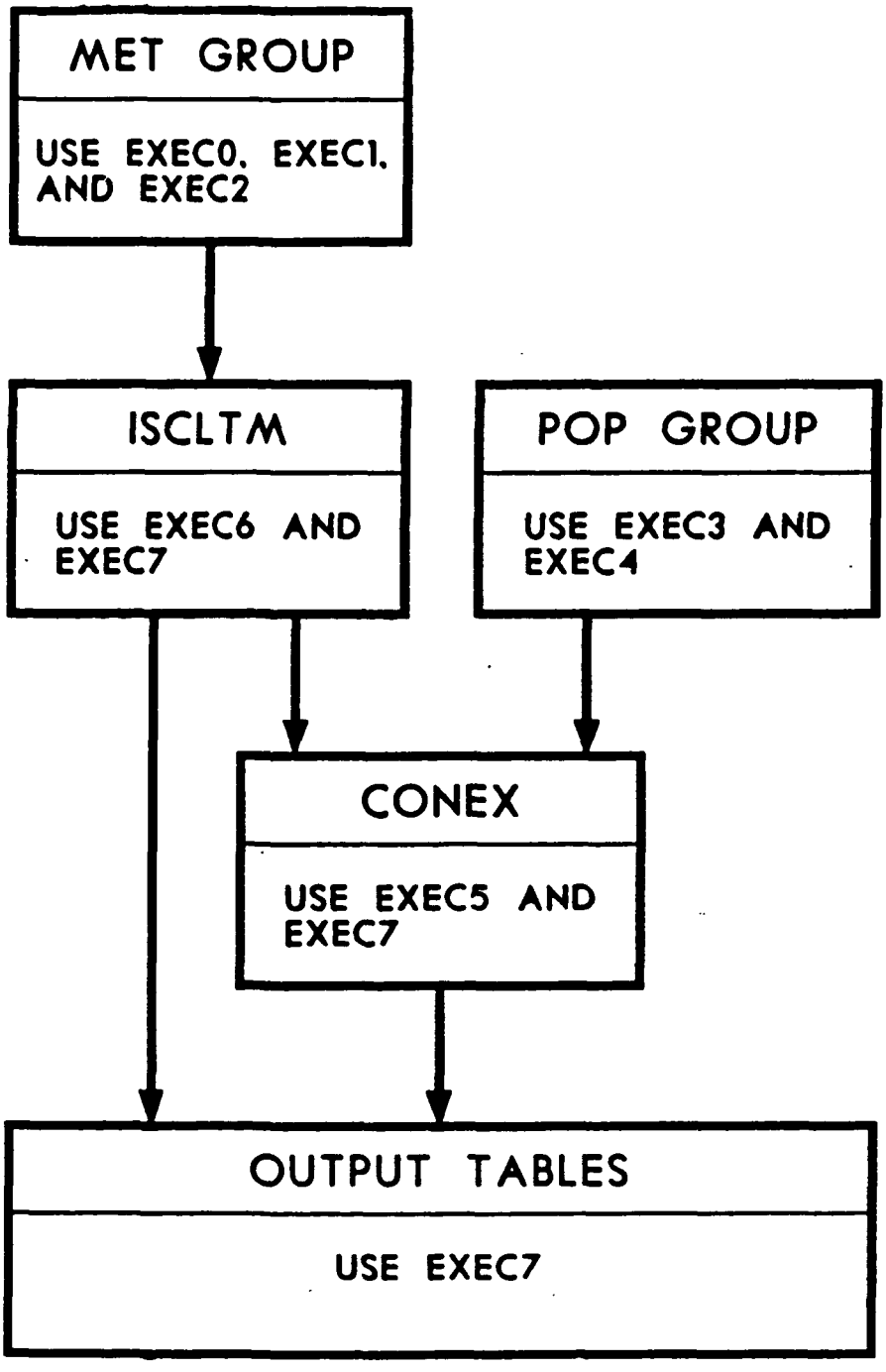

Figure 1. Schematic representation of program group interactions in the IEM and their use of executive (EXEC) programs.

The MET group is a series of three main programs (SERCH, DIREC, and STAR) that uses EXEC0, EXEC1, and EXEC2 to guide the user in identifying meteorological stations near the facility; in selecting an appropriate meteorological data set; and in naming and formatting the data set as required for compatability with the atmospheric dispersion code.

The POP group is a series of two main programs (RD80 and APORT) that uses EXEC3 and EXEC4 to guide the user in creating, naming, and formatting a population data set for use by the concentration-exposure program (CONEX).

The ISCLTM group uses EXEC6 to direct the user in creating, naming, and formatting an input data file for use by ISCLTM. Similarly, the CONEX group uses EXEC5 to direct the user in creating, naming, and formatting the input data file needed to run the concentration-exposure program (CONEX).

A final executive program, EXEC7, runs the two main computational programs, ISCLTM and CONEX. This EXEC program collects all output files prepared by the various program groups and feeds them, in proper order, to ISCLTM and CONEX.

The IEM uses two polar coordinate systems, called the "grid system" and the "centroid system". The orientations of the two coordinate systems are shown in Figure 2. Both systems are centered on a common origin and use the same set of 16 equally spaced (22.5° apart) direction vectors (Di, where i is the direction index). Vector D1 points to the North, D5 to the East, D9 to the South, D13 to the West, etc. Each direction vector lies along the center of a 22.5° wide sector. The rings of the centroid system (RCk, where k is the ring index) are located at radial distances XCk (in meters) from the origin. The centroid rings are positioned midway between successive rings of the grid system (RGj, where j is the ring index), which are located distances XGj from the origin. For example, RC1 is midway between RG1 and RG2, and RC2 is midway between RG2 and RG3. Thus, there always must be one more grid ring (maximum of 20) than there are centroid rings (maximum of 19). Also note that the area inside RG1, which is usually the source (plant) boundary, is excluded from the centroid system.

The points at which the direction vectors and grid rings intersect, PG(i,j), are the points at which ISCLTM calculates "grid-point concentrations" [GPC(i,j)]. The GPC(i,j) are annual-average, sector-averaged, centerline, ground-level, air concentrations. (See Reference 3 for details of the calculations.)

The points at which the direction vectors and centroid rings intersect, PC(i,k), are the geometric centroids of the sector segments [SS(i,k)], or the areas, over which CONEX calculates (see Sect. 3) "sector-segment concentrations" [SSC(i,k)]. Each sector segment is bounded by its two nearest grid rings and the limits of its associated sector (i.e., two imaginary lines located ±11.25° from its direction vector). The shaded area in Figure 2 shows sector segment SS(9,2), which is centered on centroid point PC(9,2). This point is located at the intersection of direction vector D9 (180° from North) and centroid ring RC2 (distance XC2 from the origin). This sector segment occupies the area bounded by directions 168.75° and 191.25° and grid rings RG2 and RG3 (distances XG2 and XG3 from origin).

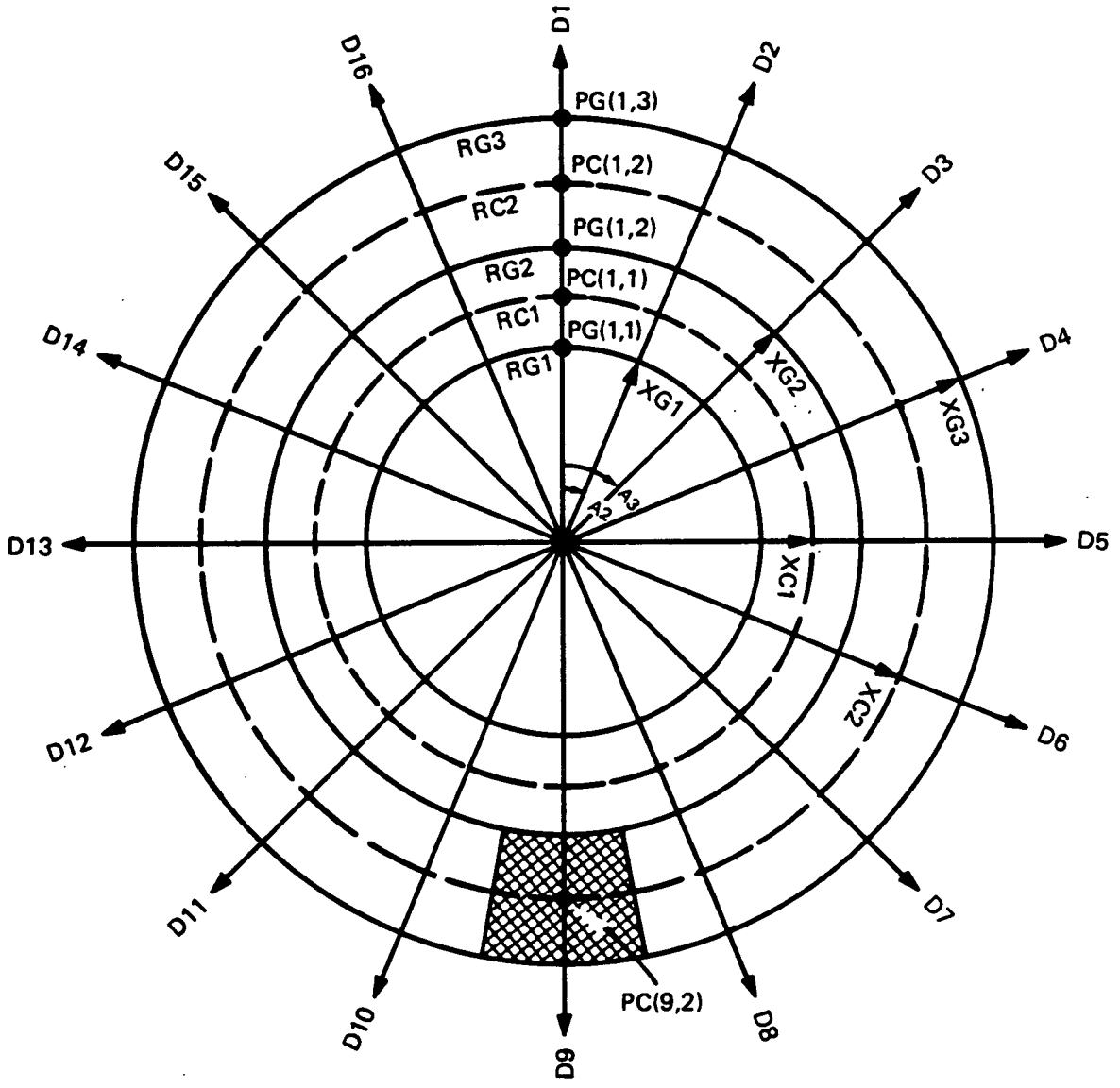

Figure 2. Orientation of the grid and centroid coordinate systems used in the IEM (see explanation in text).

SECTION 2

SUMMARY

A study was made of the sensitivity of IEM predictions to variations of the more important user-supplied input parameter values and to the use of some of the available modeling options to represent emission sources found at HWMFs. These sources have relatively low pollutant release heights, may be located near structures that influence pollutant dispersion, and, except for incinerator stacks, may have essentially no associated plume rise. Parameters affecting plume rise, which have been studied elsewhere, were not included in this study. The parameters studied in detail include atmospheric stability class, release height, and source area. Effects due to wind speed and direction, adjacent buildings, pollutant decay and deposition, the arrangement of receptor points, the use of different source geometries, and the method used to estimate exposures also are discussed. In most cases, the study assumed a unit (1 g/s) total pollutant release rate, a wind blowing from one direction, and a wind speed of 0.75 m/s (see Sect. 4). The more important findings of this study include:

(1) The IEM method for estimating the total exposed population is as accurate as any other general method. However, the accuracy of the method used to link exposed persons to specific pollutant concentrations (i.e., to calculate exposures) is unknown, but likely is comparable to the accuracy of other existing methods (Sect. 3).

(2) For the sources considered in this study, wind speed acted as an inverse, linear scaling factor on concentration and population exposure predictions, except when pollutant decay and deposition were considered. Linear scaling also would not be found for stack sources that produce plume rise, which were not part of this study (Sect. 5).

(3) Variations in atmospheric stability, pollutant release height, and source area had interdependent and strong influences on predicted concentrations and exposures. Therefore, every effort should be made to evaluate these parameters accurately (Sect. 5).

(4) Increasing stability increased exposure predictions but, depending largely on the release height, either increased or decreased maximum concentration predictions (Sect. 5).

(5) Increasing release height decreased both exposure and concentration predictions (Sect. 5).

(6) Increasing source area had little effect on exposure predictions, for the same receptor array. Maximum concentration predictions varied by as much as 60% for the source areas considered in this study (Sect. 5).

(7) Use of the building wake effects option increased concentration predictions within 200 m of the source center but had little effect on more distant concentration predictions and on population exposure predictions (Sect. 5).

(8) For pollutants that have half-lives of a few days or less, decay could reduce significantly airborne concentrations at receptors beyond 1 km. For longer-lived pollutants, decay would be unimportant (Sect. 5).

(9) Pollutant deposition affected significantly both concentration and exposure predictions, especially at sites characterized by stable atmospheric conditions and low wind speeds (Sect. 5). The IEM pollutant deposition option should be used if the emitted pollutants are particles or can form particles that can be characterized.

(10) The choice of a receptor array can bias predictions significantly. For the sources considered in this study, an array with receptors concentrated between the first allowed distance and 2 km should produce the most accurate predictions (in terms of the model's predictive capability) of maximum concentration and exposures (Sect. 5).

(11) Use of the various available emission source modeling options produced essentially the same predictions of population exposures and of airborne concentrations at receptors beyond ~1 km. At the closer receptors, use of the stack and the area source representations produced very similar concentration predictions. For the more stable atmospheric conditions, use of volume source representations resulted in predictions of close-in concentrations that were higher than those predicted using stack and area source representations. For the less stable conditions, use of volume source representations resulted in concentration predictions that generally were lower than those predicted using the other options (Sect. 6).

SECTION 3

DISCUSSION OF THE EXPOSURE ESTIMATION PROCEDURE

Exposure is defined as the product of an average airborne pollutant concentration and the number of persons immersed in that concentration over a specified time interval. In the IEM, the time interval is one year and the unit of exposure is person-$\mu g/m^3$. Three types of exposure estimates usually are of interest: the maximum individual exposure, the total population exposure, and the population exposures attributable to selected concentration levels.

The maximum individual exposure is numerically equal to the maximum grid-point concentration at an occupied grid point. Thus, the parameters that affect calculation of the maximum individual exposure are the same as those that affect calculation of the maximum grid-point air concentration. These parameters are discussed in Section 5. The remainder of this section deals with factors affecting population exposure estimates.

An accurate population exposure estimate requires (1) accurate estimates of the total number of persons involved, (2) accurate estimates of the air concentrations to which the persons are exposed, and (3) an accurate method for linking the air concentrations and the exposed persons. Reasonably accurate estimates of air concentrations at selected receptor locations can be obtained using an atmospheric dispersion model such as the ISCLTM. Similar estimates of the total exposed population can be obtained from census data or from specially prepared, site-specific data. However, the accuracies of methods for linking exposed persons and concentrations are unknown, but likely are poor. The method used in the IEM involves (1) using the grid-point concentrations to calculate an average concentration over each sector segment (area) of the centroid system, (2) manipulating the census data to give the number of persons residing in each sector segment, and (3) multiplying corresponding sector-segment concentrations and populations to give sector-segment population exposures. The sector-segment exposures then are added to give a total population exposure estimate. The sector-segment exposures also are used to determine the exposures associated with various concentration levels.

SECTOR-SEGMENT CONCENTRATIONS

The IEM calculates SSC(i,k), the average concentration ($\mu g/m^3$) over sector segment SS(i,k) of the centroid system, from the grid-point concentrations at grid points PG(i,j) and PG(i,j+1) as follows:

$$SSC(i,k) = \exp[C1 + (C2 - C1) \times RTEMP],$$

where, using the IEM orientation of coordinate systems (see Fig. 2),

k = j,

C1 = ln GPC(i,j),

GPC(i,j) = grid-point concentration ($\mu g/m^3$) at PG(i,j),

C2 = ln GPC(i,j+1),

GPC(i,j+1) = grid-point concentration ($\mu g/m^3$) at PG(i,j+1),

RTEMP = [ln(XCk/XGj)]/[ln(XGj+1/XGj)],

XCk = distance (m) from the origin to centroid point PC(i,k),

XGj = distance (m) from the origin to grid point PG(i,j), and

XGj+1 = distance (m) from the origin to grid point PG(i,j+1).

In general, the accuracy of the averaging process is as good as the accuracy of the grid-point concentration calculations. For pollutants released at heights above ~10 m under stable atmospheric conditions (e.g., stability classes E and F), grid-point concentration profiles rise sharply to their maximums. Under these conditions, sector-segment concentrations within ~1 km of the source may represent a large (one or two orders of magnitude) range of grid-point concentrations, depending also on the grid-point spacing used. (Increases in grid-point spacings increase the range of concentrations represented by the sector-segment averages.) Figure 3 illustrates the relationship between grid-point and sector-segment concentration profiles for releases from stack sources (with no plume rise) with heights of 0 and 20 m under stable (F) conditions. (As shown in the Appendixes, grid-point concentration profiles exhibit the most curvature under F stability conditions.) The receptor array described in Section 4 was used. For the 0-m release height, the grid-point concentration profile is essentially a straight line. The ranges of grid-point concentrations included in the sector-segment concentrations is small (less than a factor of 3) out to 2 km, beyond which the larger spread between grid points causes the ranges to increase to about a factor of 5. For the 20-m release height, the grid-point concentration profile rises rapidly to near its maximum value, peaks smoothly, and becomes linear beyond ~2 km. In this case, the first visible sector-segment concentration, centered at 225 m, is the average of grid-point concentrations that span two orders of magnitude. Subsequent segment-average concentrations are obtained from decreasing ranges of grid-point concentrations until the 2-km point is reached. Beyond 2 km, the relationship between the grid-point and sector-segment concentration profiles is similar to the relationship for the 0-m release. Because the sector segments nearest the source are the smallest and usually contain few people, they account for only a small fraction of the

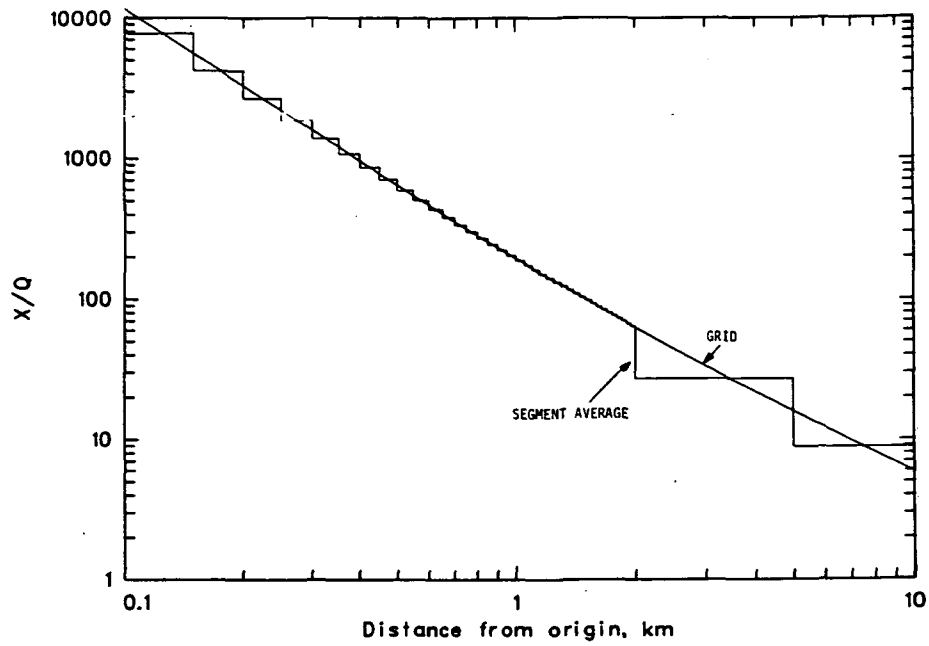

(a) Release height = 0 m

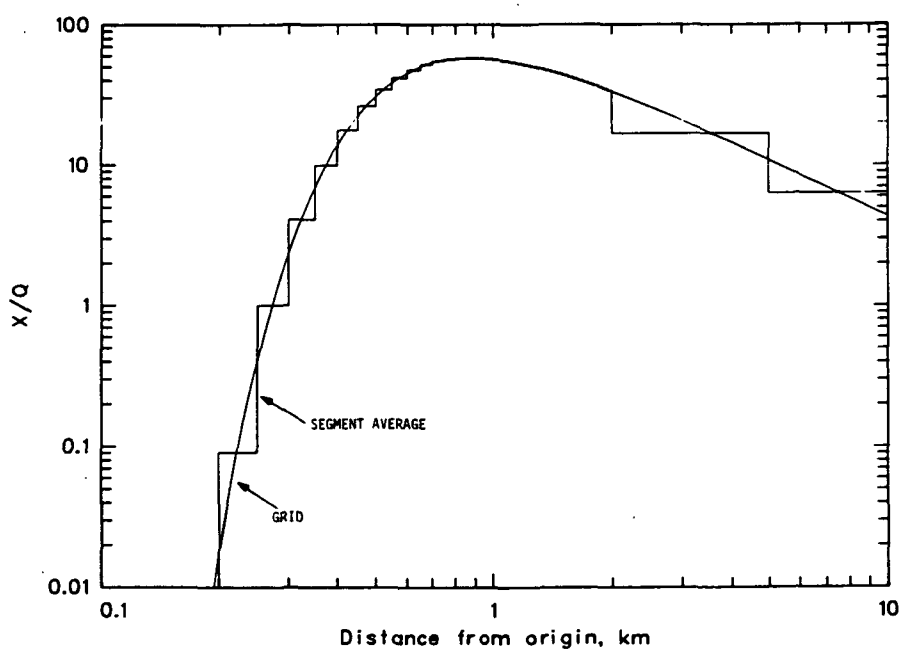

(b) Release height = 20 m

Figure 3. Comparison of grid-point and sector-segment concentrations for releases from 0- and 20-m high stack sources with no plume rise under F stability conditions.

total exposure. Thus, any significant distortions caused by the averaging process should have very little effect on the total exposure predictions. As shown in Section 5, any reasonable choice of a receptor array will produce acceptable total exposure estimates.

SECTOR-SEGMENT POPULATIONS

The population data provided with the IEM consists of 55 data sets that were prepared using 1980 census data, which lists the number of persons residing in census enumeration districts that are located at specific latitude-longitude points. One of the IEM data sets contains estimates of the number of persons in each cell of a coarse-grid (0.1° latitude by 0.1° longitude) rectangular matrix that covers the contiguous United States. At 36° latitude, such a cell would have dimensions of ~11 by ~9 km. (These dimensions would change slightly with latitude due to the curvature of the Earth). Each of the remaining 54 data sets contain estimates of the number of persons in each cell of a fine-grid (2′ latitude by 2′ longitude or ~3.7 by ~3.0 km at 36° latitude) rectangular matrix that encompasses a specific metropolitan area. The cell populations were obtained by assuming that all persons assigned to census enumeration districts located within the latitude-longitude window of a cell reside in and are distributed uniformly over the cell.

To estimate the number of persons residing in the sector segments of the centroid coordinate system, the IEM superimposes the array of sector segments (see Fig. 2) on the array of rectangular cells and calculates the areal fraction of each cell that is intersected by each sector segment. Then SSP(i,k), the population in sector segment SS(i,k), is calculated using

$$SSP(i,k) = \sum_{c=1}^{N} f_c(i,k) \times P_c,$$

where N = number of cells intersected by SS(i,k),

$f_c(i,k)$ = areal fraction of cell c that lies within SS(i,k), and

P_c = total number of persons assigned to cell c.

The accuracy of the population assignment procedure used by the IEM is unknown. The procedure can produce a distorted population distribution if a particular site is characterized by a grossly nonuniform population distribution. For example, at a site located near a large body of water, or any other uninhabited area, the IEM may assign persons to sector segments in which no one resides. Similar distortions could arise at sites characterized by isolated, small-sized, but densely populated areas. The IEM procedure also may offer some advantages. The census data have two shortcomings: (1) they locate an entire enumeration-district population at a point, and (2) they do not account for the daily movement of persons about their "point" of residence. Since the area encompassed by an enumeration district depends, to some extent, on the surrounding population density, the census data condense populations in areas of variable size to populations at points. The IEM procedure may

compensate to some degree for these shortcomings by spreading the census population over the area covered by the sector segment to which it is assigned. (We know of no good method to model in a general way the daily movement of people about their point of residence.)

A user of the IEM may, of course, supply an alternate population data set using the procedures outlined in the addendum to the IEM user's guide.[2] This option is useful if site-specific population data are available.

EXPOSURE ESTIMATION

The IEM calculates sector-segment exposures, SSE(i,k), from their corresponding sector-segment concentrations and populations using

$$SSE(i,k) = SSC(i,k) \times SSP(i,k).$$

The sector-segment exposures are combined to give exposures in:

(1) each sector, $SE(i) = \sum_{k} SSE(i,k)$,

(2) each radial band, $RBE(k) = \sum_{i=1}^{16} SSE(i,k)$, and

(3) the entire assessment area, $TE = \sum_{i=1}^{16} \sum_{k} SSE(i,k)$.

There are other methods for locating exposed persons and linking them to air concentrations. One such method is used in the Human Exposure Model (HEM).[23] This method does not manipulate the census data. Rather, it calculates an average concentration at the location of each census enumeration district. The averaging calculation is similar to the one used in the IEM, but it uses the grid-point concentrations at the four grid points nearest to and surrounding the point at which the enumeration district is located.

A comparison was made of the exposure estimates produced by the IEM and the HEM methods for maleic anhydride plants located at six different sites.[27] Table 2 summarizes the results of the comparison. Total exposures calculated using HEM differed by between -36 and +35% from those calculated using IEM. These differences may be due to two factors: (1) the different methods used to link exposed persons and air concentrations and (2) the fact that IEM results were based on 1980 census data and the HEM results, on 1970 data extrapolated to 1980. As shown in Table 2, differences (-13 to +7%) in the total populations used do not account for the exposure differences. A combination of the details of the population distributions and the methods of linking concentrations and exposed persons is the likely explanation for the total exposure differences. These differences are not large in the context of the overall uncertainties inherent in this type of calculation.

Table 2. Total exposure and exposed population estimates produced by the IEM and the HEM within 20 km of six sites

Site	IEM	HEM	% HEM difference
	Total exposure (person-ug/m^3)		
West Virginia	25,700[a]	33,600	30.7
Missouri	46,100[b]	47,300	2.6
Indiana	79,500[a]	50,900	-36.0
Illinois	28,600[a]	38,700	35.3
New Jersey	12,500[b]	9,540	-23.7
Pennsylvania	270,000[b]	267,000	-1.1
	Total exposed population (thousands of persons)		
West Virginia	56[a]	52	-7.3
Missouri	1,248[b]	1,338	7.2
Indiana	110[a]	108	-2.1
Illinois	154[a]	160	4.1
New Jersey	1,470[b]	1,277	-13.1
Pennsylvania	1,063[b]	1,090	2.6

[a]Coarse-grid population data were used.
[b]Fine-grid population data were used.

Source: Reference 27.

SECTION 4

METHOD USED FOR THE SENSITIVITY ANALYSIS

Emission sources found at HWMFs have relatively low pollutant release heights, may be located near structures that influence pollutant dispersion, and except for incinerator stacks, may have essentially no associated plume rise. Previous studies have examined the sensitivity of ISCLTM predictions to typical hazardous waste incinerator stack parameters.[28-30] Based on these studies and the fact that all stack parameters except the physical stack height affect only plume rise, which merely modifies the release height (or the effective stack height), we did not study these parameters in detail. Some general statements about the effects of stack parameters are given in Section 5. The remaining, important, user-supplied input parameters include meteorological parameters (wind speed, wind direction, and stability class), source parameters (release height, source area, and adjacent building cross sections), pollutant parameters (decay coefficient, settling velocity, and reflection coefficient), and the array of grid points chosen. The effects of varying these parameters are illustrated in Section 5. The effects of using the three source representation options to model two typical HWMF sources are illustrated in Section 6.

Several typical HWMF sources were selected for detailed study: a stack with essentially no plume rise, a 14.1-m square (200 m^2) area, an 80.6-m square (6500 m^2) area, a 316.2-m square (100,000 m^2) area, and a 2236.1-m square (5,000,000 m^2) area. Since the ISCLTM algorithm will not accept zero values for a stack diameter or gas exit velocity, our stack source was assumed to have a diameter of 1.0 m and a gas exit velocity of 1×10^{-5} m/s, the ISCLTM default value. Source (release) heights of 0, 5, 10, 15, and 20 m were considered for these sources. Limited evaluations were made of the effects of representing a 200-m^2 process building by one stack source, by two area sources, and by two volume sources; two release heights, 5 and 10 m, were considered for each representation. Similar evaluations were made for a 200-m^2 tank farm containing four tanks that were represented by four point sources with and without building wake effects, by one area source, by four area sources, by one volume source, and by four volume sources. Two release heights, 3 and 6 m, were considered for each representation.

These sources were studied using, unless otherwise indicated, the ISCLTM default parameter values and the following simplifying conditions:

(1) Source-specific pollutant emission rates were chosen to give a total emission rate of 1 g/s. This simplification makes the calculated concentrations ($\mu g/m^3$) equivalent to concentrations per unit release [$(\mu g/m^3)/(g/s)$], which are called X/Q values.

(2) The wind was assumed to blow only in one direction, from North to South. This simplification causes the highest concentrations to occur on direction vector D9 (South), which we call the "primary direction".

(3) Only one wind speed (0.75 m/s, the ISCLTM default for class 1) was considered.*

These conditions were used only if they acted as scaling factors (i.e., if they affected the magnitude but not the shape of the concentration profiles). Conditions 1 and 2 were used throughout this study; condition 3 was not used when considering the effects of pollutant decay and deposition. (Condition 3 also would not have been used if parameters that affect plume rise had been studied.)

The above simplifications were chosen to minimize the number of computer runs required and to isolate the effects of meteorological parameter values on the IEM predictions. Although the results of this study, if used properly, could be used to estimate concentrations and exposures from a real facility under real meteorological conditions, making an IEM run for the facility would be much easier and more reliable. Use of the results of this study in a real application would involve scaling the concentrations and exposures to account for (1) actual pollutant release rates; (2) actual combinations of wind speed, stability class, and wind direction; and (3) the actual population distribution. Step 1 could be accomplished easily, but accomplishment of steps 2 and 3 would be very difficult and time consuming.

Measures used to study the behavior of IEM predictions under the above conditions included:

(1) Primary Grid-Point Concentration [PGPC(j) = GPC(9,j)] profiles: plots of primary-direction grid-point concentrations vs. downwind distance (XGj),

(2) Value and location of the maximum PGPC,

(3) Primary Sector Exposure Potential [PSEP = SEP(9)]: the total exposure in the primary sector [SE(9) in Sect. 3] for a uniform site population density of 1 person/m^2,

(4) Total Grid-Ring Concentration [$TGRC(j) = \sum_{i=1}^{16} GPC(i,j)$] profiles: plots of the sums of all grid-point concentrations on the jth grid ring vs. downwind distance (XGj),

* The EPA recommends using 1.5 m/s for wind speed class 1.[31]

(5) Value and location of the maximum TGRC, and

(6) Total Exposure Potential [TEP = $\sum_{i=1}^{16}$ SEP(i)]: the sum of all sector exposure potentials, or the total population exposure for a uniform site population density of 1 person/m^2.

The TGRC and TEP measures were included because the dimensions of some of the area sources were large enough to cause substantial air concentrations to occur at grid points that lie outside the primary sector. Ignoring these concentrations would give a false impression of the importance of area size (see Sect. 5). These measures also give a better picture of IEM predictions under real meteorological conditions. They are equivalent to the PGPC and PSEP values that would be obtained if the wind was assumed to blow equally in all directions and if the pollutant release rate was 16 g/s. For the stack source, which essentially is a point source, PGPC and TGRC values are equal, as are the PSEP and TEP values. As source size increases, differences between the PGPC and TGRC values and between the PSEP and TEP values also increase.

One concern of this study, and indeed of any atmospheric modeling effort, was optimum receptor location. Concentrations at receptor locations are the output predictions of the atmospheric dispersion program, and it is important that the output reflects accurately the calculational capability of the program. To satisfy this concern, a detailed preliminary study was made of concentrations due to releases from a 30-m-high stack source, with no plume rise, under all combinations of stability and wind-speed classes. Good plume profiles and output maximum concentrations that were within a few percent of those actually calculated by the ISCLTM were obtained by locating receptors on grid rings at 50-m intervals between 100 m and 2 km, and at 5, 10, 20, 30, and 50 km. Except for location of the first grid ring, this receptor array was used throughout this study. The ISCLTM algorithms (see Ref. 4 for details) did not allow the first grid ring to be closer than 100 m for the stack, 150 m for the 200- and 6500-m^2 areas, 300 m for the 100,000-m^2 area, and 1250 m for the 5,000,000-m^2 area. Since the maximum number of grid rings used in this study (44) exceeds the number (20) normally allowed in the IEM, suggested receptor arrays are discussed in Section 5.

SECTION 5

DISCUSSION OF PARAMETERS THAT AFFECT CONCENTRATION ESTIMATES

The IEM uses a Gaussian-plume atmospheric dispersion model, ISCLTM, to calculate GPCs (annual-average, sector-averaged, centerline, ground-level, air concentrations of pollutants at user-specified receptor locations). As the name implies, a Gaussian-plume dispersion model assumes that pollutants released from a source are transported downwind in well-defined plumes. Sixteen such plumes are assumed in the IEM, one lying along and filling each of the sixteen direction vectors. Each plume is characterized by a line connecting the points of maximum concentration at each downwind (x) distance and a crosswind (y,z) distribution of pollutant concentration about the line. A maximum concentration line is an imaginary line drawn parallel to a direction vector at an elevation that, for most sources considered in this study, is determined largely by the pollutant release height. The crosswind distribution tends to be least uniform (high maximum concentration relative to concentrations at other locations) near the source and to become more uniform with increasing downwind distance. The lateral (y) component of this distribution is treated by the sector averaging procedure. Our concern is with evaluation of the distribution at the ground surface, at $z = 0$, where the ISCLTM calculates GPC values. These values are affected by the meteorological, climatological, source, and pollutant parameters and by the choice of a receptor array (the locations of the grid points at which the GPCs are calculated).

METEOROLOGICAL AND CLIMATOLOGICAL PARAMETERS

Selection of a representative meteorological data set is very important. Consultation with a professional meteorologist is recommended, especially when site-specific data are not available, when the site has complex topographic features, or when the site features differ from those at the nearest weather station.

The meteorological data supplied with the IEM consists of National Oceanic and Atmospheric Administration Stability Array (STAR) data sets for weather stations located throughout the contiguous United States. Each data set contains a time-averaged joint frequency distribution of wind direction, wind-speed class, and atmospheric (Pasquill) stability category. (An annual meteorological data set contains 576 entries. Each entry is the fraction of the year during which one of six Pasquill stability categories occurs in

combination with winds blowing into one of the sixteen 22.5°-wide sectors at speeds within the range of speeds assigned to one of six wind-speed classes.) For this study, the components of the joint frequency distribution were treated separately. Each stability category was studied, but only one wind speed and one wind direction were considered. The wind was assumed to blow only from North to South, thus, the fraction of the time that the wind blows from direction 1 toward direction 9, the primary direction, was set equal to 1.0. The fractions for all other directions were set to zero. This simplification makes the results of this study applicable to all directions. Also only one wind speed was considered in detail. Except for the situations discussed below, this simplification also allows the results of this study to be applied to other wind speeds. In principle, the results of this limited study could be applied to a real case simply by multiplying the results for a given stability category by the appropriate wind-speed scaling factors (see below) and joint frequency distributions. In practice, it would be much simpler and less error-prone to run the IEM for the problem of interest.

To illustrate the relative occurrence of each stability category and wind-speed class in real meteorological data sets, data from eight scattered weather stations were analyzed. The results of this analysis are presented in Table 3. (These results should not be used in studies of specific sites.) Stability category D tended to occur most often, while categories A and B occurred infrequently. In some STAR data sets, categories E and F are combined and listed under category E. These data sets contain either no entries or all zeros for stability category F. (This is why the minimum frequency of occurrence is zero for category F in Table 3.) Wind speed classes 2 (2.5 m/s) and 3 (4.3 m/s) occurred most often; classes 1 (0.75 m/s) and 4 (6.8 m/s) also were important; and classes 5 (9.5 m/s) and 6 (12.5 m/s) were relatively rare.

Wind Direction

The fraction of the time that the wind blows in a given direction (i.e., within ± 11.25° of a given direction vector) is an important parameter in concentration calculations using a real meteorological data set. It determines the fraction of the total pollutant release that is directed into the plume centered on the given direction. This parameter enters the atmospheric dispersion calculations, which are performed separately for each direction, as a linear, multiplicative, scaling factor. Thus, this parameter affects the magnitude of the calculated GPCs but not the shape of their profiles. For example, if the wind is assumed to blow from North to South only 10% of the time, the resulting concentrations and exposures will be 0.1 times those given in this study.

Wind Speed

Wind speed determines both the length of time it takes for a pollutant to be transported from the emission point to some downwind distance and the volume per unit time of ambient air passing the emission point. This volume flow determines the initial total quantity of pollutant contained per unit length of the plume and, thus, determines the total quantity of pollutant that can be distributed across a given plume cross section. For the sources considered in this study, wind speed and downwind GPCs were related inversely,

Table 3. Composite of stability and wind-speed class frequencies for eight scattered weather stations[a]

Class	Minimum	Mean	Maximum
		Stability class	
A	0.00286	0.01089	0.03329
B	0.02669	0.06022	0.10239
C	0.08606	0.10267	0.14081
D	0.25820	0.46934	0.62780
E	0.06127	0.17335	0.30483
F	0.0	0.18358	0.28043
		Wind-speed class	
1	0.06822	0.19650	0.36065
2	0.19485	0.25887	0.32479
3	0.25863	0.29737	0.38707
4	0.13032	0.19881	0.26425
5	0.00913	0.03881	0.08517
6	0.00186	0.01026	0.03808

[a]Annual average data, based on five years of observation, from the following weather stations:
Blythe/Riverside, CA
Eau Claire, WI
Kansas City, MO
Williamsport/Lyco, PA
Bismarck, ND
Sheridan County, WY
Morgantown, WV
Louisville, KY

except when pollutant decay and deposition were considered. (Wind speed is a linear, multiplicative, scaling factor in the denominator of the dispersion equation.) Figure 4 depicts the scaling factor (the straight line) as a function of wind speed for a reference speed of 0.75 m/s, the base speed used throughout this study. Multiplication of the concentrations and exposures presented in this study by the appropriate scaling factor will generate concentrations and exposures for any desired wind speed. For example, if the desired wind speed is 2.5 m/s, multiply the results of this study by 0.3. (Dividing by the ratio of the new and old wind speeds, 2.5/0.75 = 3.3, yields the same result.)

For sources having an associated plume rise, the linear relationship will not hold. In fact, increasing wind speed may lead to higher concentration and exposure predictions for these sources.[30] This reversal occurs because increasing the wind speed reduces plume rise and, thus, lowers the effective pollutant release height.

Uncertainties that could be introduced into IEM predictions due to the use of discrete (mean) wind speeds to represent ranges of values are illustrated by the stepped curve in Figure 4. For example, for wind speed class 2, with an average wind speed of 2.5 m/s and limits of 1.5 and 3.4 m/s, the calculated concentrations and exposures could be between a factor of 1.7 low and a factor of 1.4 high. Largest uncertainties would occur in wind speed classes 1 and 6, which are open ended. In practice, these potential uncertainties may not be realized. Bowman and Crowder ran the ISCLT using either mean wind speeds or true hourly average wind speeds and found less than a 3% difference between the two sets of concentration predictions.[30]

Stabilty Class

A stability class is a measure of atmospheric turbulence; it determines the rapidity with which emitted pollutants mix with the available ambient air. Thus, this parameter affects the crosswind distribution of pollutant concentration. The rapid mixing that occurs under unstable (e.g, A) conditions causes the distribution to become uniform sooner (nearer to the source) than does the slower mixing that occurs under stable (e.g., F) conditions. The effects of stability on concentration and exposure predictions also are affected by the pollutant release height, the source area, and the location of the first receptor.

The effects of stability class on PGPC and TGRC profiles are illustrated, respectively, in Appendix A (Figs. 13-17) and Appendix B (Figs. 18-21). For ground-level (0-m) releases, increasing stability (from A to F) increased the concentration at every receptor location. Maximum concentrations always occurred under F stability, at the first allowed receptor location for the source being considered (see Tables 4-8). Increasing stability in combination with increasing release height caused concentrations at receptors near the source to decrease faster than concentrations at more distant locations, moved the locations of the maximum concentrations farther downwind, and caused the maxima to occur under less stable conditions. This effect was most pronounced for stack (0-m^2 area) source releases (Table 4). For ground-level releases, maximum concentrations always occurred at 100 m and increased with the following stability-class sequence: A B C D E F. For 10-m releases, maximum

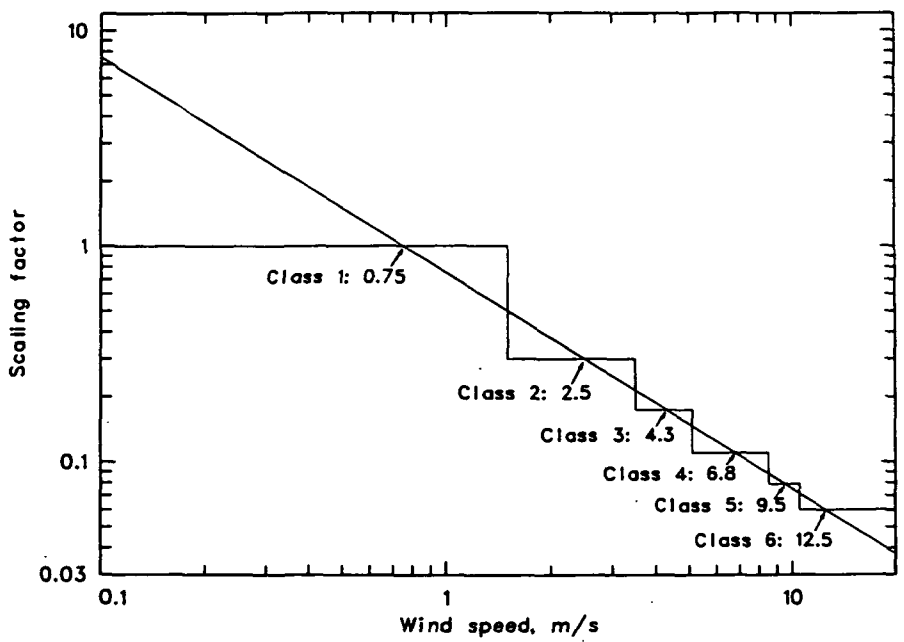

Figure 4. The wind-speed scaling factor (equals 1.0 for 0.75 m/s).

Table 4. Summary of maximum concentrations and exposures, stack

Stability class	Release height, m				
	0	5	10	15	20
	Values and locations of maximum PGPCs, $\mu g/m^3$(km)				
A	1938(0.10)[a]	1818(0.10)	1499(0.10)	1044(0.10)	647(0.10)
B	2550(0.10)	2282(0.10)	1635(0.10)	883(0.10)	455(0.15)
C	3634(0.10)	2900(0.10)	1473(0.10)	586(0.15)	304(0.20)
D	5814(0.10)	3263(0.10)	869(0.15)	329(0.25)	164(0.35)
E	7650(0.10)	2813(0.10)	600(0.20)	216(0.35)	101(0.50)
F	11630(0.10)	1688(0.15)	352(0.35)	124(0.60)	57(0.85)
	PSEPs, 10^8 person-$\mu g/m^3$				
A	0.79	0.79	0.78	0.74	0.71
B	0.98	0.98	0.96	0.88	0.83
C	1.35	1.34	1.29	1.15	1.04
D	3.63	3.55	3.40	2.96	2.66
E	6.26	6.08	5.78	4.90	4.32
F	10.80	10.27	9.63	8.04	6.94
	Values and locations of maximum TGRCs, $\mu g/m^3$(km)				
A	1938(0.10)[a]	1818(0.10)	1499(0.10)	1044(0.10)	647(0.10)
B	2550(0.10)	2282(0.10)	1635(0.10)	883(0.10)	455(0.15)
C	3634(0.10)	2900(0.10)	1473(0.10)	586(0.15)	304(0.20)
D	5814(0.10)	3263(0.10)	869(0.15)	329(0.25)	164(0.35)
E	7650(0.10)	2813(0.10)	600(0.20)	216(0.35)	101(0.50)
F	11630(0.10)	1688(0.15)	352(0.35)	124(0.60)	57(0.90)
	TEPs, 10^8 person-$\mu g/m^3$				
A	0.79	0.79	0.78	0.74	0.71
B	0.98	0.98	0.96	0.88	0.83
C	1.35	1.34	1.29	1.15	1.04
D	3.63	3.55	3.40	2.96	2.66
E	6.26	6.08	5.78	4.90	4.32
F	10.80	10.27	9.63	8.04	6.94

[a]The closest distance allowed for this source.

Table 5. Summary of maximum concentrations and exposures, 200-m^2 area

Stability class	Release height, m				
	0	5	10	15	20
	Values and locations of maximum PGPCs, $\mu g/m^3$(km)				
A	602(0.15)[a]	589(0.15)	551(0.15)	473(0.15)	392(0.15)
B	845(0.15)	808(0.15)	708(0.15)	534(0.15)	376(0.15)
C	1214(0.15)	1108(0.15)	843(0.15)	493(0.15)	267(0.20)
D	1986(0.15)	1556(0.15)	748(0.15)	298(0.25)	152(0.35)
E	2679(0.15)	1719(0.15)	541(0.20)	201(0.35)	97(0.50)
F	4081(0.15)	1457(0.15)	330(0.35)	119(0.60)	56(0.85)
	PSEPs, 10^8 person-$\mu g/m^3$				
A	0.74	0.74	0.74	0.70	0.68
B	0.91	0.91	0.90	0.84	0.79
C	1.25	1.24	1.22	1.10	1.02
D	3.44	3.41	3.33	2.92	2.63
E	6.00	5.91	5.71	4.86	4.29
F	10.42	10.11	9.56	8.00	6.92
	Values and locations of maximum TGRCs, $\mu g/m^3$(km)				
A	878(0.15)[a]	858(0.15)	799(0.15)	682(0.15)	562(0.15)
B	1227(0.15)	1172(0.15)	1021(0.15)	763(0.15)	530(0.15)
C	1763(0.15)	1603(0.15)	1205(0.15)	691(0.15)	351(0.20)
D	2882(0.15)	2235(0.15)	1045(0.15)	375(0.25)	181(0.30)
E	3883(0.15)	2449(0.15)	706(0.20)	239(0.35)	110(0.50)
F	5913(0.15)	2032(0.15)	392(0.35)	133(0.60)	60(0.85)
	TEPs, 10^8 person-$\mu g/m^3$				
A	0.76	0.76	0.76	0.73	0.70
B	0.95	0.95	0.94	0.88	0.83
C	1.32	1.31	1.28	1.15	1.06
D	3.58	3.53	3.43	2.99	2.68
E	6.19	6.08	5.83	4.94	4.35
F	10.72	10.34	9.71	8.09	6.98

[a]The closest distance allowed for this source.

Table 6. Summary of maximum concentrations and exposures, 6500-m^2 area

Stability class	Release height, m				
	0	5	10	15	20
	Values and locations of maximum PGPCs, $\mu g/m^3$(km)				
A	208(0.15)[a]	206(0.15)	199(0.15)	181(0.15)	164(0.15)
B	307(0.15)	300(0.15)	280(0.15)	235(0.15)	191(0.15)
C	447(0.15)	426(0.15)	368(0.15)	266(0.15)	178(0.15)
D	743(0.15)	649(0.15)	433(0.15)	211(0.20)	116(0.30)
E	1020(0.15)	791(0.15)	369(0.15)	154(0.30)	80(0.50)
F	1562(0.15)	860(0.15)	256(0.35)	101(0.60)	49(0.85)
	PSEPs, 10^8 person-$\mu g/m^3$				
A	0.69	0.69	0.69	0.66	0.64
B	0.82	0.82	0.82	0.77	0.73
C	1.10	1.10	1.09	1.00	0.93
D	3.17	3.16	3.12	2.76	2.52
E	5.61	5.56	5.45	4.69	4.16
F	9.80	9.63	9.25	7.80	6.77
	Values and locations of maximum TGRCs, $\mu g/m^3$(km)				
A	603(0.15)[a]	596(0.15)	574(0.15)	518(0.15)	462(0.15)
B	883(0.15)	860(0.15)	795(0.15)	655(0.15)	522(0.15)
C	1282(0.15)	1212(0.15)	1026(0.15)	718(0.15)	462(0.15)
D	2123(0.15)	1823(0.15)	1157(0.15)	494(0.15)	216(0.25)
E	2903(0.15)	2185(0.15)	939(0.15)	283(0.30)	130(0.45)
F	4439(0.15)	2289(0.15)	465(0.30)	156(0.55)	70(0.80)
	TEPs, 10^8 person-$\mu g/m^3$				
A	0.75	0.75	0.75	0.72	0.69
B	0.94	0.94	0.93	0.87	0.83
C	1.30	1.29	1.28	1.16	1.07
D	3.57	3.55	3.47	3.05	2.75
E	6.21	6.13	5.93	5.05	4.44
F	10.76	10.47	9.90	8.24	7.10

[a]The closest distance allowed for this source.

Table 7. Summary of maximum concentrations and exposures, 100,000-m^2 area

Stability class	Release height, m				
	0	5	10	15	20
	Values and locations of maximum PGPCs, $\mu g/m^3$(km)				
A	14(0.30)[a]	14(0.30)	14(0.30)	13(0.30)	13(0.30)
B	35(0.30)	35(0.30)	35(0.30)	32(0.30)	30(0.30)
C	58(0.30)	57(0.30)	56(0.30)	49(0.30)	44(0.30)
D	104(0.30)	102(0.30)	94(0.30)	74(0.30)	57(0.30)
E	151(0.30)	143(0.30)	121(0.30)	81(0.30)	50(0.30)
F	229(0.30)	201(0.30)	137(0.30)	67(0.40)	36(0.70)
	PSEPs, 10^8 person-$\mu g/m^3$				
A	0.62	0.62	0.62	0.60	0.58
B	0.69	0.69	0.69	0.65	0.62
C	0.89	0.89	0.89	0.82	0.77
D	2.72	2.71	2.70	2.42	2.23
E	4.92	4.90	4.86	4.24	3.81
F	8.70	8.63	8.45	7.23	6.35
	Values and locations of maximum TGRCs, $\mu g/m^3$(km)				
A	98(0.30)[a]	98(0.30)	98(0.30)	93(0.30)	89(0.30)
B	207(0.30)	206(0.30)	203(0.30)	186(0.30)	171(0.30)
C	328(0.30)	323(0.30)	311(0.30)	269(0.30)	233(0.30)
D	581(0.30)	559(0.30)	497(0.30)	372(0.30)	268(0.30)
E	831(0.30)	768(0.30)	609(0.30)	372(0.30)	208(0.30)
F	1267(0.30)	1054(0.30)	625(0.30)	248(0.30)	91(0.45)
	TEPs, 10^8 person-$\mu g/m^3$				
A	0.71	0.71	0.71	0.68	0.66
B	0.85	0.85	0.85	0.80	0.76
C	1.16	1.16	1.16	1.07	1.00
D	3.39	3.38	3.35	2.99	2.74
E	5.99	5.96	5.87	5.08	4.52
F	10.45	10.32	9.99	8.44	7.32

[a]The closest distance allowed for this source.

Table 8. Summary of maximum concentrations and exposures, 5,000,000-m^2 area

Stability class	Release height, m				
	0	5	10	15	20
	Values and locations of maximum PGPCs, $\mu g/m^3$(km)				
A	<1(1.25)[a]	<1(1.25)	<1(1.25)	<1(1.25)	<1(1.25)
B	1(1.25)	1(1.25)	1(1.25)	1(1.25)	1(1.25)
C	2(1.25)	2(1.25)	2(1.25)	2(1.25)	2(1.25)
D	5(1.25)	5(1.25)	5(1.25)	4(1.25)	4(1.25)
E	8(1.25)	8(1.25)	8(1.25)	7(1.25)	6(1.25)
F	12(1.25)	12(1.25)	12(1.25)	10(1.25)	8(1.25)
	PSEPs, 10^8 person-$\mu g/m^3$				
A	0.48	0.48	0.48	0.46	0.45
B	0.48	0.48	0.48	0.45	0.44
C	0.54	0.54	0.54	0.50	0.47
D	1.71	1.71	1.71	1.54	1.43
E	3.27	3.27	3.25	2.86	2.61
F	5.94	5.92	5.86	5.10	4.56
	Values and locations of maximum TGRCs, $\mu g/m^3$(km)				
A	3(1.25)[a]	3(1.25)	3(1.25)	3(1.25)	3(1.25)
B	7(1.25)	7(1.25)	7(1.25)	6(1.25)	6(1.25)
C	14(1.25)	14(1.25)	14(1.25)	13(1.25)	12(1.25)
D	37(1.25)	36(1.25)	36(1.25)	32(1.25)	29(1.25)
E	56(1.25)	56(1.25)	55(1.25)	47(1.25)	41(1.25)
F	88(1.25)	87(1.25)	82(1.25)	66(1.25)	54(1.25)
	TEPs, 10^8 person-$\mu g/m^3$				
A	0.72	0.72	0.72	0.69	0.67
B	0.74	0.74	0.74	0.70	0.67
C	0.91	0.91	0.91	0.84	0.79
D	2.91	2.91	2.90	2.62	2.42
E	5.38	5.37	5.34	4.69	4.25
F	9.60	9.56	9.43	8.16	7.25

[a]The closest distance allowed for this source.

concentrations occurred between 100 and 350 m and increased in the sequence F E D C A B. For 20-m releases, maximum concentrations occurred between 100 and 850 m and increased in the sequence F E D C B A, the reverse of the ground-level sequence.

As source area was increased, the distance to the first allowed receptor increased and the above effects of stability class were, at least apparently, mitigated. For the 5,000,000-m^2 area source (Table 8), maximum concentrations always occurred at the first allowed receptor (at 1250 m) and always increased in the same sequence, A B C D E F. This consistency is due largely to the fact that the first allowed receptor was beyond the range of distances that are affected strongly by the joint interaction of stability and release height. There was also a small mitigation of the stability/release height effects with increasing area for the other sources considered. Tables 9-14 present the values and locations of of maximum PGPCs and TGRCs that were obtained when the first receptors were located at 150, 300, or 1250 m. Table 15 is a summary of the stability-class sequences (in order of increasing stability) given in Tables 9-14. Note that the larger areas tend to slow the release-height-dependent reversal of sequences.

The effects of stability class on the concentration profiles are related directly to the degree of mixing associated with the stabilities. For ground-level releases, the maximum concentration line is always at ground level. Therefore, ground-level releases always predicted the highest GPCs. Also, since the line concentration decreases with distance from the source, the maximum GPC always occurred at the first receptor. Concentrations decrease with increasing distance from the source due to dispersion, which distributes the pollutants throughout the plume cross section by depleting the line concentration. Increasing the release height raises the maximum concentration line and leads to an overall reduction in ground-level concentrations. As release height is increased, the slower mixing associated with stable conditions does not allow significant concentrations of pollutants to reach ground level at the close-in receptors. As the plume travels downwind, dispersion spreads the plume, and maximum GPCs occur when the plume reaches ground level, at more distant receptors. As stability is decreased, maximum GPCs tend to occur at closer receptors. In fact, for the sources studied, the maximum GPCs always occurred at the closest receptor under A stability conditions.

Tables 4-8 and 16-21 list PSEPs and TEPs for each source, stability class, and release height studied. These exposure measures always increased with increasing stability. This effect is expected because (1) sector-segment areas and, in this case, their populations increase with distance from the origin and (2) sector-segment concentrations in segments beyond ~1250 m downwind always increase with increasing stability. This relationship is likely to hold for real population distributions.

The behavior of IEM predictions with changes in stability are important when modeling low-level releases. Using either urban stability mode option to model a ground-level release may result in concentration and exposure predictions that are lower than those obtained when using the rural mode option. (Both urban mode options move stabilities E and F to D, and urban mode 2 moves D to C; C to B; and B to A.) For a ground-level release, the

Table 9. Values ($\mu g/m^3$) and locations[a] (km) of maximum PGPCs for receptors beginning at 0.15 km downwind

Stability class	Release height, m				
	0	5	10	15	20
			Stack source		
A	842(0.15)	820(0.15)	755(0.15)	633(0.15)	508(0.15)
B	1164(0.15)	1105(0.15)	945(0.15)	685(0.15)	455(0.15)
C	1671(0.15)	1501(0.15)	1087(0.15)	586(0.15)	304(0.20)
D	2723(0.15)	2047(0.15)	869(0.15)	329(0.25)	164(0.35)
E	3656(0.15)	2185(0.15)	600(0.20)	216(0.35)	101(0.50)
F	5566(0.15)	1688(0.15)	352(0.35)	124(0.60)	57(0.85)
			200-m^2 source		
A	602(0.15)	589(0.15)	551(0.15)	473(0.15)	392(0.15)
B	845(0.15)	808(0.15)	708(0.15)	534(0.15)	376(0.15)
C	1214(0.15)	1108(0.15)	843(0.15)	493(0.15)	267(0.20)
D	1986(0.15)	1556(0.15)	748(0.15)	298(0.25)	152(0.35)
E	2679(0.15)	1719(0.15)	541(0.20)	201(0.35)	97(0.50)
F	4081(0.15)	1457(0.15)	330(0.35)	119(0.60)	56(0.85)
			6500-m^2 source		
A	208(0.15)	206(0.15)	199(0.15)	181(0.15)	164(0.15)
B	307(0.15)	300(0.15)	280(0.15)	235(0.15)	191(0.15)
C	447(0.15)	426(0.15)	368(0.15)	266(0.15)	178(0.15)
D	743(0.15)	649(0.15)	433(0.15)	211(0.20)	116(0.30)
E	1020(0.15)	791(0.15)	369(0.15)	154(0.30)	80(0.50)
F	1562(0.15)	860(0.15)	256(0.35)	101(0.60)	49(0.85)

[a]Distances are given in parentheses ().

Table 10. Values ($\mu g/m^3$) and locations[a] (km) of maximum TGRCs for receptors beginning at 0.15 km downwind

Stability class	Release height, m				
	0	5	10	15	20
			Stack source		
A	842(0.15)	820(0.15)	755(0.15)	633(0.15)	508(0.15)
B	1164(0.15)	1105(0.15)	945(0.15)	685(0.15)	455(0.15)
C	1671(0.15)	1501(0.15)	1087(0.15)	586(0.15)	304(0.20)
D	2723(0.15)	2047(0.15)	869(0.15)	329(0.25)	164(0.35)
E	3656(0.15)	2185(0.15)	600(0.20)	216(0.35)	101(0.50)
F	5566(0.15)	1688(0.15)	352(0.35)	124(0.60)	57(0.85)
			200-m^2 source		
A	878(0.15)	858(0.15)	799(0.15)	682(0.15)	562(0.15)
B	1227(0.15)	1172(0.15)	1021(0.15)	763(0.15)	530(0.15)
C	1763(0.15)	1603(0.15)	1205(0.15)	691(0.15)	351(0.20)
D	2882(0.15)	2235(0.15)	1045(0.15)	375(0.25)	181(0.30)
E	3883(0.15)	2449(0.15)	706(0.20)	239(0.35)	110(0.50)
F	5913(0.15)	2032(0.15)	392(0.35)	133(0.60)	60(0.85)
			6500-m^2 source		
A	603(0.15)	596(0.15)	574(0.15)	518(0.15)	462(0.15)
B	883(0.15)	860(0.15)	795(0.15)	655(0.15)	522(0.15)
C	1282(0.15)	1212(0.15)	1026(0.15)	718(0.15)	462(0.15)
D	2123(0.15)	1823(0.15)	1157(0.15)	494(0.15)	216(0.25)
E	2903(0.15)	2185(0.15)	939(0.15)	283(0.30)	130(0.45)
F	4439(0.15)	2289(0.15)	465(0.30)	156(0.55)	70(0.80)

[a]Distances are given in parentheses ().

Table 11. Values ($\mu g/m^3$) and locations[a] (km) of maximum PGPCs for receptors beginning at 0.3 km downwind

Stability class	Release height, m				
	0	5	10	15	20
			Stack source		
A	190(0.30)	189(0.30)	186(0.30)	174(0.30)	162(0.30)
B	299(0.30)	295(0.30)	283(0.30)	249(0.30)	217(0.30)
C	444(0.30)	431(0.30)	393(0.30)	312(0.30)	238(0.30)
D	746(0.30)	685(0.30)	530(0.30)	312(0.30)	164(0.35)
E	1037(0.30)	879(0.30)	534(0.30)	216(0.35)	101(0.50)
F	1604(0.30)	1080(0.30)	352(0.35)	124(0.60)	57(0.85)
			200-m^2 source		
A	157(0.30)	156(0.30)	154(0.30)	144(0.30)	136(0.30)
B	252(0.30)	249(0.30)	240(0.30)	212(0.30)	186(0.30)
C	375(0.30)	365(0.30)	336(0.30)	269(0.30)	209(0.30)
D	634(0.30)	585(0.30)	461(0.30)	280(0.30)	152(0.35)
E	883(0.30)	757(0.30)	477(0.30)	201(0.35)	97(0.50)
F	1364(0.30)	945(0.30)	330(0.35)	119(0.60)	56(0.85)
			6500-m^2 source		
A	77(0.30)	77(0.30)	76(0.30)	72(0.30)	69(0.30)
B	134(0.30)	133(0.30)	130(0.30)	117(0.30)	106(0.30)
C	203(0.30)	199(0.30)	187(0.30)	157(0.30)	129(0.30)
D	349(0.30)	329(0.30)	277(0.30)	187(0.30)	116(0.30)
E	492(0.30)	438(0.30)	310(0.30)	154(0.30)	80(0.50)
F	755(0.30)	575(0.30)	256(0.35)	101(0.60)	49(0.85)
			100,000-m^2 source		
A	14(0.30)	14(0.30)	14(0.30)	13(0.30)	13(0.30)
B	35(0.30)	35(0.30)	35(0.30)	32(0.30)	30(0.30)
C	58(0.30)	57(0.30)	56(0.30)	49(0.30)	44(0.30)
D	104(0.30)	102(0.30)	94(0.30)	74(0.30)	57(0.30)
E	151(0.30)	143(0.30)	121(0.30)	81(0.30)	50(0.30)
F	229(0.30)	201(0.30)	137(0.30)	67(0.40)	36(0.70)

[a]Distances are given in parentheses ().

Table 12. Values ($\mu g/m^3$) and locations[a] (km) of maximum TGRCs for receptors beginning at 0.3 km downwind

Stability class	Release height, m				
	0	5	10	15	20
			Stack source		
A	190(0.30)	189(0.30)	186(0.30)	174(0.30)	162(0.30)
B	299(0.30)	295(0.30)	283(0.30)	249(0.30)	217(0.30)
C	444(0.30)	431(0.30)	393(0.30)	312(0.30)	238(0.30)
D	746(0.30)	685(0.30)	530(0.30)	312(0.30)	164(0.35)
E	1037(0.30)	879(0.30)	536(0.30)	216(0.35)	101(0.50)
F	1604(0.30)	1080(0.30)	352(0.35)	124(0.60)	57(0.85)
			200-m^2 source		
A	198(0.30)	197(0.30)	194(0.30)	182(0.30)	170(0.30)
B	316(0.30)	312(0.30)	300(0.30)	264(0.30)	231(0.30)
C	469(0.30)	456(0.30)	419(0.30)	334(0.30)	259(0.30)
D	792(0.30)	730(0.30)	572(0.30)	344(0.30)	181(0.30)
E	1102(0.30)	941(0.30)	586(0.30)	239(0.35)	110(0.50)
F	1703(0.30)	1168(0.30)	392(0.35)	133(0.60)	60(0.85)
			6500-m^2 source		
A	151(0.30)	151(0.30)	149(0.30)	141(0.30)	134(0.30)
B	260(0.30)	258(0.30)	251(0.30)	225(0.30)	203(0.30)
C	391(0.30)	383(0.30)	360(0.30)	300(0.30)	245(0.30)
D	672(0.30)	632(0.30)	527(0.30)	351(0.30)	213(0.30)
E	945(0.30)	838(0.30)	583(0.30)	283(0.30)	130(0.45)
F	1453(0.30)	1093(0.30)	465(0.30)	156(0.55)	70(0.80)
			100,000-m^2 source		
A	98(0.30)	98(0.30)	98(0.30)	93(0.30)	89(0.30)
B	207(0.30)	206(0.30)	203(0.30)	186(0.30)	171(0.30)
C	328(0.30)	323(0.30)	311(0.30)	269(0.30)	233(0.30)
D	581(0.30)	559(0.30)	497(0.30)	372(0.30)	268(0.30)
E	831(0.30)	768(0.30)	609(0.30)	372(0.30)	208(0.30)
F	1267(0.30)	1054(0.30)	625(0.30)	248(0.30)	91(0.45)

[a]Distances are given in parentheses ().

Table 13. Values ($\mu g/m^3$) and locations[a] (km) of maximum PGPCs for receptors beginning at 1.25 km downwind

Stability class	Release height, m				
	0	5	10	15	20
			Stack source		
A	3.1(1.25)	3.1(1.25)	3.1(1.25)	3.0(1.25)	2.9(1.25)
B	15.5(1.25)	15.5(1.25)	15.5(1.25)	14.5(1.25)	13.8(1.25)
C	28.8(1.25)	28.8(1.25)	28.6(1.25)	26.1(1.25)	24.2(1.25)
D	58.4(1.25)	57.8(1.25)	56.3(1.25)	48.6(1.25)	42.4(1.25)
E	86.9(1.25)	85.1(1.25)	80.1(1.25)	64.2(1.25)	51.1(1.25)
F	134.6(1.25)	128.3(1.25)	110.9(1.25)	77.1(1.25)	50.4(1.25)
			200-m^2 source		
A	3.0(1.25)	3.0(1.25)	3.0(1.25)	2.8(1.25)	2.8(1.25)
B	14.8(1.25)	14.8(1.25)	14.8(1.25)	13.9(1.25)	13.2(1.25)
C	27.7(1.25)	27.6(1.25)	27.5(1.25)	25.0(1.25)	23.3(1.25)
D	56.2(1.25)	55.7(1.25)	54.2(1.25)	46.8(1.25)	40.9(1.25)
E	83.7(1.25)	82.0(1.25)	77.3(1.25)	61.9(1.25)	49.4(1.25)
F	129.6(1.25)	123.6(1.25)	107.1(1.25)	74.7(1.25)	49.1(1.25)
			6500-m^2 source		
A	2.4(1.25)	2.4(1.25)	2.4(1.25)	2.4(1.25)	2.3(1.25)
B	12.3(1.25)	12.3(1.25)	12.2(1.25)	11.5(1.25)	10.9(1.25)
C	23.1(1.25)	23.0(1.25)	22.9(1.25)	20.9(1.25)	19.5(1.25)
D	47.5(1.25)	47.1(1.25)	45.9(1.25)	39.8(1.25)	34.9(1.25)
E	70.7(1.25)	69.4(1.25)	65.7(1.25)	53.0(1.25)	42.7(1.25)
F	109.6(1.25)	104.8(1.25)	91.6(1.25)	64.9(1.25)	43.5(1.25)
			100,000-m^2 source		
A	1.6(1.25)	1.6(1.25)	1.6(1.25)	1.5(1.25)	1.5(1.25)
B	7.0(1.25)	7.0(1.25)	7.0(1.25)	6.6(1.25)	6.3(1.25)
C	13.7(1.25)	13.6(1.25)	13.6(1.25)	12.4(1.25)	11.6(1.25)
D	29.4(1.25)	29.2(1.25)	28.6(1.25)	25.0(1.25)	22.2(1.25)
E	43.9(1.25)	43.2(1.25)	41.3(1.25)	33.9(1.25)	28.0(1.25)
F	67.9(1.25)	65.5(1.25)	58.7(1.25)	43.4(1.25)	30.8(1.25)
			5,000,000-m^2 source		
A	0.4(1.25)	0.4(1.25)	0.4(1.25)	0.4(1.25)	0.4(1.25)
B	0.8(1.25)	0.8(1.25)	0.8(1.25)	0.8(1.25)	0.7(1.25)
C	1.9(1.25)	1.9(1.25)	1.9(1.25)	1.7(1.25)	1.6(1.25)
D	5.0(1.25)	5.0(1.25)	5.0(1.25)	4.4(1.25)	4.0(1.25)
E	7.7(1.25)	7.7(1.25)	7.6(1.25)	6.5(1.25)	5.7(1.25)
F	12.3(1.25)	12.1(1.25)	11.6(1.25)	9.5(1.25)	7.9(1.25)

[a] Distances are given in parentheses ().

Table 14. Values ($\mu g/m^3$) and locations[a] (km) of maximum TGRCs for receptors beginning at 1.25 km downwind

Stability class	Release height, m				
	0	5	10	15	20
			Stack source		
A	3.1(1.25)	3.1(1.25)	3.1(1.25)	3.0(1.25)	2.9(1.25)
B	15.5(1.25)	15.5(1.25)	15.5(1.25)	14.5(1.25)	13.8(1.25)
C	28.8(1.25)	28.8(1.25)	28.6(1.25)	26.1(1.25)	24.2(1.25)
D	58.4(1.25)	57.8(1.25)	56.3(1.25)	48.6(1.25)	42.4(1.25)
E	86.9(1.25)	85.1(1.25)	80.1(1.25)	64.2(1.25)	51.1(1.25)
F	134.6(1.25)	128.3(1.25)	110.9(1.25)	77.1(1.25)	50.4(1.25)
			200-m^2 source		
A	3.2(1.25)	3.2(1.25)	3.2(1.25)	3.0(1.25)	3.0(1.25)
B	15.8(1.25)	15.8(1.25)	15.8(1.25)	14.8(1.25)	14.1(1.25)
C	29.5(1.25)	29.4(1.25)	29.3(1.25)	26.7(1.25)	24.8(1.25)
D	59.8(1.25)	59.3(1.25)	57.7(1.25)	49.8(1.25)	43.5(1.25)
E	89.0(1.25)	87.3(1.25)	82.2(1.25)	65.8(1.25)	52.5(1.25)
F	138.0(1.25)	131.5(1.25)	113.8(1.25)	79.3(1.25)	52.0(1.25)
			6500-m^2 source		
A	3.3(1.25)	3.3(1.25)	3.3(1.25)	3.1(1.25)	3.1(1.25)
B	16.3(1.25)	16.3(1.25)	16.3(1.25)	15.3(1.25)	14.6(1.25)
C	30.7(1.25)	30.6(1.25)	30.4(1.25)	27.8(1.25)	25.8(1.25)
D	62.8(1.25)	62.3(1.25)	60.7(1.25)	52.5(1.25)	46.0(1.25)
E	93.6(1.25)	91.8(1.25)	86.7(1.25)	69.8(1.25)	56.0(1.25)
F	145.0(1.25)	138.5(1.25)	120.7(1.25)	85.0(1.25)	56.6(1.25)
			100,000-m^2 source		
A	2.9(1.25)	2.9(1.25)	2.9(1.25)	2.8(1.25)	2.7(1.25)
B	13.5(1.25)	13.5(1.25)	13.4(1.25)	12.6(1.25)	12.0(1.25)
C	26.0(1.25)	25.9(1.25)	25.8(1.25)	23.6(1.25)	22.1(1.25)
D	55.4(1.25)	55.0(1.25)	53.9(1.25)	47.0(1.25)	41.6(1.25)
E	82.7(1.25)	81.4(1.25)	77.7(1.25)	63.6(1.25)	52.2(1.25)
F	128.1(1.25)	123.4(1.25)	110.1(1.25)	80.7(1.25)	56.8(1.25)
			5,000,000-m^2 source		
A	2.9(1.25)	2.9(1.25)	2.9(1.25)	2.8(1.25)	2.7(1.25)
B	6.6(1.25)	6.6(1.25)	6.6(1.25)	6.2(1.25)	5.9(1.25)
C	14.3(1.25)	14.3(1.25)	14.3(1.25)	13.1(1.25)	12.4(1.25)
D	36.5(1.25)	36.4(1.25)	36.1(1.25)	32.1(1.25)	29.2(1.25)
E	56.1(1.25)	55.7(1.25)	54.5(1.25)	46.5(1.25)	40.5(1.25)
F	88.1(1.25)	86.6(1.25)	82.0(1.25)	66.4(1.25)	53.7(1.25)

[a]Distances are given in parentheses ().

Table 15. Stability category sequences, in order of increasing maximum concentration, for each source, release height, and first receptor location

Source area, m^2	Release height, m		
	0	10	20
		First recptor at 150 m	
0	A B C D E F	F E A D B C	F E D C B A
200	A B C D E F	F E A B C D	F E D C B A
6,500	A B C D E F	A F B C E D	F E D A C B
		First recptor at 300 m	
0	A B C D E F	A B F C D E	F E A D B C
200	A B C D E F	A B F C D E	F E A D B C
6,500	A B C D E F	A B C F D E	F A E B D C
100,000	A B C D E F	A B C D E F	A B F C E D
		First recptor at 1250 m	
0	A B C D E F	A B C D E F	A B C D F E
200	A B C D E F	A B C D E F	A B C D F E
6,500	A B C D E F	A B C D E F	A B C D E F
100,000	A B C D E F	A B C D E F	A B C D E F
5,000,000	A B C D E F	A B C D E F	A B C D E F

Table 16. PSEPs (10^8 person-$\mu g/m^3$) for first receptor at 0.15 km

Stability class	Release height, m				
	0	5	10	15	20
			Stack source		
A	0.76	0.76	0.75	0.72	0.70
B	0.94	0.94	0.93	0.86	0.82
C	1.30	1.29	1.26	1.13	1.04
D	3.53	3.49	3.39	2.95	2.66
E	6.13	6.02	5.78	4.90	4.32
F	10.61	10.24	9.63	8.04	6.94
			200-m^2 source		
A	0.74	0.74	0.74	0.70	0.68
B	0.91	0.91	0.90	0.84	0.79
C	1.25	1.24	1.22	1.10	1.02
D	3.44	3.41	3.33	2.92	2.63
E	6.00	5.91	5.71	4.86	4.29
F	10.42	10.11	9.56	8.00	6.92
			6500-m^2 source		
A	0.69	0.69	0.69	0.66	0.64
B	0.82	0.82	0.82	0.77	0.73
C	1.10	1.10	1.09	1.00	0.93
D	3.17	3.16	3.12	2.76	2.52
E	5.61	5.56	5.45	4.69	4.16
F	9.80	9.63	9.25	7.80	6.77

Table 17. TEPs (10^8 person-$\mu g/m^3$) for first receptor at 0.15 km

Stability class	Release height, m				
	0	5	10	15	20
			Stack source		
A	0.76	0.76	0.75	0.72	0.70
B	0.94	0.94	0.93	0.86	0.82
C	1.30	1.29	1.26	1.13	1.04
D	3.53	3.49	3.39	2.95	2.66
E	6.13	6.02	5.78	4.90	4.32
F	10.61	10.24	9.63	8.04	6.94
			200-m^2 source		
A	0.76	0.76	0.76	0.73	0.70
B	0.95	0.95	0.94	0.88	0.83
C	1.32	1.31	1.28	1.15	1.06
D	3.58	3.53	3.43	2.99	2.68
E	6.19	6.08	5.83	4.94	4.35
F	10.72	10.34	9.71	8.09	6.98
			6500-m^2 source		
A	0.75	0.75	0.75	0.72	0.69
B	0.94	0.94	0.93	0.87	0.83
C	1.30	1.29	1.28	1.16	1.07
D	3.57	3.55	3.47	3.05	2.75
E	6.21	6.13	5.93	5.05	4.44
F	10.76	10.47	9.90	8.24	7.10

Table 18. PSEPs (10^8 person-$\mu g/m^3$) for first receptor at 0.30 km

Stability class	Release height, m				
	0	5	10	15	20
			Stack source		
A	0.71	0.71	0.71	0.68	0.66
B	0.87	0.87	0.87	0.81	0.77
C	1.19	1.19	1.18	1.08	1.00
D	3.36	3.34	3.29	2.91	2.64
E	5.89	5.84	5.70	4.88	4.31
F	10.25	10.06	9.60	8.04	6.94
			200-m^2 source		
A	0.70	0.70	0.70	0.67	0.65
B	0.85	0.85	0.85	0.80	0.76
C	1.16	1.16	1.15	1.05	0.98
D	3.31	3.29	3.25	2.88	2.62
E	5.81	5.77	5.64	4.84	4.29
F	10.13	9.95	9.53	7.99	6.92
			6500-m^2 source		
A	0.67	0.67	0.67	0.64	0.62
B	0.79	0.79	0.79	0.74	0.71
C	1.07	1.07	1.06	0.97	0.91
D	3.11	3.10	3.07	2.74	2.50
E	5.52	5.49	5.40	4.67	4.16
F	9.66	9.54	9.22	7.79	6.77
			100,000-m^2 source		
A	0.62	0.62	0.62	0.60	0.58
B	0.69	0.69	0.69	0.65	0.62
C	0.89	0.89	0.89	0.82	0.77
D	2.72	2.71	2.70	2.42	2.23
E	4.92	4.90	4.86	4.24	3.81
F	8.70	8.63	8.45	7.23	6.35

Table 19. TEPs (10^8 person-$\mu g/m^3$) for first receptor at 0.30 km

Stability class	Release height, m				
	0	5	10	15	20
			Stack source		
A	0.71	0.71	0.71	0.68	0.66
B	0.87	0.87	0.87	0.81	0.77
C	1.19	1.19	1.18	1.08	1.00
D	3.36	3.34	3.29	2.91	2.64
E	5.89	5.84	5.70	4.88	4.31
F	10.25	10.06	9.60	8.04	6.94
			200-m^2 source		
A	0.71	0.71	0.71	0.68	0.66
B	0.88	0.88	0.87	0.82	0.78
C	1.20	1.20	1.19	1.09	1.01
D	3.39	3.37	3.33	2.94	2.67
E	5.94	5.89	5.75	4.92	4.34
F	10.33	10.13	9.67	8.08	6.98
			6500-m^2 source		
A	0.71	0.71	0.71	0.68	0.66
B	0.88	0.88	0.88	0.82	0.79
C	1.21	1.21	1.20	1.10	1.03
D	3.43	3.42	3.37	2.99	2.72
E	6.01	5.97	5.84	5.01	4.43
F	10.45	10.28	9.84	8.23	7.10
			100,000-m^2 source		
A	0.71	0.71	0.71	0.68	0.66
B	0.85	0.85	0.85	0.80	0.76
C	1.16	1.16	1.16	1.07	1.00
D	3.39	3.38	3.35	2.99	2.74
E	5.99	5.96	5.87	5.08	4.52
F	10.45	10.32	9.99	8.44	7.32

Table 20. PSEPs (10^8 person-$\mu g/m^3$) for first receptor at 1.25 km

Stability class	Release height, m				
	0	5	10	15	20
			Stack source		
A	0.65	0.65	0.65	0.62	0.61
B	0.72	0.72	0.72	0.68	0.65
C	0.95	0.95	0.95	0.88	0.83
D	2.93	2.92	2.91	2.62	2.41
E	5.27	5.25	5.21	4.55	4.10
F	9.29	9.23	9.04	7.75	6.80
			200-m^2 source		
A	0.65	0.65	0.65	0.62	0.60
B	0.72	0.72	0.72	0.68	0.65
C	0.95	0.95	0.94	0.87	0.82
D	2.91	2.90	2.89	2.60	2.40
E	5.24	5.22	5.18	4.53	4.08
F	9.24	9.18	9.00	7.72	6.78
			6500-m^2 source		
A	0.64	0.64	0.64	0.61	0.60
B	0.70	0.70	0.70	0.66	0.63
C	0.91	0.91	0.91	0.84	0.79
D	2.82	2.82	2.81	2.53	2.33
E	5.10	5.09	5.05	4.42	3.98
F	9.02	8.97	8.80	7.55	6.65
			100,000-m^2 source		
A	0.61	0.61	0.61	0.59	0.57
B	0.65	0.65	0.65	0.61	0.59
C	0.82	0.82	0.82	0.76	0.72
D	2.58	2.58	2.57	2.31	2.14
E	4.72	4.71	4.68	4.10	3.71
F	8.39	8.34	8.21	7.07	6.26
			5,000,000-m^2 source		
A	0.48	0.48	0.48	0.46	0.45
B	0.48	0.48	0.48	0.45	0.44
C	0.54	0.54	0.54	0.50	0.47
D	1.71	1.71	1.71	1.54	1.43
E	3.27	3.27	3.25	2.86	2.61
F	5.94	5.92	5.86	5.10	4.56

Table 21. TEPs (10^8 person-$\mu g/m^3$) for first receptor at 1.25 km

Stability class	Release height, m				
	0	5	10	15	20
			Stack source		
A	0.65	0.65	0.65	0.62	0.61
B	0.72	0.72	0.72	0.68	0.65
C	0.95	0.95	0.95	0.88	0.83
D	2.93	2.92	2.91	2.62	2.41
E	5.27	5.25	5.21	4.55	4.10
F	9.29	9.23	9.04	7.75	6.80
			200-m^2 source		
A	0.65	0.65	0.65	0.63	0.61
B	0.73	0.73	0.73	0.68	0.65
C	0.96	0.96	0.96	0.88	0.83
D	2.94	2.94	2.93	2.63	2.43
E	5.29	5.28	5.23	4.57	4.12
F	9.33	9.27	9.08	7.78	6.83
			6500-m^2 source		
A	0.66	0.66	0.66	0.63	0.61
B	0.74	0.74	0.74	0.69	0.66
C	0.97	0.97	0.97	0.89	0.84
D	2.99	2.98	2.97	2.67	2.46
E	5.37	5.35	5.31	4.64	4.18
F	9.46	9.40	9.21	7.89	6.93
			100,000-m^2 source		
A	0.68	0.68	0.68	0.65	0.63
B	0.74	0.74	0.74	0.70	0.67
C	0.98	0.98	0.98	0.90	0.85
D	3.04	3.03	3.02	2.72	2.51
E	5.47	5.45	5.41	4.74	4.27
F	9.65	9.59	9.40	8.08	7.11
			5,000,000-m^2 source		
A	0.72	0.72	0.72	0.69	0.67
B	0.74	0.74	0.74	0.70	0.67
C	0.91	0.91	0.91	0.84	0.79
D	2.91	2.91	2.90	2.62	2.42
E	5.38	5.37	5.34	4.69	4.25
F	9.60	9.56	9.43	8.16	7.25

maximum concentration, which might correspond to the maximum individual exposure, always occurred under F stability conditions. (Stability class F always produced the worst case, or the highest, population exposure predictions.) Table 22 gives the stability class under which the maximum concentration occurred for each release height, source area, and first receptor location studied. For most combinations, use of an urban mode option will predict lower maximum concentrations than will use of the rural mode option.

Other Parameters

Other meteorological and climatological parameters used by the ISCLT that may be specified by the modeler include: ambient air temperatures, mixing layer heights, vertical gradient of potential temperature, height above ground at which the wind speed was measured, air entrainment coefficients for unstable and stable atmospheres, and acceleration due to gravity. Default values are supplied for several of the parameters. The default values of the vertical gradient of potential temperature should be used unless site-specific measurements are available for each stability class. These values are used in the calculation of buoyant plume rise. The default values for air entrainment coefficients and the acceleration due to gravity also should be used.

Ambient air temperatures must be supplied for each stability category and each season. These temperatures can be obtained from a variety of sources, including publications by the U.S. Department of Commerce[32] and by Ruffner,[33] and various climatological atlases. Ambient air temperature affects only the calculation of buoyant plume rise. The developers of the ISCLT suggest using the average seasonal daily maximum temperature for stability classes A, B, and C; the average seasonal temperature for stability class D; and the average seasonal daily minimum temperature for stability classes E and F.

Mixing heights also must be supplied by the user for each wind-speed class, stability class, and season. The ISCLTM automatically sets mixing heights for stability classes E and F to 10 km if the rural mode stability class option is chosen. Annual-average and seasonal morning and afternoon mixing heights may be found in Holzworth's publication.[34] This parameter is not very important for low-level releases; small errors in mixing height specification, except possibly under very unstable conditions, likely will have little or no effect on GPC calculations within 50 km of the source.

Specification of the height at which the wind speed measurements used to define the meteorological data were taken is very important. The modeler should confirm this height with the supplier of the data. An inaccurate height may cause an incorrect wind speed to be calculated at the pollutant release height (see following discussion of release height effects). The default height supplied by the ISCLTM is 10 m; it applies to the STAR data supplied with the IEM.

Table 22. Stability categories giving maximum PGPCs and TGRCs for each source, release height, and first receptor location

Source area, m^2	Release height, m				
	0	5	10	15	20
			First receptor at 100 m		
0	F	D	B	A	A
			First recptor at 150 m		
0	F	E	C	B	A
200	F	E	C	B	A
6,500	F	F	D	C	B
			First recptor at 300 m		
0	F	F	E	C,D	C
200	F	F	E	D	C
6,500	F	F	E	D	C
100,000	F	F	F	E	D
			First recptor at 1250 m		
0	F	F	F	F	E
200	F	F	F	F	E
6,500	F	F	F	F	F
100,000	F	F	F	F	F
5,000,000	F	F	F	F	F

SOURCE RELATED PARAMETERS

Source related parameters studied in detail were release height and area. In general, the effects of these parameters on the IEM predictions were influenced by stability class and allowed receptor locations. Enhanced ground level turbulence due to structures near the sources was considered by using the building wake effects option to model a hypothetical tank farm. Some general comments are given regarding parameters affecting plume rise, which affects only emissions from incinerator stacks, not those from the other sources commonly found at HWMFs.

Release Height

The effects of release height on PGPC and TGRC profiles are illustrated, respectively, in Appendixes C (Figs. 23-27) and D (Figs. 28-31). In all cases, predicted concentrations decreased with increasing release height. In general, the decreases were largest nearest the source and diminished as downwind distance increased. Increasing atmospheric stability magnified the decreases at close-in receptors; increasing source area lessened the effects slightly, even after correcting for effects due to first receptor location. Note that concentration profiles for releases at or below 10 m (the height at which the wind speed measurements were made) converged as downwind distance increased. Concentration profiles for releases above 10 m did not converge.

Tables 4-14 illustrate release-height related changes in maximum PGPCs and TGRCs for each stability class, source, and first receptor location. These changes followed the pattern noted above for the overall concentration profiles. Under the conditions of this study, increasing the release height from 0 to 20 m reduced maximum concentration predictions by between ~7% (Table 14, all sources under A stability) and ~99.5% (Table 4, stack source under F stability). The magnitude of the reductions depended strongly on stability class and first receptor location, and to a lesser extent on source area. Note also that increasing release height tended to increase the distance to the maximum concentration.

Exposure predictions also decreased with increasing release height (Tables 4-8 and 16-21). However, the effects of release height changes on exposure predictions were smaller than the effects on maximum concentration predictions. Increasing the release height from 0 to 20 m decreased exposure predictions by between ~6% (Table 21, all sources under A stability) and ~36% (Table 4, stack source under F stability). The decreases depended strongly on stability class, moderately on first receptor location, and weakly on source area. The relative insensitivity of exposure predictions to changes in release height is explained by the tendency of concentration profiles for different release heights to merge at downwind distances of a few kilometers and by the large fraction of the total study area affected by the merged concentrations.

Source Area

The effects of source area on PGPC and TGRC profiles are illustrated, respectively, in Appendixes E (Figs. 32-36) and F (Figs. 37-41). Except at

close-in receptors for the higher release heights under the more stable conditions, increasing source size always lowered the PGPC curves out to ~10 km, where the profiles for the three smaller sources tended to merge. The TGRC curves exhibited the same trend but (1) differences due to increasing release height were smaller; (2) the stack (0-m wide) and 200-m^2 (14.1-m wide) area source profiles were very similar but reversed, the area source curves were slightly higher than the stack curves; and (3) all profiles tended to merge and, in fact, to cross over so that increasing source size always increased concentrations beyond 10 km (not shown in Figs. 37-41). The differences between the PGPC and TGRC profiles are explained by the fact that the TGRC curves account for GPCs in sectors other than the primary one. These GPCs become more important as source size increases and, thus, allows pollutants to be spread over a larger area. As noted in Section 4, TGRCs represent concentrations that would arise under conditions corresponding to the wind blowing equally in all directions with a pollutant release rate of 16 g/s. Therefore, we prefer to use TGRCs when discussing source-size effects. Also, source-size effects should be compared using receptor arrays that have the same starting point.

Tables 10, 12, and 14 show the effects of source size on maximum TGRCs. Increasing area tended to reduce the distance to the maximum TGRC. Except for the stack source, which always predicts maximum TGRCs that are lower than those predicted by the 200-m^2 area source, increasing source area decreased maximum TGRCs for ground-level releases and for releases under A stability conditions. For the other release heights and stabilities, area-size effects depended on the combination of release height, stability class, and first receptor location. Increasing the distance to the first receptor always decreased maximum TGRC values, regardless of the actual source area.

Three sources can have their first receptors at 150 m. For this receptor array, the largest source-size related difference in maximum TGRC values occurred for a 10-m release under E stability conditions; the maximum TGRC predicted by the stack source was ~36% lower than the one predicted by the 6500-m^2 area source (Table 10). The 200-m^2 area always predicted the highest TGRCs for ground-level releases and for releases under stability classes A and B. As stability and release height were increased, the 6500-m^2 source tended to predict the highest TGRCs.

Four sources can have their first receptors at 300 m. For this array, the largest source-size related difference in maximum TGRC values occurred for a 20-m release under E stability conditions; the maximum TGRC predicted by the stack source was ~51% lower than the one predicted by the 100,000-m^2 area source (Table 12). The 200-m^2 area always yielded the highest TGRCs for ground-level and 5-m releases, and for releases under stability classes A through C. Except for 10-m releases under D stability, the 100,000-m^2 source predicted the highest TGRCs for releases at or above 10 m under stabilities D through F.

All five sources can have their first receptors at 1250 m. For this array, the largest source-size related difference in maximum TGRC values occurred for a ground-level release under B stability conditions; the maximum TGRC predicted by the 5,000,000-m^2 area source was ~60% lower than the one predicted by the 6500-m^2 area source (Table 14). The 6500-m^2 area always

yielded the highest TGRCs, except for 20-m releases under stability class F.

Tables 17, 19, and 21 show that source size had little effect on predicted TEPs. Increasing the distance to the first receptor always decreased TEPs, regardless of the actual source area. For each receptor array, TEPs tended to increase with increasing source area, but the increases were small. For the array beginning at 150 m, the maximum increase was ~3% and occurred for 10-m releases under F stability (Table 17). For the remaining arrays, maximum increases occurred for 20-m releases under F stability. The increases were ~5% for the 300-m array (Table 19) and ~7% for the 1250-m array (Table 21). These increases were due largely to the tendency for the larger areas to predict higher concentrations at the more distant receptor locations.

Building Wake Effects

The building wake effects option attempts to simulate the increased atmospheric turbulence caused by air flowing over and around structures adjacent to or near the source. This option is invoked by specifying the height and the crosswind width of a building adjacent to a stack source. Provision is also made to account for squat buildings (see Reference 3).

To study how use of the building wake effects option affects the IEM predictions for low release heights, a tank farm containing four 6.1-m high tanks was modeled as four 6.1-m high stack sources with no plume rise. Each tank was assumed to have an adjacent structure (i.e., a tank) with a crosswind width of 7.1 m. Four structure heights were studied, 0 (no building), 3, 4.5, and 6.0 m. As shown in Figure 5a, PGPC profiles were similar for all building heights under A stability conditions. The same was true under B stability conditions. The already high turbulence associated with these stabilities apparently masked the effects of the building wake. As stability was increased, the 0-m profile (no building) began to show the characteristic close-in dip (see Fig. 13). Profiles for the 3- and 4.5-m high buildings do not exhibit the characteristic close-in dip, while those for the 6-m high building show increasingly lower concentrations relative to the other building heights. These effects were greatest under F stability conditions (Fig. 5b). One explanation for the effects of the 6-m building is that it produces the most turbulence and directs much of the emissions into sectors other than the primary one. This explanation is supported by the TGRC profiles (Fig. 6), which essentially are identical except for the characteristic close-in dip exhibited for the 0-m high adjacent building under F stability conditions (Fig. 6b). Thus, it appears that use of the building wake effects option will maximize concentration predictions at receptors very near the source.

Maximum TGRCs were identical for all building heights under A stability conditions (Table 23). As stability was increased, differences between the maximum TGRCs remained small (<12%), except for the 0-m building under F stability conditions (~39% less than the 3-m building maximum). Note that the maximum TGRCs always occurred on the first allowed (150 m) ring, except for the 0-m structure under F stability conditions, which occurred on the 200-m ring.

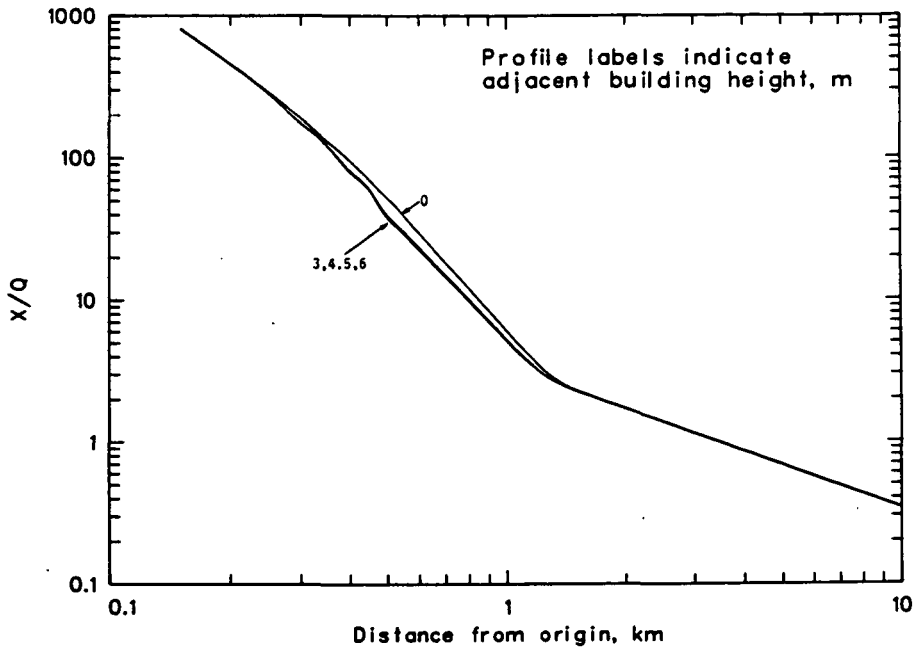

(a) Stability class A

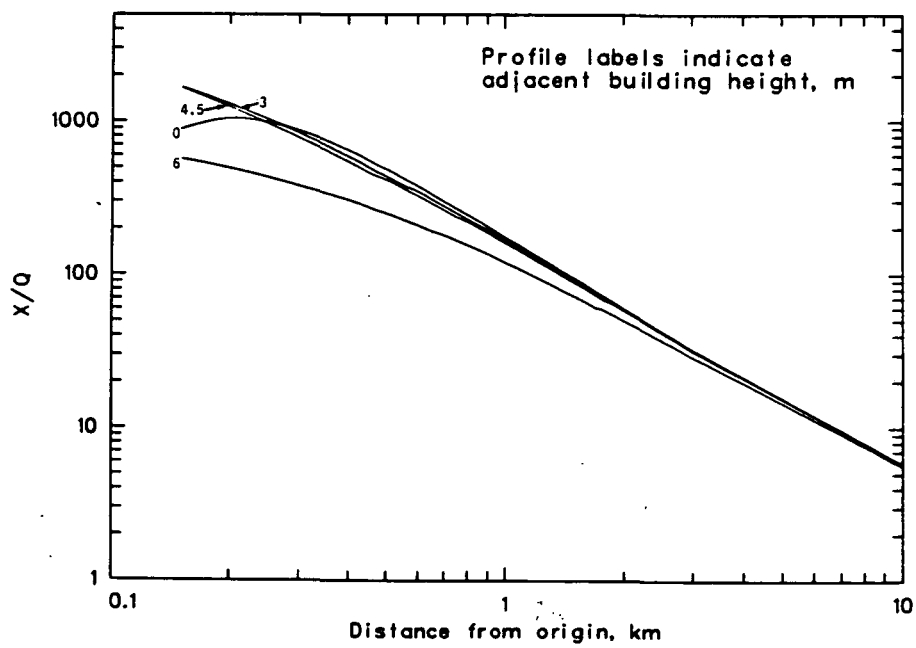

(b) Stability class F

Figure 5. PGPC profiles for releases from a 6.1-m high tank farm represented as four stack sources with adjacent structures.

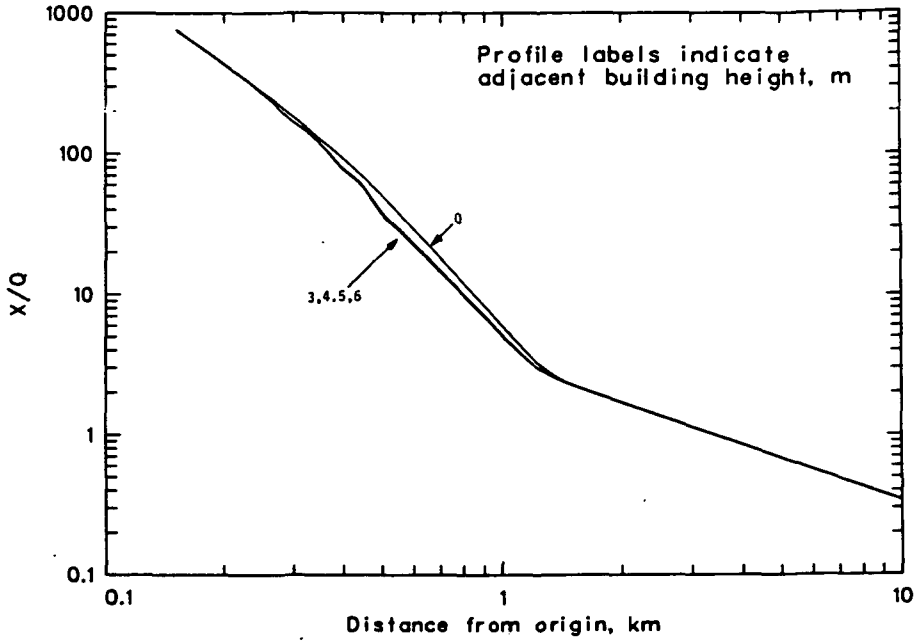

(a) Stability class A

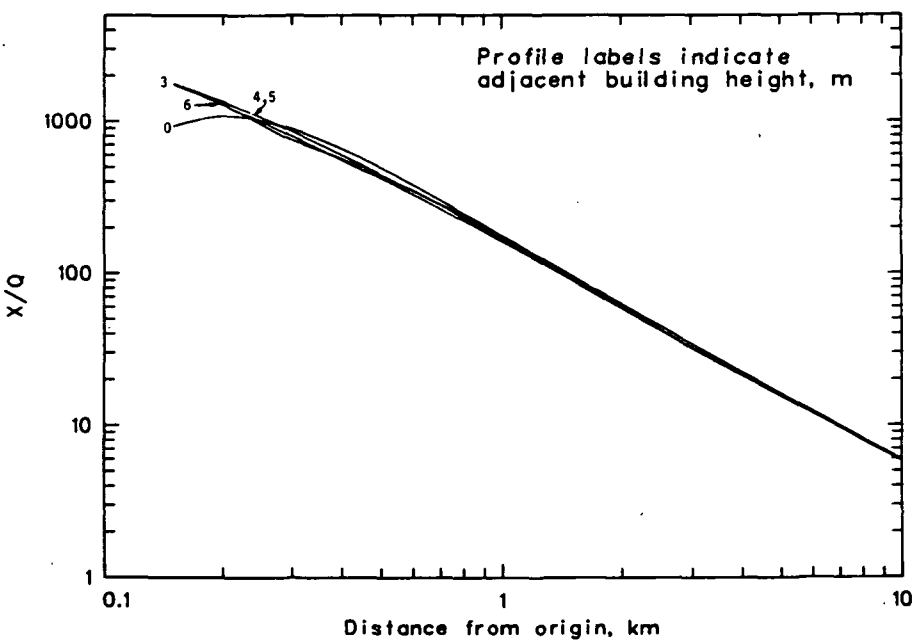

(b) Stability class F

Figure 6. TGRC profiles for releases from a 6.1-m high tank farm represented as four stack sources with adjacent structures.

Table 23. Summary of maximum concentrations and exposures for building wake effects study

Building height, m	Maximum[a] PGPC, X/Q	Maximum[a] TGRC, X/Q	PSEP ($\times 10^{-8}$)	TEP ($\times 10^{-8}$)
		Stability class A		
0.0	762	811	0.77	0.78
3.0	762	811	0.76	0.77
4.5	762	811	0.76	0.77
6.0	762	811	0.76	0.77
		Stability class B		
0.0	1016	1079	0.96	0.96
3.0	1009	1072	0.95	0.96
4.5	998	1060	0.95	0.96
6.0	977	1047	0.95	0.95
		Stability class C		
0.0	1342	1425	1.31	1.32
3.0	1261	1339	1.29	1.30
4.5	1211	1285	1.28	1.29
6.0	930	1356	1.24	1.31
		Stability class D		
0.0	1677	1777	3.49	3.51
3.0	1562	1656	3.47	3.48
4.5	1466	1555	3.44	3.46
6.0	850	1571	3.29	3.52
		Stability class E		
0.0	1600	1691	5.98	6.01
3.0	1670	1769	5.95	5.97
4.5	1583	1678	5.91	5.93
6.0	749	1610	5.61	6.04
		Stability class F		
0.0	1040	1082	10.10	10.13
3.0	1667	1764	10.08	10.11
4.5	1664	1763	10.01	10.04
6.0	569	1755	9.39	10.26

[a]All maximums occur at 150 m, except those for the 0-m release under F stability, which occur at 200 m.

TEP predictions were not affected significantly by building wake effects for low sources because most of the effects occurred close to the source. Variations on the order of 2% or less were found for changes in adjacent building height under the same stability conditions.

From the above observations, one could conclude that use of the building wake effects option makes little difference in IEM predictions for low-level releases. It would be desirable to confirm the findings of this limited analysis by investigating the effects of other building geometries and release heights.

Plume Rise

The importance of plume rise is that it increases the release height, with all the attendant ramifications thereof. In the ISCLTM, plume rise may be momentum- or buoyancy-driven, or both. Parameters affecting plume rise include the stack exit gas velocity and temperature, the stack diameter, the ambient air temperature, the mixing layer height, the acceleration due to gravity, and the wind speed. As noted above, increasing wind speed may decrease plume rise. Of the source parameters in this group, exit gas velocity and temperature have the greatest effects. Stack diameter is relatively unimportant. Ambient air temperature can be important, but, for low sources, the mixing layer height is unlikely to be important. The acceleration due to gravity is a constant. Since others have studied the sensitivity of the ISCLT predictions to variations in the parameters affecting plume rise,[28-30] the above brief description is all that we attempted in this regard.

POLLUTANT RELATED PARAMETERS

Pollutant parameters considered were the decay coefficient and the deposition related parameters, particle size and reflection coefficient. Only brief consideration was given to deposition since its use is not recommended for small particles.

Decay Coefficient

The decay coefficient is defined by $\lambda = \ln(2)/t_{1/2}$, where $t_{1/2}$ is the pollutant half-life. This coefficient enters the concentration calculations through a multiplicative decay term defined by:

$$\text{Decay term} = \exp[-\lambda x/u(h)],$$

where x is the downwind distance (m) and u(h) is the mean wind speed (m/s) at release height h (m). Typical degradation (decay) half-lives for reactive pollutants that might be released from HWMFs range from 0.41 day (for Resorcinol) to 27 days (for CO).[35] Nonreactive pollutants, including trace metals, have essentially infinite half-lives.

Figure 7 illustrates the effect of the decay term for pollutants with half-lives of one hour and one day as functions of wind speed and downwind

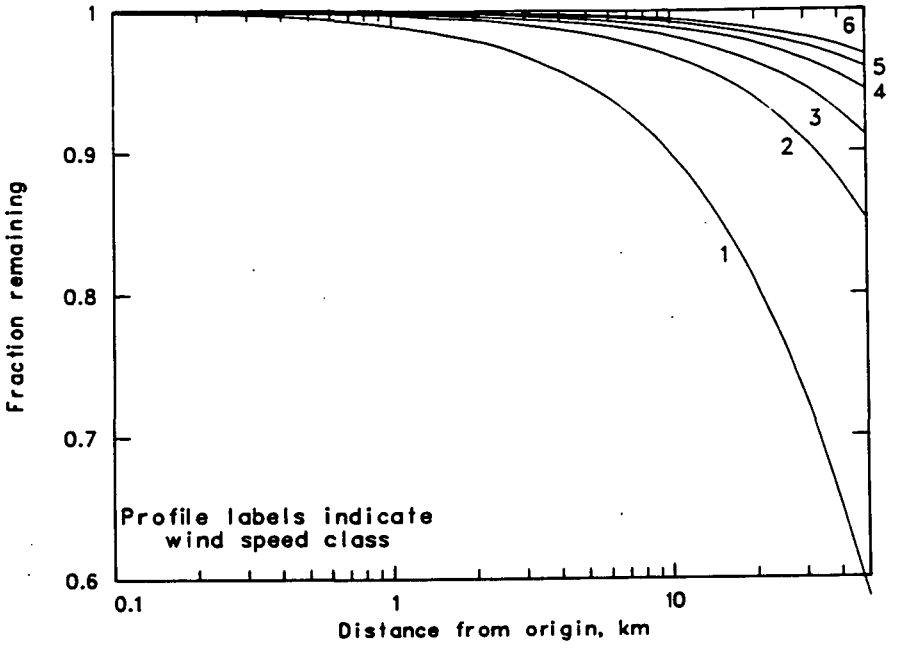

(b) $t_{1/2}$ = 1 day

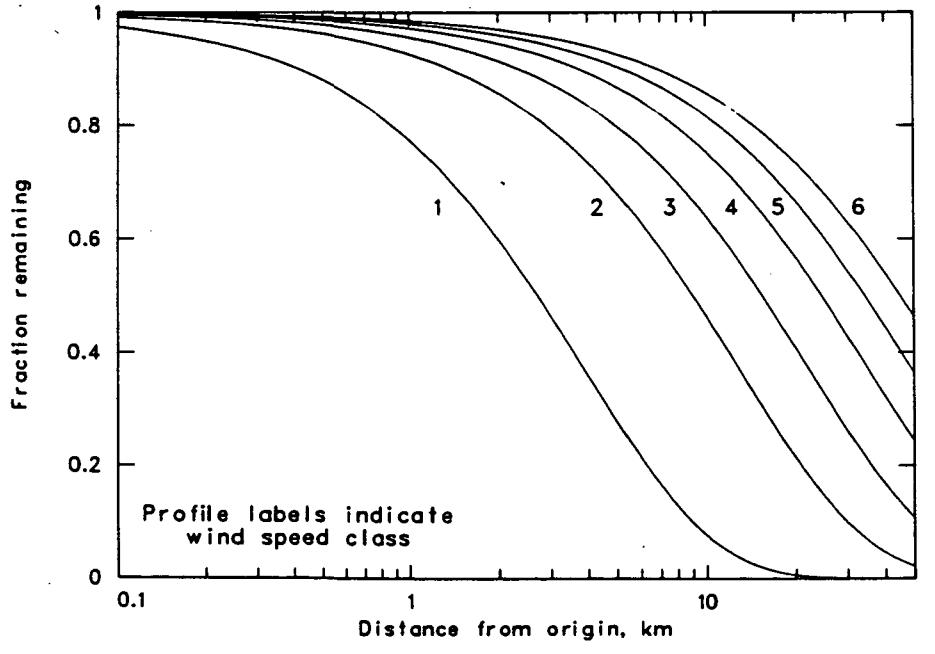

(a) $t_{1/2}$ = 1 hour

Figure 7. Illustration of decay term behavior.

distance. For pollutants having half-lives greater than a few days, decay should have negligible effect on IEM predictions. For half-lives less than one day, under real meteorological conditions, the decay term could reduce exposures appreciably because concentrations at the farther downwind distances will be substantially reduced. Effects on maximum concentrations, which usually occur within 1 km, will not be greatly affected, unless very short half-lives are involved. For example, less than 10% of a pollutant with a one-hour half-life will decay by the time it travels 1 km downwind under all but the lowest wind-speed class, for which about 30% would decay.

Deposition Parameters

The ISCLTM contains an algorithm to account for deposition of airborne particles onto the ground surface. To use this option, the modeler must specify the number of particle-size categories to be considered (i.e., enter a positive integer for NVS on card 17 of the input data file). Subsequent input cards must specify, for each particle-size category, a settling velocity (m/s), the fraction of the total particulate mass in that category, and a surface reflection coefficient. Guidance is given in the ISCLT user's guide for calculating settling velocities and determining reflection coefficients.[3] Use of this option to model particles with diameters smaller than ~20 μm should be undertaken cautiously.[3,22]

To indicate the effects of using the ISCLTM deposition option, we considered releases of 5-μm-diameter, stable (nondecaying) particles from a 20-m high stack source. Particles of this size are respirable and could be formed during HWMF operations or after emission of smaller-sized particulate or gaseous pollutants that attach to ambient air particles. These particles were assigned a settling velocity of 0.0072 m/s and a reflection coefficient of 0.8. The releases were studied under the following combinations of wind speed and stability: wind-speed class 1 (0.75 m/s), stability classes B, D, and F; wind-speed class 3 (4.3 m/s), stability classes B and D; and wind-speed class 6 (12.5 m/s), stability class D. The results of this study are summarized in Figure 8 and Table 24.

Figure 8 illustrates PGPC and TGRC profiles obtained with and without deposition. (Recall that PGPC and TGRC concentrations, and PSEPs and TEPs are identical for stack sources of small diameter.) For the lowest wind speed (Figs. 8a-c), accounting for deposition produced close-in concentrations that equaled or exceeded those obtained when not accounting for deposition. At some downwind distance, the profiles crossed and concentrations predicted without considering deposition exceeded those obtained with deposition. Increasing stability magnified the differences between the concentrations and lengthened the distance to the crossover point. Under the least stable conditions (A and B), concentrations with and without deposition were equal at the first few receptors; at subsequent receptors, concentrations with no deposition exceeded those with deposition. Increasing wind speed (Figs. 8a, 8d, and 8e), in addition to lowering all concentrations, moved the crossover point to the first receptor location, thus causing concentrations without deposition to exceed those with deposition at all downwind receptor locations. Thus, increasing wind speed reduced concentrations obtained when accounting for deposition more than it did when deposition was ignored. This means that wind speed is not a linear scaling factor when deposition is considered.

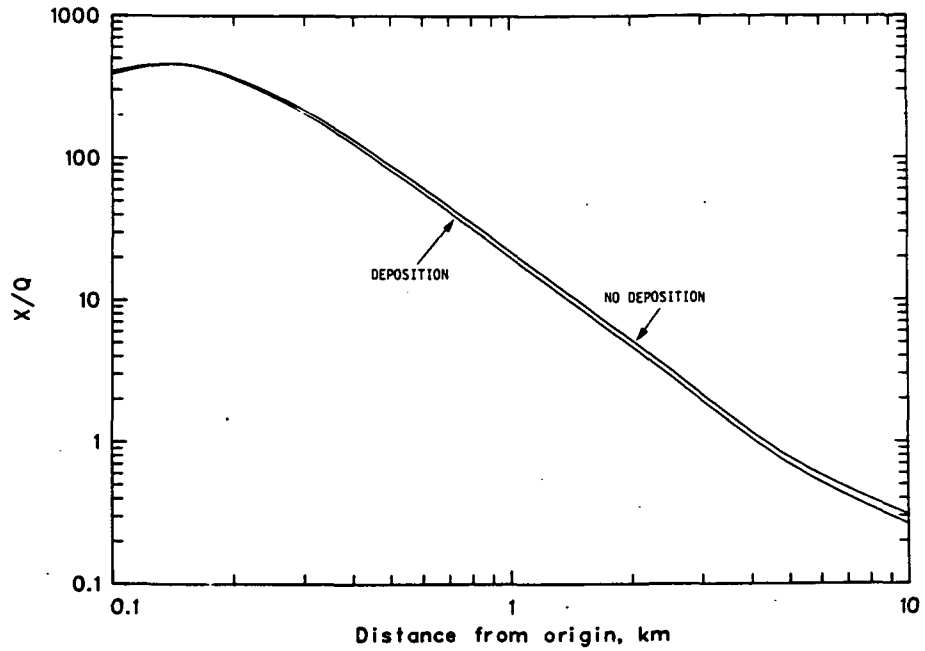

(a) Stability class B, wind-speed class 1

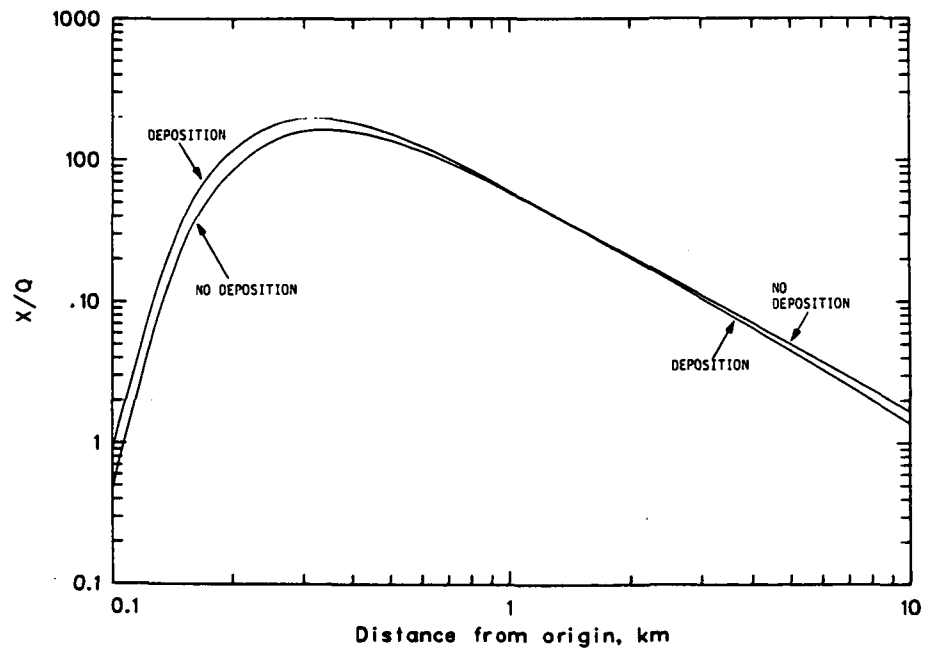

(b) Stability class D, wind-speed class 1

Figure 8. Effects of deposition on concentration predictions for releases from a 20-m high stack source.

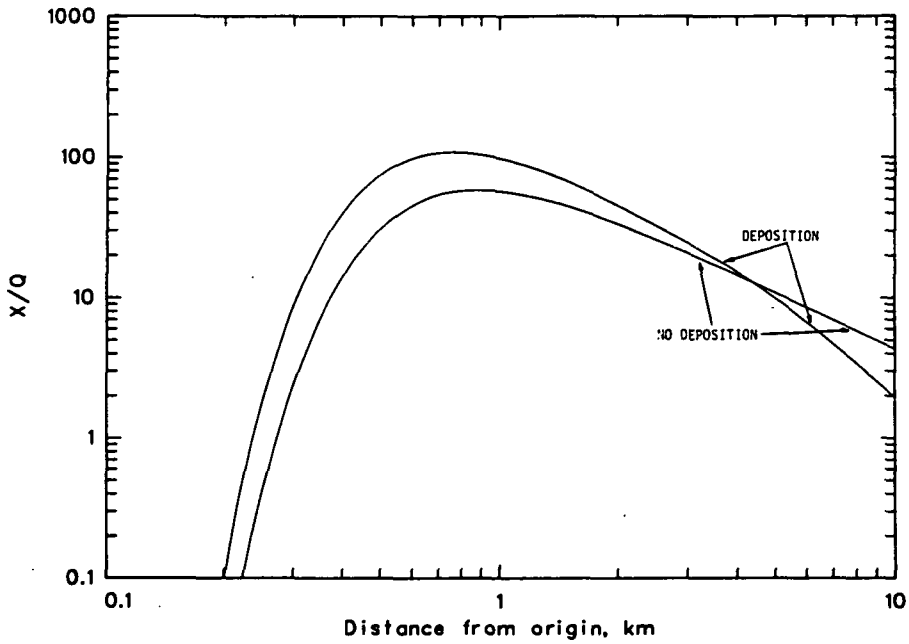

(c) Stability class F, wind-speed class 1

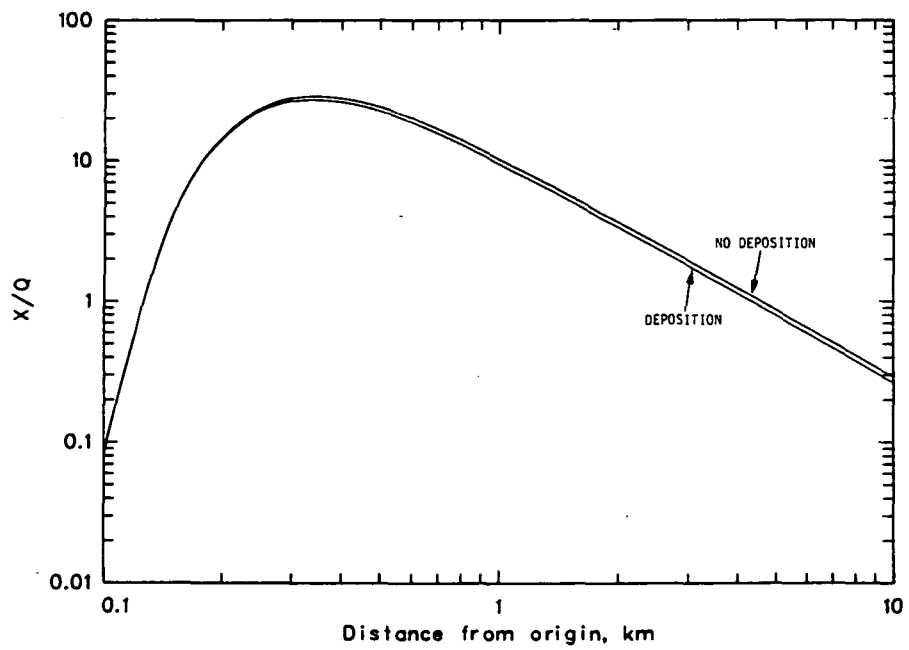

(d) Stability class D, wind-speed class 3

Figure 8. Continued.

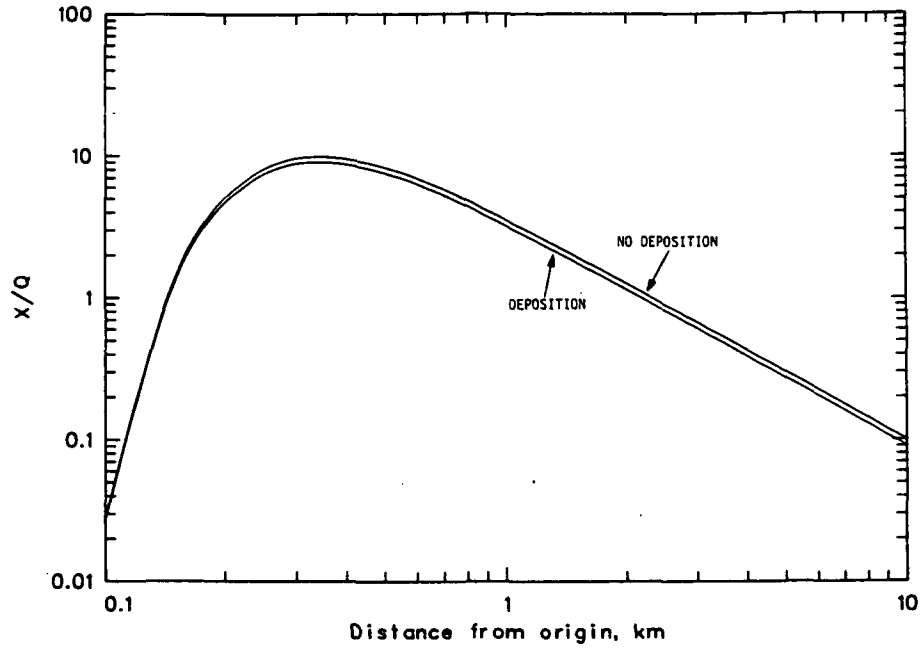

(e) Stability class D, wind-speed class 6

Figure 8. Continued.

Table 24 summarizes the behavior of maximum concentration and exposure potential predictions with and without deposition. Accounting for deposition tended to shorten the distance to the location of the maximum. Also, for the lowest wind speed and the stabilities considered, accounting for deposition gave maximum concentrations that were 0-87% higher than those obtained without accounting for deposition. At higher wind speeds, accounting for deposition produced maximum concentrations that were 5-8% lower. Estimates of exposure potential were always lower when deposition was considered, by 9-70% for the conditions considered. Differences in the exposure predictions tended to increase with increasing stability. This effect is explained largely by differences between the concentration profiles at the farther downwind distances.

Based on the above limited observations, one could conclude that the deposition option should be used if well-characterized particles are emitted from the sources. Ignoring deposition likely will maximize predicted concentrations and exposures under real meteorological conditions. However, at sites characterized by substantial time periods of calm winds and stable conditions, failure to account for deposition could lead to substantial underestimates of maximum concentrations and, therefore, of maximum individual exposures and to substantial overestimates of population exposures.

RECEPTOR LOCATION

As noted in Section 4, careful receptor location will ensure that the predictive capabilities of any atmospheric model are fully reflected in its output. Predictions obtained using four alternate receptor arrays were compared with predictions obtained using our base receptor array. The following arrays were compared:

* Base array, receptors at 0.1, 0.15, 0.2, 0.25, 0.3, 0.35, 0.4, 0.45, 0.5, 0.55, 0.6, 0.65, 0.7, 0.75, 0.8, 0.85, 0.9, 0.95 ,1.0, 1.05, 1.1, 1.15, 1.2, 1.25, 1.3, 1.35, 1.4, 1.45, 1.5, 1.55, 1.6, 1.65, 1.7, 1.75, 1.8, 1.85, 1.9, 1.95, 2.0, 5.0, 10.0, 20.0, 30.0, and 50.0 km;
* Array 1, receptors at 0.1, 0.3, 0.5, 0.7, 1.0, 1.5, 2.0, 5.0, 10.0, 20.0, 30.0, 40.0, and 50.0 km;
* Array 2, receptors at 0.1, 0.5, 1.0, 5.0, 10.0, and 50.0 km;
* Array 3, receptors at 0.1, 1.0, 10.0, and 50.0 km; and
* Array 4, receptors at 0.1 and 50.0 km.

Table 25 summarizes the comparison results for a 0-m (ground-level) and a 20-m high release from a stack source, without plume rise, under D stability conditions and a wind speed of 0.75 m/s. For a ground level release, all receptor arrays gave the same maximum concentration, because it occurs at the first allowed receptor location, which was the same in all the arrays. As the receptor arrays become more open, predicted exposure potentials diverged downward from the base case. However, even the most open array (4), which contains only the first and last receptors of the base case, predicted an exposure potential that was only ~28% lower than the one predicted by the base case.

Table 24. Summary of maximum concentrations and exposures for the deposition effects study

Stability class	Wind speed, m/s	Deposition	No deposition	% difference, Dep./No dep.
		Maximum PGPCs and TGRCs, X/Q(location in km)		
B	0.75	455 (0.15)	455 (0.15)	~0
B	4.3	73 (0.15)	79 (0.15)	-8
D	0.75	196 (0.30)	164 (0.35)	20
D	4.3	27 (0.35)	29 (0.35)	-5
D	12.5	9 (0.35)	10 (0.35)	-8
F	0.75	107 (0.75)	57 (0.90)	87
		PSEPs and TEPs ($\times 10^{-8}$)		
B	0.75	0.65	0.83	-22
B	4.3	0.11	0.14	-22
D	0.75	2.03	2.66	-24
D	4.3	0.42	0.46	-9
D	12.5	0.14	0.16	-10
F	0.75	2.11	6.94	-70

Table 25. Effects of several receptor array choices on maximum concentration and total exposure predictions

Receptor array[a]	Maximum PGPCs and TGRCs		PEPs and TEPs	
	Value, X/Q	% difference from base	Value, $x10^8$	% difference from base
		Ground-level release		
Base	5814[b]	-	3.63	-----
1	5814[b]	0	3.60	-0.6
2	5814[b]	0	3.42	-5.6
3	5814[b]	0	3.24	-10.5
4	5814[b]	0	2.61	-28.2
		20-m release		
Base	163.6[c]	-----	2.66	-----
1	159.8[d]	-2.3	2.64	-0.6
2	136.8[e]	-16.4	2.48	-6.8
3	58.4[f]	-64.3	2.29	-13.8
4	0.5[g]	-99.7	0.78	-70.6

[a]See text for receptor array descriptions.

[b]Occurs at 0.1 km.

[c]Occurs at 0.35 km.

[d]Predicted at 0.3 km instead of at 0.35 km.

[e]Predicted at 0.5 km instead of at 0.35 km.

[f]Predicted at 1.0 km instead of at 0.35 km.

[g]Predicted at 0.1 km instead of at 0.35 km.

For a 20-m release, maximum concentration predictions dropped rapidly as receptor separation increased. Arrays 3 and 4 yielded predictions of maximum concentration and, therefore, of maximum individual exposure that are unacceptably lower than the base case predictions. Array 2 produced marginally acceptable values. Except for Array 4, which gave an unacceptably low (-71% or a factor of 3.3) prediction, exposure potential predictions behaved like those for the ground-level release.

Based on this study, alternate receptor Array 1 would be a reasonable choice for modeling releases from HWMF sources. Since this array contains only 13 receptors and the IEM allows specification of up to 20 receptors, additional receptors could be included. For example, Tables 4-14 could be used to locate the receptors giving the maximum concentrations for the particular sources being considered. These receptors could be added, as necessary to Array 1. (Note that, for some sources, it might be necessary to move the location of the first receptor beyond 0.1 km.) Also, for the higher release heights, for stack sources with plume rise, or for sources that cover a large area, it might be appropriate to include more receptors between the first one and the one at 2 km.

SECTION 6

DISCUSSION OF SOURCE REPRESENTATION OPTIONS

Many of the sources commonly found at HWMFs can be modeled using one of the source-representation options available in the ISCLTM. The source area discussion in Section 5 illustrates the effects of representing a source by a stack (essentially a point) and by one or more different-sized area sources. These representation options normally are not considered when modeling an actual source. Rather, one tries to match the area of the model source with the area of the actual source. In this section, we discuss differences in concentration and exposure potential predictions due to modeling two typical HWMF components, a process building and a small tank farm, using source representations that, except for the stack representations, keep the source area constant. The results summarized in this section merely show differences in predictions due to use of the various source representations; they do not address the question of which representation gives the most accurate results. This question can be answered only by comparing the various predictions with measurements made under similar conditions.

The process building was assumed to be 10-m high, to cover 200 m^2, and to release pollutants either from a rooftop or a midheight vent. The building was modeled as one stack source, as one 14.1-m square area source, as two 10-m square area sources, and as two volume sources having standard deviations of 2.33 for their crosswind source distributions and 4.65 for their vertical source distributions (see Ref. 3 for an explanation of these terms). Figures 9 and 10 illustrate the TGRC profiles obtained for the source representations used to model the 5- and 10-m releases, respectively. Only profiles for A and F stability conditions are given because they bound the effects due to stability. Maximum TGRCs and TEPs are given in Table 26 for each source representation and stability class.

The tank farm was assumed to contain four 6.1-m high tanks, to cover 200 m^2, and to release pollutants from vents located on top of the tanks. The tanks were modeled as four stack sources, as four stack sources with adjacent 6.0-m high structures, as one 14.1-m square area source, as four 7.07-m square area sources, as one volume source having standard deviations of 3.29 for its crosswind source distribution and 2.84 for its vertical source distribution, and as four volume sources having standard deviations of 1.64 for their crosswind source distributions and 2.84 for their vertical source distributions. Midheight (3.05-m) releases were considered only for the single area and and volume source representations. Figures 11 and 12 illustrate the TGRC profiles obtained for the source representations used to

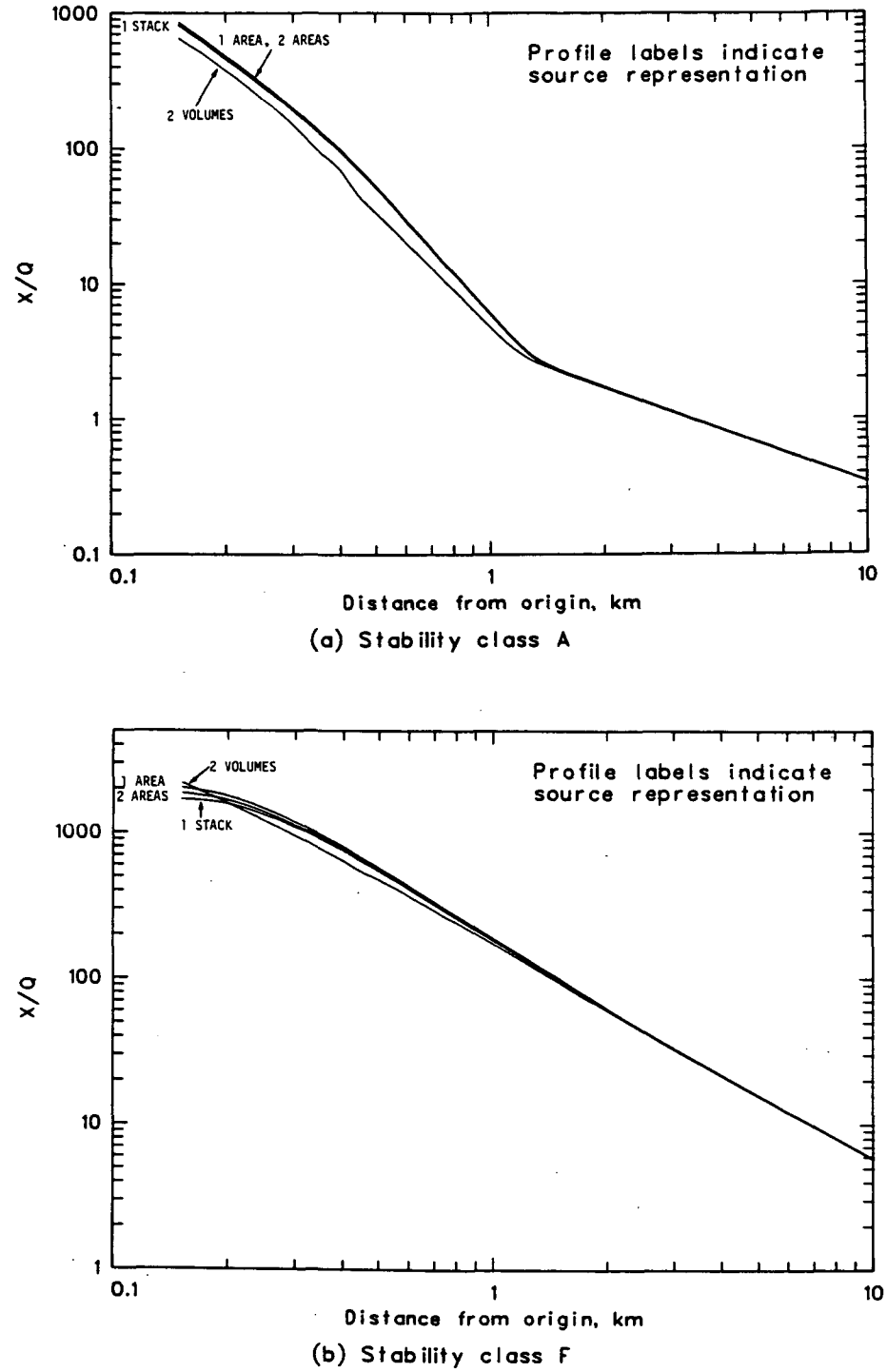

Figure 9. TGRC profiles for releases from a 5-m high process building.

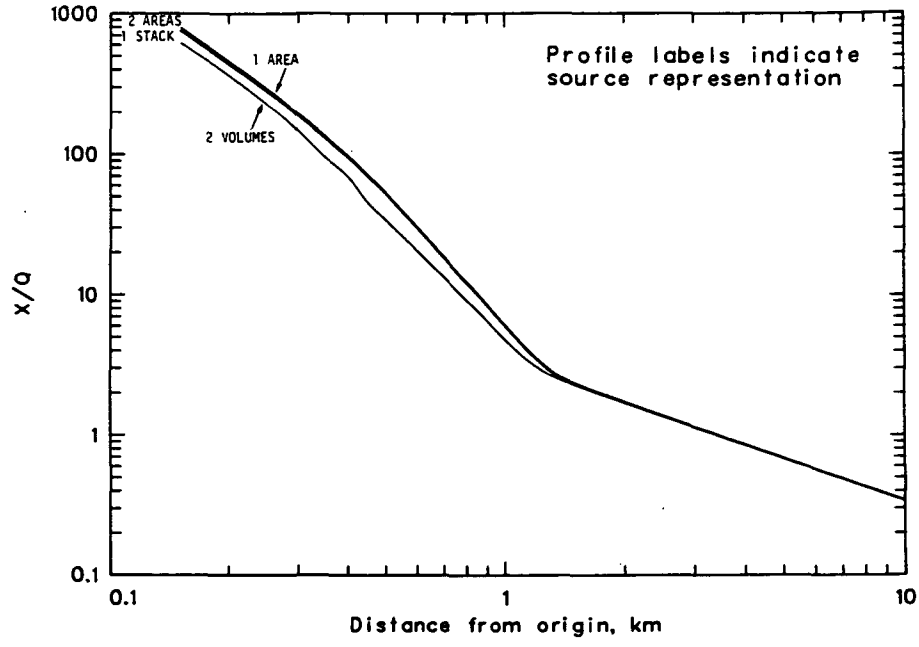

(a) Stability class A

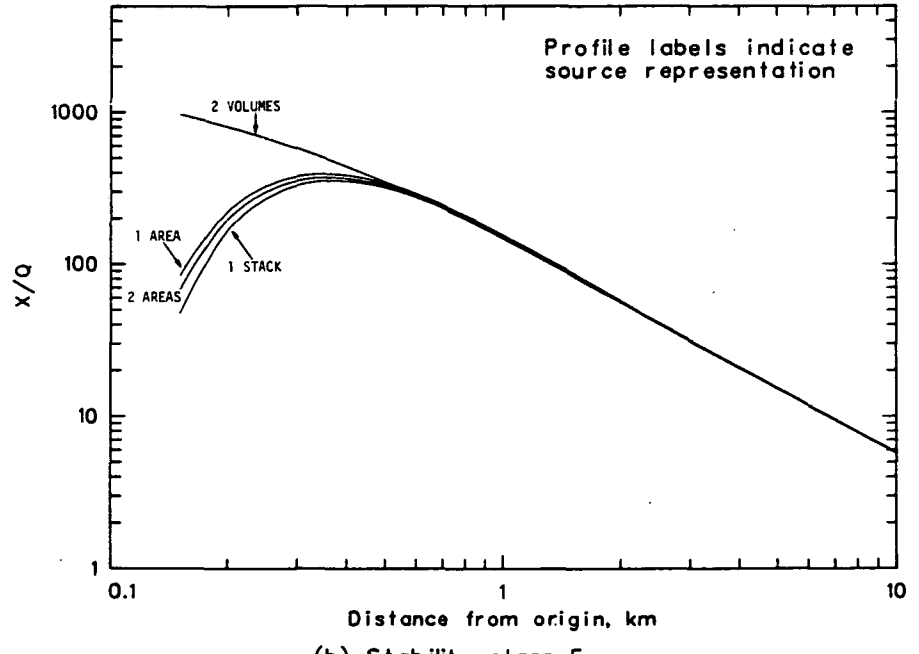

(b) Stability class F

Figure 10. TGRC profiles for releases from a 10-m high process building.

Table 26. Summary of maximum concentrations and exposures for the process building simulation calculations

Stability class	Source representation			
	1 stack	1 area	2 areas	2 volumes
	TGRCs, X/Q (5-m release)			
A	820	858	822	653
B	1105	1172	1119	900
C	1501	1603	1527	1182
D	2047	2235	2113	1632
E	2185	2449	2295	1918
F	1688	2032	1861	2195
	TEPs $x10^{-8}$ (5-m release)			
A	0.76	0.76	0.76	0.73
B	0.94	0.95	0.94	0.91
C	1.29	1.31	1.29	1.25
D	3.49	3.53	3.51	3.43
E	6.02	6.08	6.04	5.95
F	10.24	10.34	10.29	10.19
	TGRCs, X/Q (10-m release)			
A	755	799	763	620
B	945	1021	968	813
C	1087	1205	1134	989
D	869	1045	957	1139
E	600	706	653	1123
F	352	392	371	972
	TEPs $x10^{-8}$ (10-m release)			
A	0.75	0.76	0.76	0.73
B	0.93	0.94	0.94	0.91
C	1.26	1.28	1.27	1.23
D	3.39	3.43	3.41	3.37
E	5.78	5.83	5.80	5.79
F	9.63	9.71	9.67	9.76

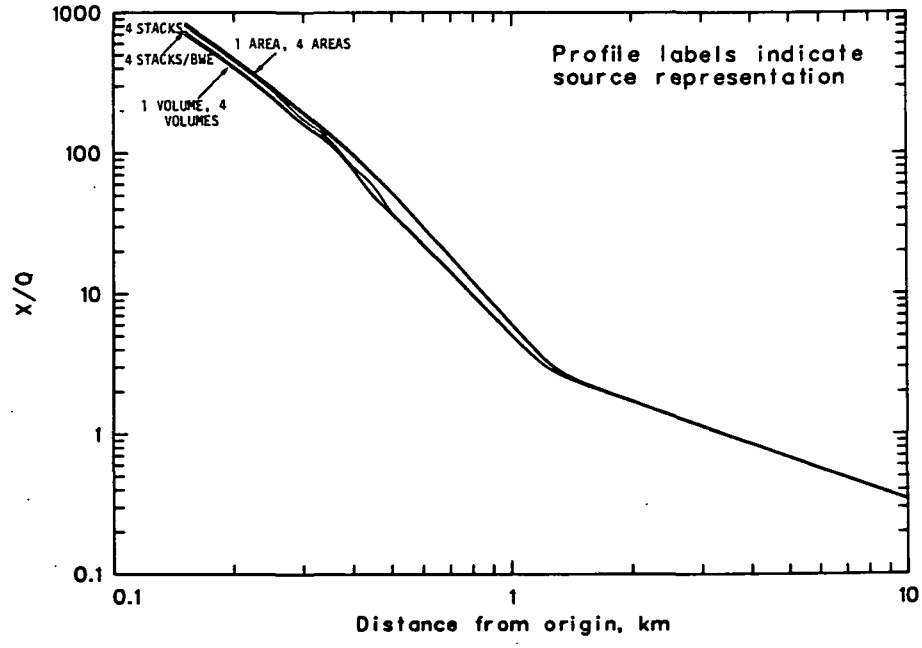

(a) Stability class A

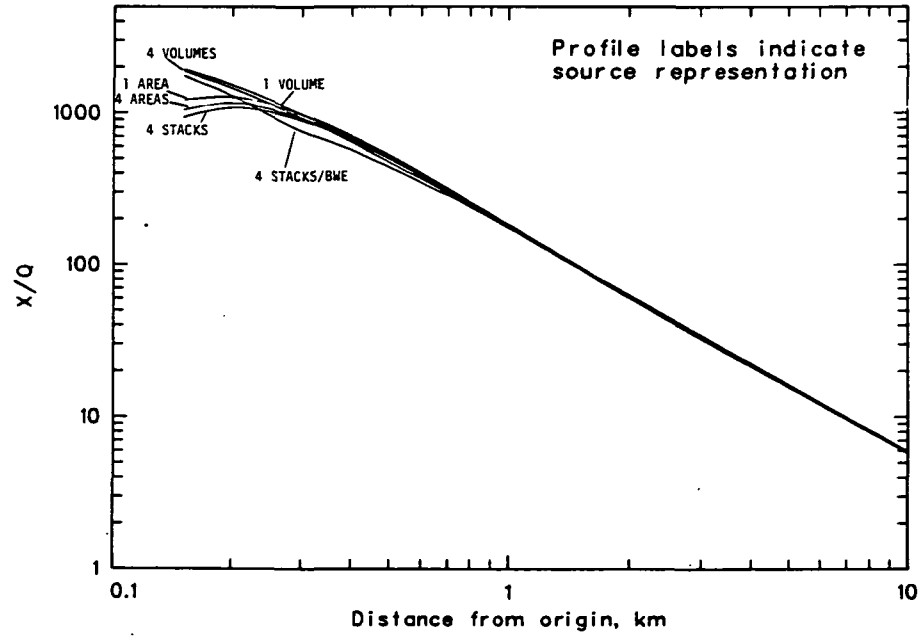

(b) Stability class F

Figure 11. TGRC profiles for releases from a 6.1-m high tank farm.

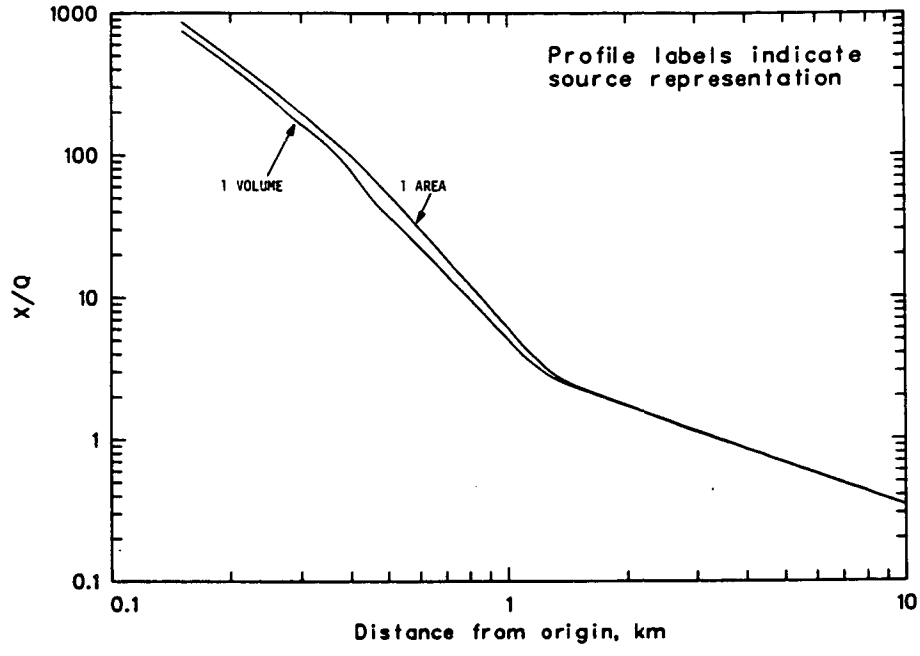

(a) Stability class A

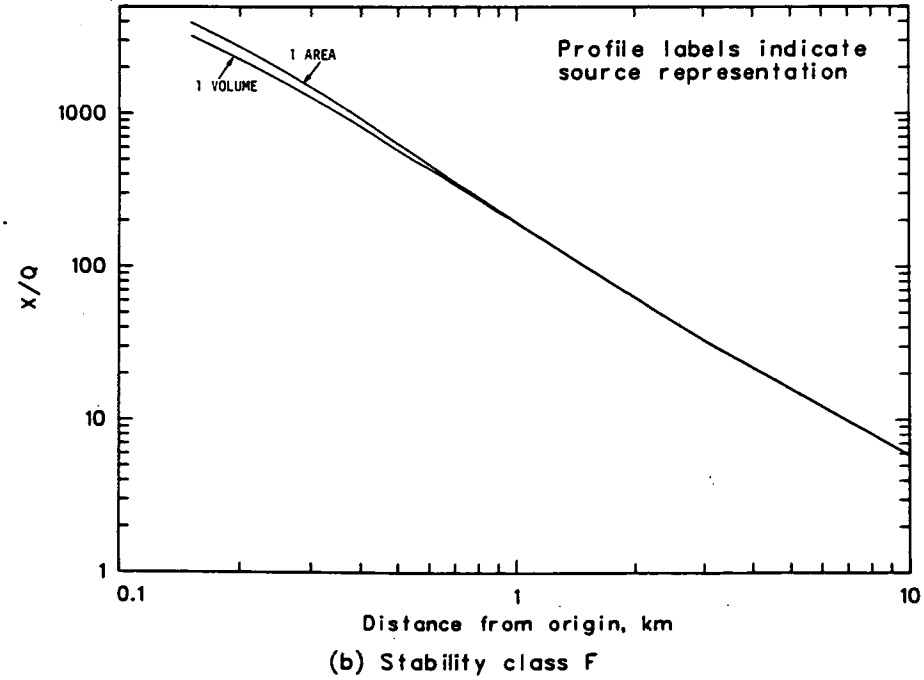

(b) Stability class F

Figure 12. TGRC profiles for releases from a 3.05-m high tank farm.

model the 6.1- and 3.05-m releases, respectively. Again, only profiles for A and F stability conditions are given. Maximum TGRCs and TEPs are given in Table 27 for each source representation and stability class.

Differences between predictions made using the various source representations were small and generally occurred within 1 km of the origin. As illustrated in Table 28, differences between maximum TGRC predictions rarely exceeded a factor of two. (A factor of two difference corresponds to percentage differences of -50% and +100% in Tables 28 and 29. As noted in Section 1, the expected accuracy of Gaussian-plume model predictions under favorable conditions is a factor of two.) As shown in Table 29, differences between TEP predictions never exceeded 5%.

STACKS VS. STACKS WITH BUILDING WAKE EFFECTS

In agreement with the discussion of building wake effects in Section 5, stack sources with and without building wake effects gave the same maximum concentration under A stability. For stabilities B through E, stacks without wake effects gave slightly (3-13%) higher maximum concentrations. Considering wake effects produced higher (38%) maximum concentrations under F stability, because use of this option did not produce the characteristic close-in dip in the TGRC profile. Using the building wake effects option produced slightly (0.8-1.3%) lower TEP predictions under stabilities A through C and slightly (0.3-1.3%) higher predictions for the remaining stabilities. These differences are not significant.

STACKS VS. AREAS

All stack and area source representations of a given source produced similar TGRC profiles. The curves essentially are superimposed, except near the first receptor, where the effects of increasing stability and release height caused the curves to deviate slightly. In this region, the area source profiles tended to be slightly higher than the the stack source profiles, except for stacks affected by building wakes under F stability conditions. Maximum TGRC predictions confirmed this trend. Maximums due to stack representations were always lower (0.2-20%) than those due to corresponding area source representations, except for stacks with building wake effects under F stability, whose maximums were 39-53% higher than those predicted using area source representations. Total exposure potential predictions for stack vs. area source representations differed by between -1.6 and 2.6%. Again, the TEP predictions are not significantly different.

STACKS VS. VOLUMES

Stack source representations produced higher close-in concentrations than did corresponding volume source representations for the lower stability classes. As stability and release height increased, this situation reversed, and volume sources tended to predict higher concentrations. This effect is especially noticeable for 10-m releases under F stability (Fig. 10b). Volume sources even outpredicted point sources with building wake effects under F stability (Fig. 12b). Maximum TGRC predictions confirmed the above observations. Under the less stable conditions, stack sources produced higher (2-27%) concentrations. Under the more stable conditions, stack source

Table 27. Summary of maximum concentrations and exposures for the tank-farm simulation calculations

Stability class	Source representation					
	Stacks		Areas		Volumes	
	4	4w/BW	1	4	1	4
	TGRCs, X/Q (6.1-m release)					
A	811	811	848	818	738	699
B	1079	1047	1147	1097	1030	961
C	1425	1356	1531	1457	1371	1257
D	1777	1571	1976	1848	1824	1678
E	1691	1610	1957	1794	1998	1868
F	1082	1755	1261	1151	1936	1887
	TEPs $x10^{-8}$ (6.1-m release)					
A	0.78	0.77	0.76	0.76	0.74	0.74
B	0.96	0.95	0.95	0.94	0.93	0.92
C	1.32	1.31	1.30	1.29	1.28	1.26
D	3.51	3.52	3.51	3.48	3.48	3.45
E	6.01	6.04	6.03	5.99	6.01	5.95
F	10.13	10.26	10.21	10.15	10.25	10.17
	TGRCs, X/Q (3.05-m release)					
A			871		755	
B			1207		1077	
C			1703		1492	
D			2624		2201	
E			3273		2699	
F			3975		3251	
	TEPs $x10^{-8}$ (3.05-m release)					
A			0.76		0.74	
B			0.95		0.93	
C			1.31		1.28	
D			3.56		3.52	
E			6.15		6.09	
F			10.61		10.51	

Table 28. Percent differences in predicted maximum TGRC values between the first and second source representations of the indicated pairs

Source pair, release height	Stability class					
	A	B	C	D	E	F
Stacks vs. Stacks w/BW						
4 stacks:4 stacks w/BW, 6.1 m	0.0	3.1	5.1	13.1	5.0	-38.3
Stacks vs. areas						
4 stacks:1 area, 6.1 m	-4.4	-5.9	-6.9	-10.1	-13.6	-14.2
4 stacks:4 areas, 6.1 m	-0.9	-1.6	-2.2	-3.8	-5.7	-6.0
1 stack:1 area, 5 m	-4.4	-5.7	-6.4	-8.4	-10.8	-16.9
1 stack:1 area, 10 m	-5.5	-7.4	-9.8	-16.8	-15.0	-10.2
1 stack:2 areas, 5 m	-0.2	-1.3	-1.7	-3.1	-4.8	-9.3
1 stack:2 areas, 10 m	-1.1	-2.4	-4.1	-9.2	-8.1	-5.1
4 stacks w/BW:1 area, 6.1 m	-4.4	-8.7	-11.4	-20.5	-17.7	39.2
4 stacks w/BW:4 areas, 6.1 m	-0.9	-4.6	-6.9	-15.0	-10.3	52.5
Stacks vs. volumes						
4 stacks:1 volume, 6.1 m	9.9	4.8	3.9	-2.6	-15.4	-44.1
4 stacks:4 volumes, 6.1 m	16.0	12.3	13.4	5.9	-9.5	-42.7
1 stack:2 volumes, 5 m	25.6	22.8	27.0	25.4	13.9	-23.1
1 stack:2 volumes, 10 m	21.8	16.2	9.9	-23.7	-46.6	-63.8
4 stacks w/BW:1 volume, 6.1 m	9.9	1.7	-1.1	-13.9	-19.4	-9.3
4 stacks w/BW:4 volumes, 6.1 m	16.0	8.9	7.9	-6.4	-13.8	-7.0
Area vs. areas						
1 area:4 areas, 6.1 m	3.7	4.6	5.1	6.9	9.1	9.6
1 area:2 areas, 5 m	4.4	4.7	5.0	5.8	6.7	9.2
1 area:2 areas, 10 m	4.7	5.5	6.3	9.2	8.1	5.7
Areas vs. volumes						
1 area:1 volume, 3.05 m	15.4	12.1	14.1	19.2	21.3	22.3
1 area:1 volume, 6.1 m	14.9	11.4	11.7	8.3	-2.1	-34.9
1 area:4 volumes, 6.1 m	21.3	19.4	21.8	17.8	4.8	-33.2
1 area:2 volumes, 5 m	31.4	30.2	35.6	37.0	27.7	-7.4
1 area:2 volumes, 10 m	28.9	25.6	21.8	-8.3	-37.1	-59.7
2 areas:2 volumes, 5 m	25.9	24.3	29.2	29.5	19.7	-15.2
2 areas:2 volumes, 10 m	23.1	19.1	14.7	-16.0	-41.9	-61.8
Volume vs. volumes						
1 volume:4 volumes, 6.1 m	5.6	7.2	9.1	8.7	7.0	2.6

Table 29. Percent differences in predicted TEP values between the first and second source representations of the indicated pairs

Source pair, release height	Stability class					
	A	B	C	D	E	F
Stacks vs. Stacks w/BW						
4 stacks:4 stacks w/BW, 6.1 m	1.3	1.1	0.8	-0.3	-0.5	-1.3
Stacks vs. areas						
4 stacks:1 area, 6.1 m	2.6	1.1	1.5	0.0	-0.3	-0.8
4 stacks:4 areas, 6.1 m	2.6	2.1	2.3	0.9	0.3	-0.2
1 stack:1 area, 5 m	0.0	-1.1	-1.5	-1.1	-1.0	-1.0
1 stack:1 area, 10 m	-1.3	-1.1	-1.6	-1.2	-0.9	-0.8
1 stack:2 areas, 5 m	0.0	0.0	0.0	-0.6	-0.3	-0.5
1 stack:2 areas, 10 m	-1.3	-1.1	-0.8	-0.6	-0.3	-0.4
4 stacks w/BW:1 area, 6.1 m	1.3	0.0	0.8	0.3	0.2	0.5
4 stacks w/BW:4 areas, 6.1 m	1.3	1.1	1.6	1.1	0.8	1.1
Stacks vs. volumes						
4 stacks:1 volume, 6.1 m	5.4	3.2	3.1	0.9	0.0	-1.2
4 stacks:4 volumes, 6.1 m	5.4	4.3	4.8	1.7	1.0	-0.4
1 stack:2 volumes, 5 m	4.1	3.3	3.2	1.8	1.2	0.5
1 stack:2 volumes, 10 m	2.7	2.2	2.4	0.6	-0.2	-1.3
4 stacks w/BW:1 volume, 6.1 m	4.1	2.2	2.3	1.1	0.5	0.1
4 stacks w/BW:4 volumes, 6.1 m	4.1	3.3	4.0	2.0	1.5	0.9
Area vs. areas						
1 area:4 areas, 6.1 m	0.0	1.1	0.8	0.9	0.7	0.6
1 area:2 areas, 5 m	0.0	1.1	1.6	0.6	0.7	0.5
1 area:2 areas, 10 m	0.0	0.0	0.8	0.6	0.5	0.4
Areas vs. volumes						
1 area:1 volume, 3.05 m	2.7	2.2	2.3	1.1	1.0	1.0
1 area:1 volume, 6.1 m	2.7	2.2	1.6	0.9	0.3	-0.4
1 area:4 volumes, 6.1 m	2.7	3.3	3.2	1.7	1.3	0.4
1 area:2 volumes, 5 m	4.1	4.4	4.8	2.9	2.2	1.5
1 area:2 volumes, 10 m	4.1	3.3	4.1	1.8	0.7	-0.5
2 areas:2 volumes, 5 m	4.1	3.3	3.2	2.3	1.5	-1.0
2 areas:2 volumes, 10 m	4.1	3.3	3.3	1.2	0.2	-0.8
Volume vs. volumes						
1 volume:4 volumes, 6.1 m	0.0	1.1	1.6	0.9	1.0	0.8

predictions were between 1 and 64% lower than the corresponding volume source predictions. Note that the 1 stack vs. 2 volumes comparison in Table 28 shows that the stack predicted higher maximum concentrations under all stability classes except F. Total exposure predictions made using stack source representations generally were higher (≤5%) than those made using volume source representations. Under the more stable conditions, a few stack source representations yielded slightly lower (≤1.5%) TEPs.

AREA VS. AREAS

Using one area source to represent an emission area always produced slightly higher concentrations and exposures than did using more than one area source. Maximum TGRC predictions were between 4 and 10% higher, and TEP predictions ranged from equal to 1.6% higher.

AREAS VS. VOLUMES

Differences between predictions made using area and volume source representations were similar to the differences between stack and volume source representations. Under the less stable conditions, area sources produced higher (≤37%) maximum TGRCs. Under the more stable conditions, some area source predictions were between 2 and 62% lower than the corresponding volume source predictions. Total exposure predictions made using area source representations generally were higher (≤5%) than those made using volume source representations. Under the more stable conditions, a few area source representations yielded slightly lower (≤1%) TEPs.

VOLUME VS. VOLUMES

Using one volume source to represent an emission source always produced slightly higher concentrations and exposures than did using more than one volume source. Maximum TGRC predictions were between 2 and 9% higher, and TEP predictions ranged from equal to 1.6% higher. These relationships are similar to those found in the one area vs. multiple areas comparison.

REFERENCES

1. O'Donnell, F. R., P. M. Mason, J. E. Pierce, G. A. Holton, and E. Dixon, User's Guide for the Automated Inhalation Exposure Methodology (IEM), EPA-600/2-83-029 (1983).

2. O'Donnell, F. R., and A. C. Cooper, User's Guide for the Automated Inhalation Exposure Methodology (IEM), Addendum 1, (In Press).

3. Bowers, J. F., J. R. Bjorklund, and C. S. Cheney, Industrial Source Complex (ISC) Dispersion Model User's Guide, Volumes I and II, EPA-450/4-79-030 and EPA-450/4-79-031 (1979).

4. H. E. Cramer Company, Inc., "Program Library Update Packages 1-13 to the Industrial Source Complex (ISC) Dispersion Model User's Guide," H. E. Cramer Company, Inc., Salt Lake City, Utah (April 11, 1980 through August 15, 1983).

5. Miller, C. W., and C. A. Little, A Review of Uncertainty Estimates Associated with Models for Assessing the Impact of Breeder Reactor Radioactivity Releases, ORNL-5832 (1982).

6. Pasquill, F., Atmospheric Diffusion, 2nd Edition, John Wiley and Sons, New York (1974).

7. Weber, A. H., Atmospheric Dispersion Parameters in Gaussian Plume Modeling Part I. Review of Current Systems and Possible Future Developments, EPA-600/4-76-030a (1976).

8. Gogolak, C. V., Data Set for Noble Gas Plume Exposure Model Validation, HASL-296 (1975).

9. Gogolak, C. V., H. L. Beck, and M. M. Pendergast, Calculated and observed ^{85}Kr concentrations within 10 km of the Savannah River Plant chemical separation facilities, Atmos. Environ. 15:497-507(1981).

10. Ruff, R.E., H. S. Javitz, and J. S. Irwin, Development and Application of a Statistical Methodology to Evaluate the Realtime Air Quality Model (RAM), pp. 663-669 in Conference on Applications of Air Pollution Meteorology, American Meteorological Society, Boston (1980).

11. Buckner, M. R., ed., Proceedings of the First SRL Model Validation Workshop, (held November 19-21, 1980 at Hilton Head, South Carolina), DP-1597 (1981).

12. Draxler, R. R., An Improved Gaussian Model for Long-Term Average Air Concentration Estimates, Atmos. Environ. 14:597-601(1980).

13. Fields, D. E., C. W. Miller, and S. J. Cotter, The AIRDOS-EPA Computer Code and Its Application to Intermediate Range Transport of ^{85}Kr from the Savannah River Plant, pp. 49-60 in Proceedings, Symposium on Intermediate Range Atmospheric Transport Processes and Technology Assessment, CONF-801064 (1981).

14. Huang, J. C., Evaluation of a Modified Gaussian Plume Model for Travel Distances 25-150 km, in Conference Papers, Second Joint Conference on Applications of Air Pollution Meteorology, American Meteorological Society, Boston (1980).

15. Pendergast, M. M., Model Evaluation for Travel Distances 30-40 km, in Proceedings, Fourth Symposium on Turbulence, Diffusion, and Air Pollution, American Meteorological Society, Boston (1979).

16. Telegadas, K., G. J. Ferber, J. L. Heffter, and R. R. Draxler, Calculated and Observed Seasonal and Annual Krypton-85 Concentrations at 30-150 km from a Point Source, Atmos. Environ. 12:1769-1775(1978)

17. U.S. Environmental Protection Agency, Regional Workshop on Air Quality Modeling: A Summary Report, EPA-450/4-82-015 (1981, rev. 1982).

18. Heron, T. M., J. F. Kelly, and P. G. Haataja, "Validation of the Industrial Source Complex Dispersion Model in a Rural Setting," J. Air Poll. Control Assoc. 31(4):365-369 (1984).

19. Miller, C. W., and R. E. Moore, Verification of a Methodology for Computing Ground-Level Air Concentration of SO_2 and Suspended Particulates for Both Point and Dispersed Sources, pp. 321-326 in Preprint Volume, Joint Conference on Applications of Air Pollution Meteorology, American Meteorological Society, Boston (1977).

20. Smith, D. B., and R. B. Ruch, Jr., Comparative Performance in Complex Terrain of Several Air Quality Impact Assessment Models Based on Aerometric Program Data, pp. 225-228 in Preprints, Fourth Symposium on Turbulence, Diffusion, and Air Pollution, American Meteorological Society, Boston (1979).

21. Wilson, A. D., H. E. Cramer, J. F. Bowers, Jr., and H. V. Geary, Jr., Detailed Diffusion Modeling As a Method of Interpreting and Supplementing Air Quality Data, pp. 315-320 in Preprint Volume, Joint Conference on Applications of Air Pollution Meteorology, American Meteorological Society, Boston (1977).

22. Bowers, J. F., and A. J. Anderson, An Evaluation Study for the Industrial Source Complex (ISC) Dispersion Model, EPA-450/4-81-002 (1981).

23. Anderson, G. E., C. S. Lin, J. Y. Holman, and J. P. Killus, Human Exposure to Atmospheric Concentrations of Selected Chemicals, Volumes I and II, EPA-2/250-1 and EPA-2/250-2 (1980).

24. The MITRE Corporation, Air Emission Control Practices at Hazardous Waste Management Facilities, Working Paper WP-83-W00048, Produced under Contact Number 68-01-6092 with the Office of Solid Waste, U.S. Environmental Protection Agency, Washington, D.C. (1983).

25. B. L. Blaney, U.S. Environmental Protection Agency, Cincinnati, Ohio, Personal Communication, 1984.

26. Eldridge, K., and G. Gschwandtner, Applicationf of CDM, ISC-LT, and TCM-2 to Point and Area Sources, Pacific Environmental Services, Inc., Final Report on Task Assignment No. 29, EPA Contract No. 68-02-3511 with the U.S. Environmental Protection Agency, Research Triangle Park, North Carolina (1983).

27. O'Donnell, F. R., and G. A. Holton, "Automated Methodology for Assessing Inhalation Exposure to Hazardous Waste Incinerator Emissions," pp. 225-234 in Incineration and Treatment of Hazardous Waste: Proceedings of the Ninth Annual Research Symposium at Ft. Mitchell, Kentucky, May 2-4, 1983, EPA-600/9-84-015, (July 1984).

28. Holton, G. A., C. A. Little, F. R. O'Donnell, E. L. Etnier, and C. C. Travis, Initial Atmospheric Dispersion Modeling in Support of the Multiple-Site Incineration Study, ORNL/TM-8181 (1982).

29. Gunthorpe, P., and C. Maxwell, Inhalation Exposure Methodology (IEM) Modeling of Hazardous Waste Incinerators, Midwest Research Institute, Final Report under EPA Contract No. 68-01-6322 with the U.S. Environmental Protection Agency, Washington, D.C. (1983).

30. Bowman, J. T., and J. W. Crowder, "A Comparison of the Short-Term and Long-Term Dispersion Algorithms for the Industrial Source Complex Model," presented at the 76th Annual Meeting of the Air Pollution Control Association, Atlanta, Georgia, June 19-24, 1983.

31. D. E. Layland, U.S. Environmental Protection Agency, Research Triangle Park, North Carolina, Personal Communication, August 30, 1984.

32. U.S. Department of Commerce, Comparative Climatic Data for the United States Through 1981, National Oceanic and Atmospheric Administration, National Climatic Center, Asheville, North Carolina (August 1982).

33. Ruffner, J. A., Climates of the States, Volumes 1 and 2, Gayle Research Company, Detroit, Michigan (1978).

34. Holzworth, G. C., Mixing Heights, Wind Speeds, and Potential for Urban Air Pollution Throughout the Contiguous United States, Office of Air Programs Publication No. AP-101, U.S. Environmental Protection Agency, Research Triangle Park, North Carolina (January 1972).

35. Oak Ridge National Laboratory, Health and Environmental Effects Document on Coal Liquefication - 1982, Volume2. Appendices, ORNL/TM-8624/V2 (September 1983).

APPENDIX A

PGPC (X/Q) PROFILES BY STABILITY CATEGORY FOR SEVERAL RELEASE HEIGHTS AND EACH SOURCE

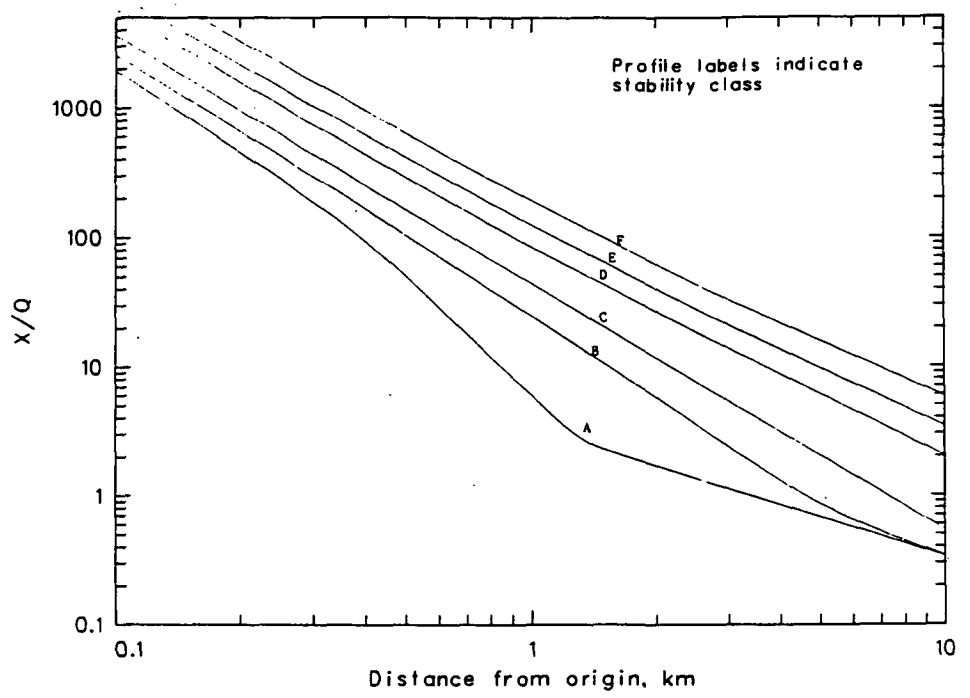

(a) Release height = 0 m

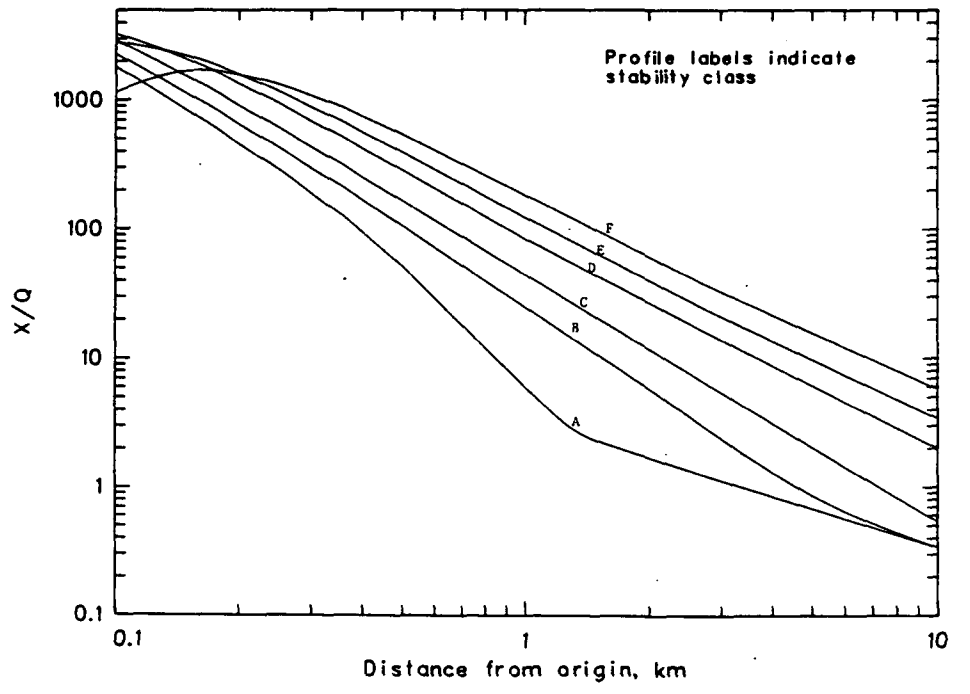

(b) Release height = 5 m

Figure 13. PGPC (X/Q) profiles by stability category for several release heights from the stack source.

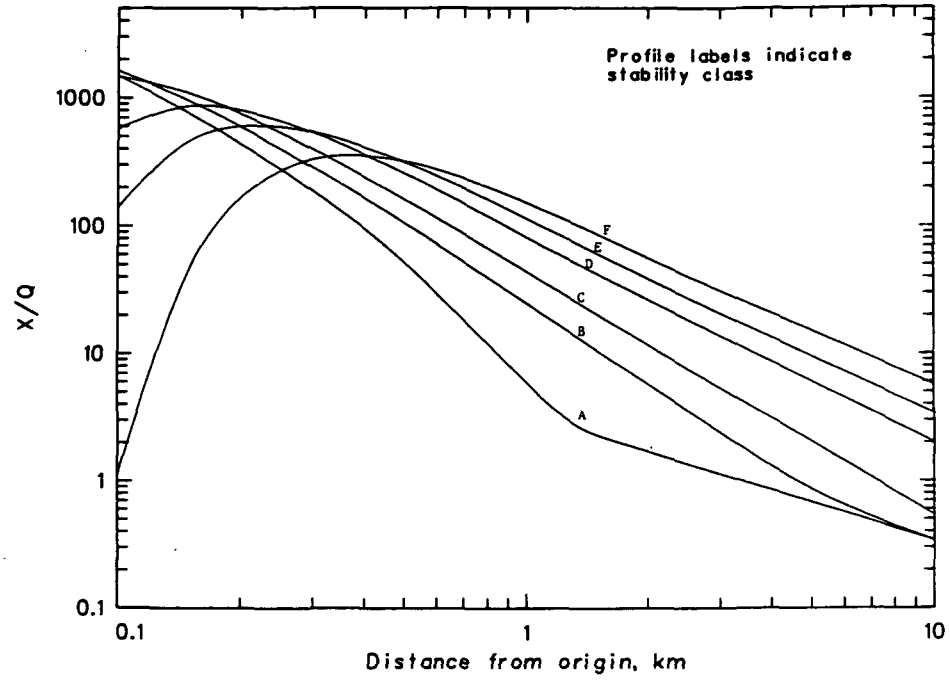

(c) Release height = 10 m

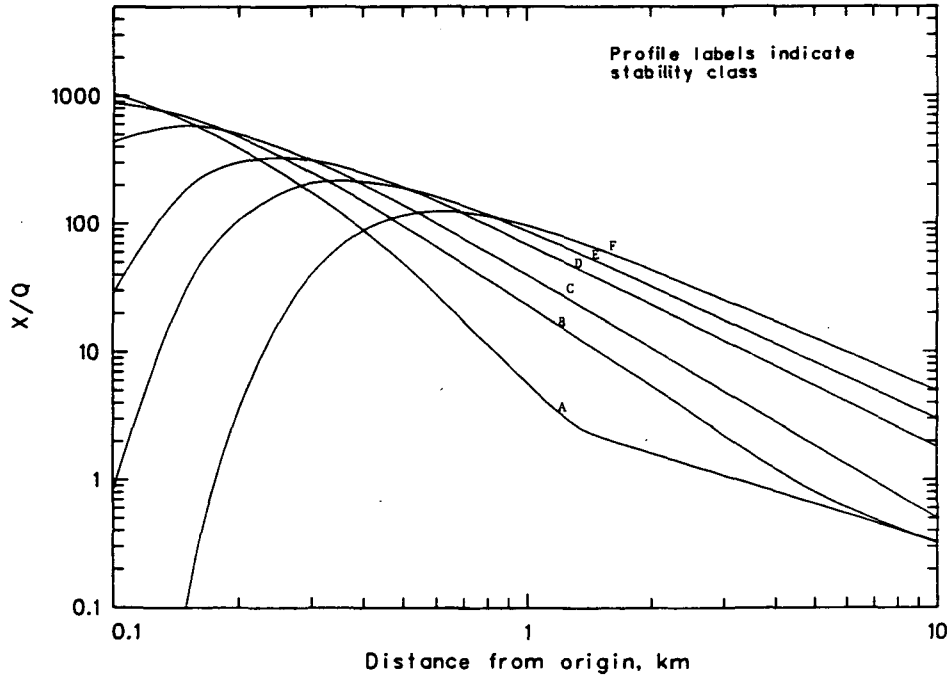

(d) Release height = 15 m

Figure 13. Continued.

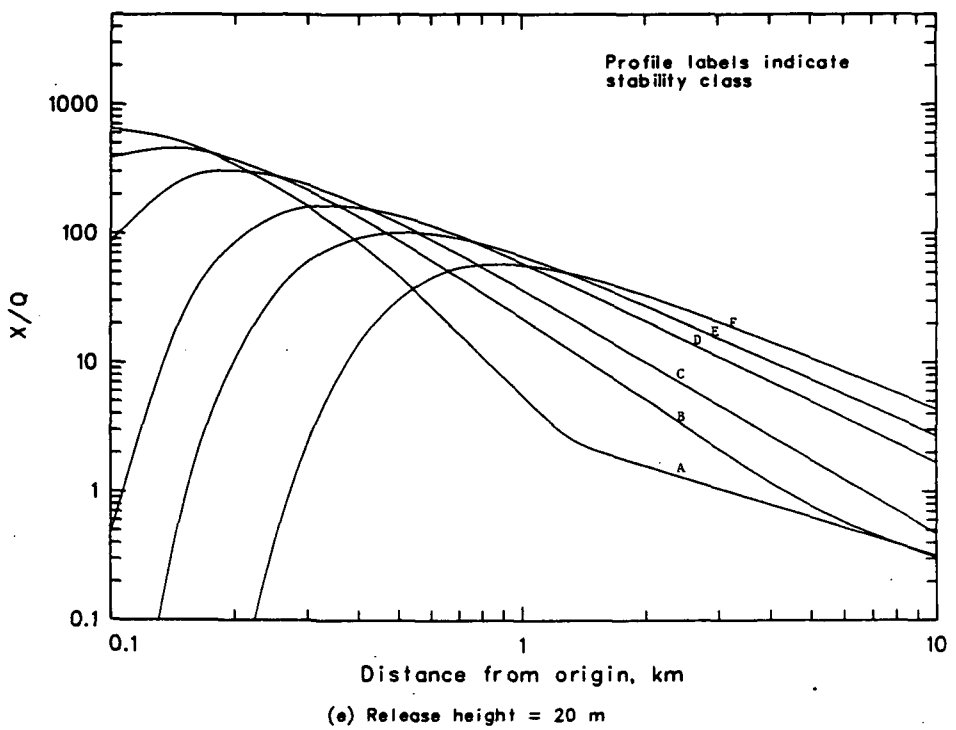

(e) Release height = 20 m

Figure 13. Continued.

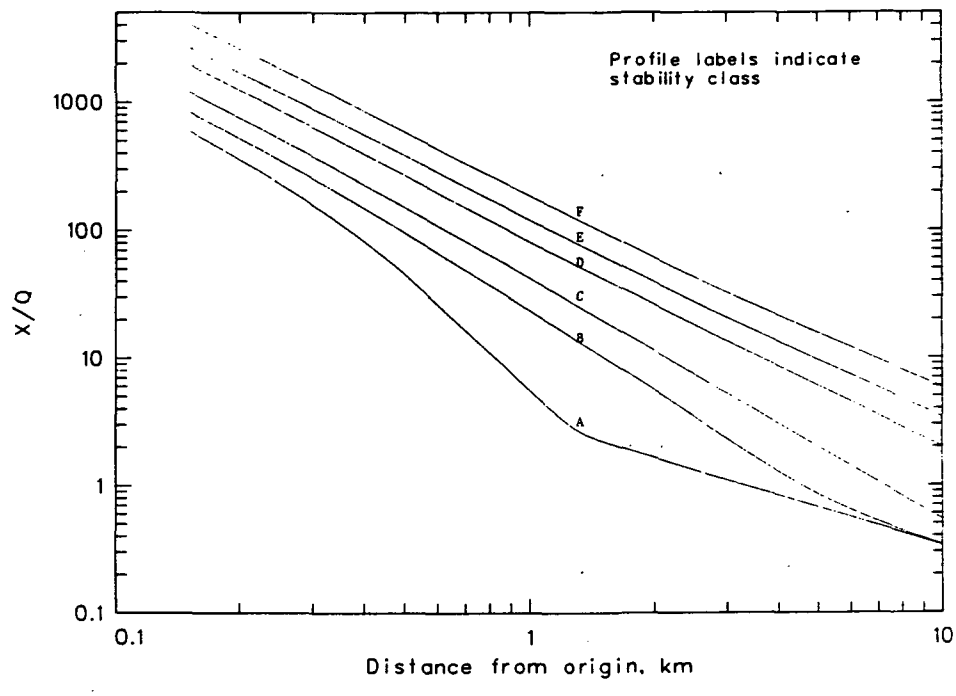

(a) Release height = 0 m

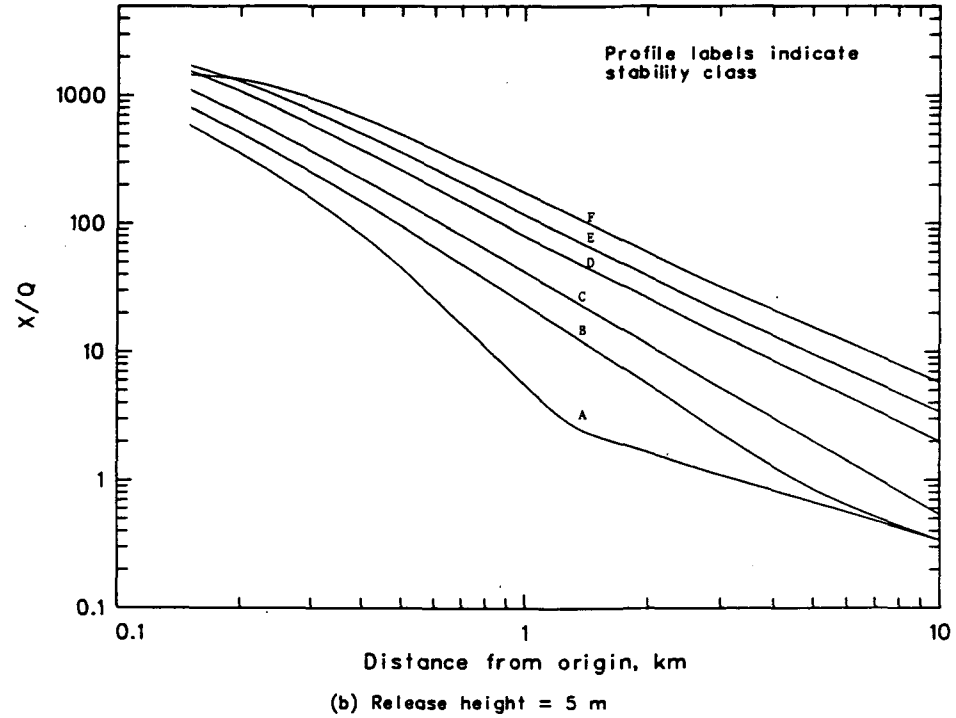

(b) Release height = 5 m

Figure 14. PGPC (X/Q) profiles by stability category for several release heights from the 14.1-m square source.

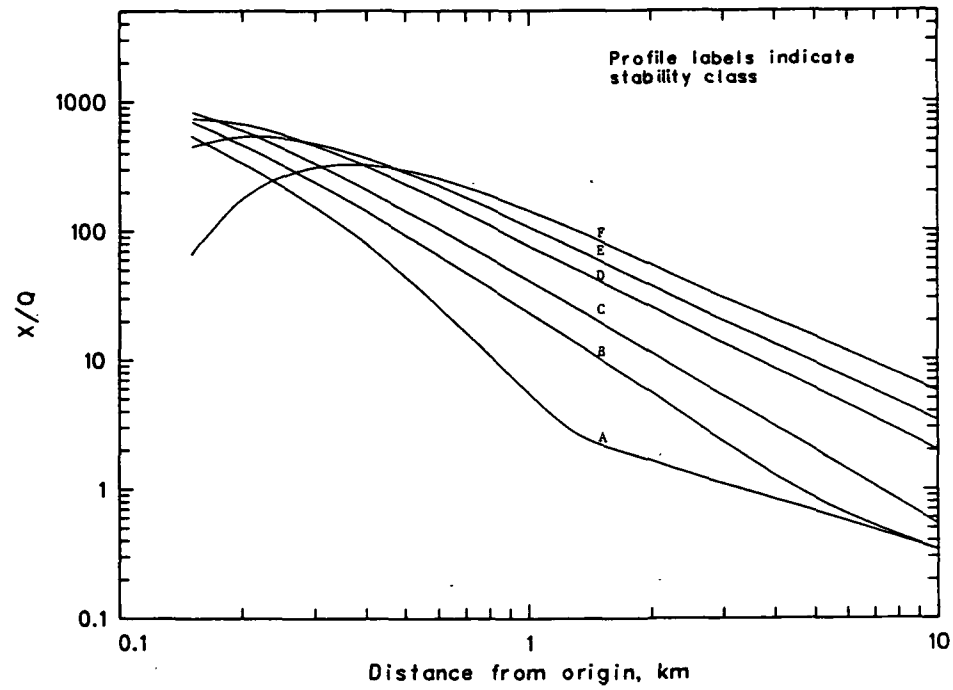

(c) Release height = 10 m

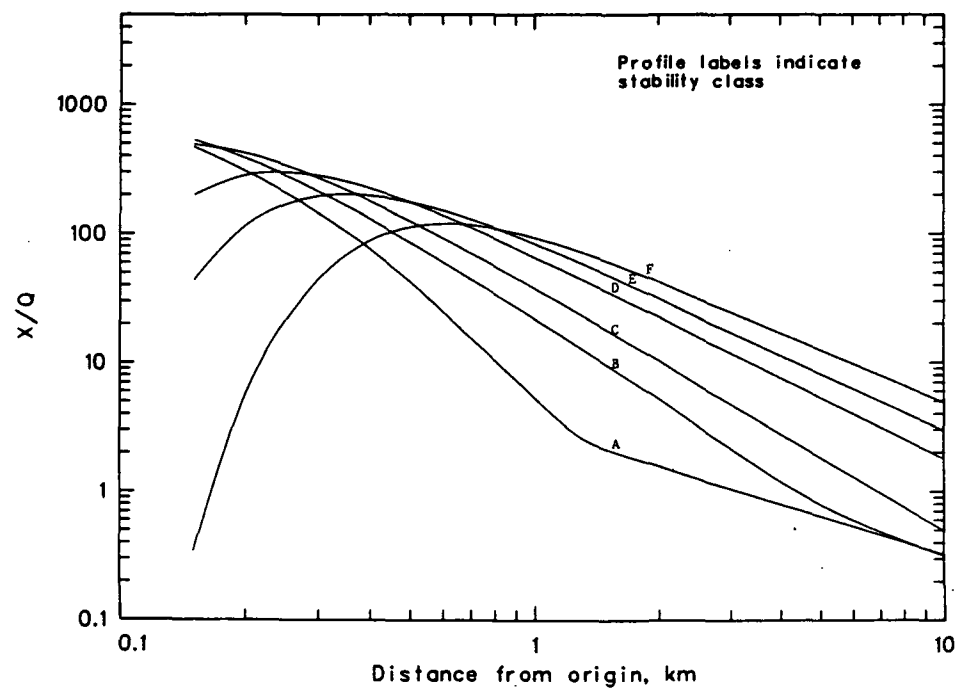

(d) Release height = 15 m

Figure 14. Continued.

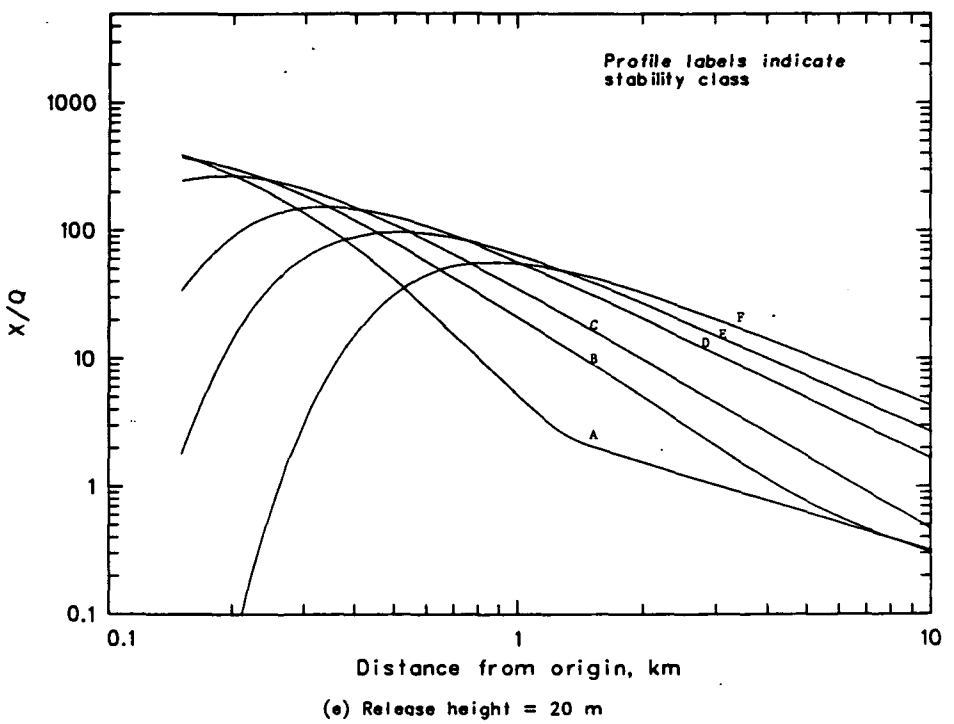

(e) Release height = 20 m

Figure 14. Continued.

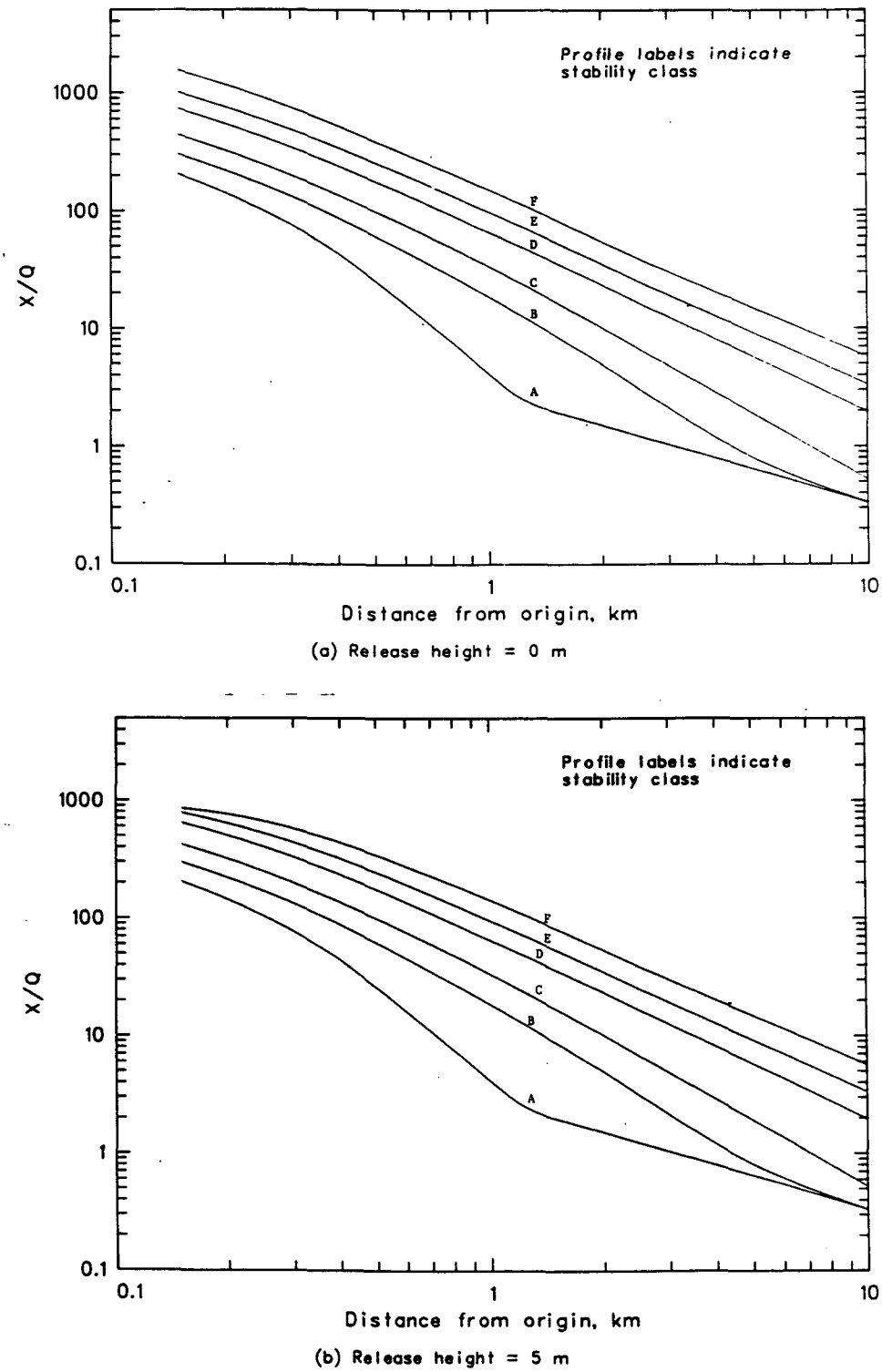

Figure 15. PGPC (X/Q) profiles by stability category for several release heights from the 80.6-m square source.

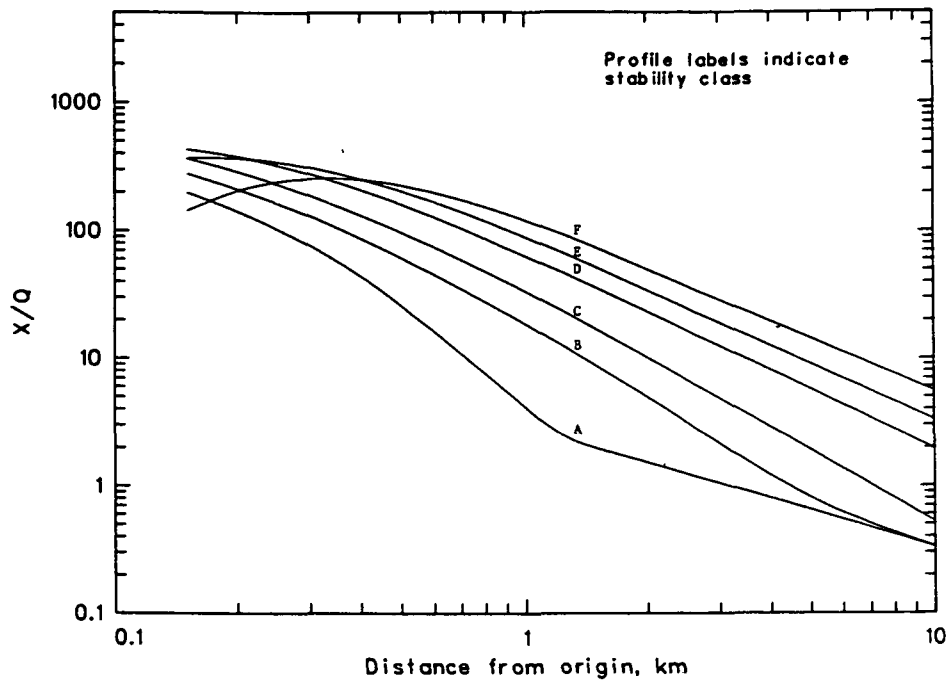

(c) Release height = 10 m

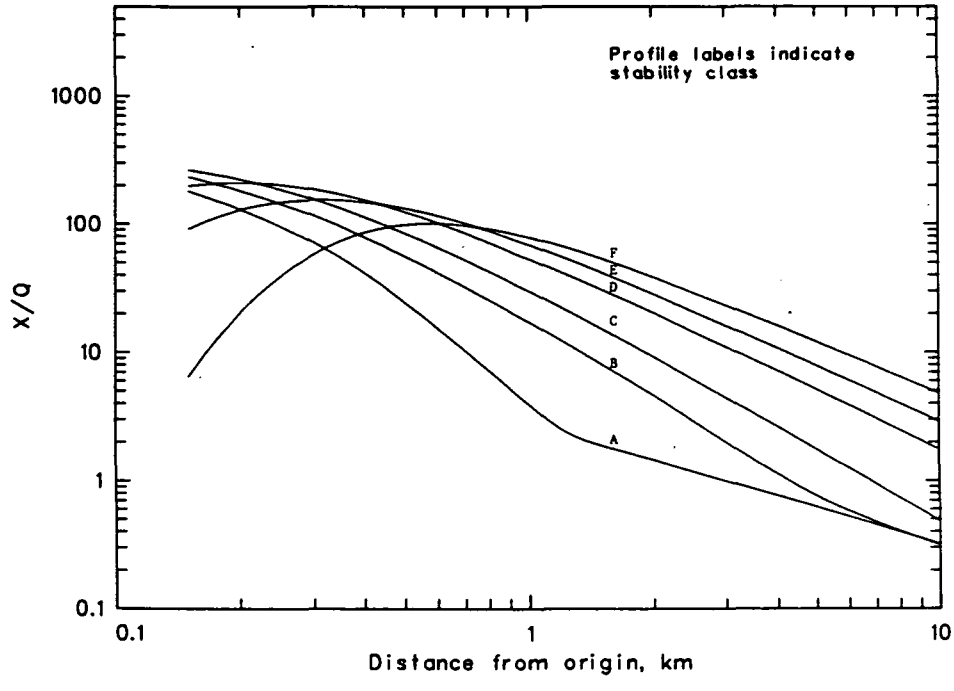

(d) Release height = 15 m

Figure 15. Continued.

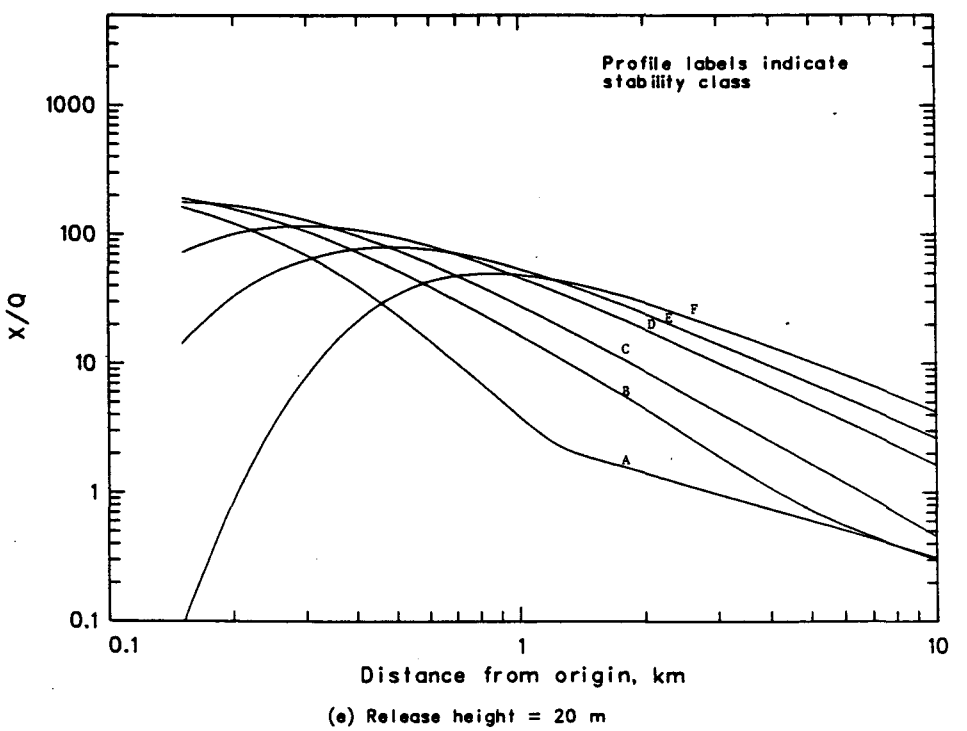

(e) Release height = 20 m

Figure 15. Continued.

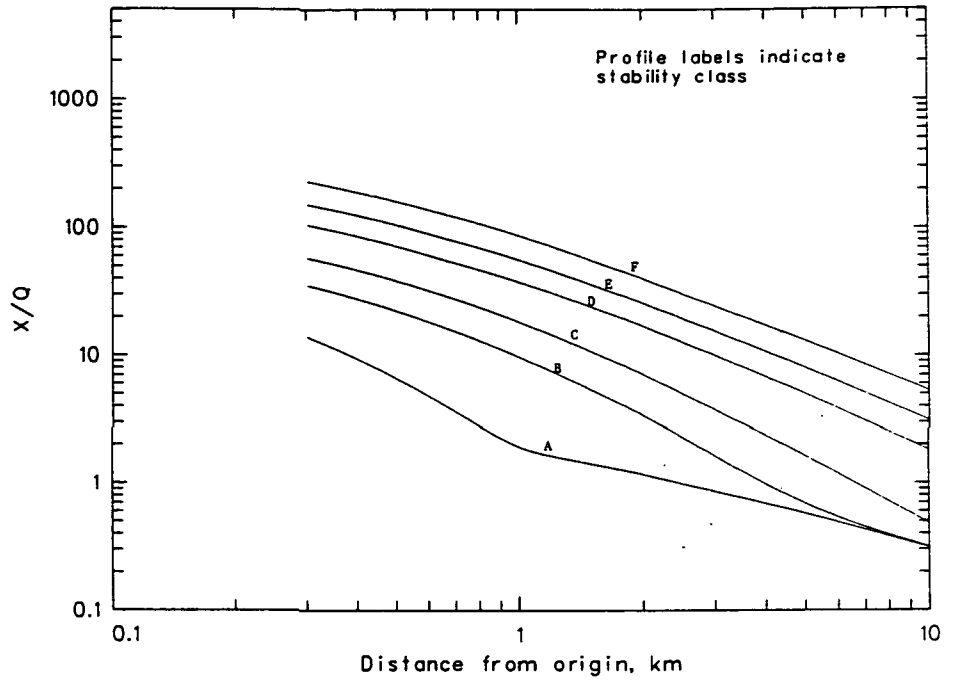

(a) Release height = 0 m

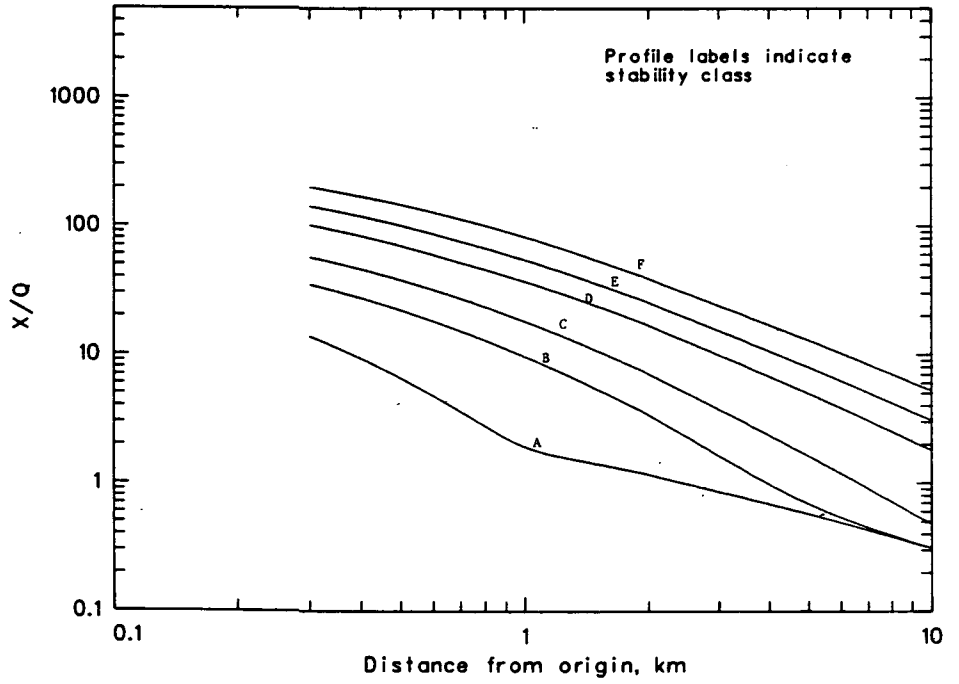

(b) Release height = 5 m

Figure 16. PGPC (X/Q) profiles by stability category for several release heights from the 316.2-m square source.

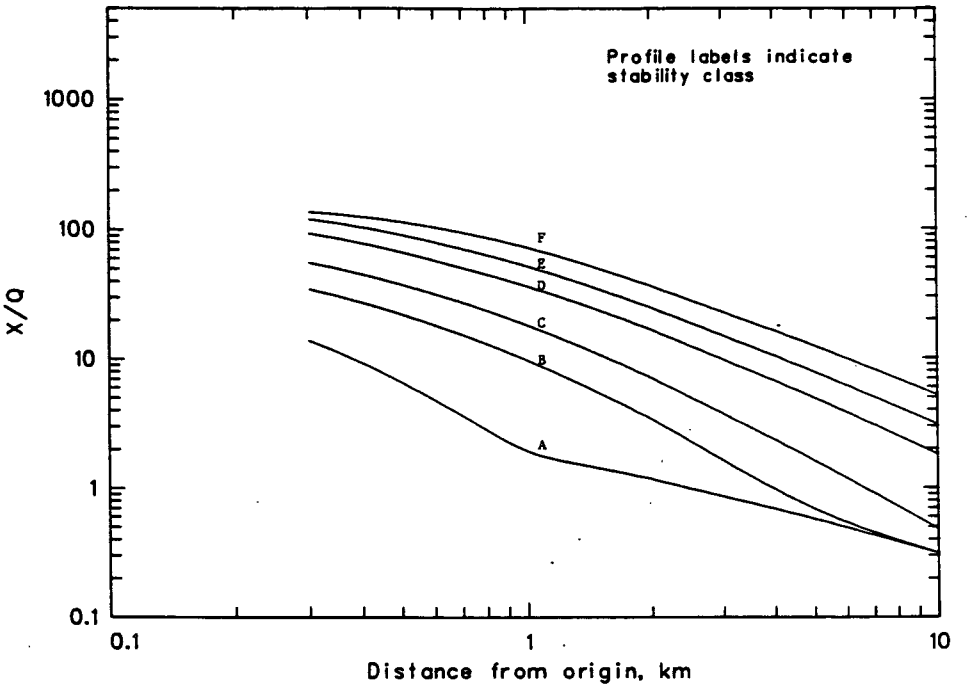

(c) Release height = 10 m

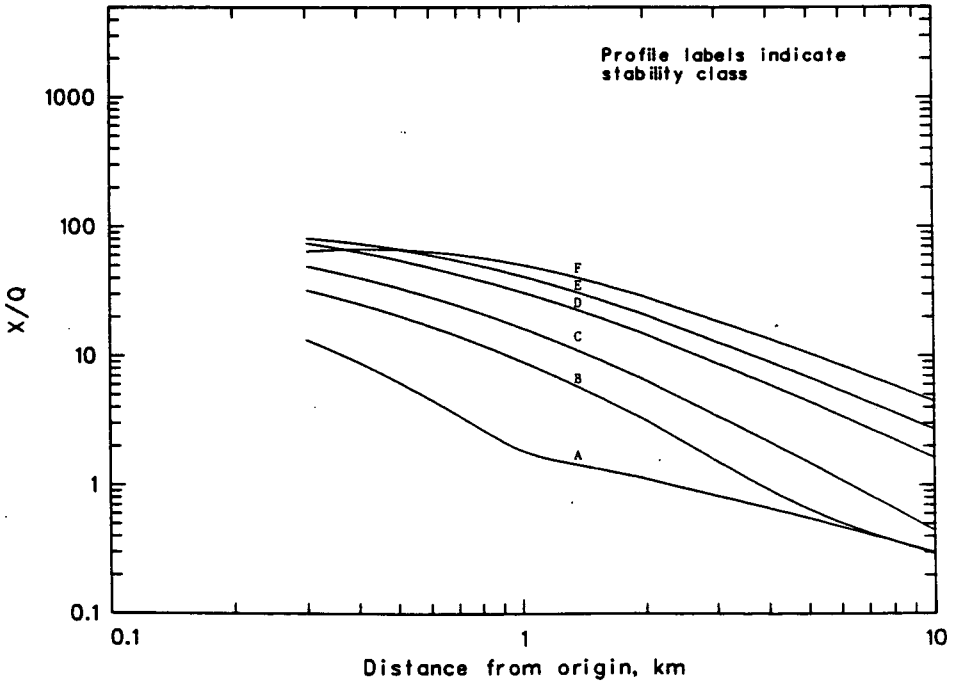

(d) Release height = 15 m

Figure 16. Continued.

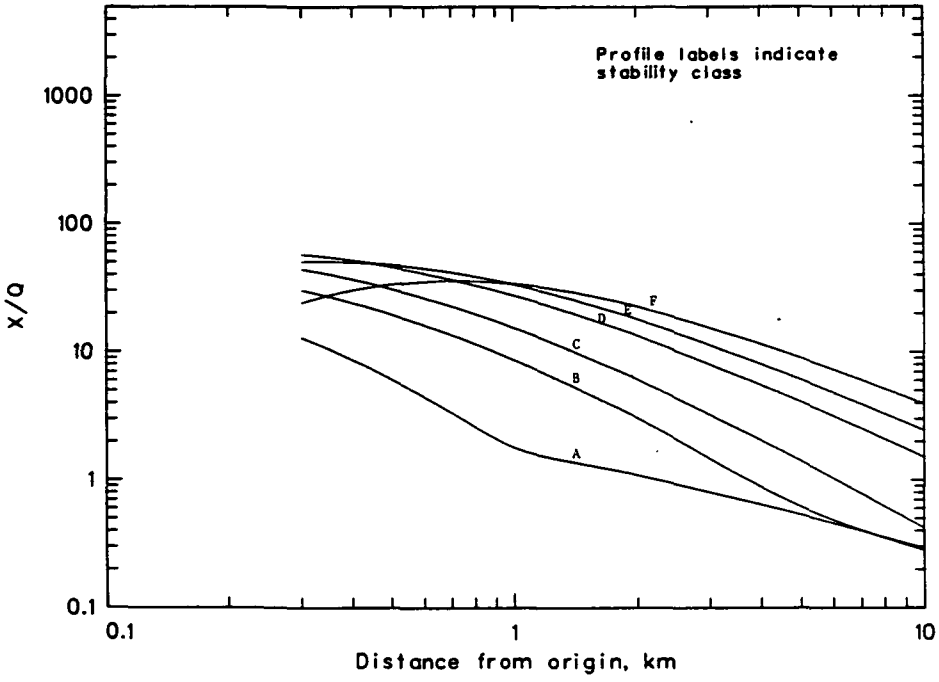

(e) Release height = 20 m

Figure 16. Continued.

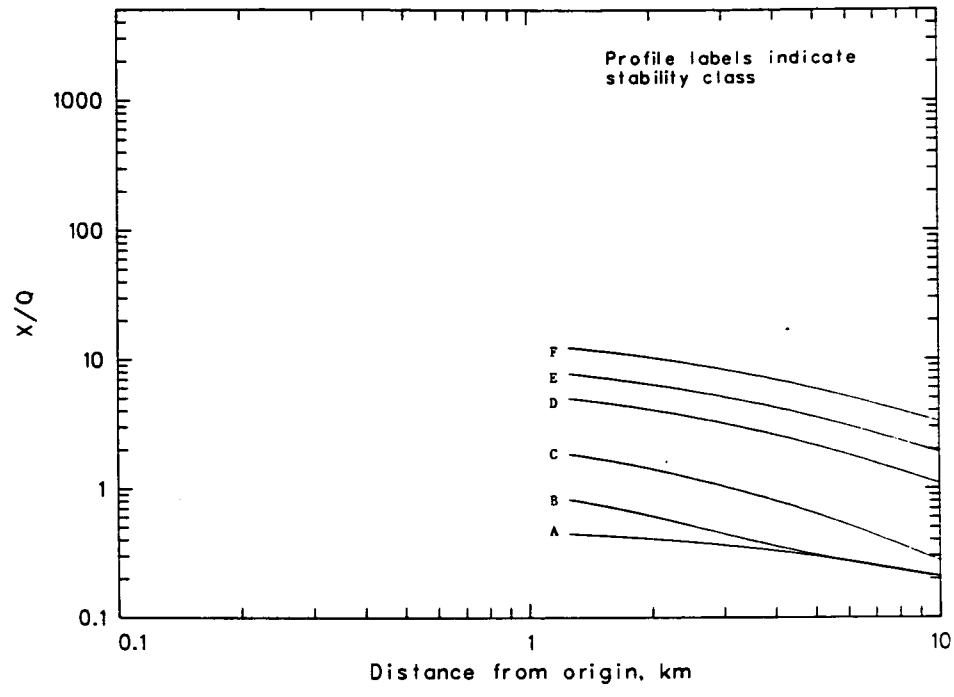

(a) Release height = 0 m

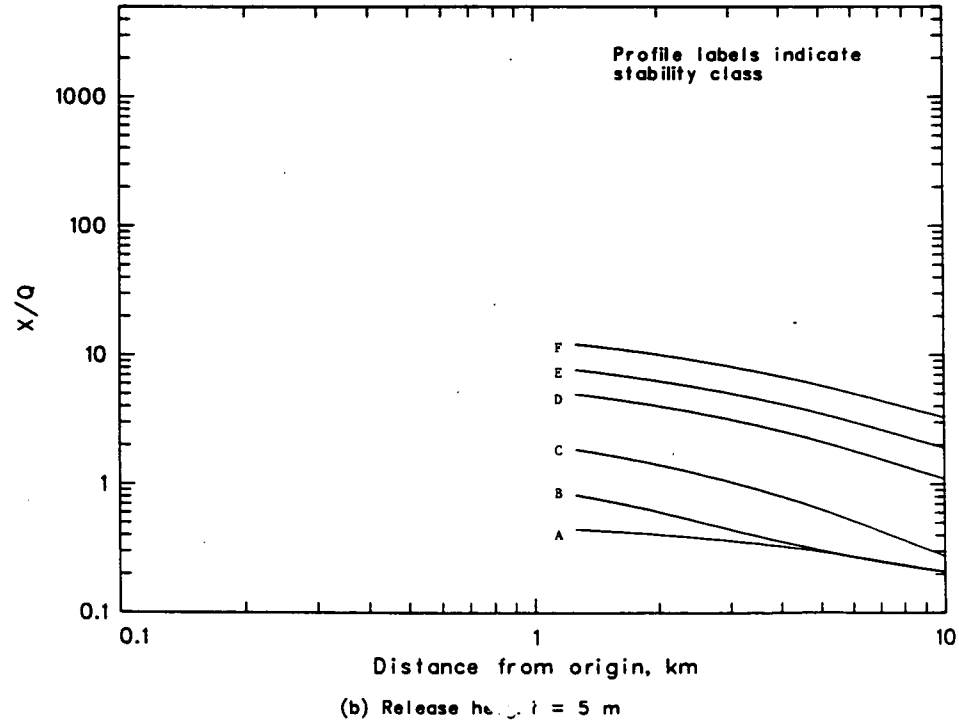

(b) Release height = 5 m

Figure 17. PGPC (X/Q) profiles by stability category for several release heights from the 2236.1-m square source

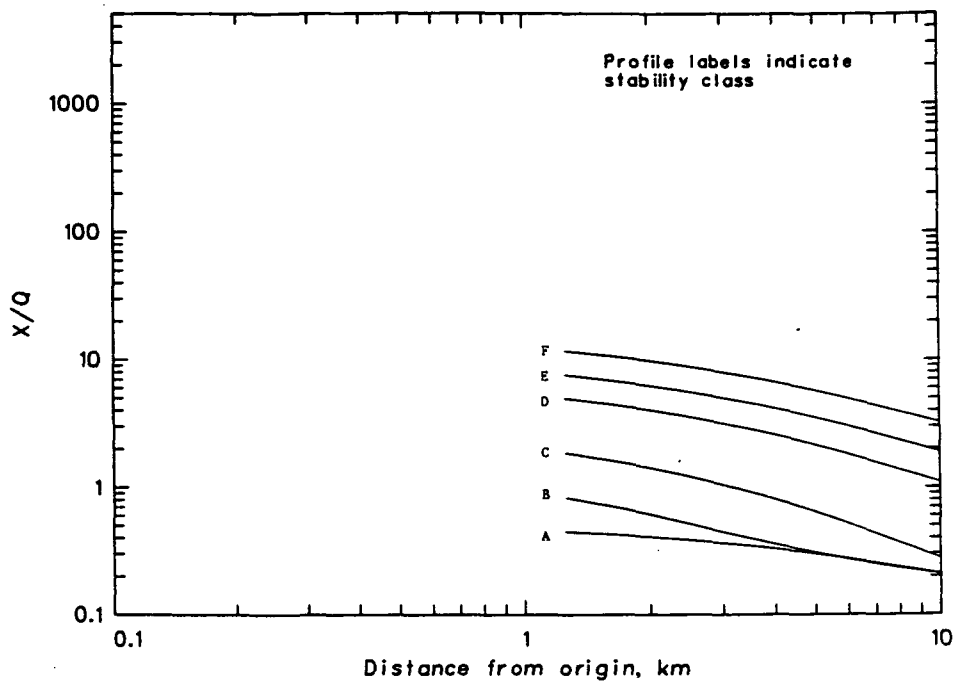

(c) Release height = 10 m

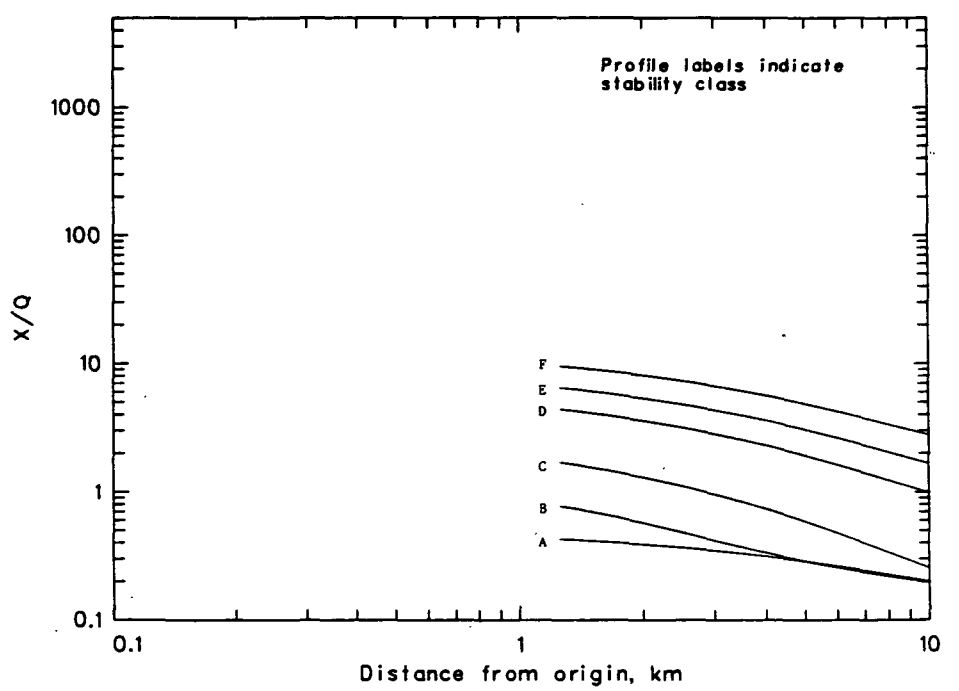

(d) Release height = 15 m

Figure 17. Continued.

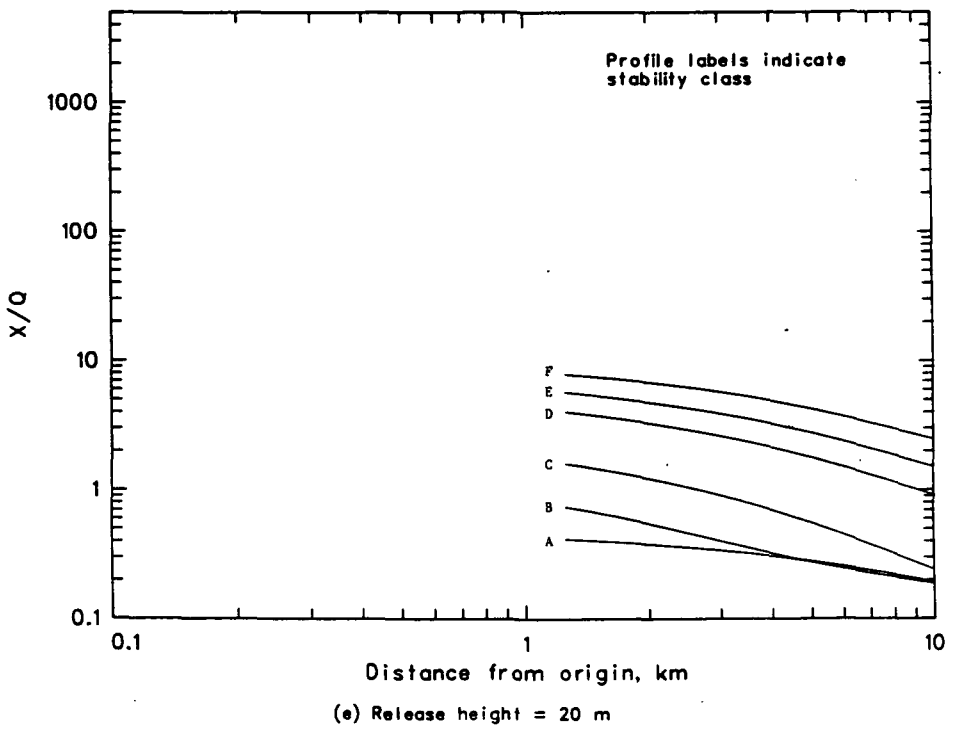

(e) Release height = 20 m

Figure 17. Continued.

APPENDIX B

TGRC (X/Q) PROFILES BY STABILITY CATEGORY FOR SEVERAL RELEASE HEIGHTS AND EACH SOURCE

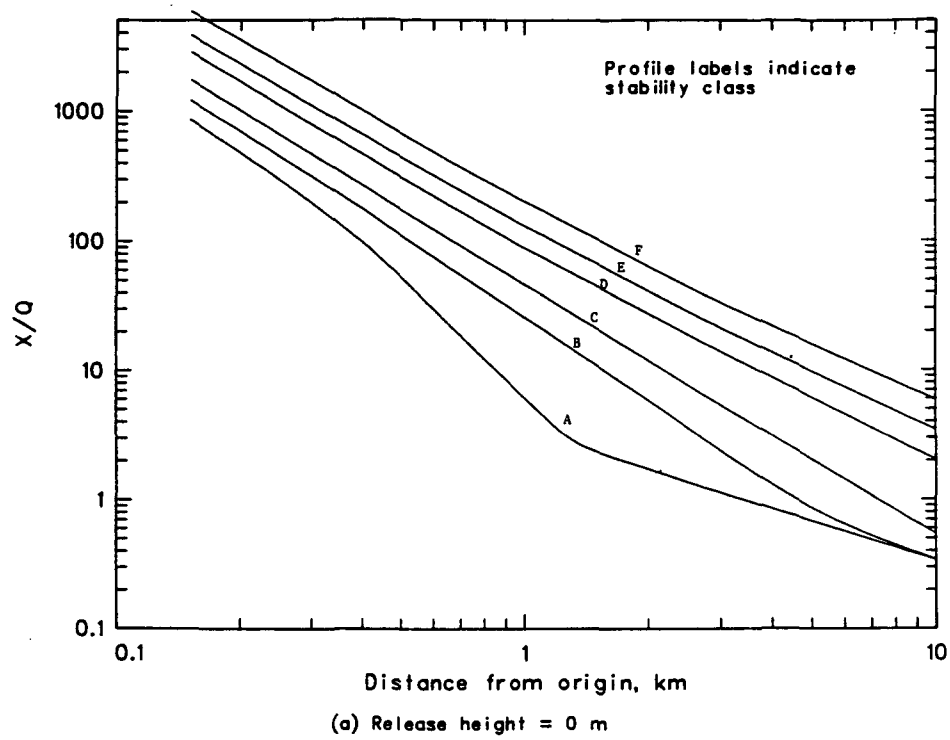

(a) Release height = 0 m

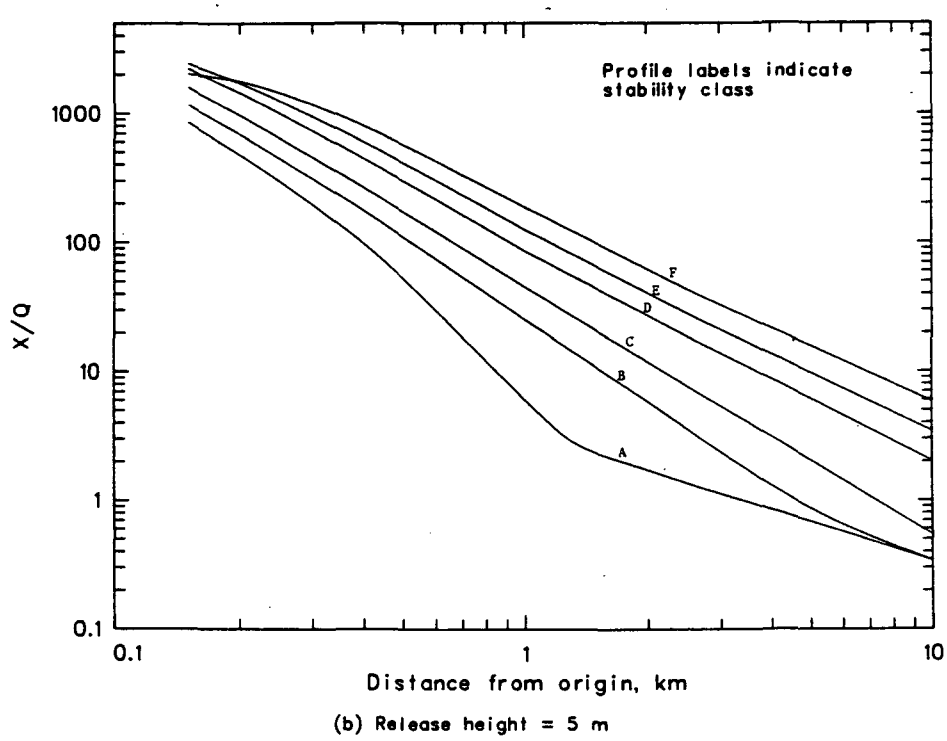

(b) Release height = 5 m

Figure 18. TGRC (X/Q) profiles by stability category for several release heights from the 14.1-m square source.

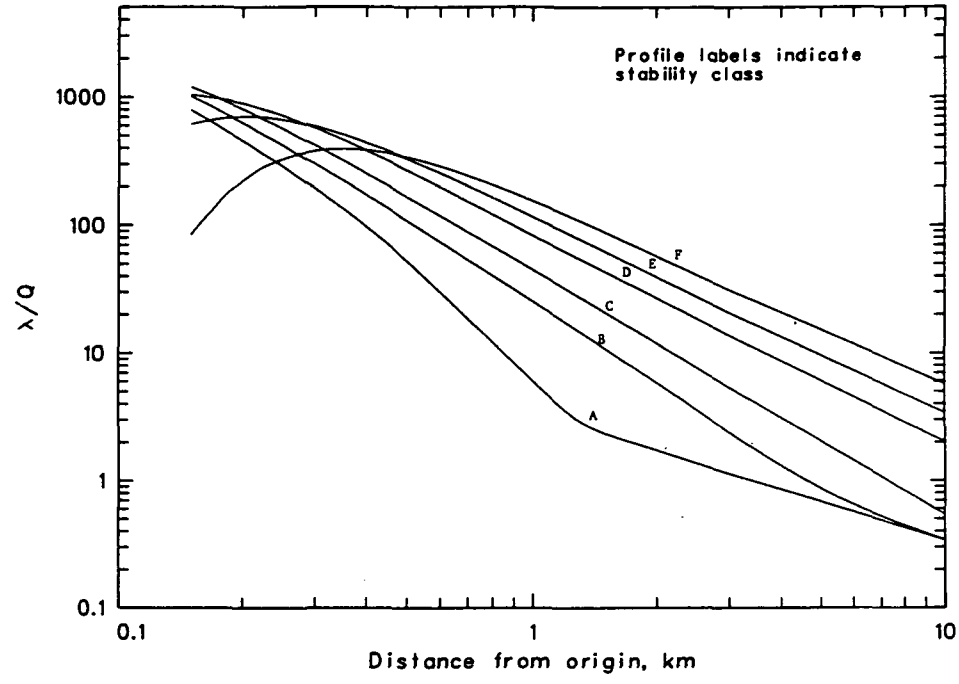

(c) Release height = 10 m

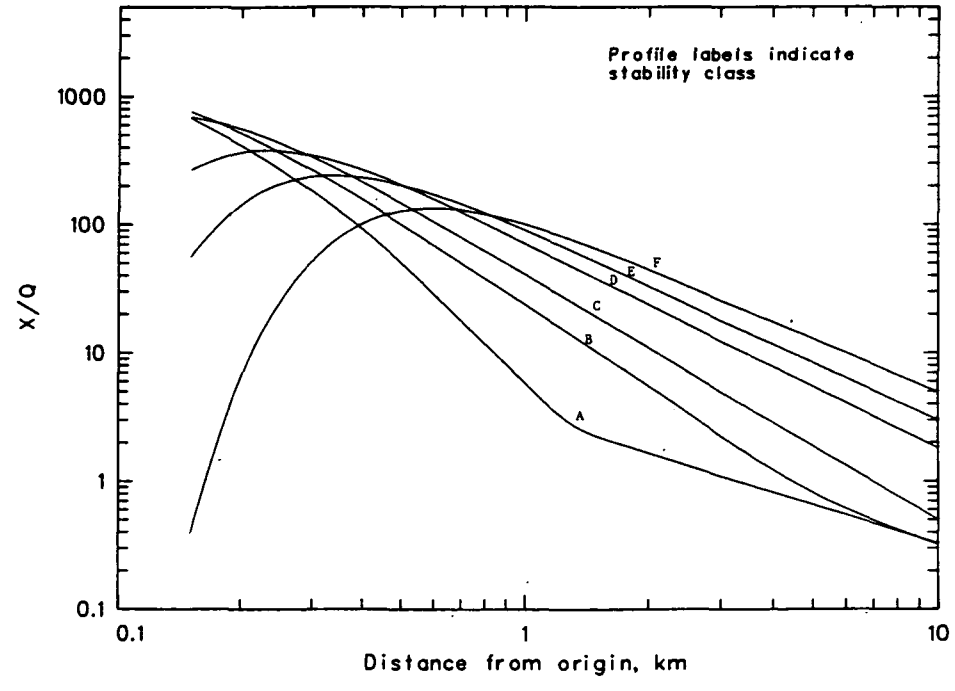

(d) Release height = 15 m

Figure 18. Continued.

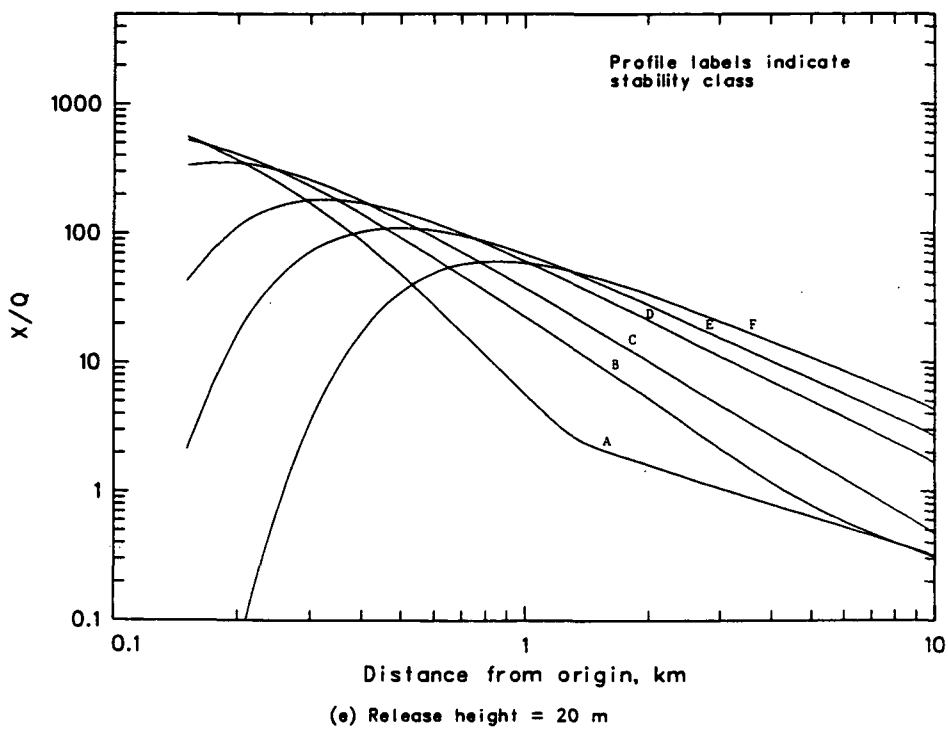

(e) Release height = 20 m

Figure 18. Continued.

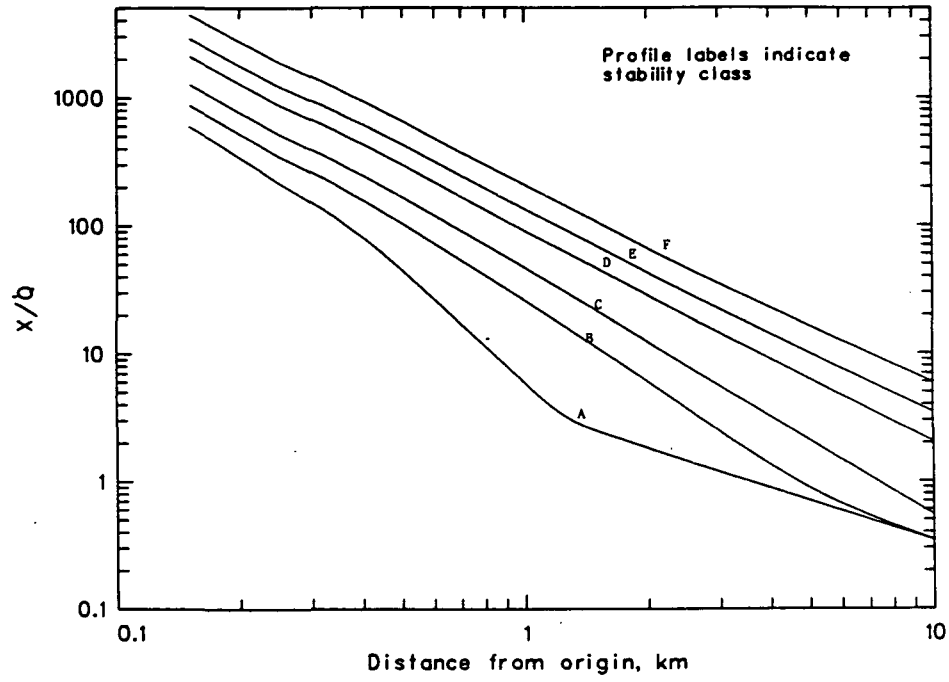

(a) Release height = 0 m

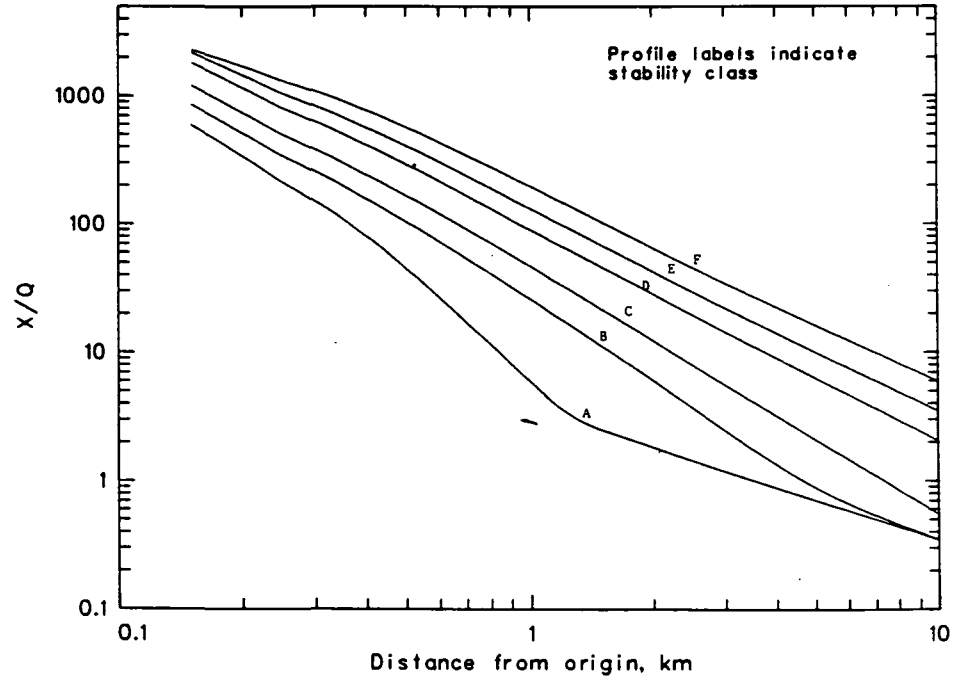

(b) Release height = 5 m

Figure 19. TGRC (X/Q) profiles by stability category for several release heights from the 80.6-m square source.

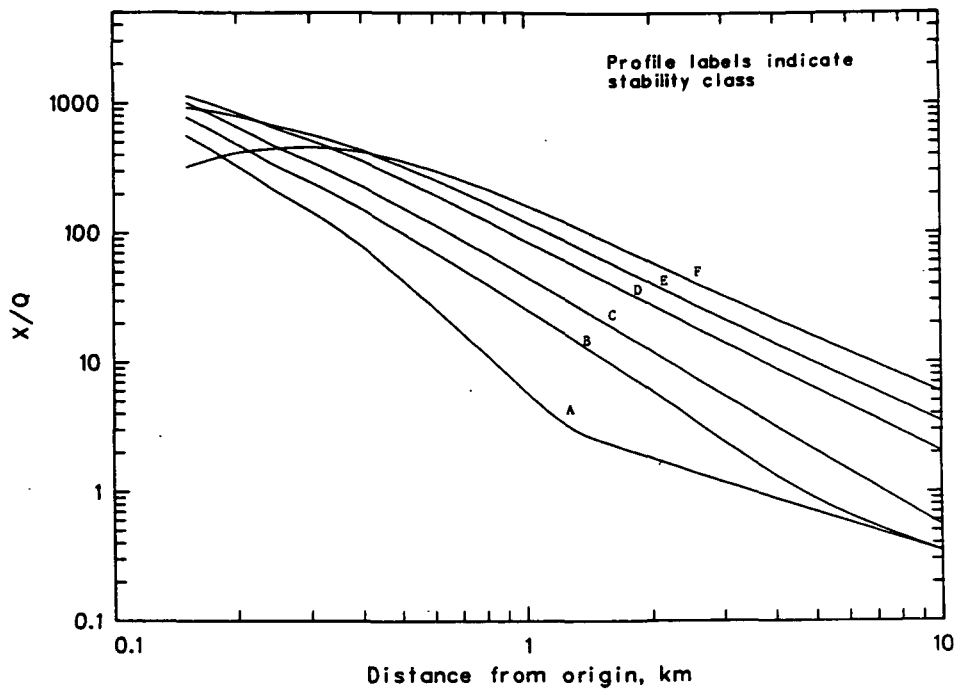

(c) Release height = 10 m

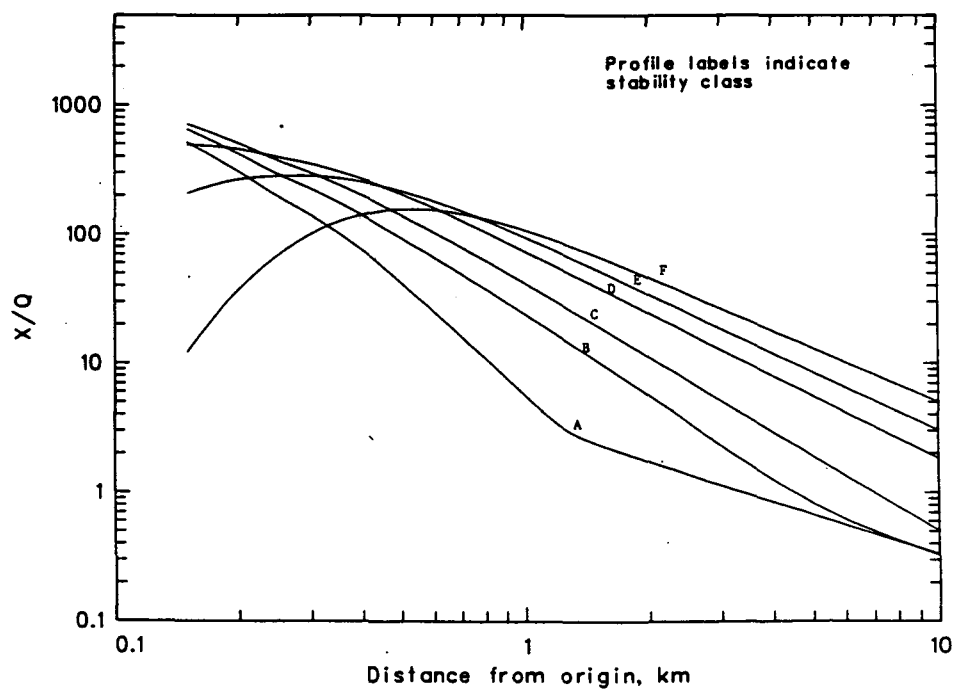

(d) Release height = 15 m

Figure 19. Continued.

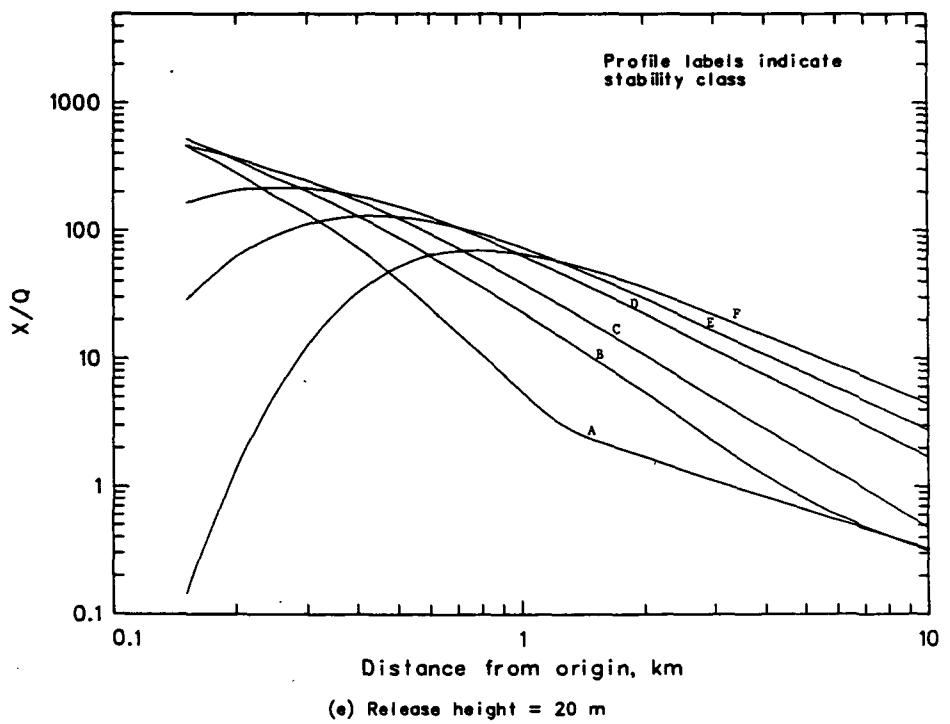

(e) Release height = 20 m

Figure 19. Continued.

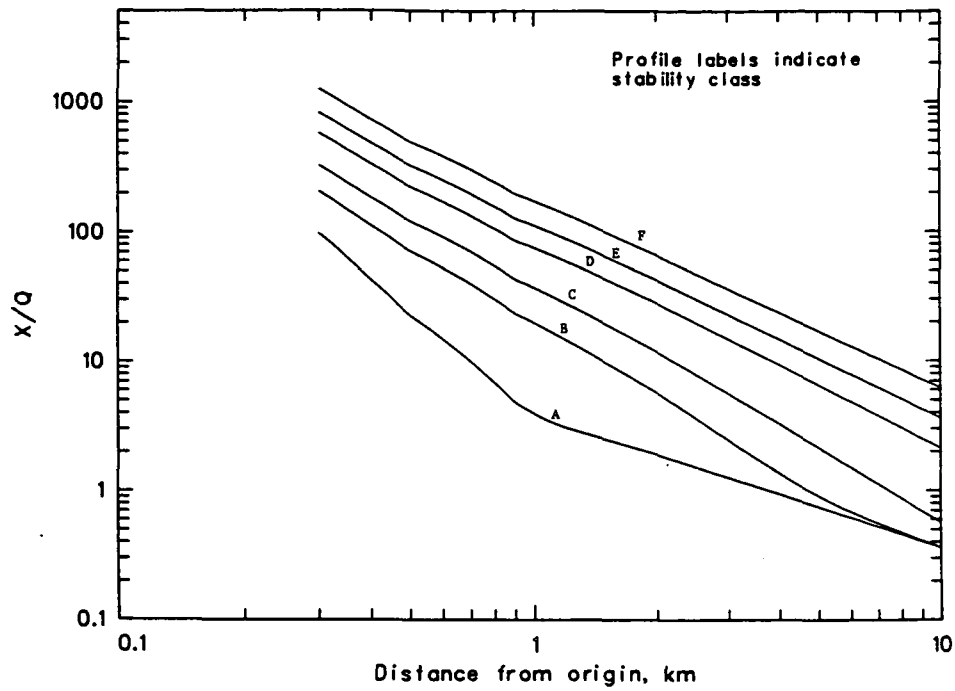

(a) Release height = 0 m

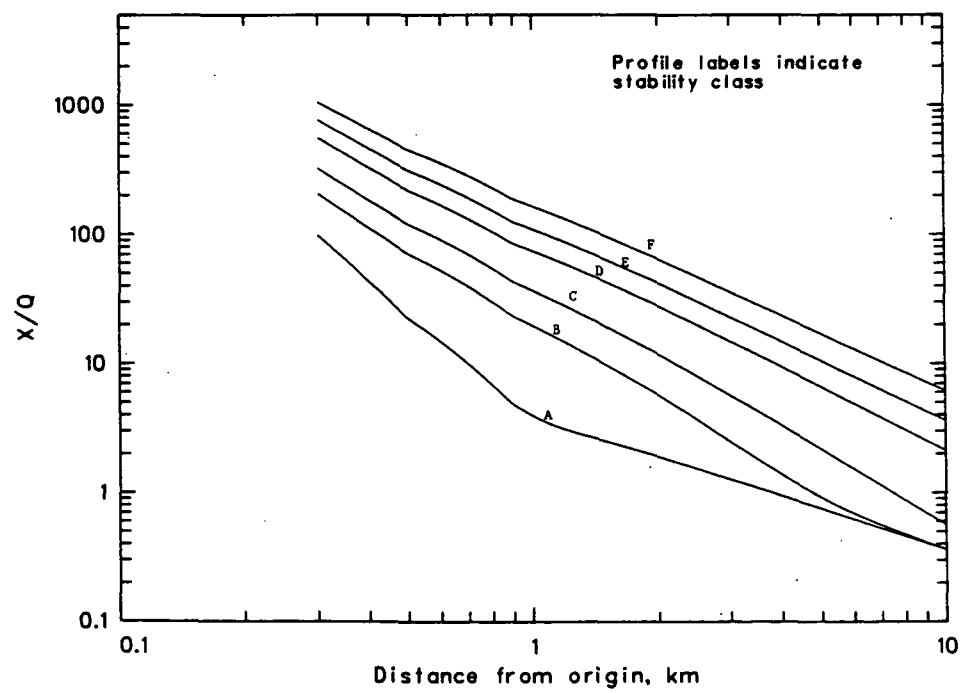

(b) Release height = 5 m

Figure 20. TGRC (X/Q) profiles by stability category for several release heights from the 316.2-m square source.

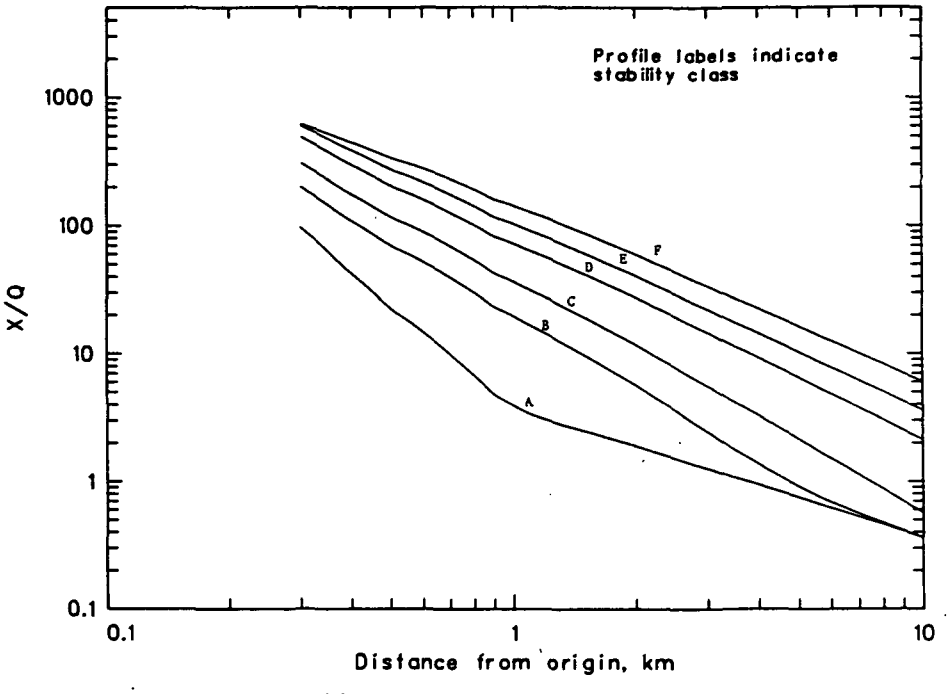

(c) Release height = 10 m

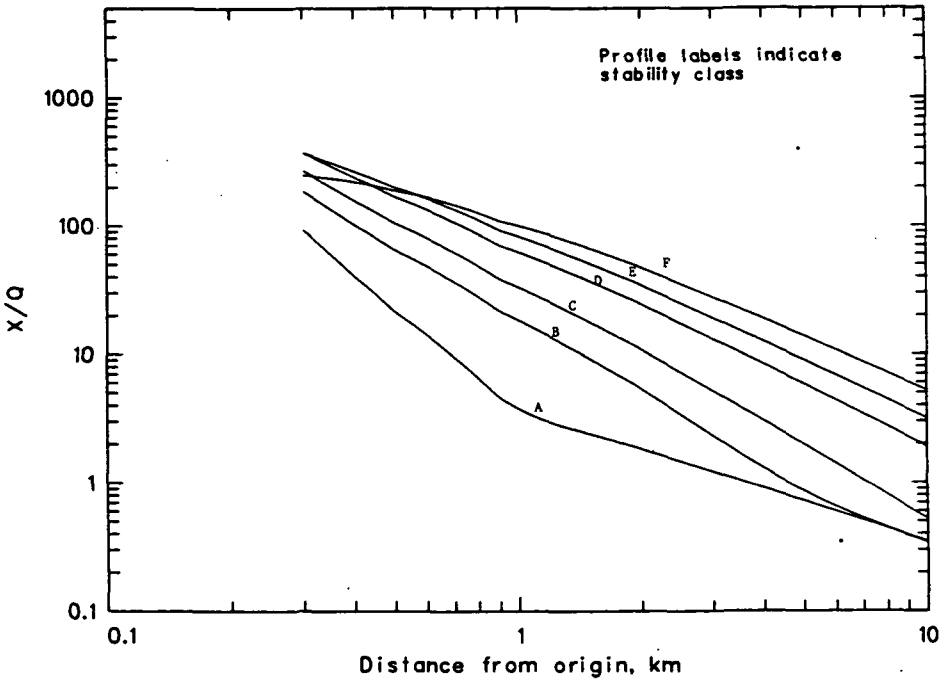

(d) Release height = 15 m

Figure 20. Continued.

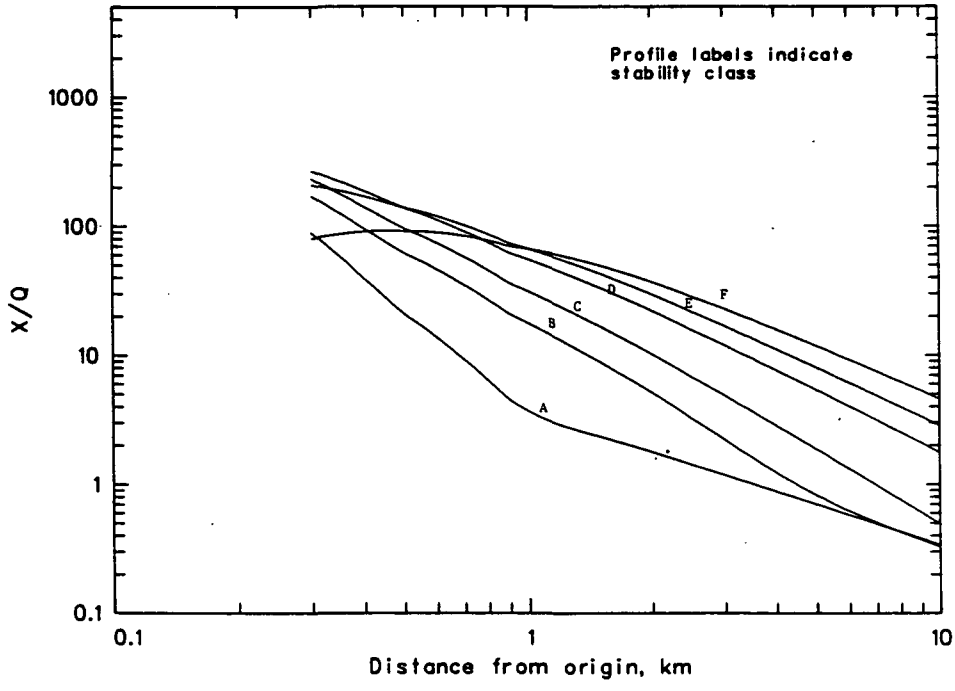

(e) Release height = 20 m

Figure 20. Continued.

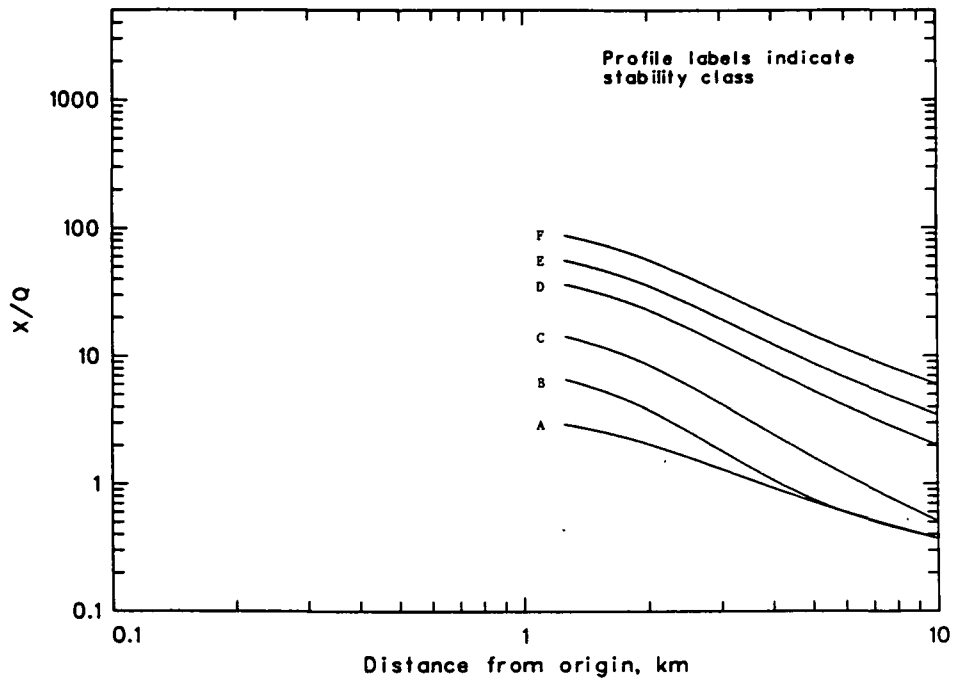

(a) Release height = 0 m

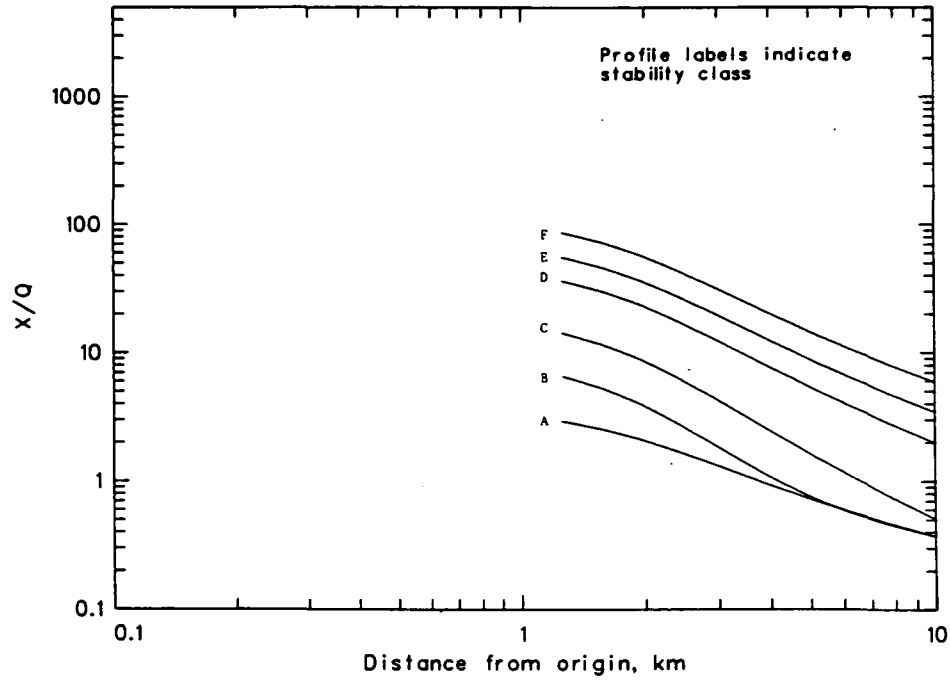

(b) Release height = 5 m

Figure 21. TGRC (X/Q) profiles by stability category for several release heights from the 2236.1-m square source

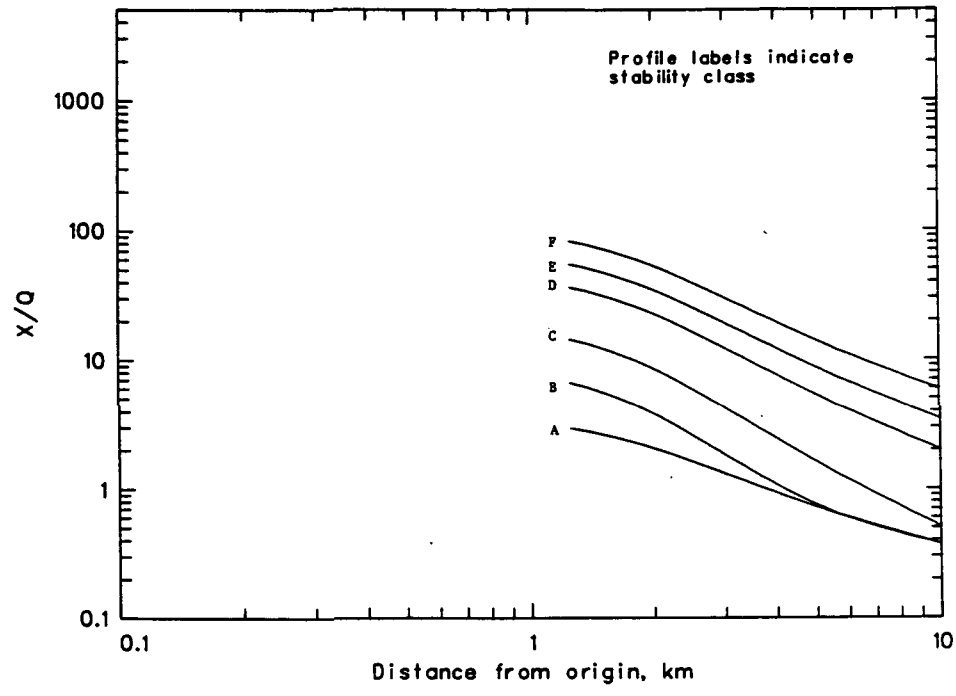

(c) Release height = 10 m

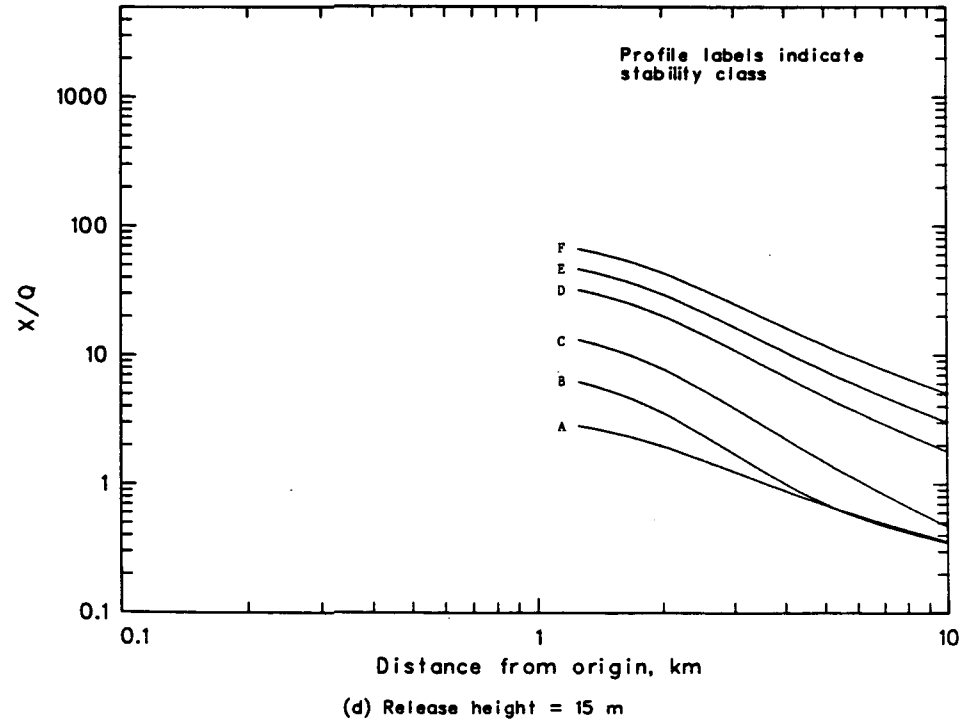

(d) Release height = 15 m

Figure 21. Continued.

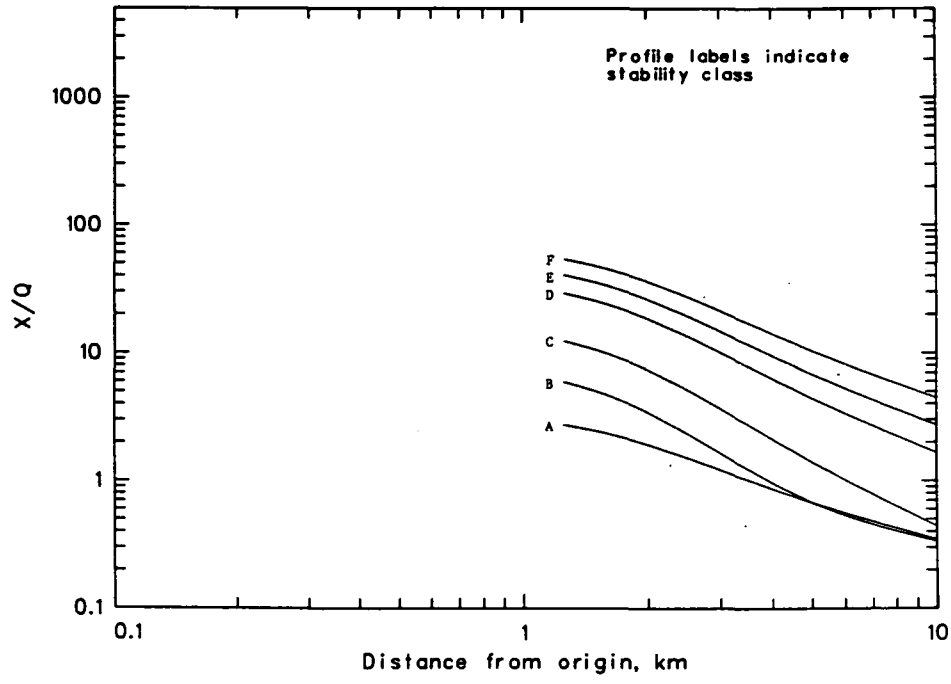

(e) Release height = 20 m

Figure 21. Continued.

APPENDIX C

PGPC (X/Q) PROFILES BY RELEASE HEIGHT FOR EACH STABILITY CATEGORY AND EACH SOURCE

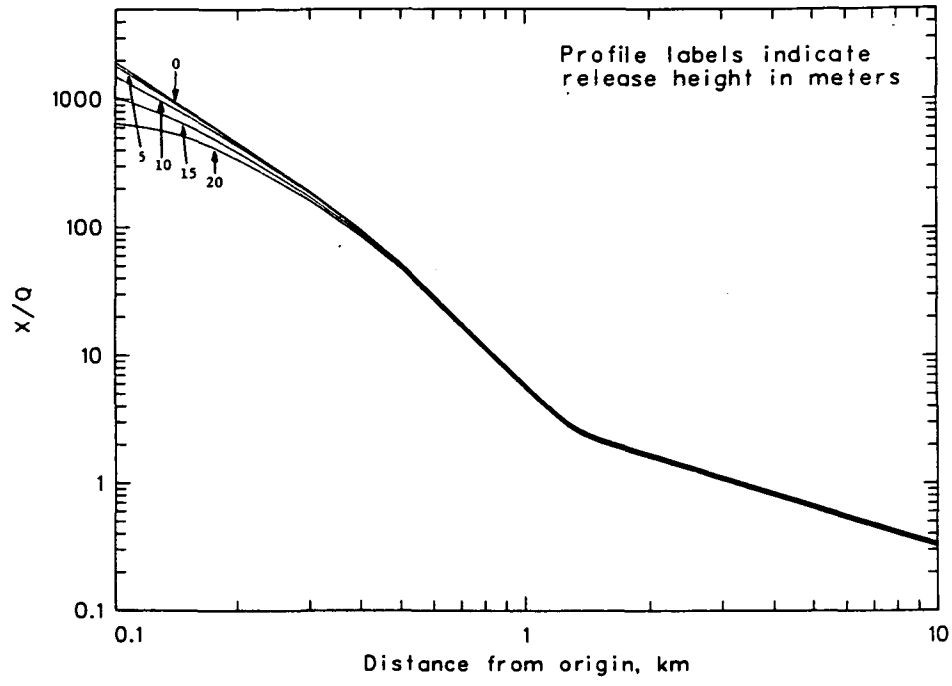

(a) Stability class A

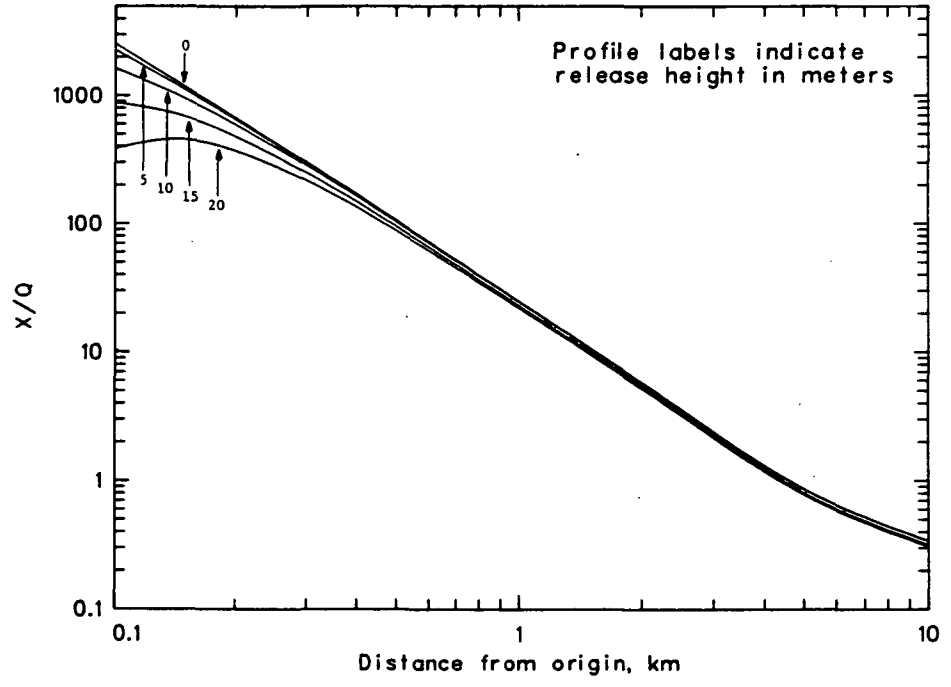

(b) Stability class B

Figure 22. PGPC (X/Q) profiles by release height for each stability class from the stack source.

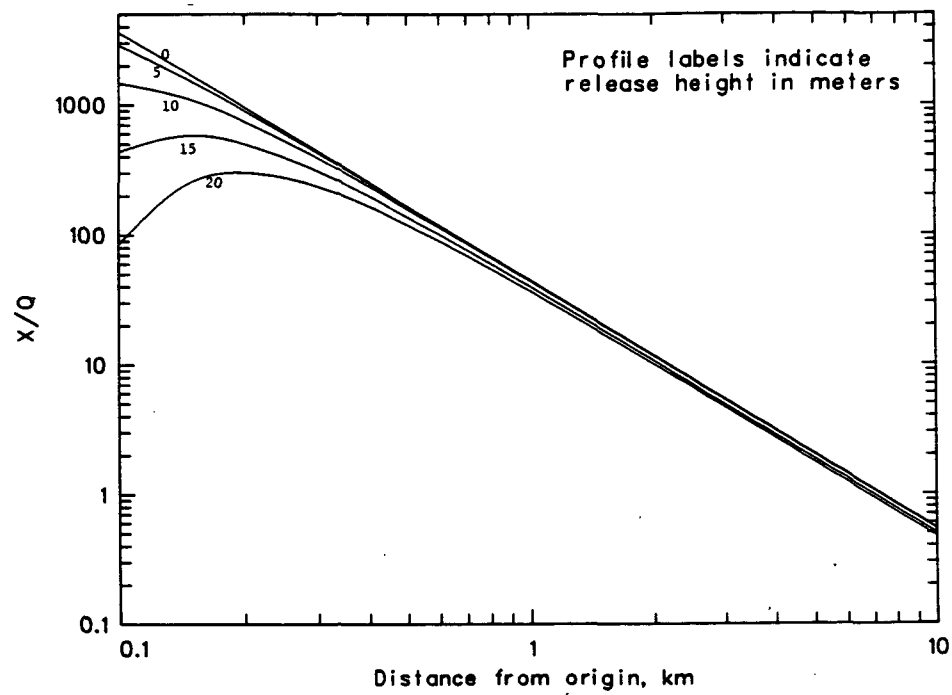

(c) Stability class C

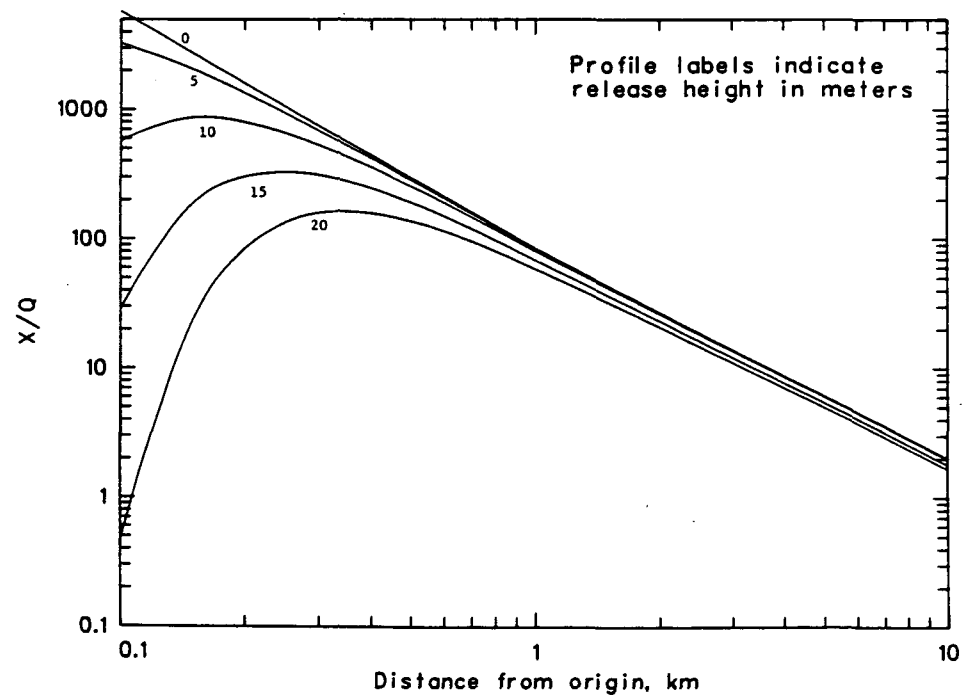

(d) Stability class D

Figure 22. Continued.

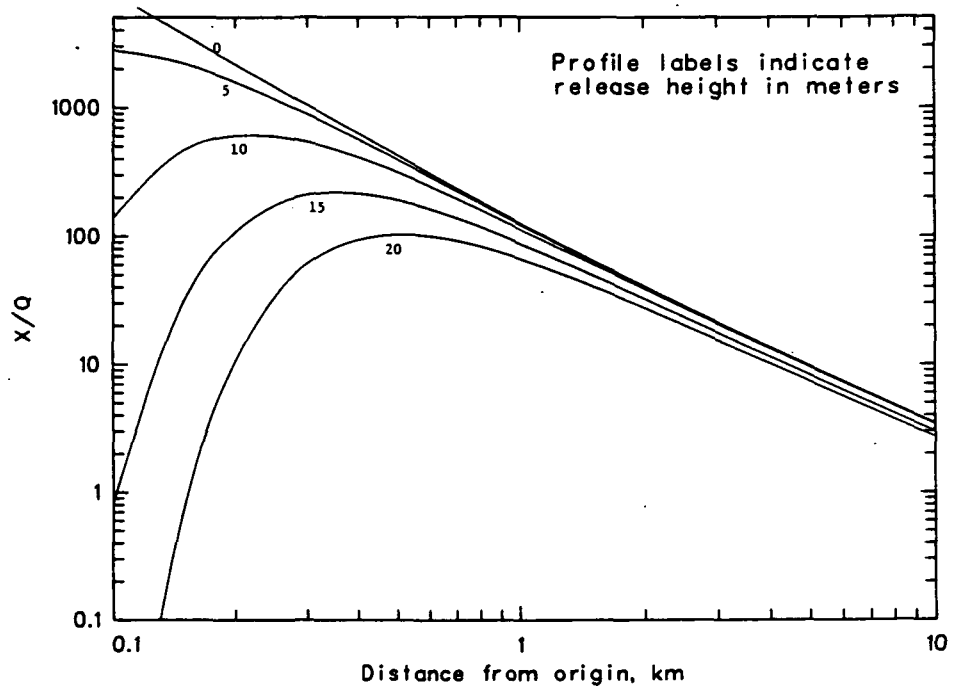

(e) Stability class E

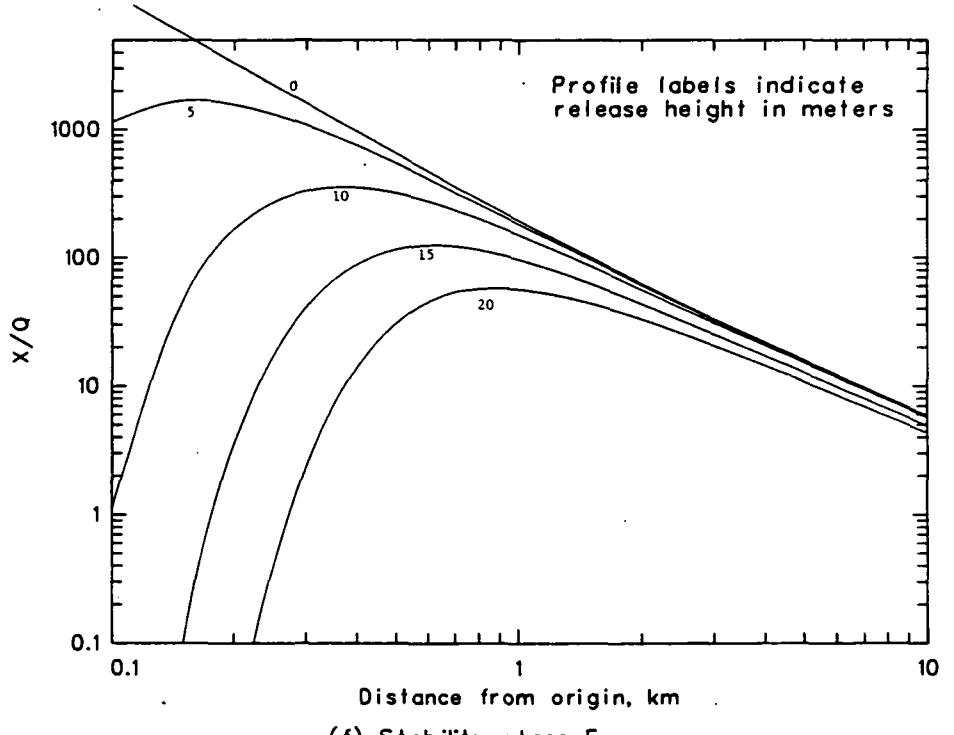

(f) Stability class F

Figure 22. Continued.

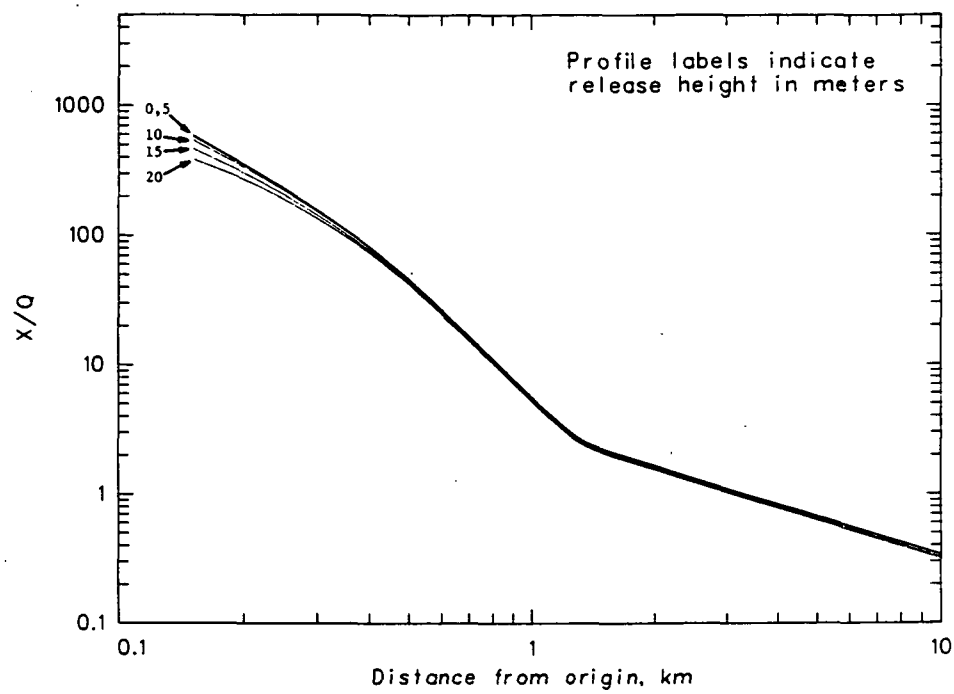

(a) Stability class A

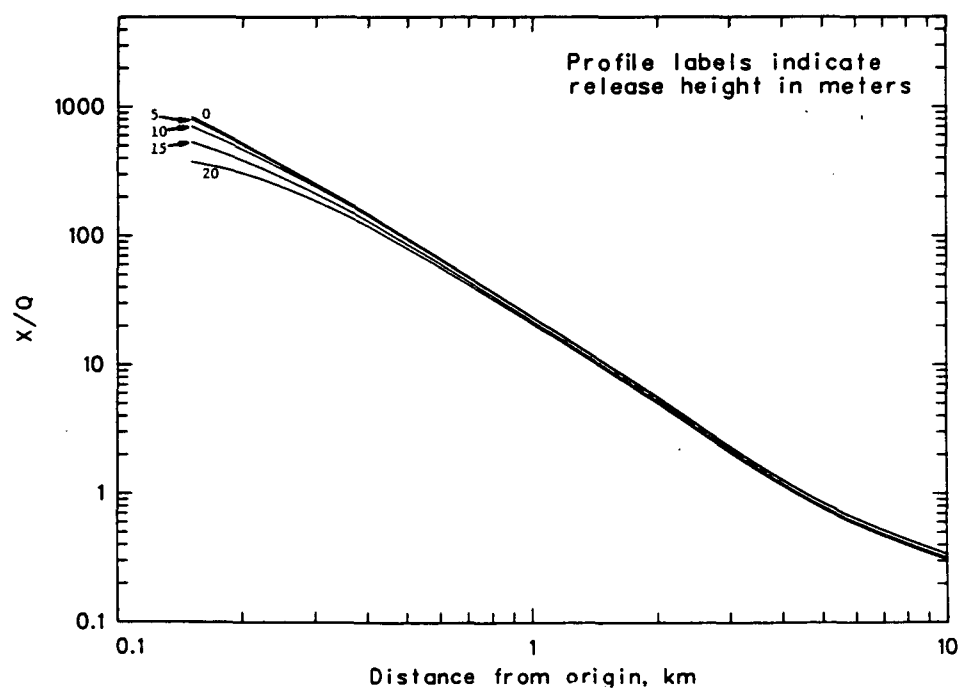

(b) Stability class B

Figure 23. PGPC (X/Q) profiles by release height for each stability class from the 14.1-m square source.

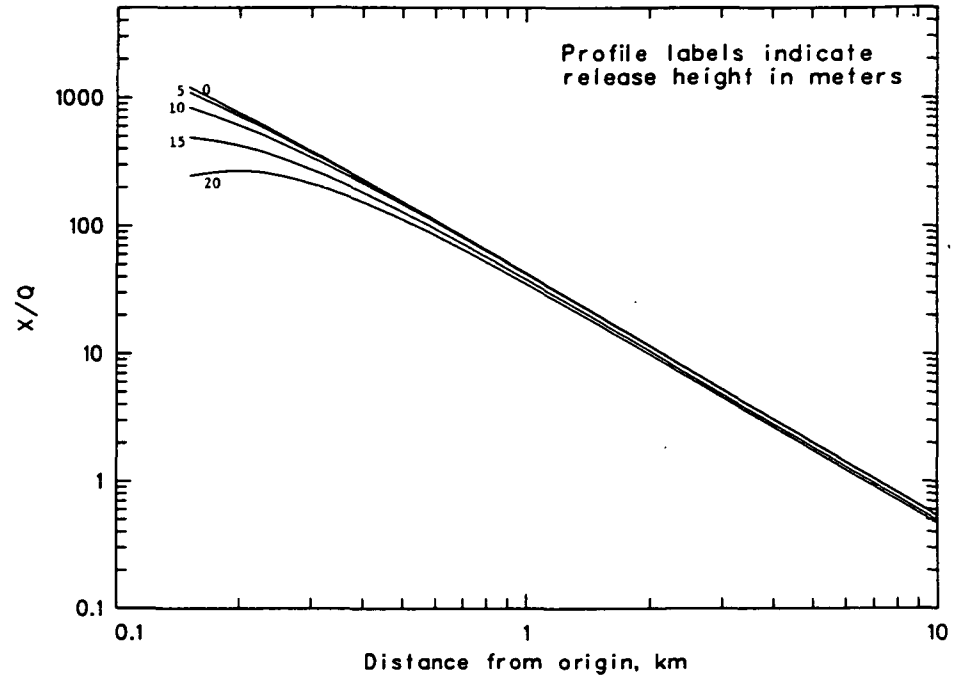

(c) Stability class C

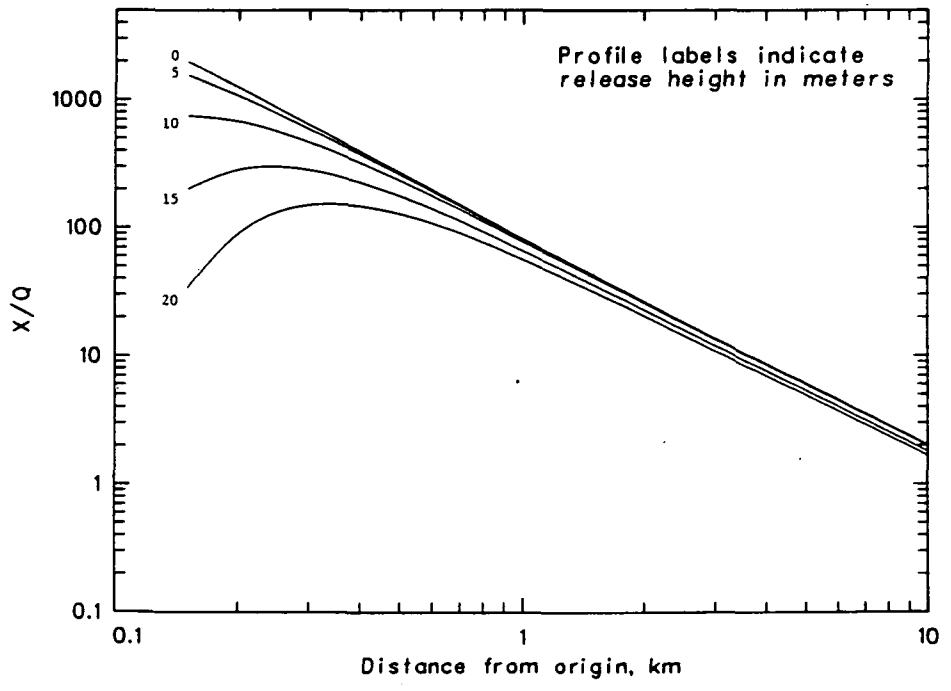

(d) Stability class D

Figure 23. Continued.

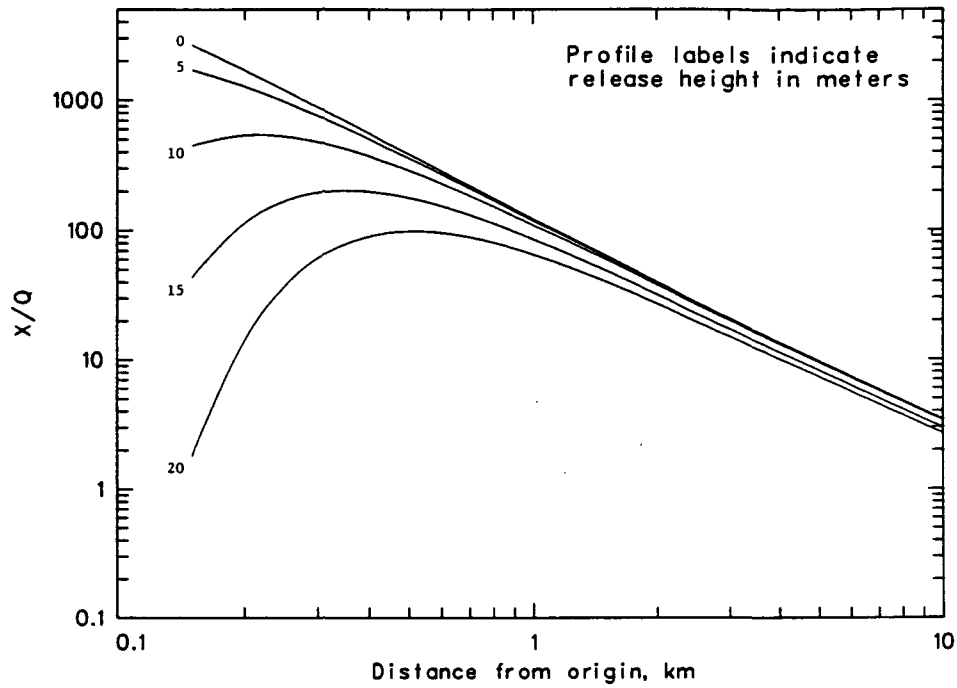

(e) Stability class E

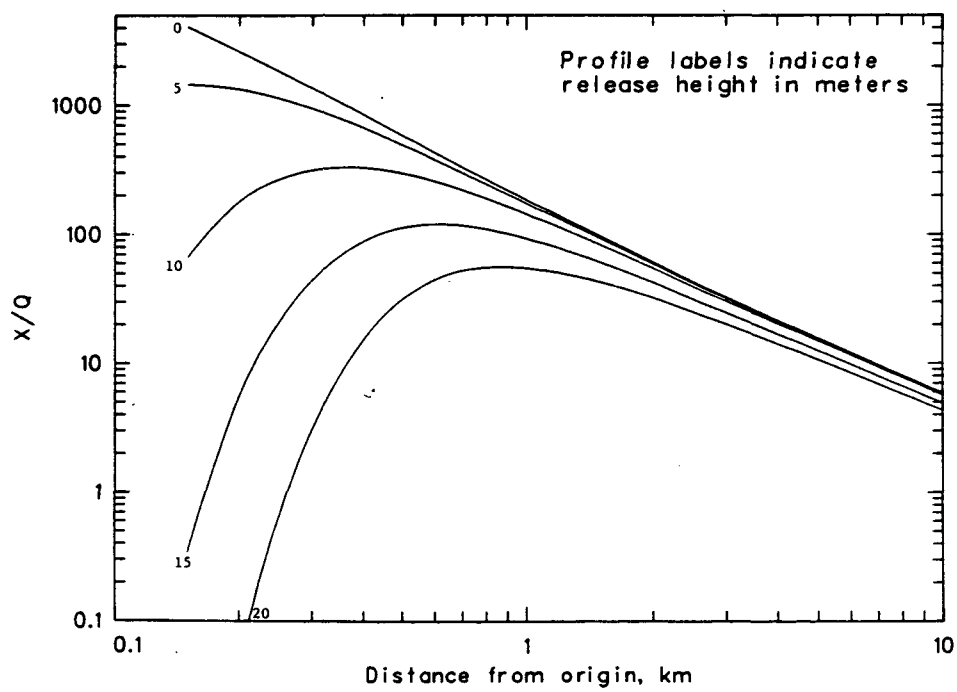

(f) Stability class F

Figure 23. Continued.

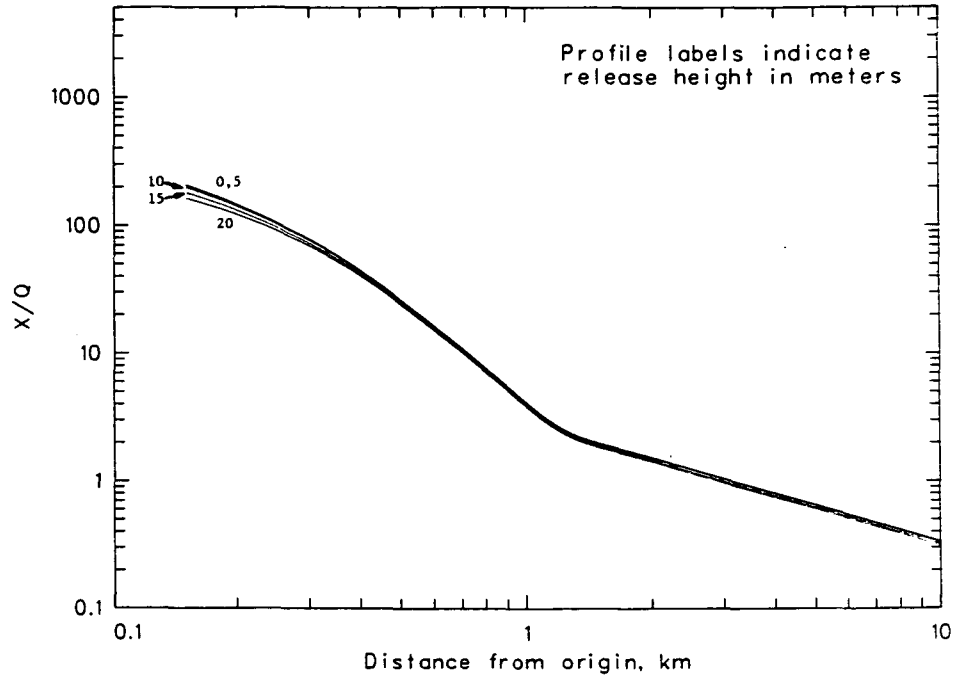

(a) Stability class A

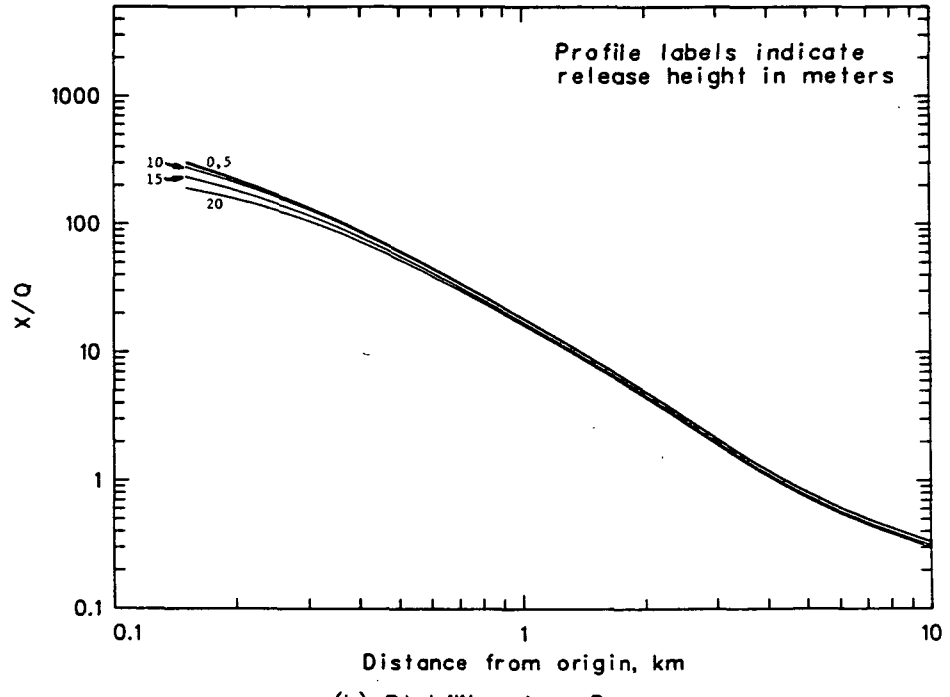

(b) Stability class B

Figure 24. PGPC (X/Q) profiles by release height for each stability class from the 80.6-m square source.

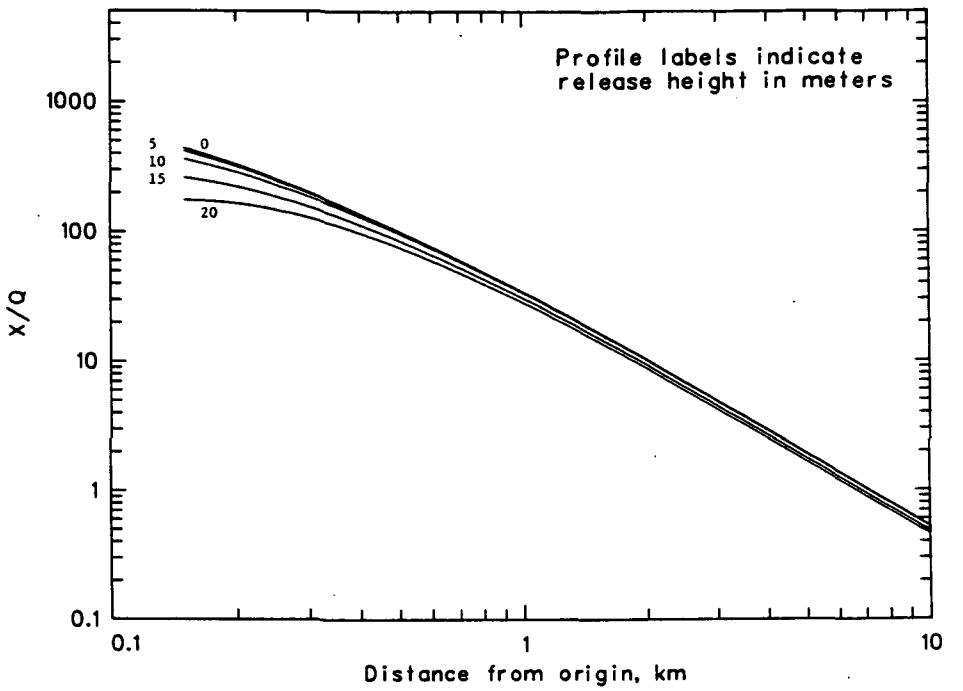

(c) Stability class C

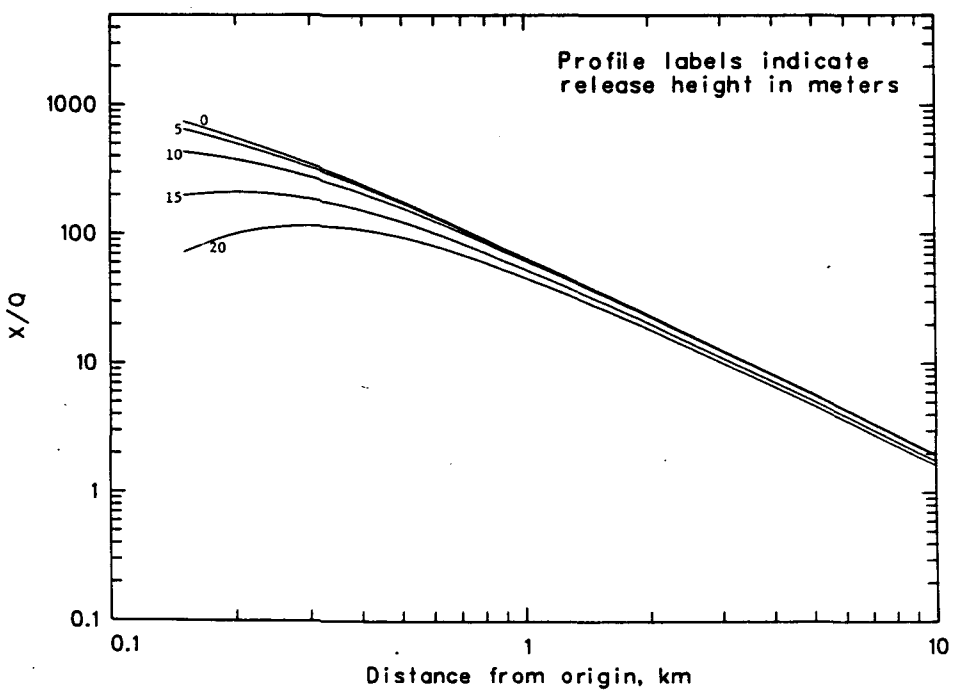

(d) Stability class D

Figure 24. Continued.

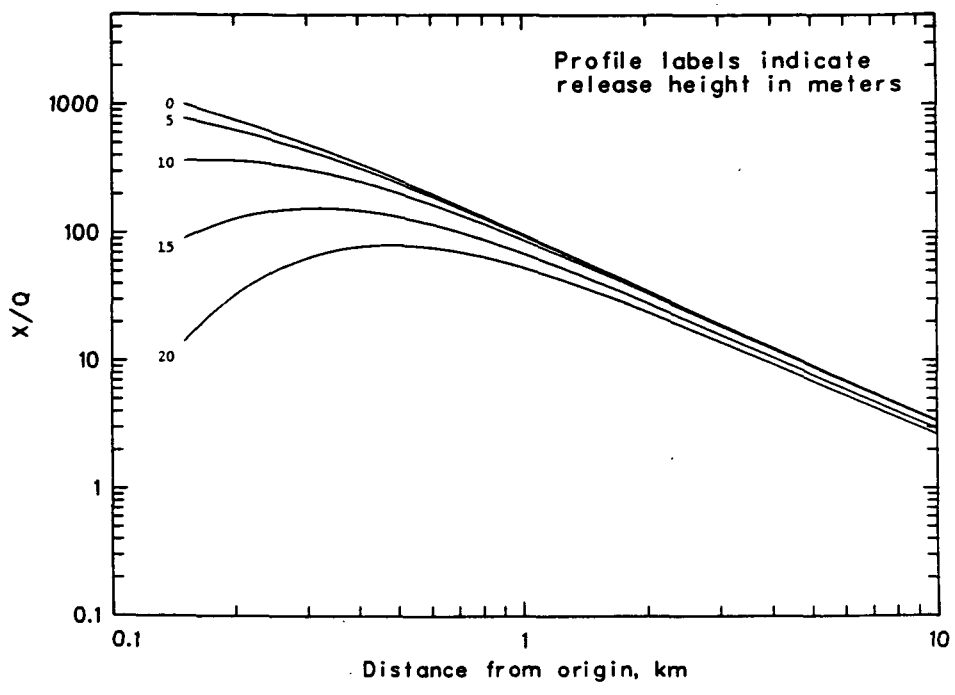

(e) Stability class E

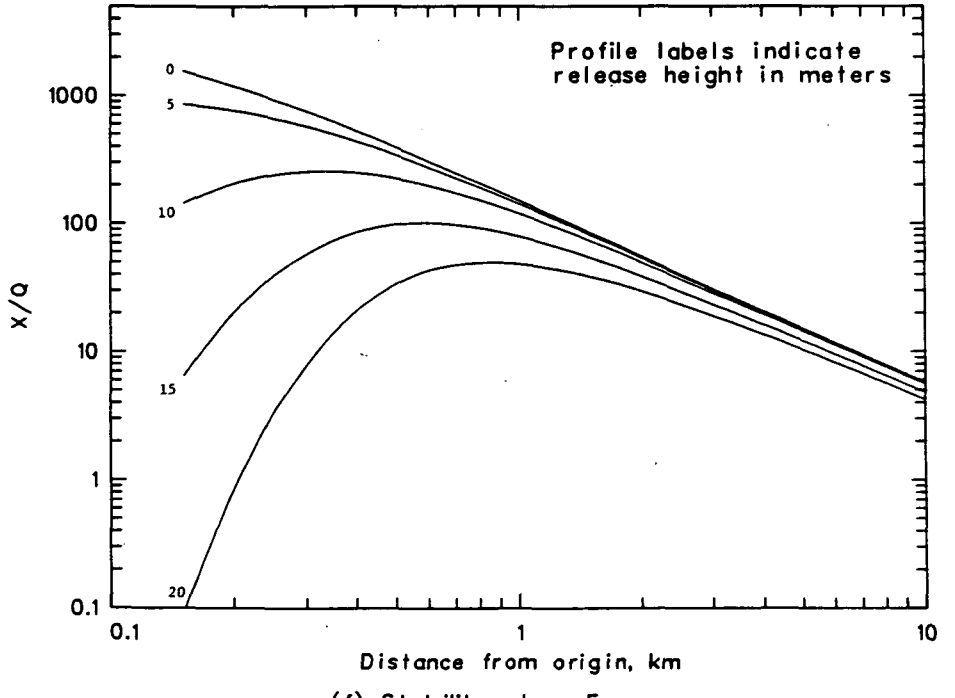

(f) Stability class F

Figure 24. Continued.

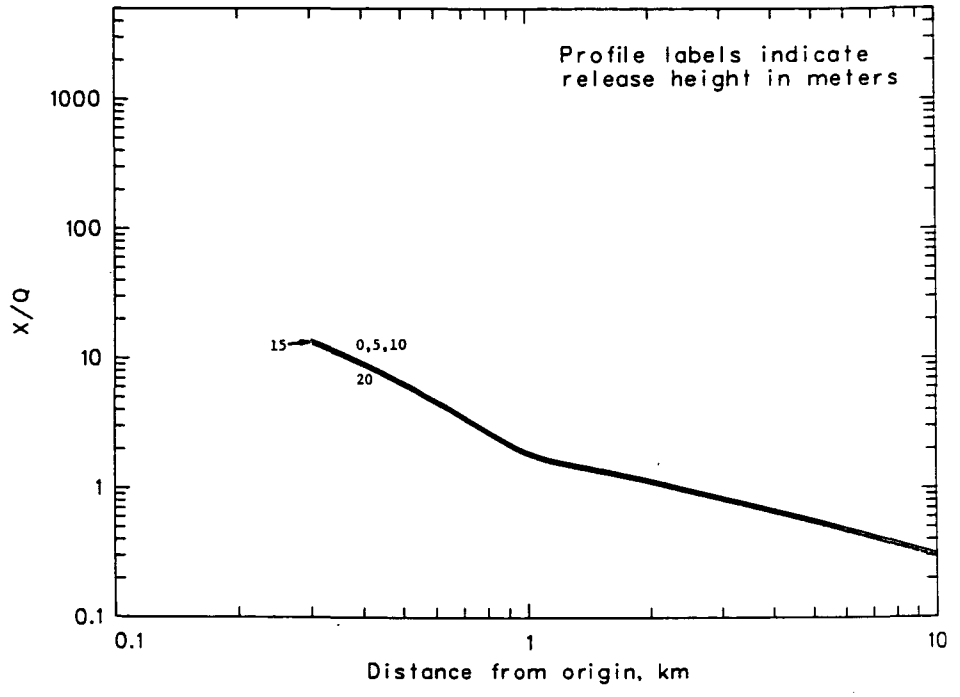

(a) Stability class A

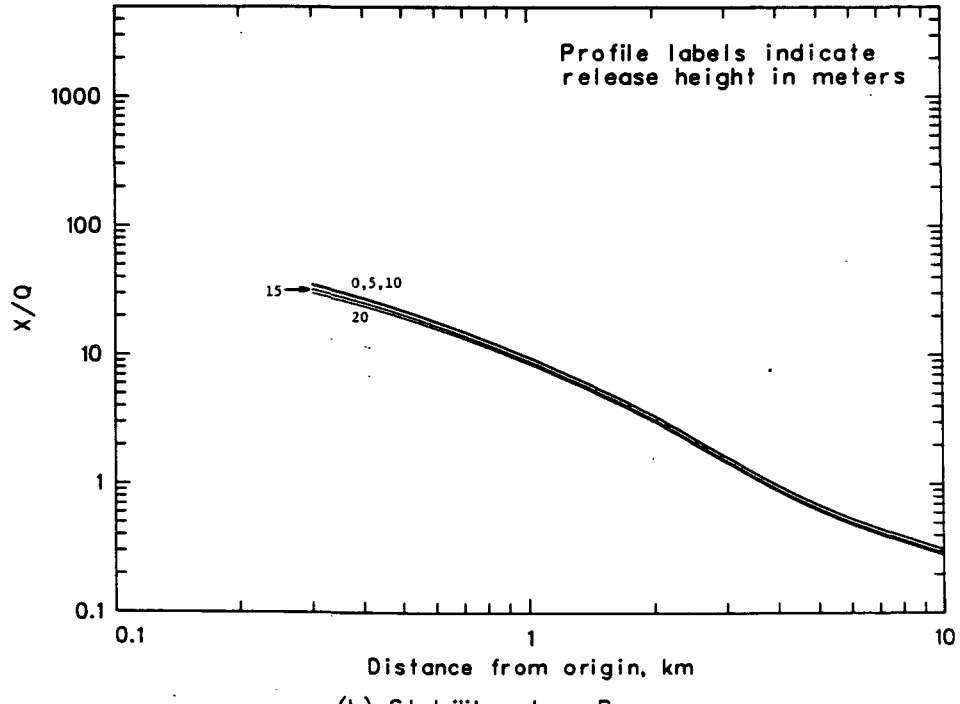

(b) Stability class B

Figure 25. PGPC (X/Q) profiles by release height for each stability class from the 316.2-m square source.

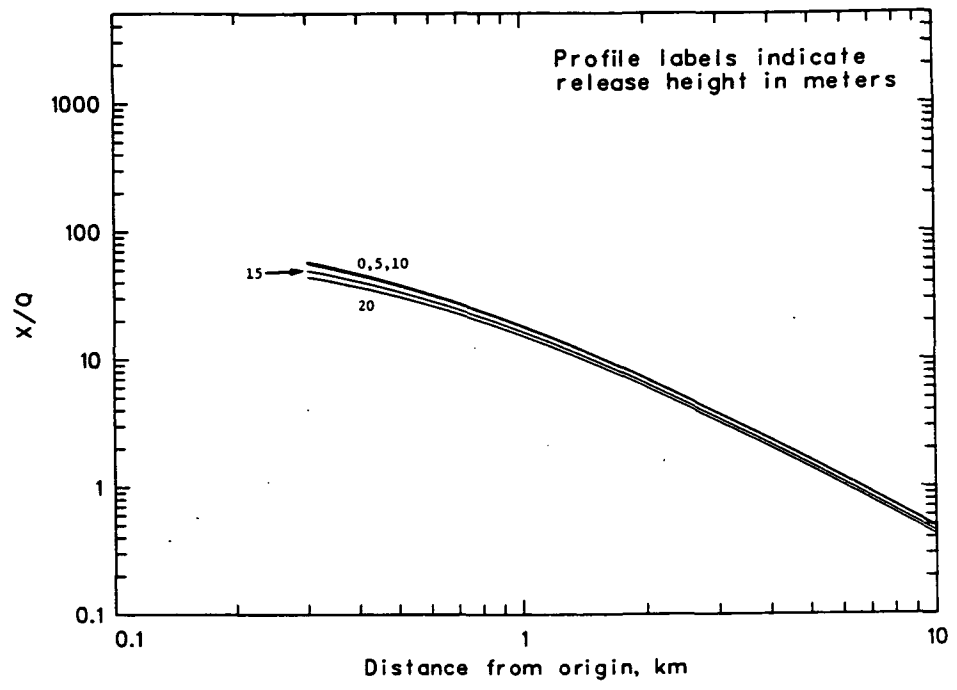

(c) Stability class C

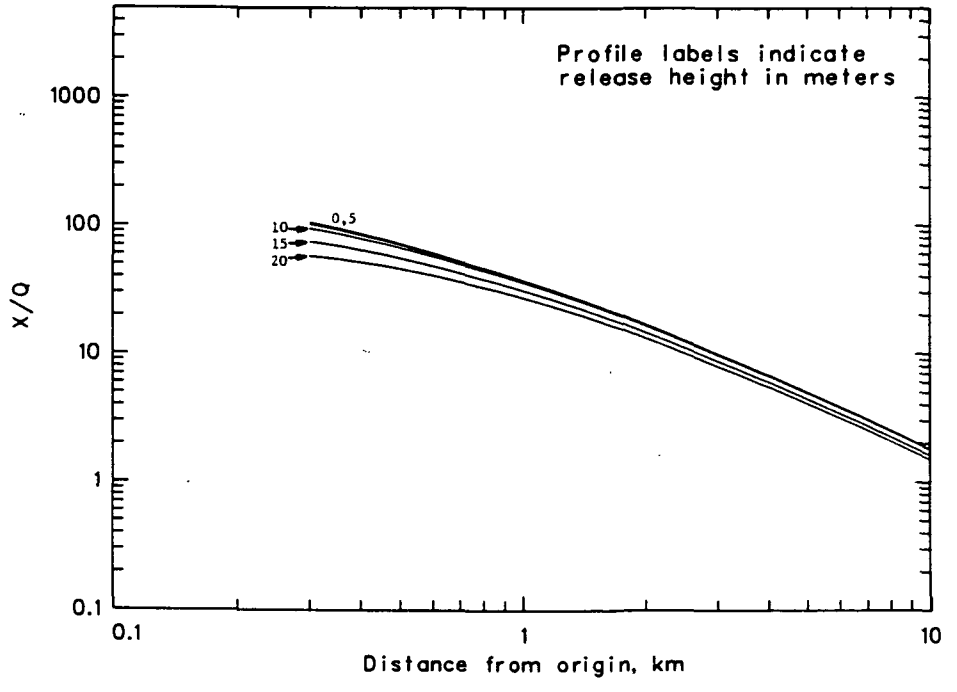

(d) Stability class D

Figure 25. Continued.

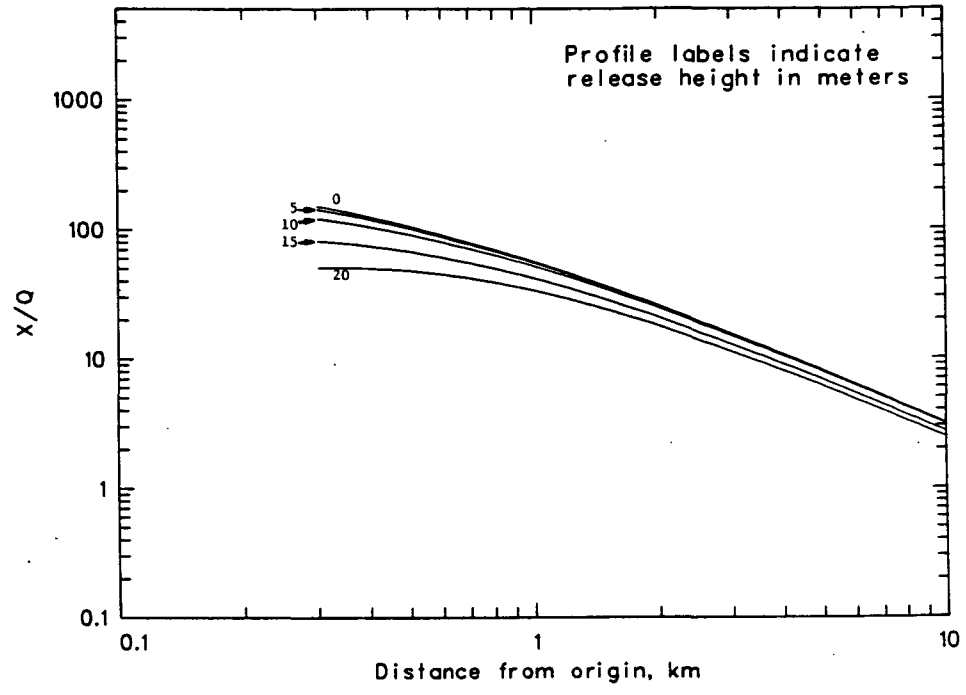

(e) Stability class E

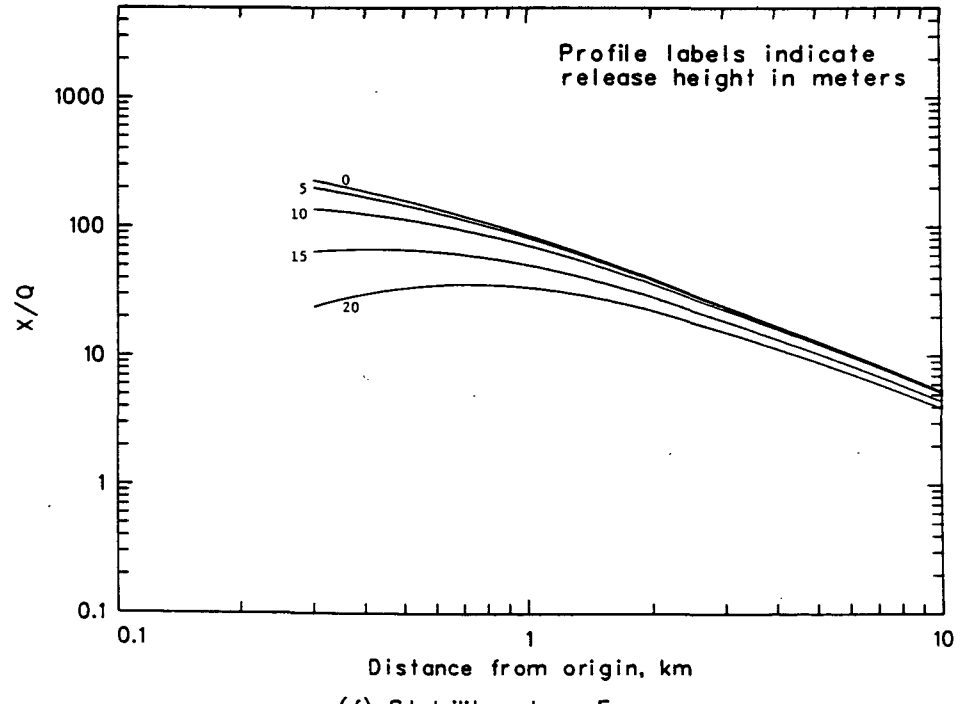

(f) Stability class F

Figure 25. Continued.

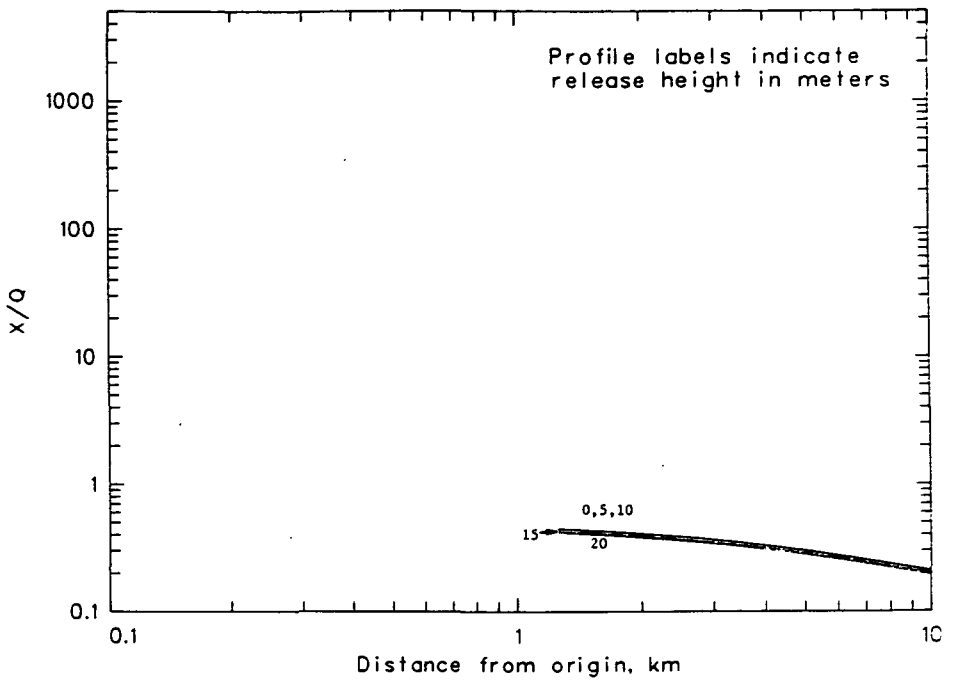

(a) Stability class A

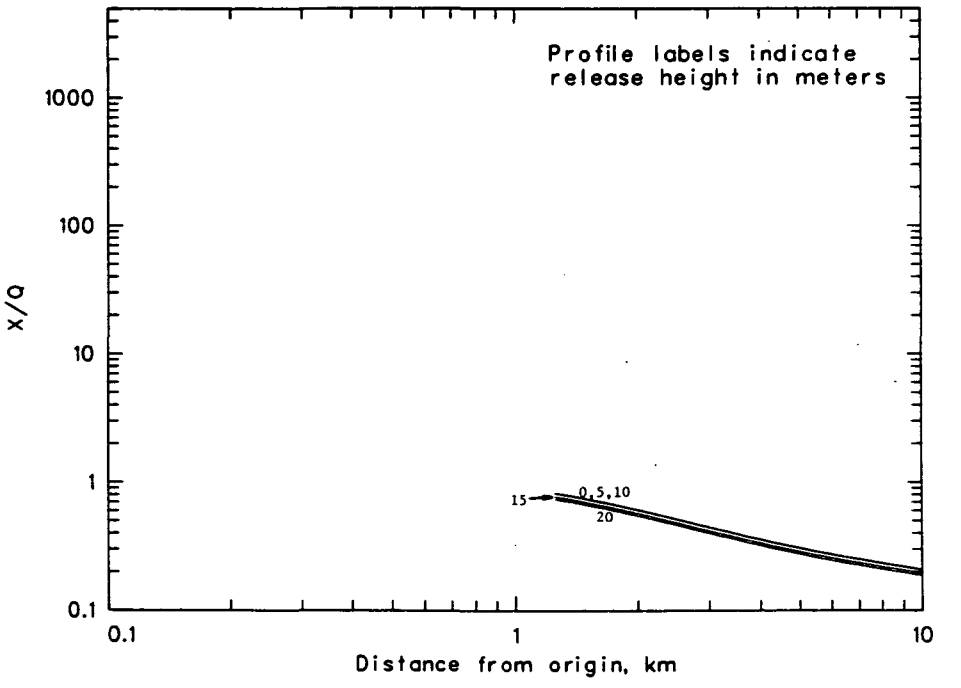

(b) Stability class B

Figure 26. PGPC (X/Q) profiles by release height for each stability class from the 2236.1-m square source.

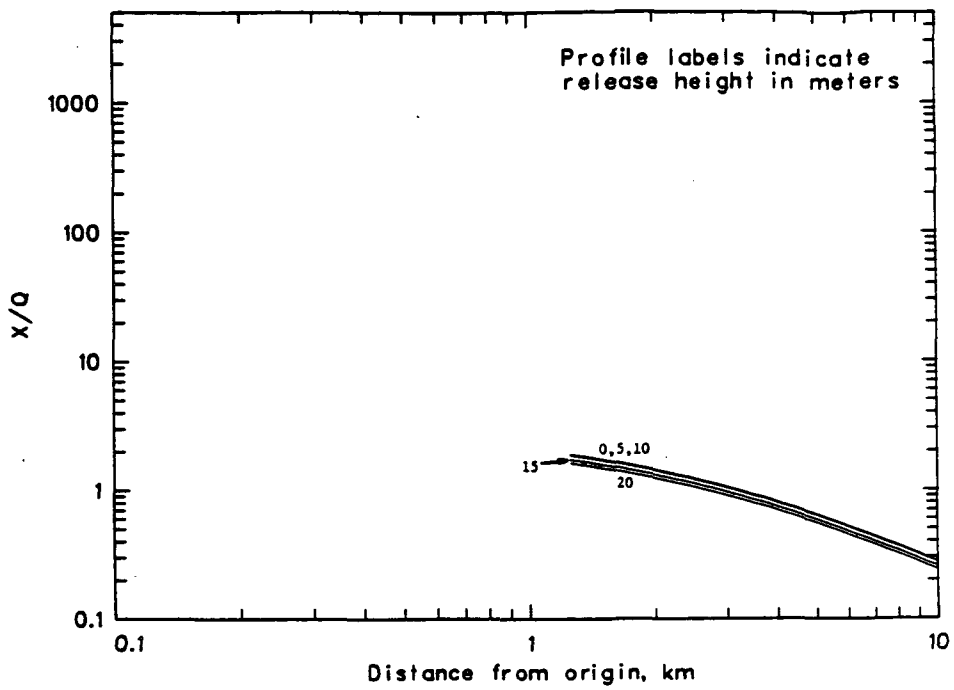

(c) Stability class C

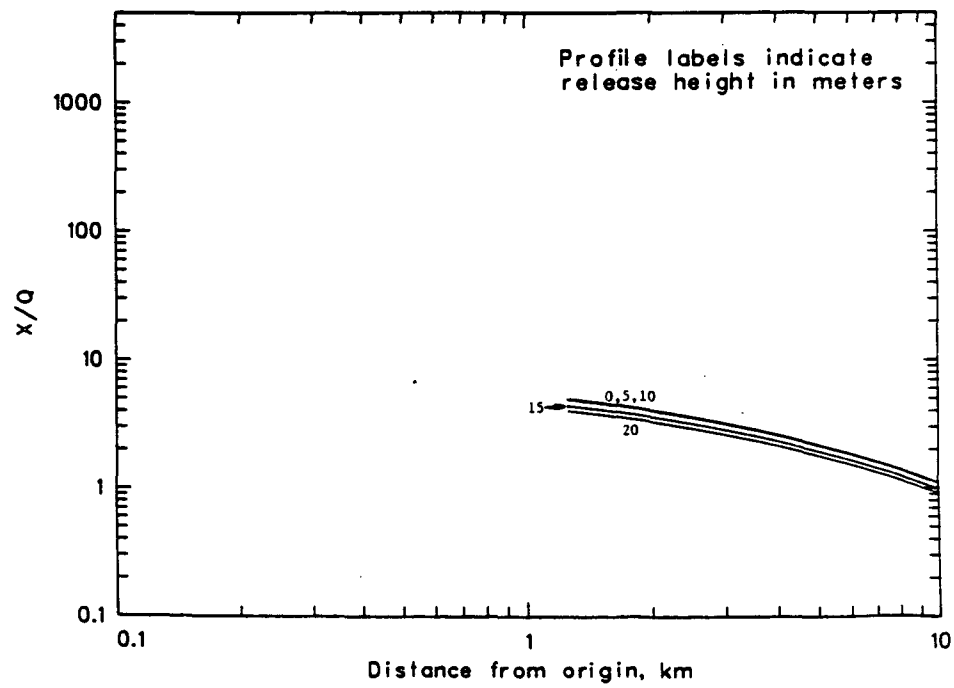

(d) Stability class D

Figure 26. Continued.

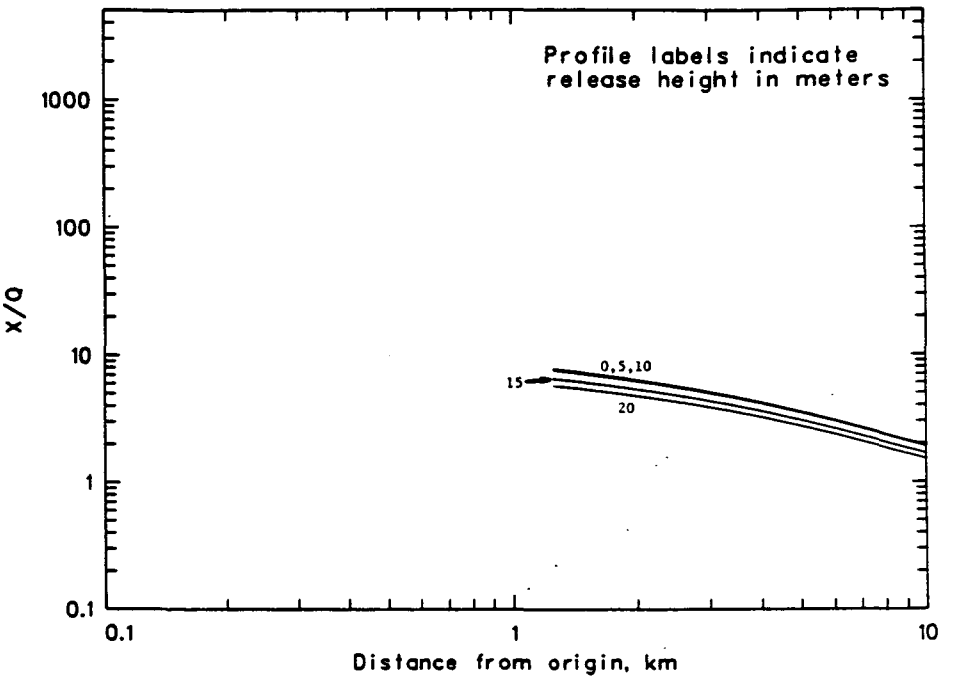

(e) Stability class E

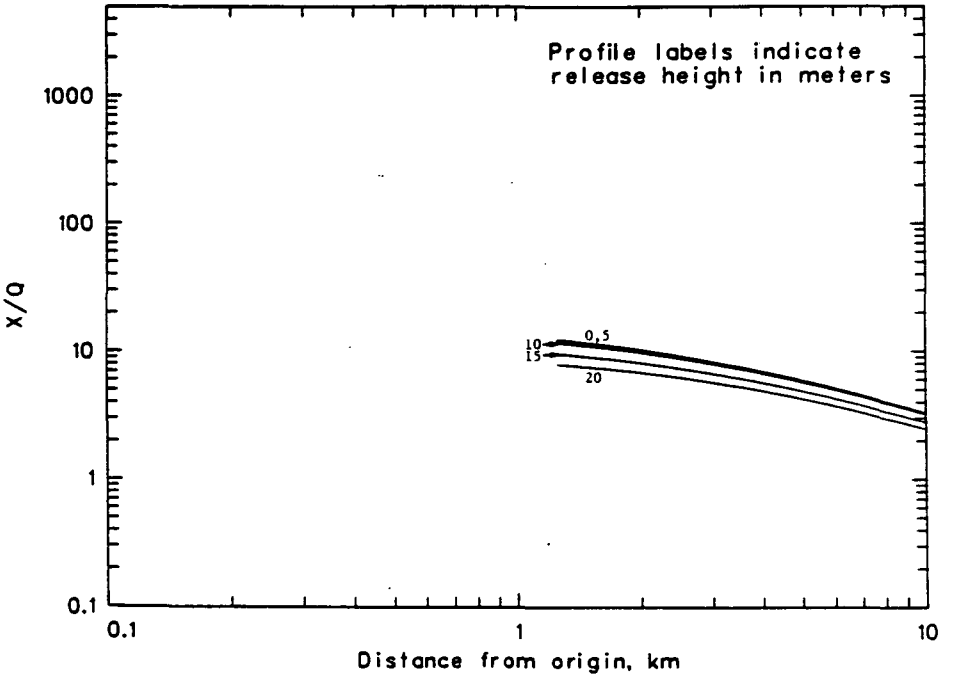

(f) Stability class F

Figure 26. Continued.

APPENDIX D

TGRC (X/Q) PROFILES BY RELEASE HEIGHT FOR EACH STABILITY CATEGORY AND EACH SOURCE

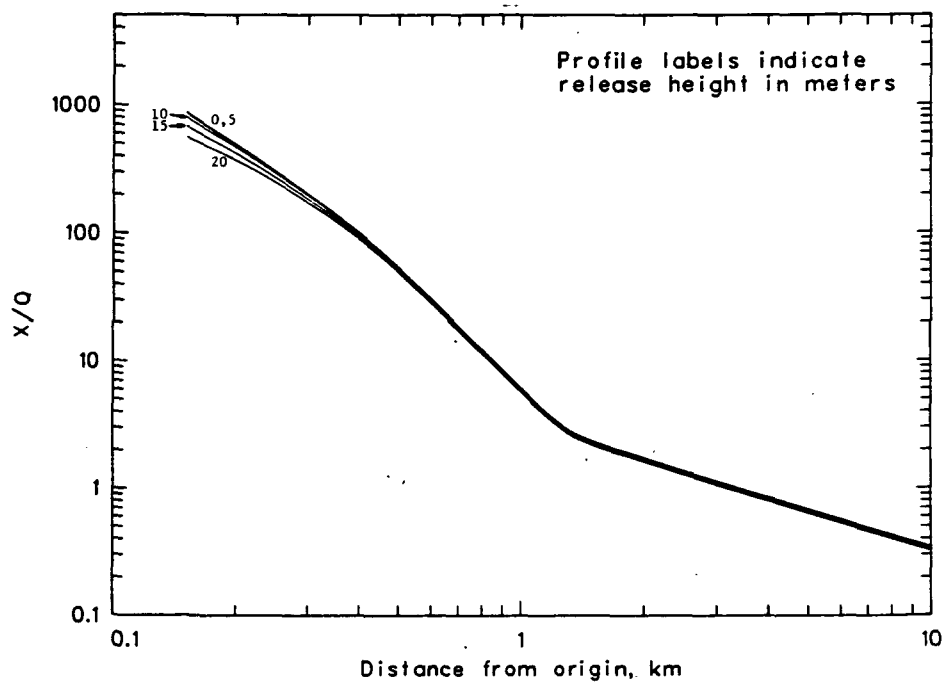

(a) Stability class A

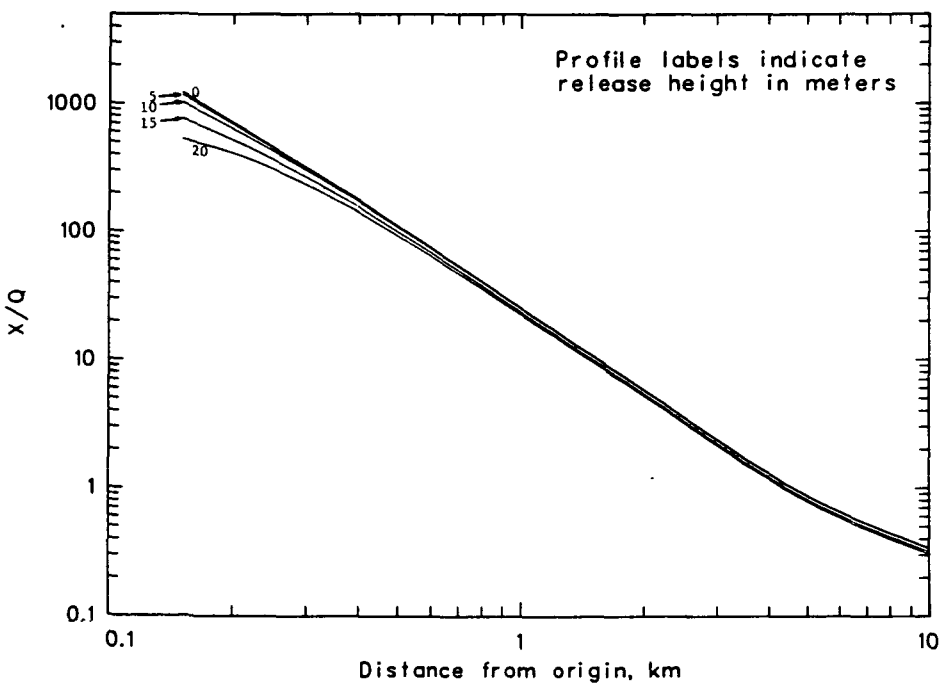

(b) Stability class B

Figure 27. TGRC (X/Q) profiles by release height for each stability class from the 14.1-m square source.

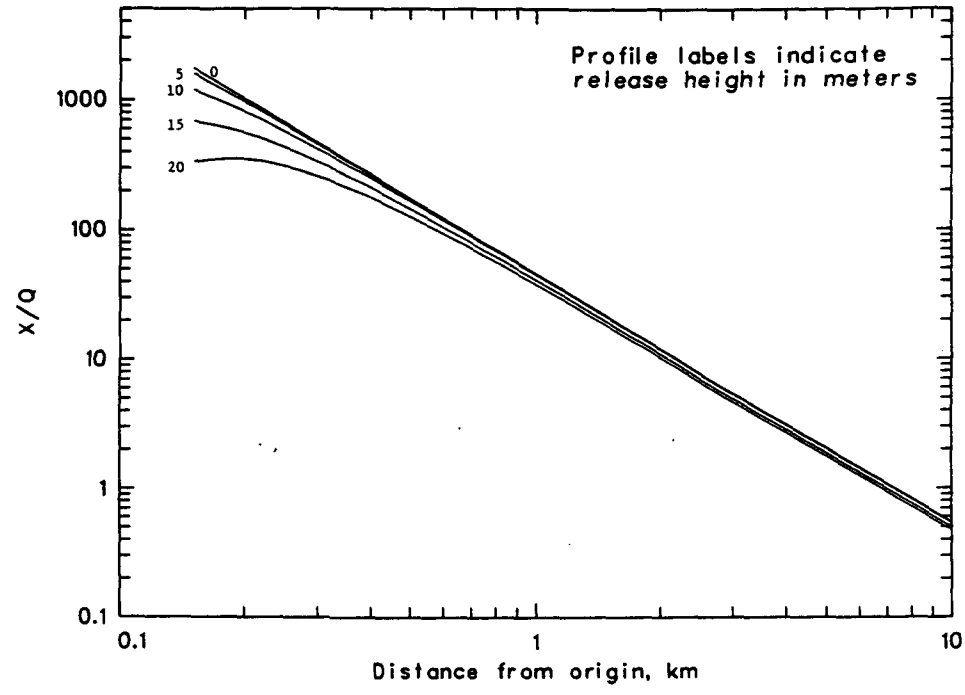

(c) Stability class C

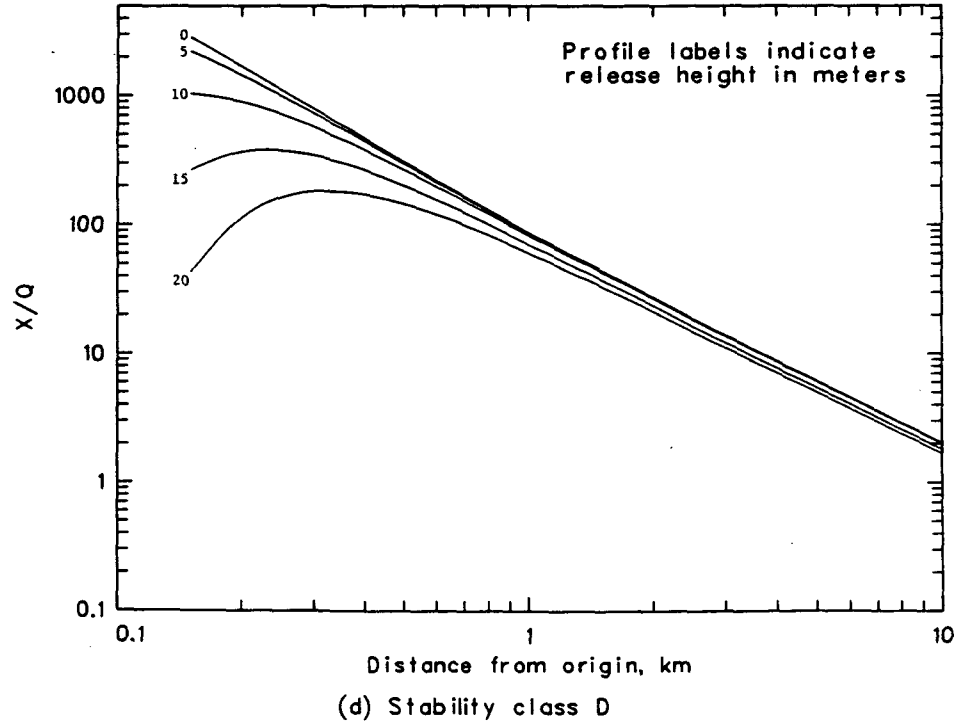

(d) Stability class D

Figure 27. Continued.

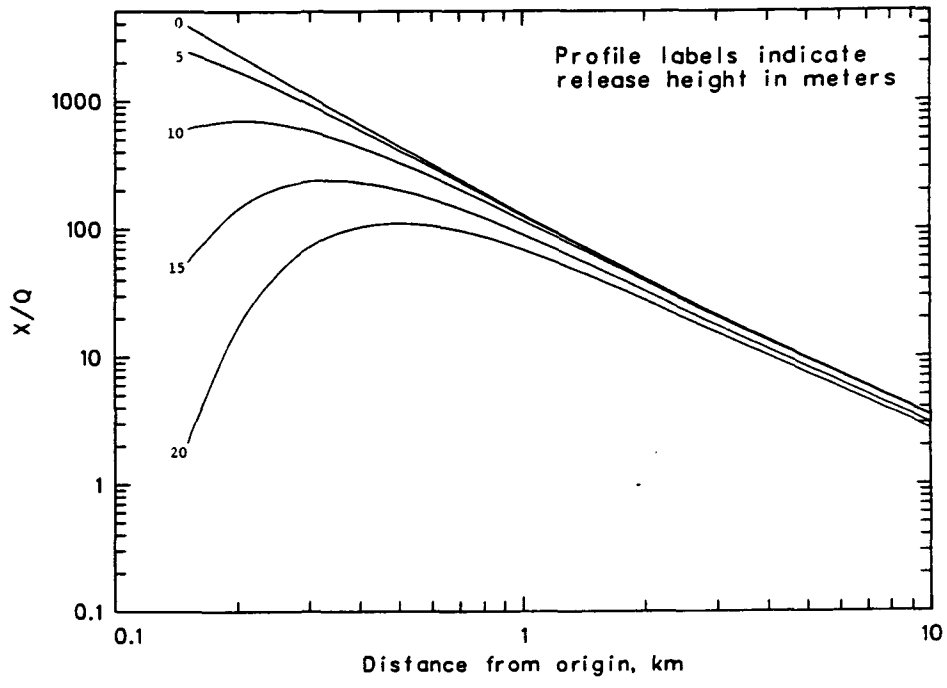

(e) Stability class E

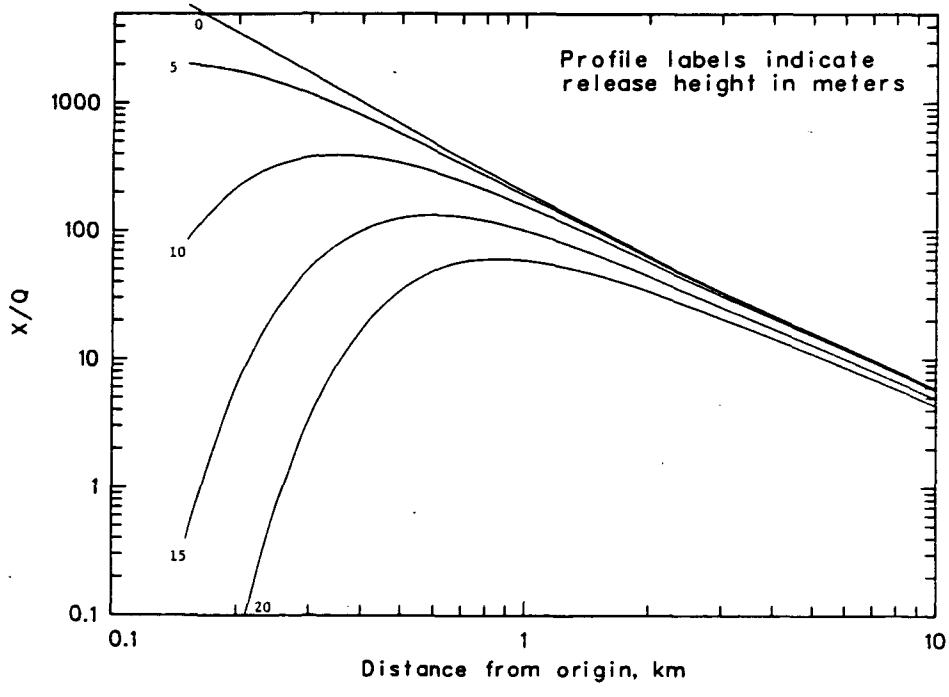

(f) Stability class F

Figure 27. Continued.

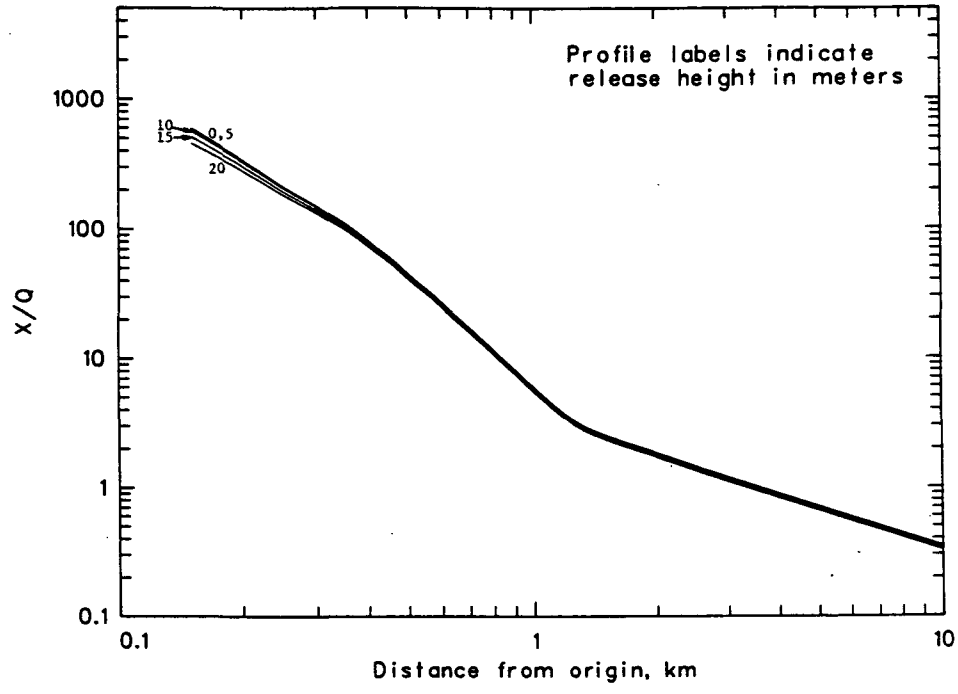

(a) Stability class A

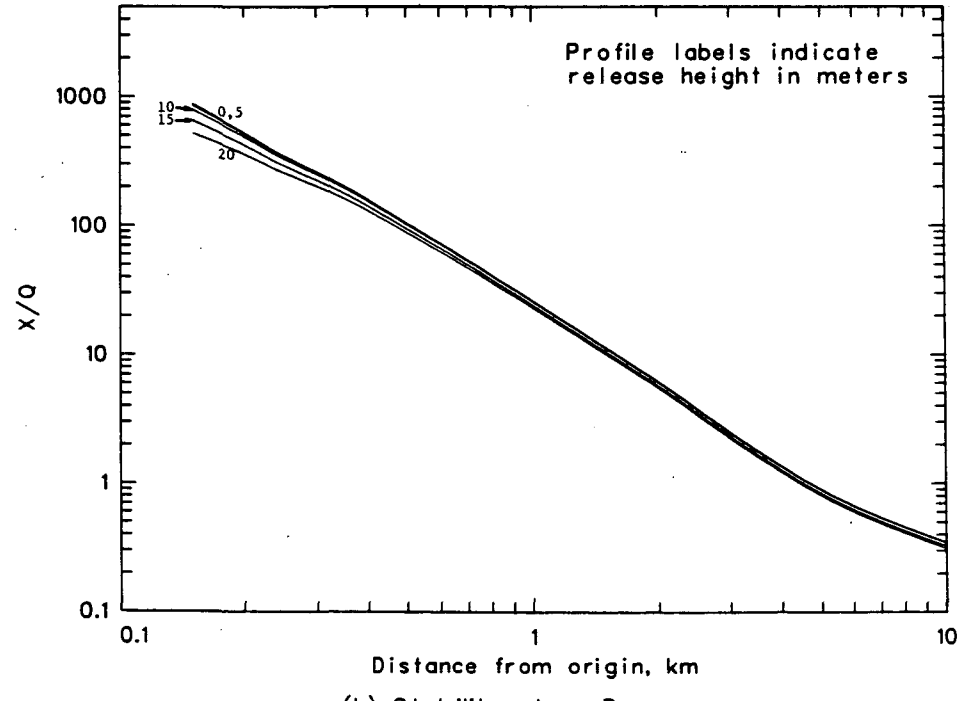

(b) Stability class B

Figure 28. TGRC (X/Q) profiles by release height for each stability class from the 80.6-m square source.

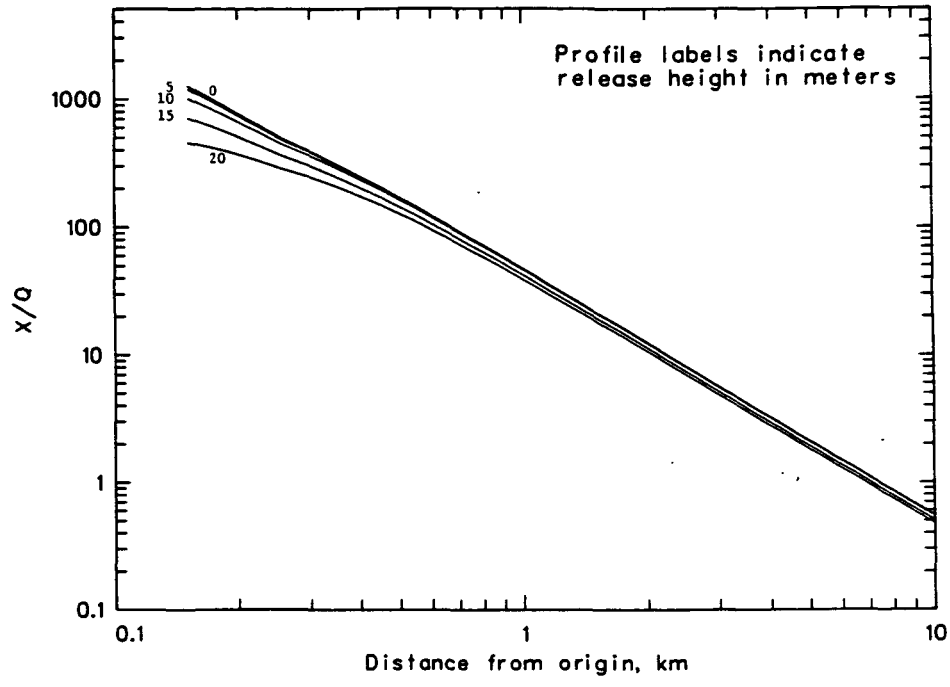

(c) Stability class C

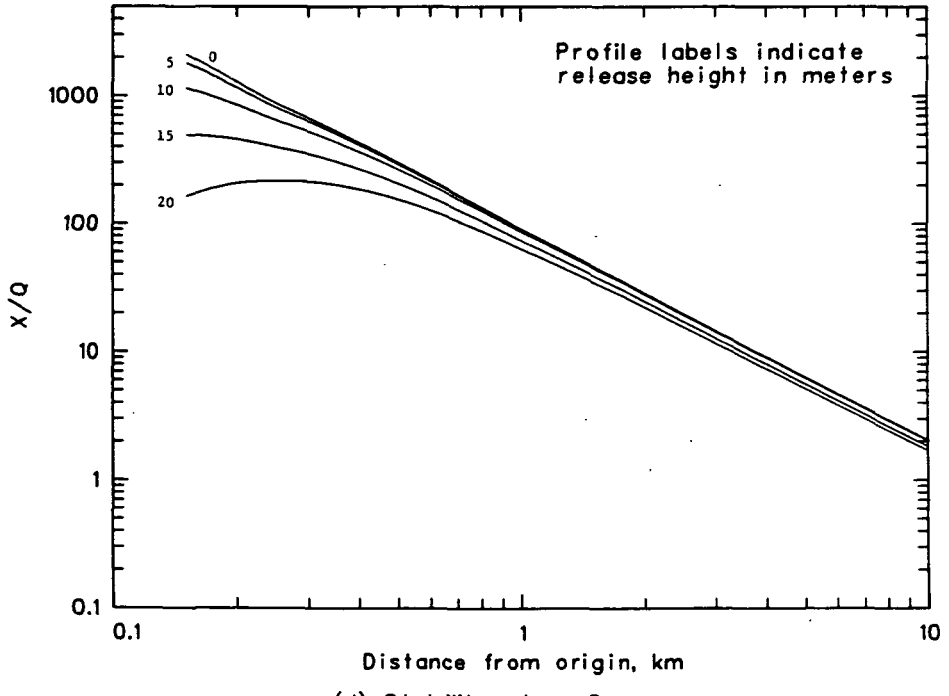

(d) Stability class D

Figure 28. Continued.

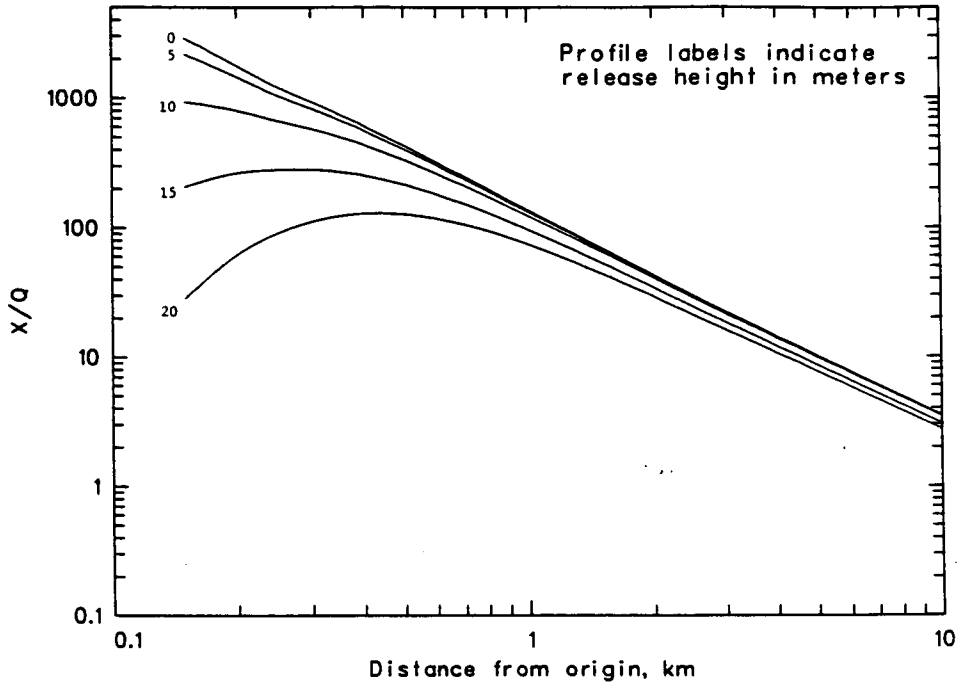

(e) Stability class E

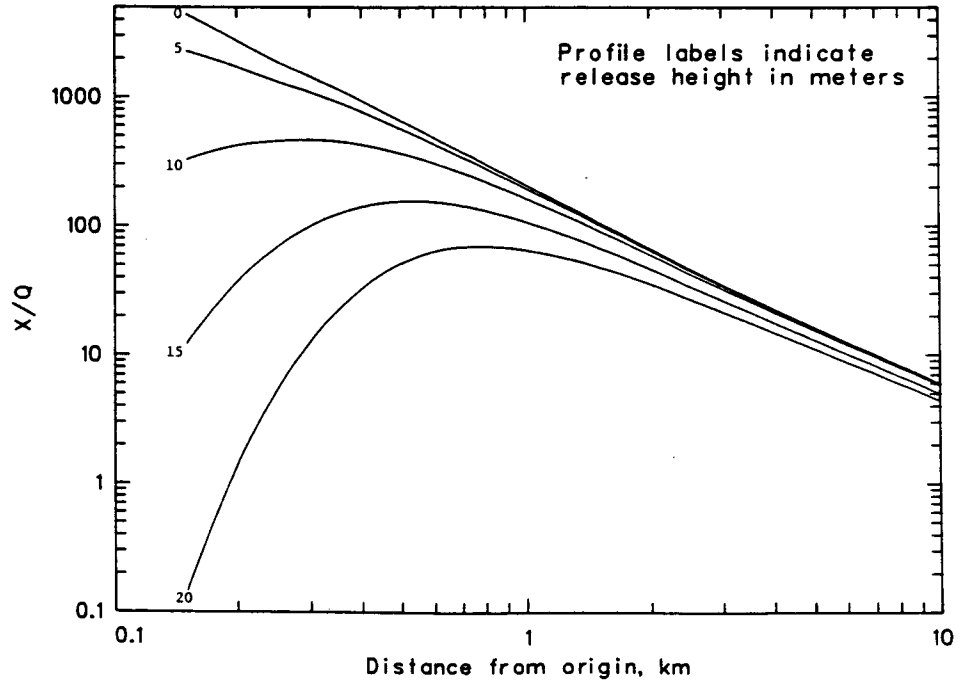

(f) Stability class F

Figure 28. Continued.

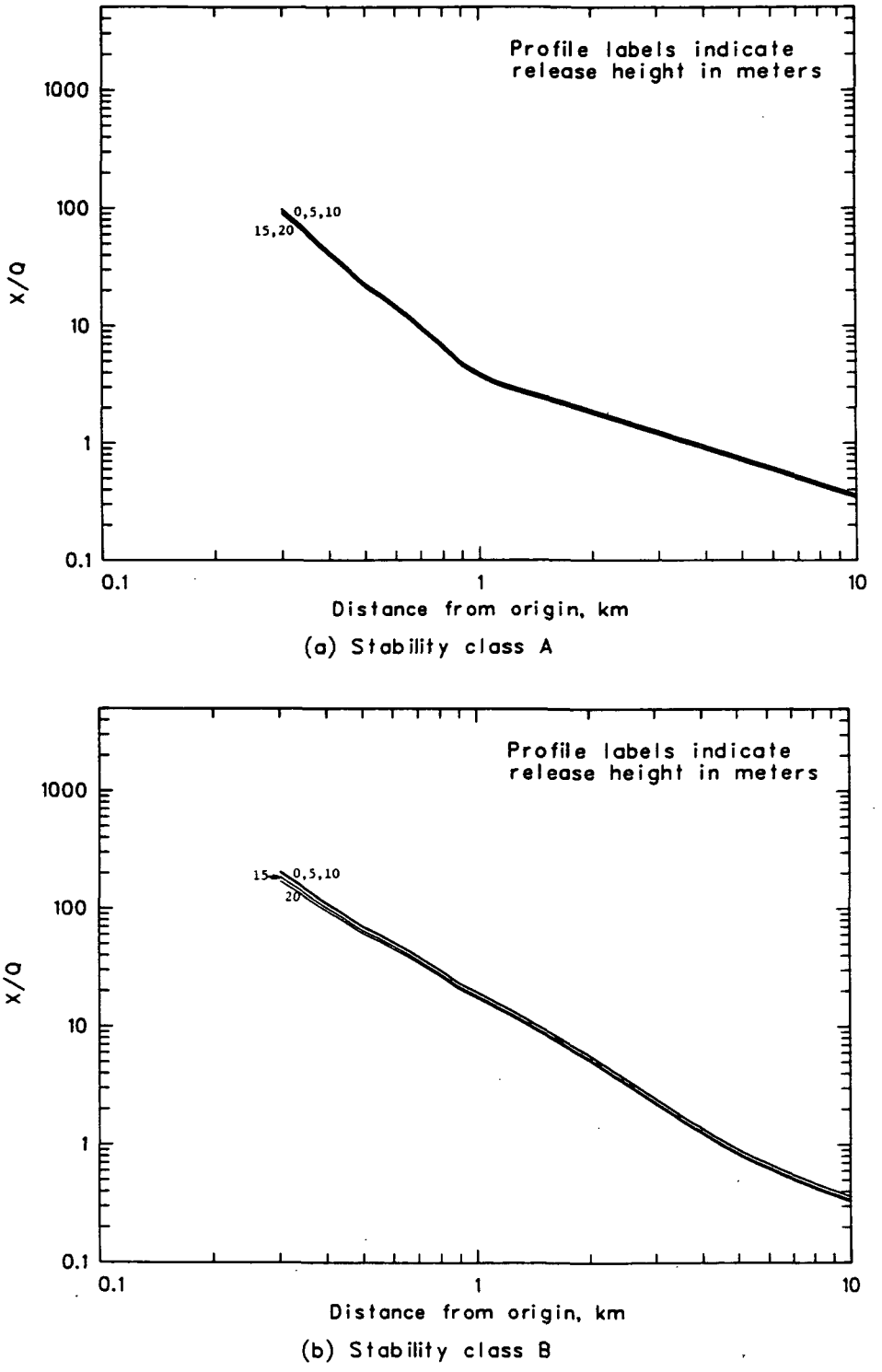

Figure 29. TGRC (X/Q) profiles by release height for each stability class from the 316.2-m square source.

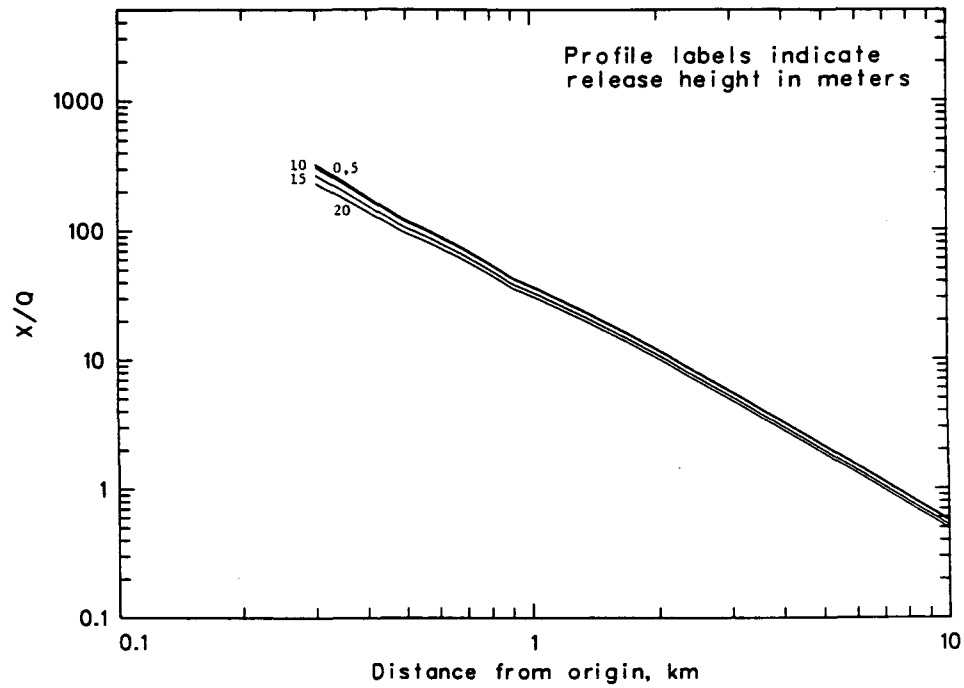

(c) Stability class C

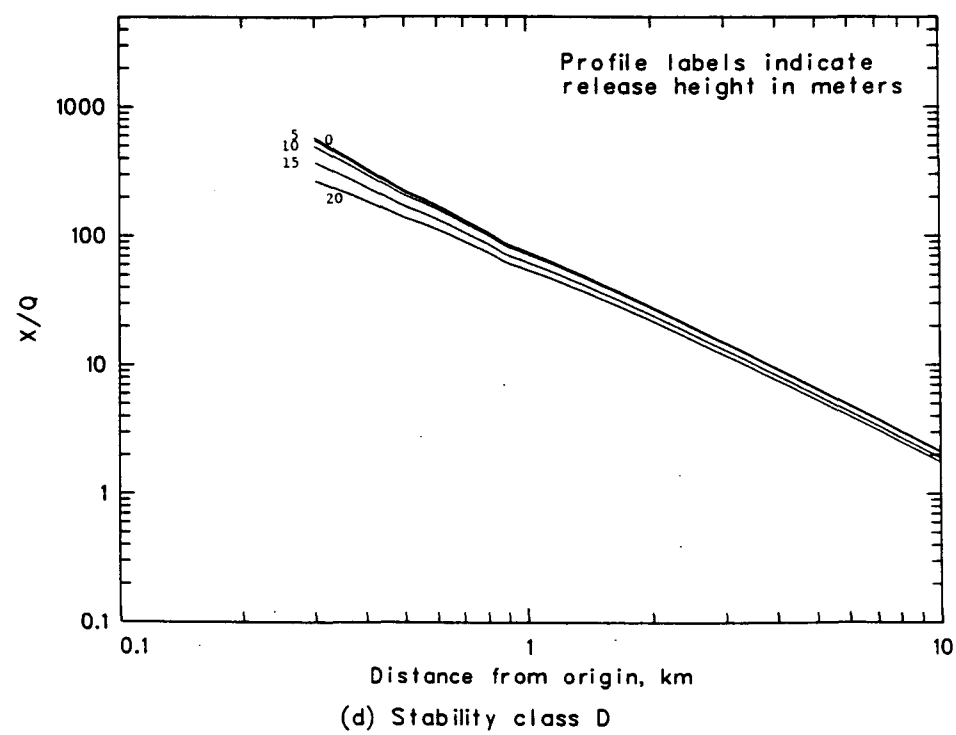

(d) Stability class D

Figure 29. Continued.

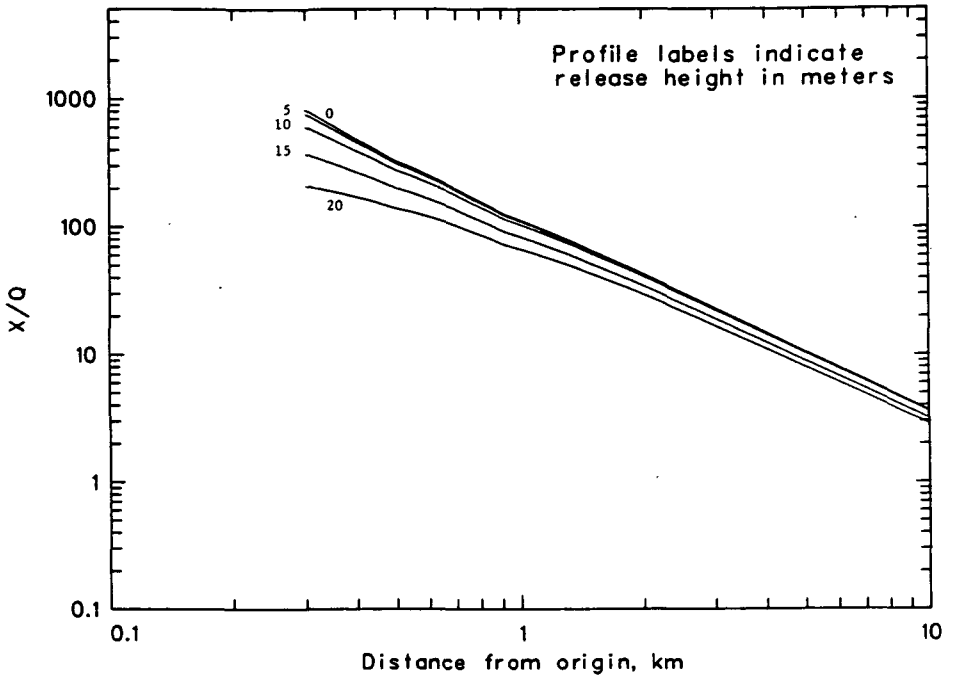

(e) Stability class E

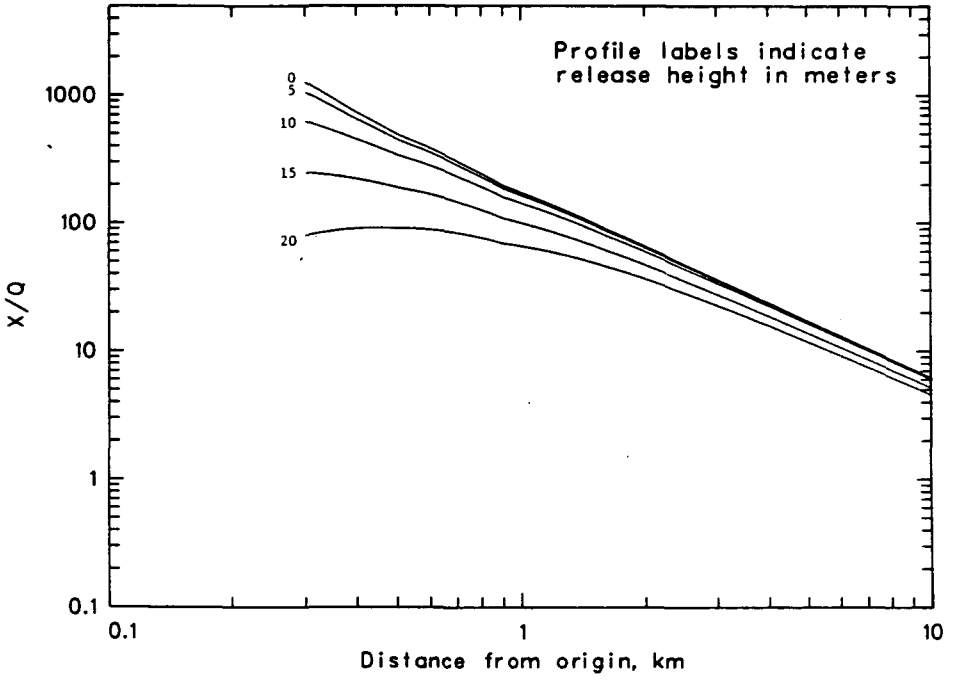

(f) Stability class F

Figure 29. Continued.

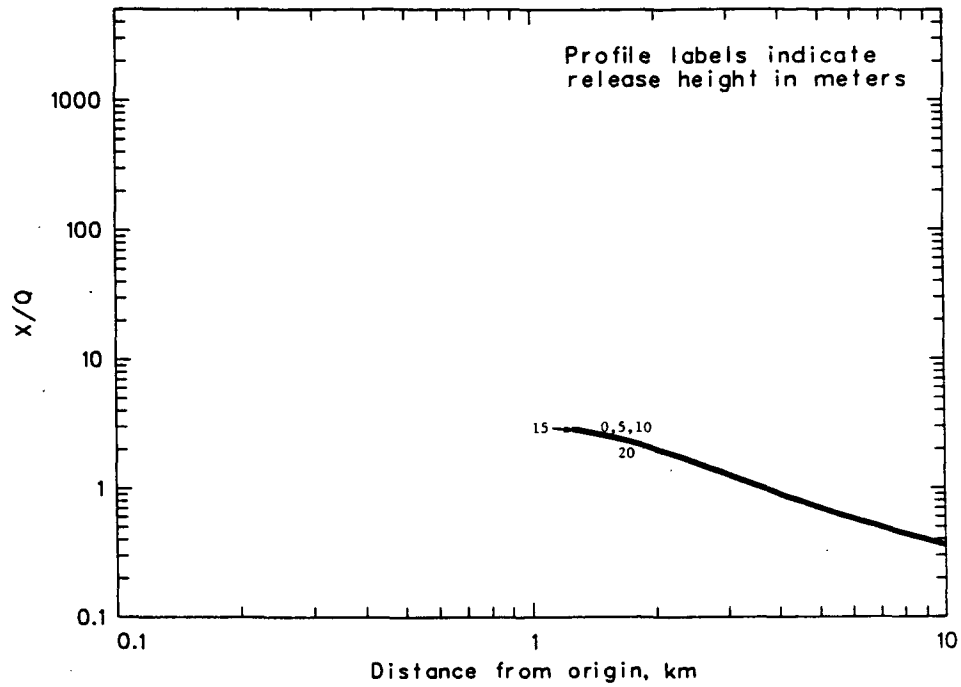

(a) Stability class A

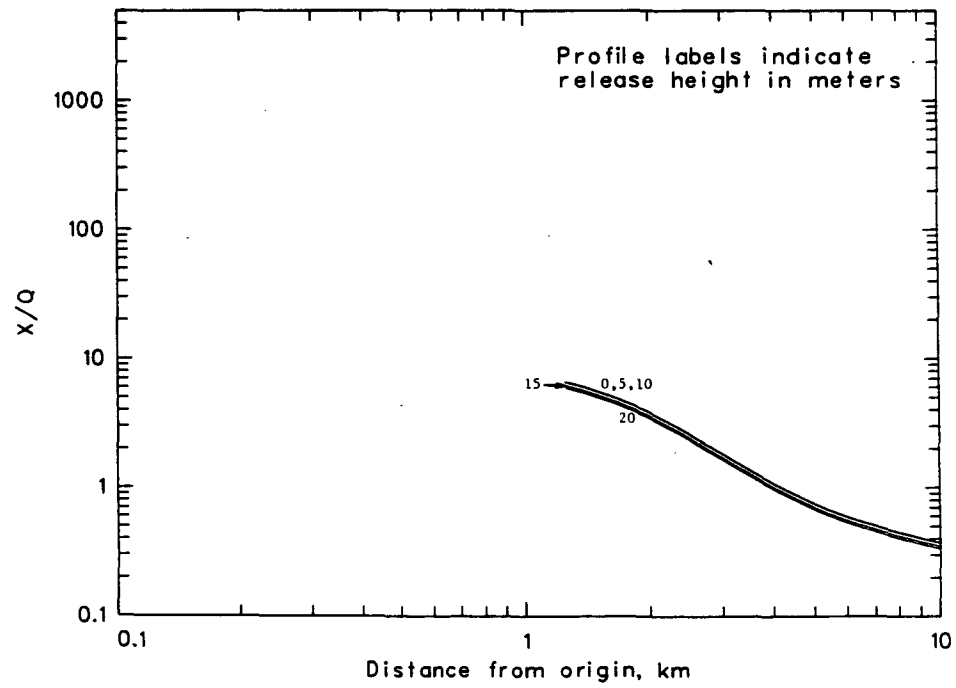

(b) Stability class B

Figure 30. TGRC (X/Q) profiles by release height for each stability class from the 2236.1-m square source.

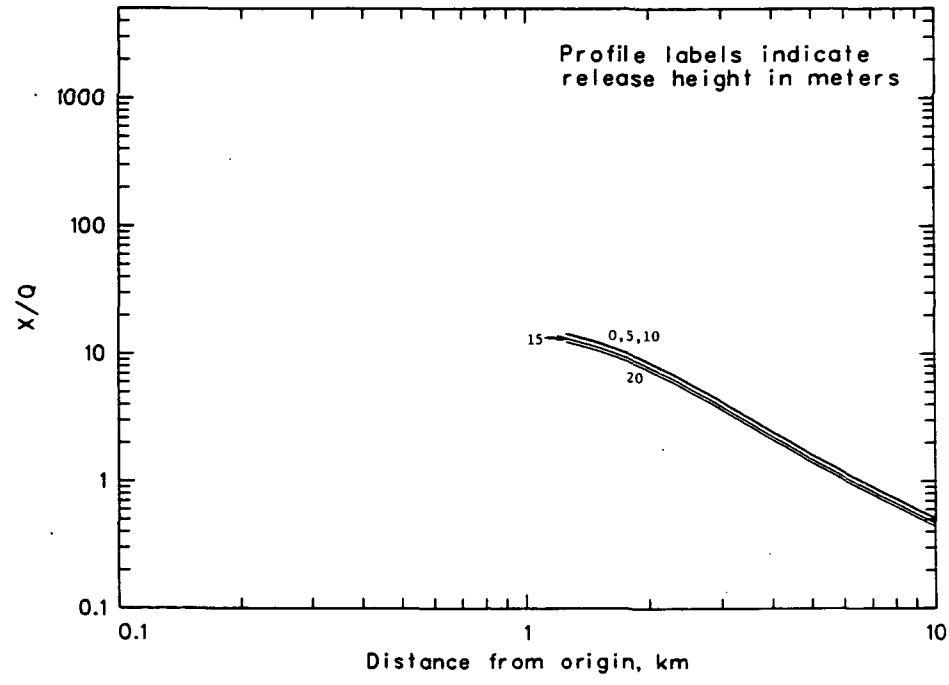

(c) Stability class C

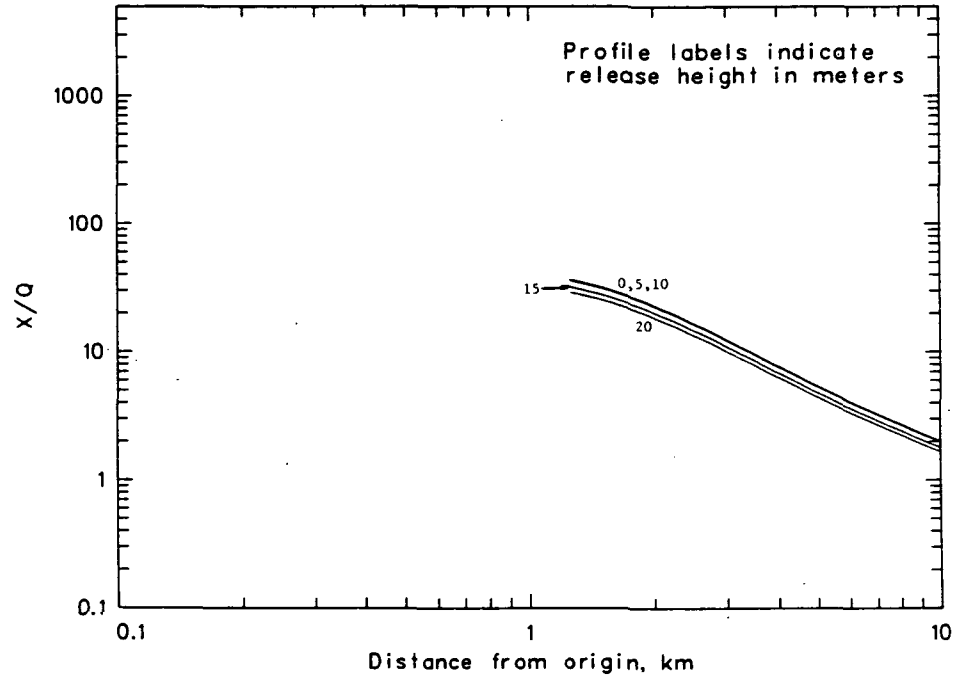

(d) Stability class D

Figure 30. Continued.

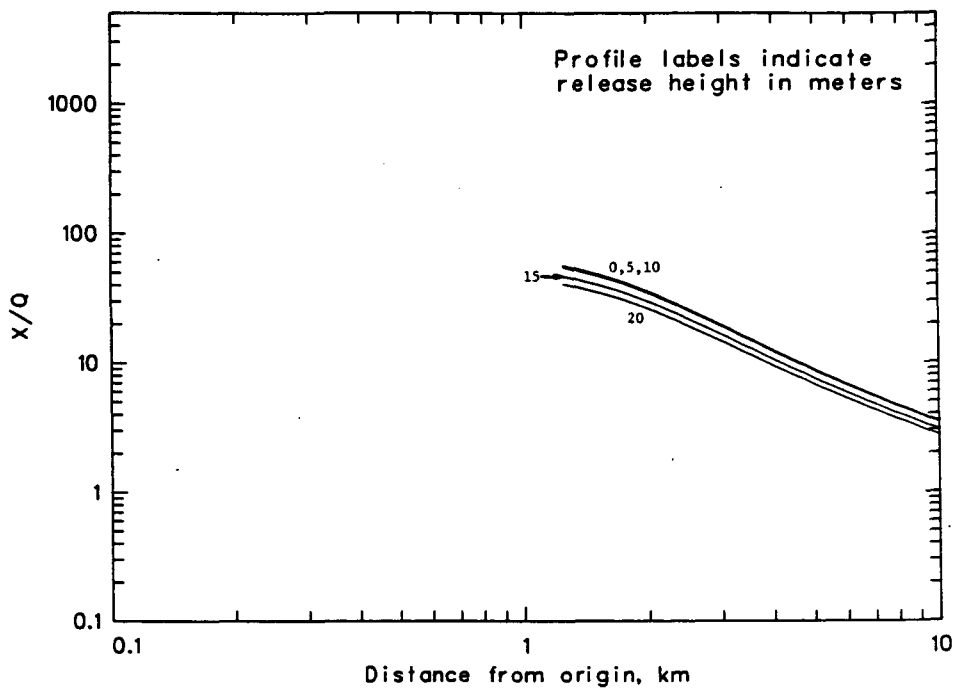

(e) Stability class E

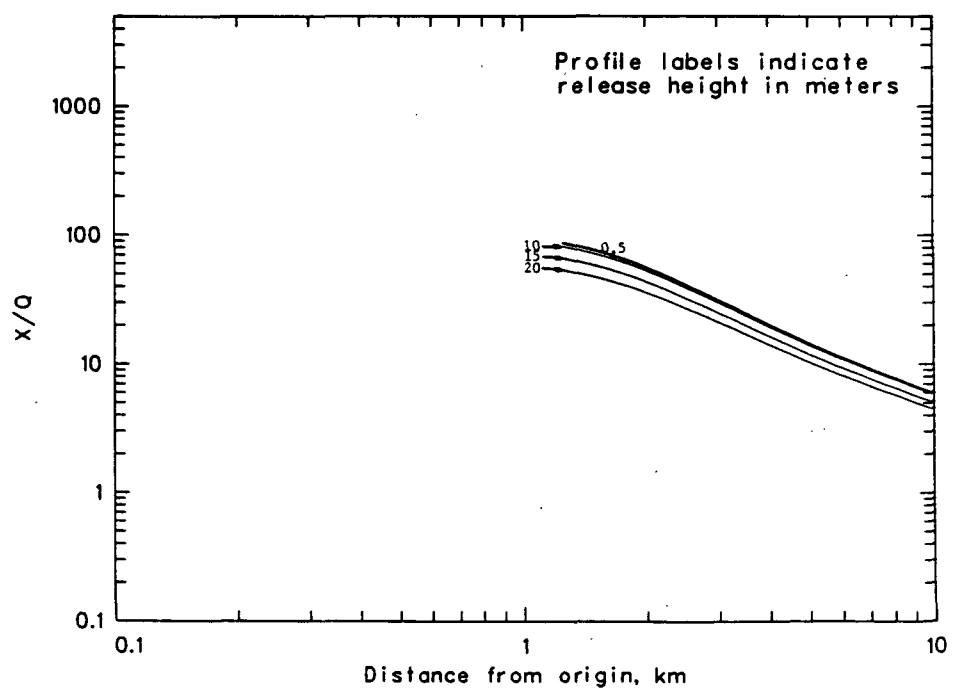

(f) Stability class F

Figure 30. Continued.

APPENDIX E

PGPC (X/Q) PROFILES BY SOURCE WIDTH FOR EACH STABILITY CATEGORY AND RELEASE HEIGHT

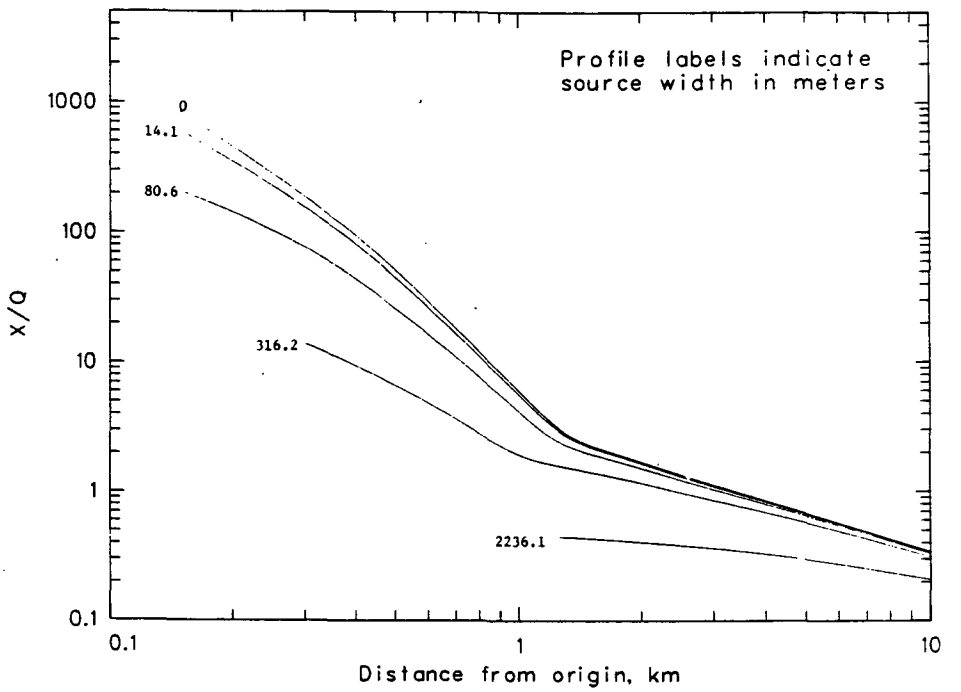

(a) Stability class A

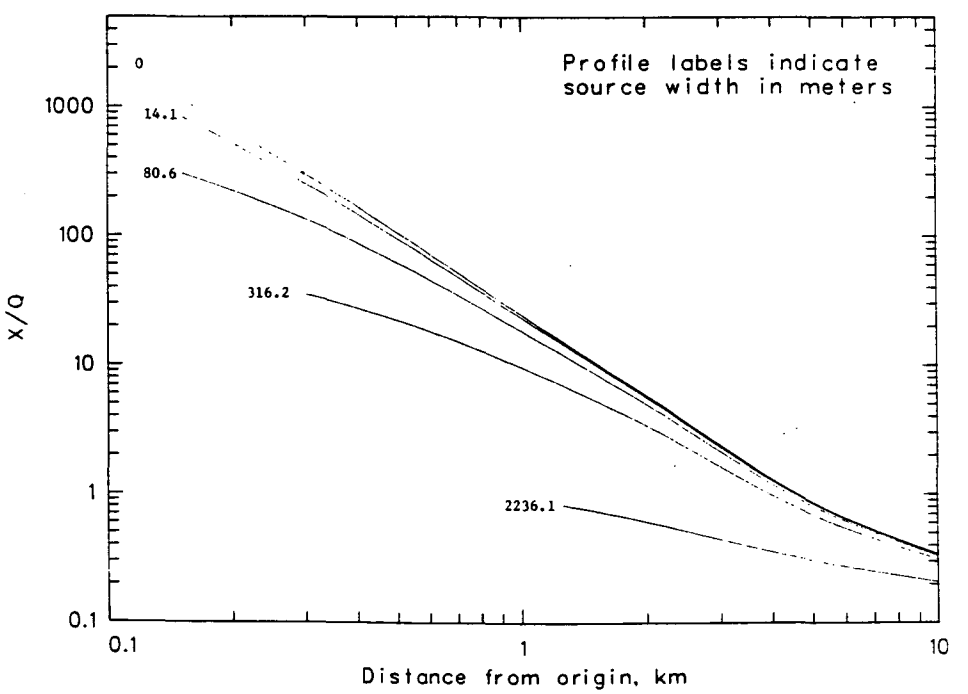

(b) Stability class B

Figure 31. PGPC (X/Q) profiles by source width for each stability class and 0-m-high releases.

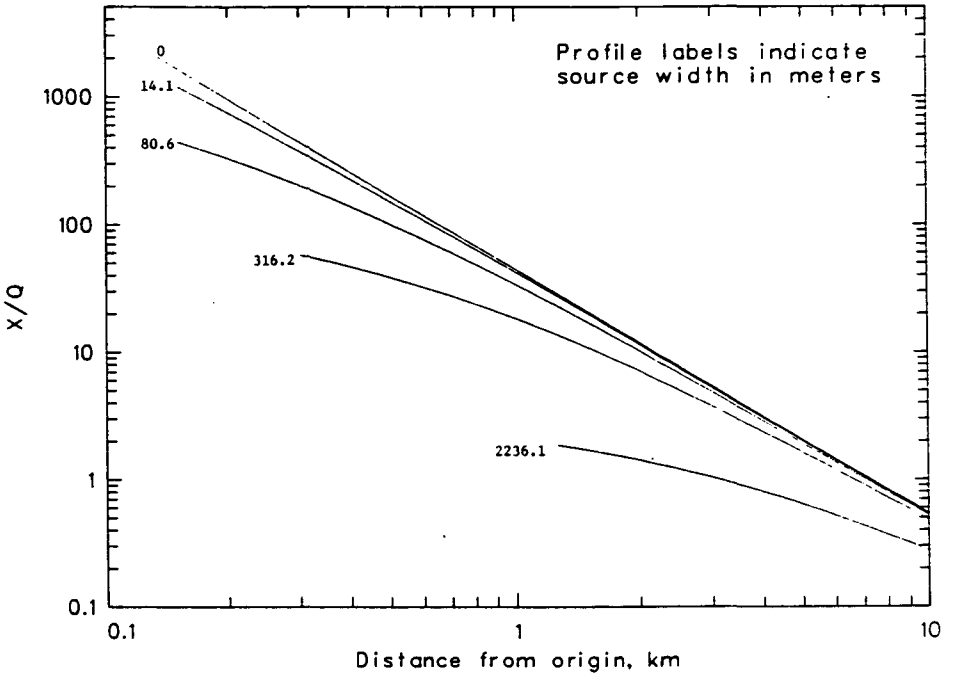

(c) Stability class C

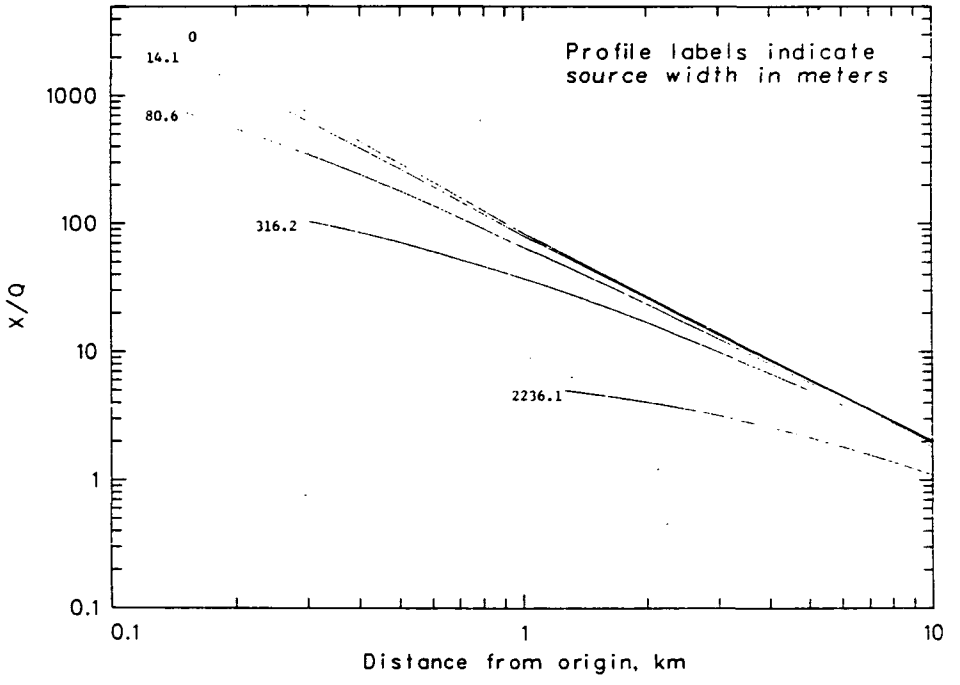

(d) Stability class D

Figure 31. Continued.

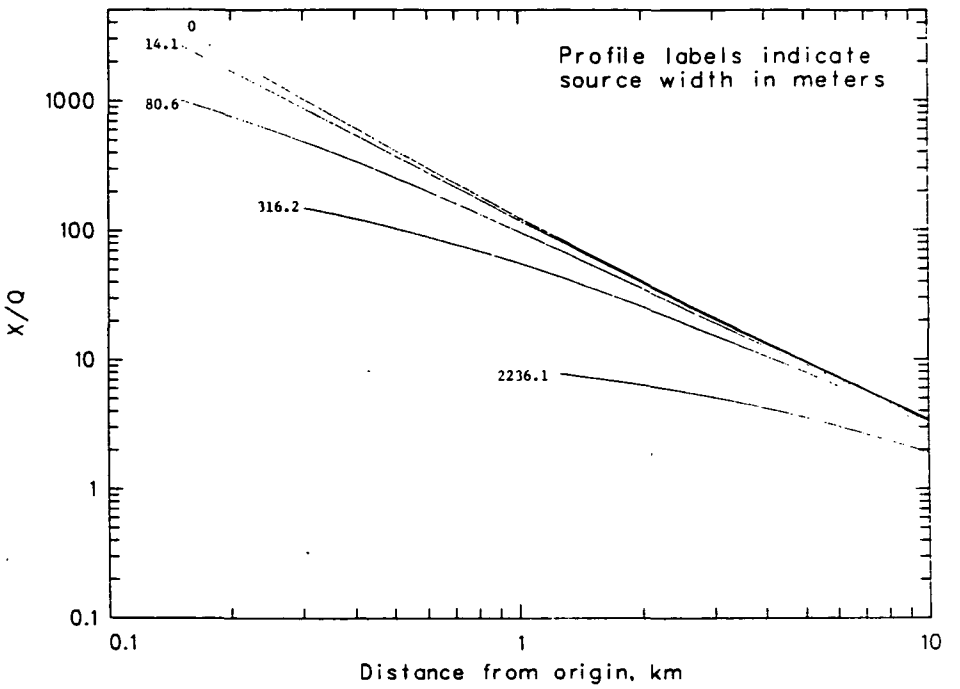

(e) Stability class E

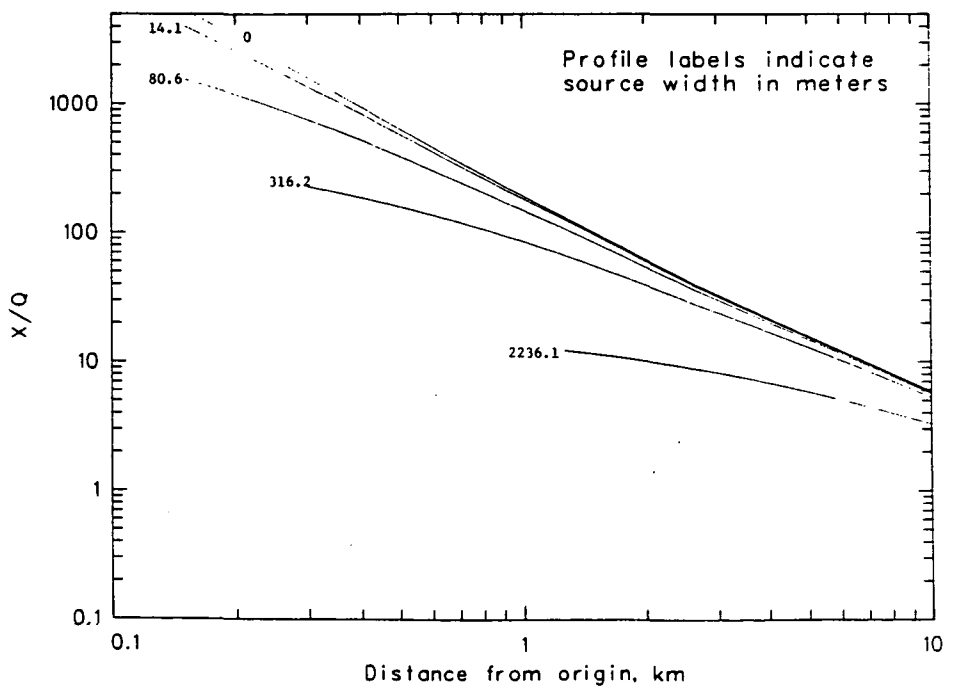

(f) Stability class F

Figure 31. Continued.

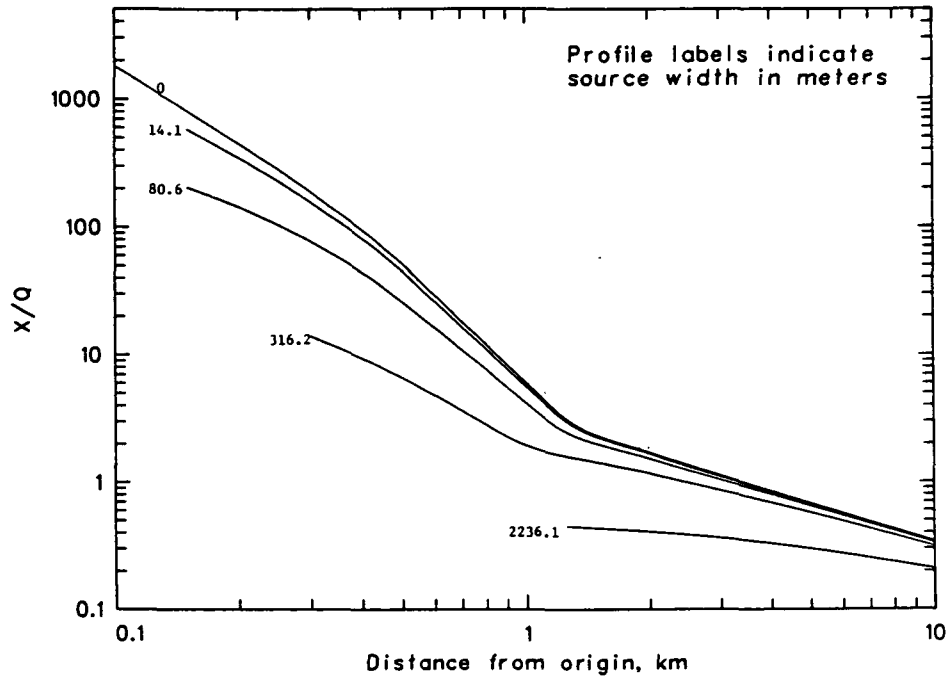

(a) Stability class A

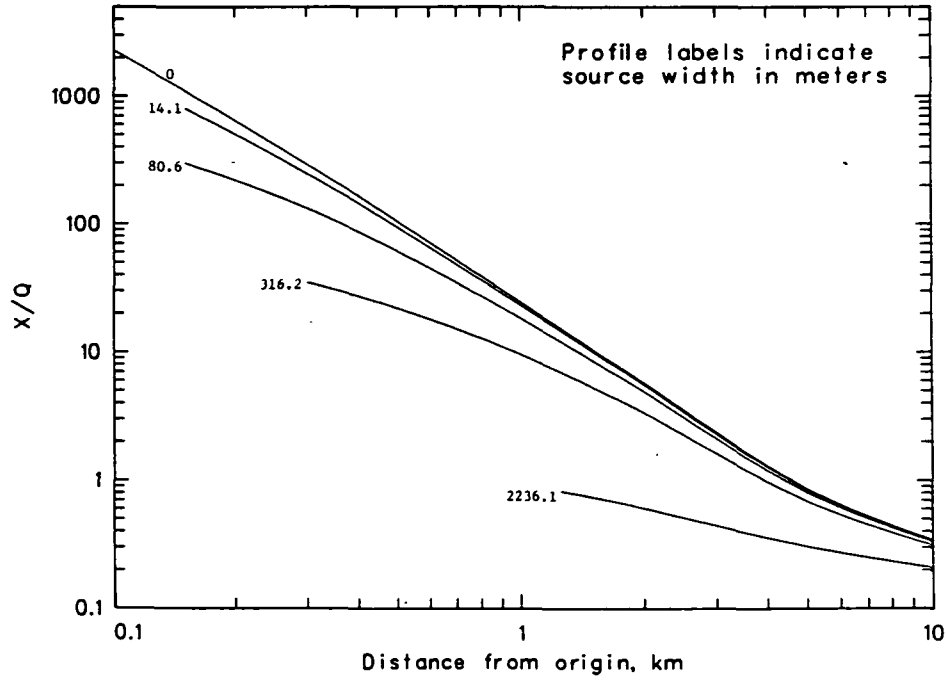

(b) Stability class B

Figure 32. PGPC (X/Q) profiles by source width for each stability class and 5-m-high releases.

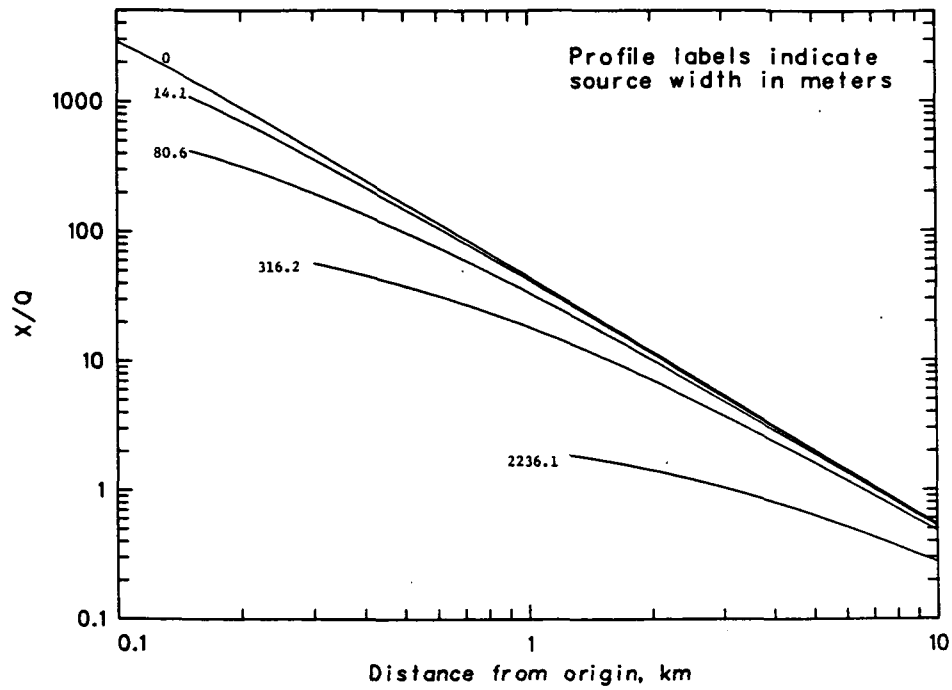

(c) Stability class C

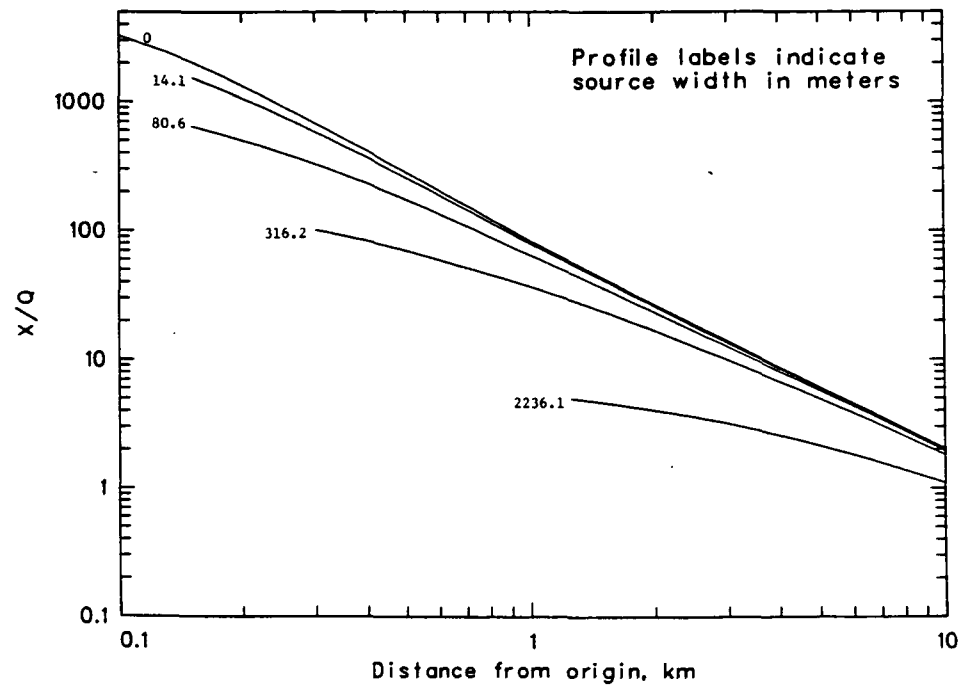

(d) Stability class D

Figure 32. Continued.

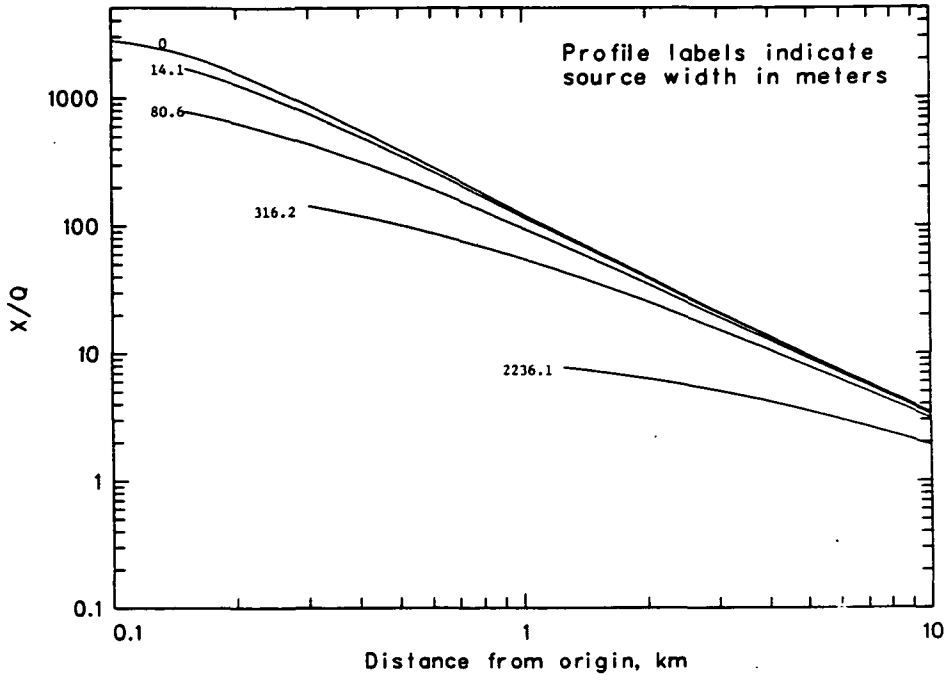

(e) Stability class E

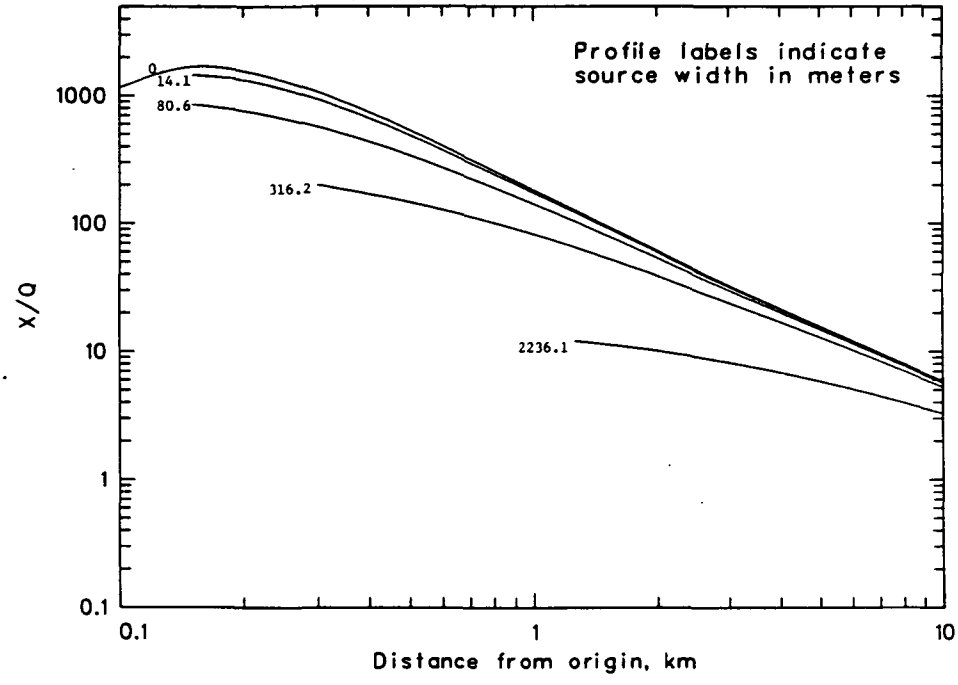

(f) Stability class F

Figure 32. Continued.

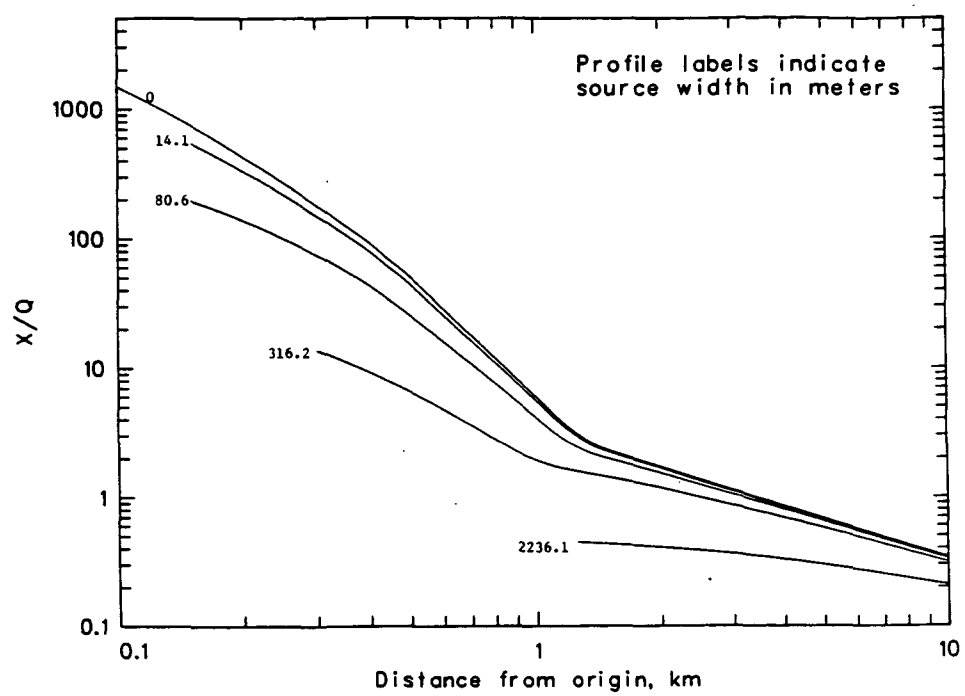

(a) Stability class A

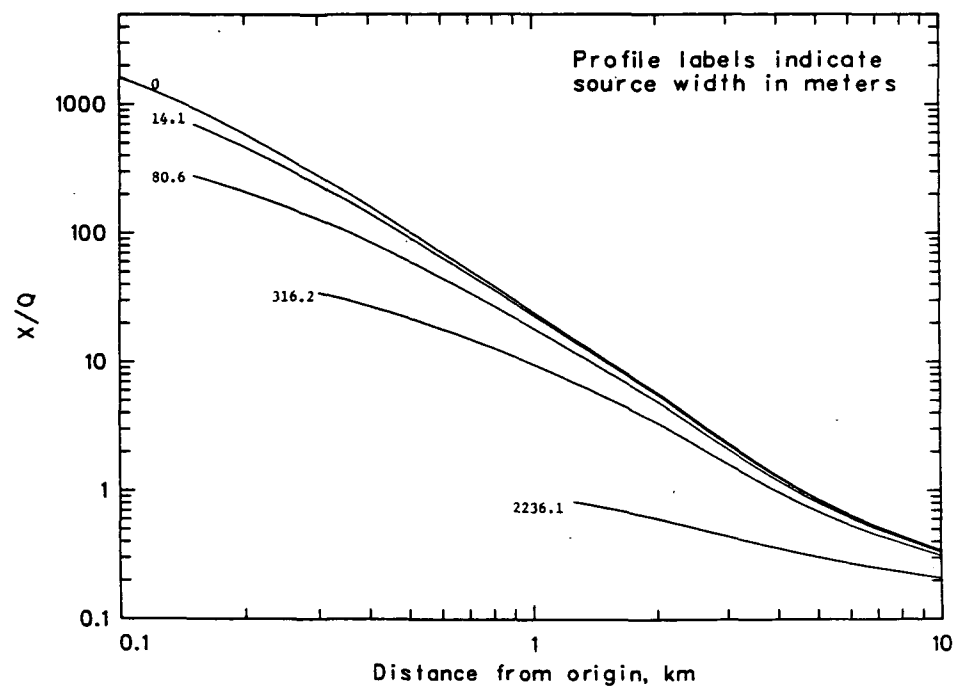

(b) Stability class B

Figure 33. PGPC (X/Q) profiles by source width for each stability class and 10-m-high releases.

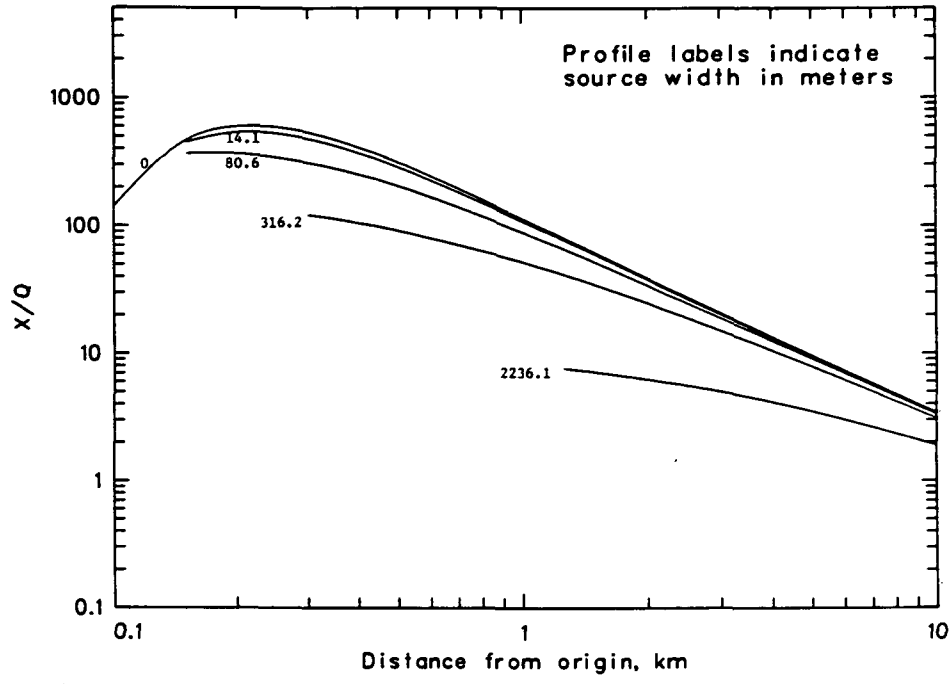

(e) Stability class E

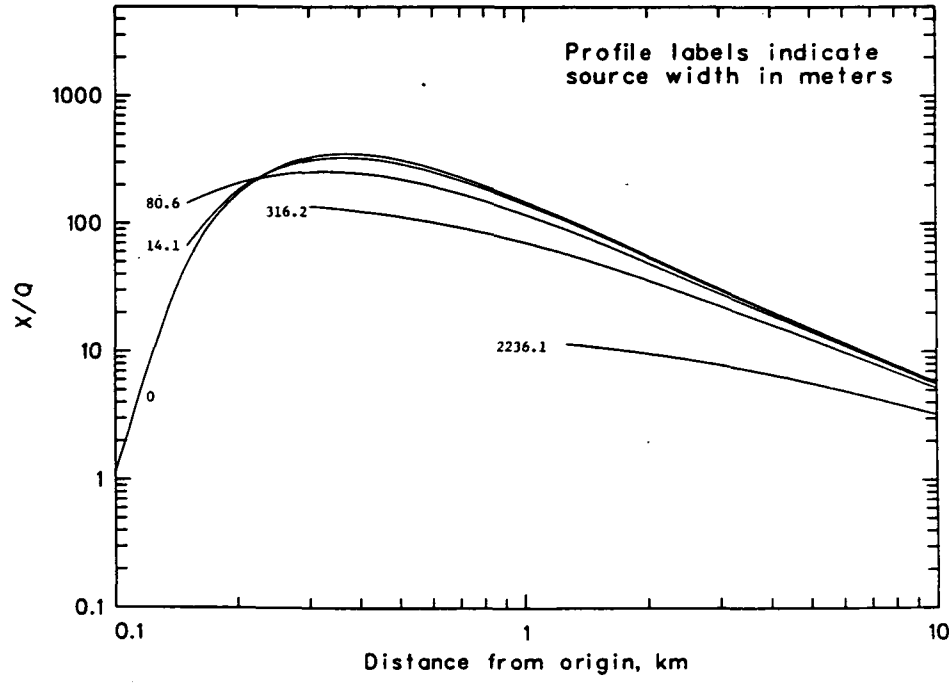

(f) Stability class F

Figure 33. Continued.

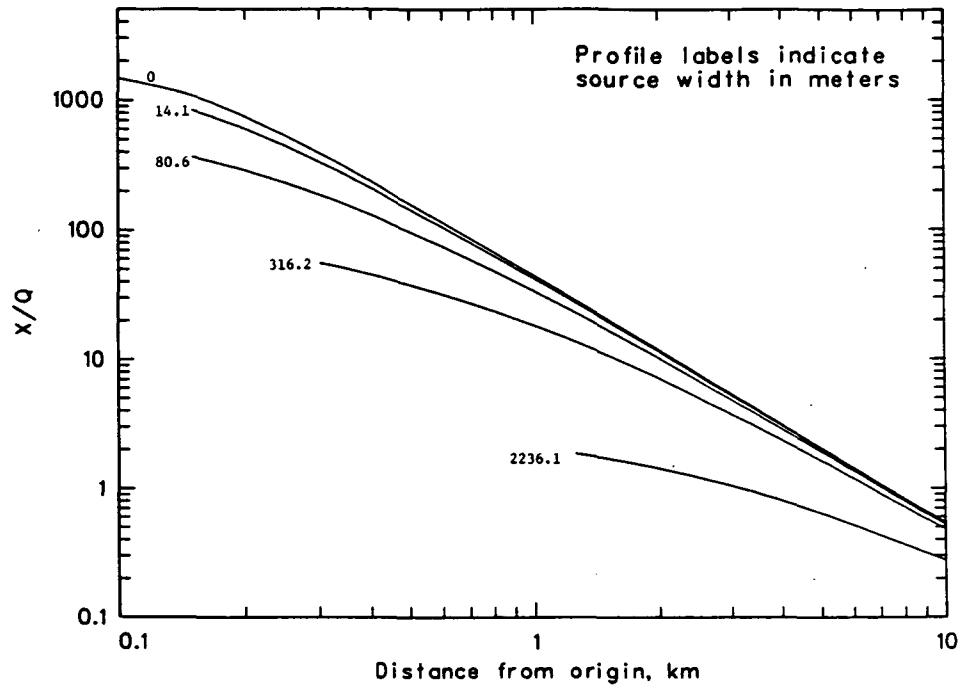

(c) Stability class C

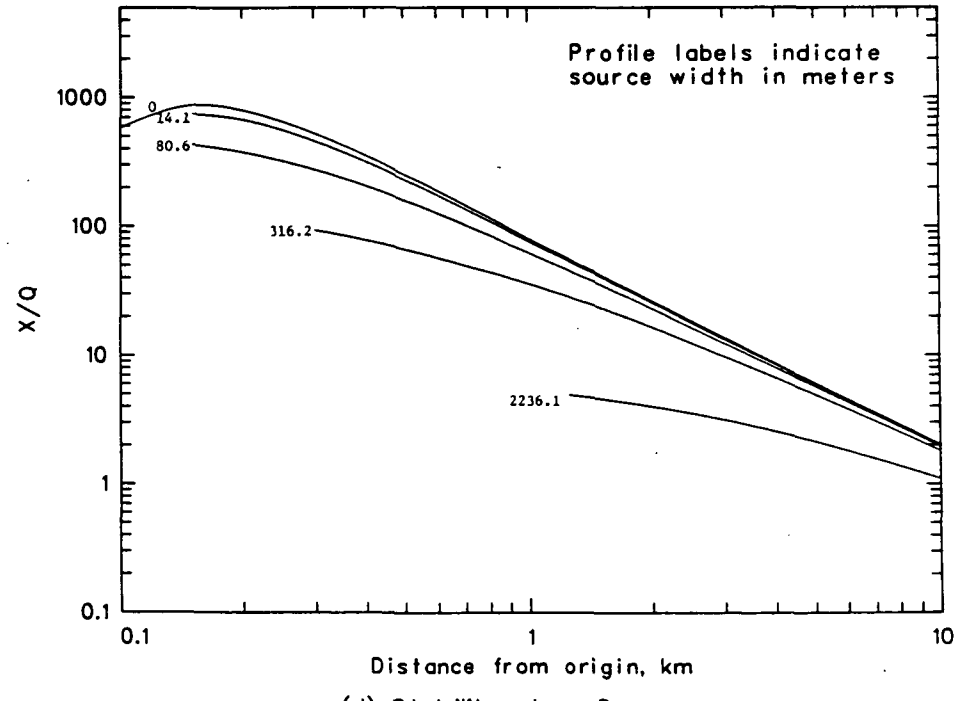

(d) Stability class D

Figure 33. Continued.

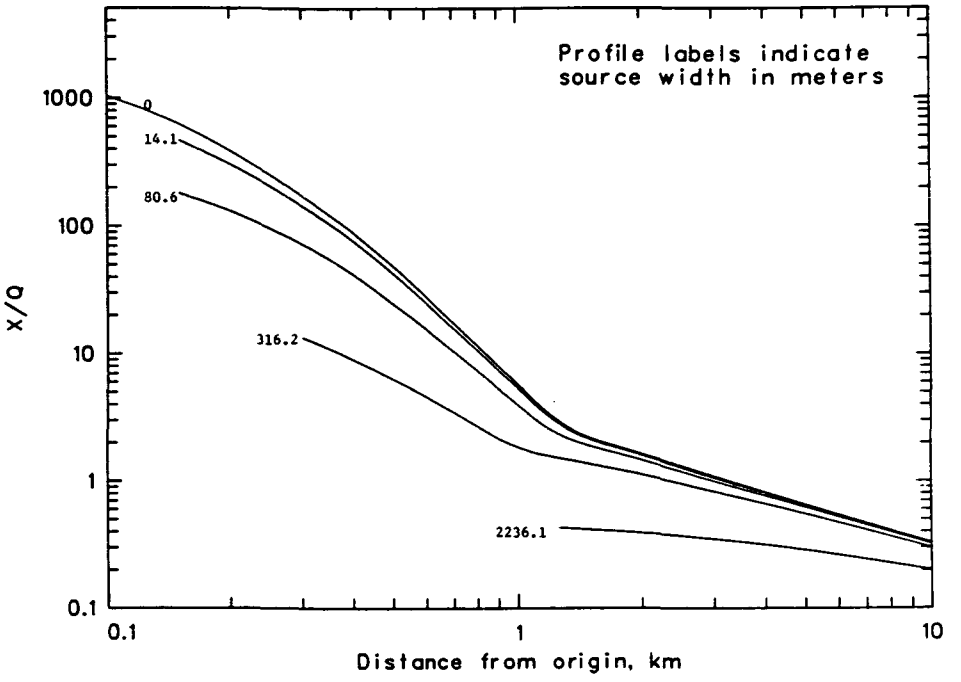

(a) Stability class A

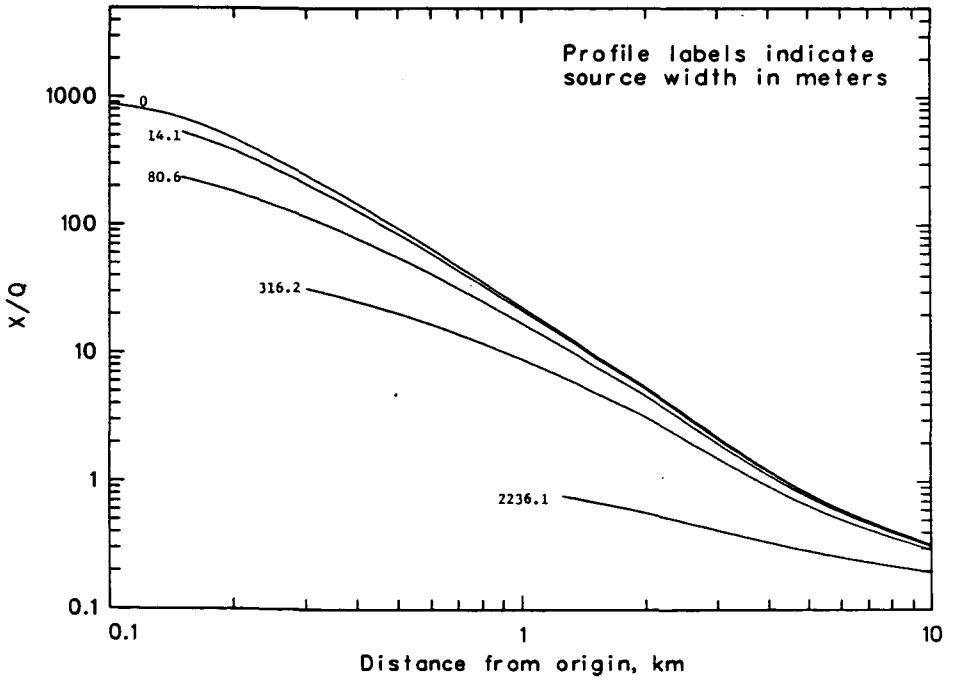

(b) Stability class B

Figure 34. PGPC (X/Q) profiles by source width for each stability class and 15-m-high releases.

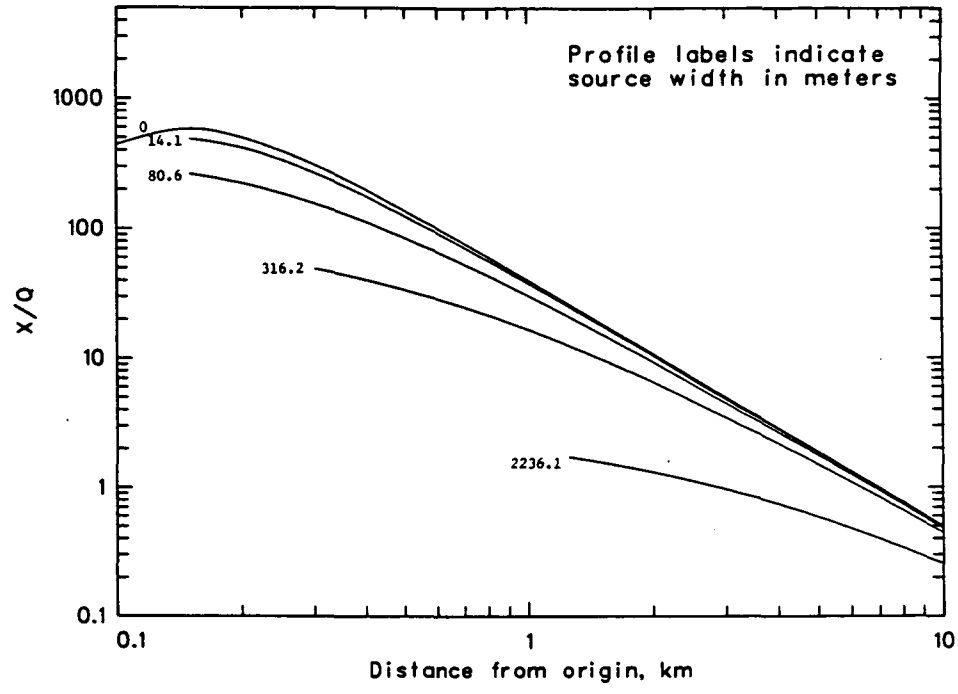

(c) Stability class C

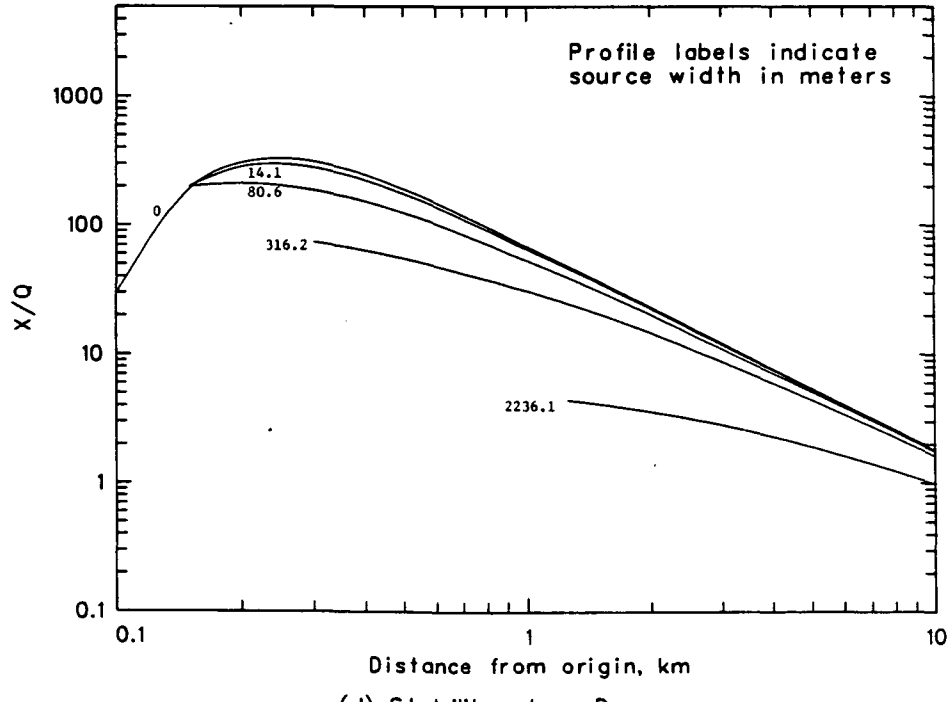

(d) Stability class D

Figure 34. Continued.

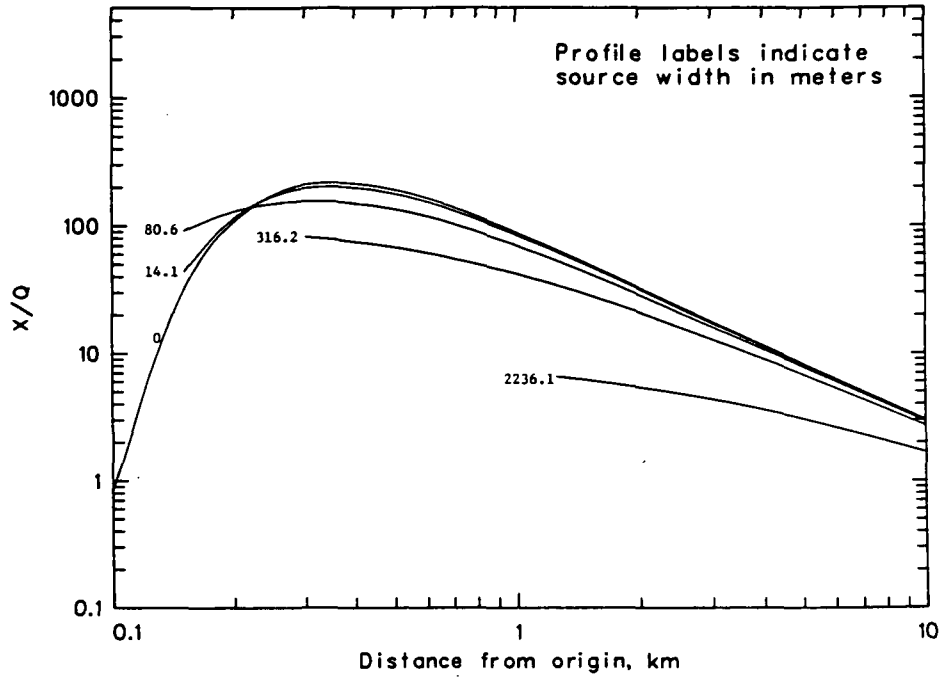

(e) Stability class E

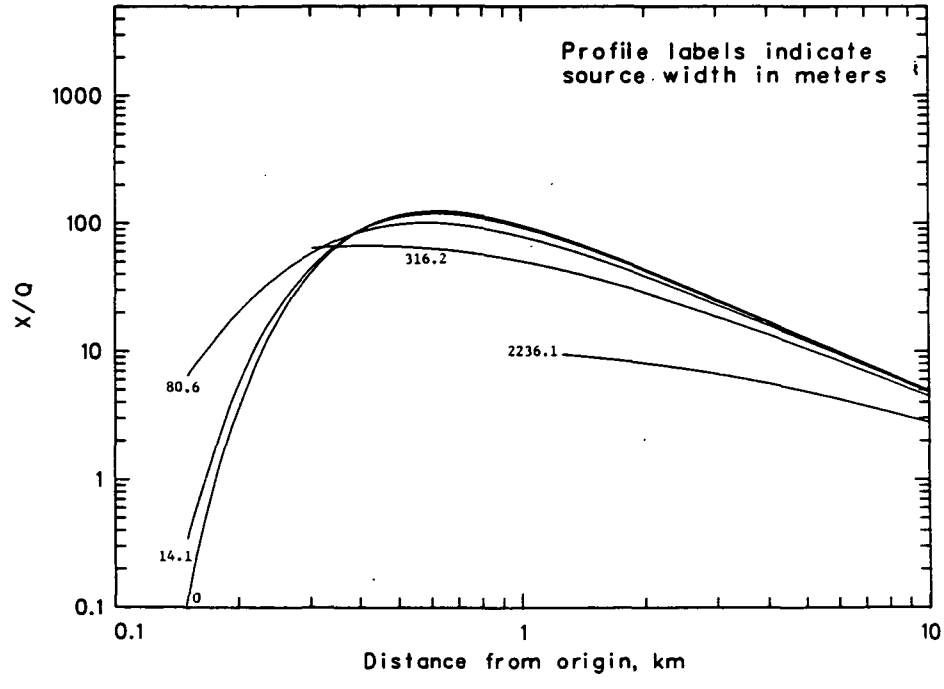

(f) Stability class F

Figure 34. Continued.

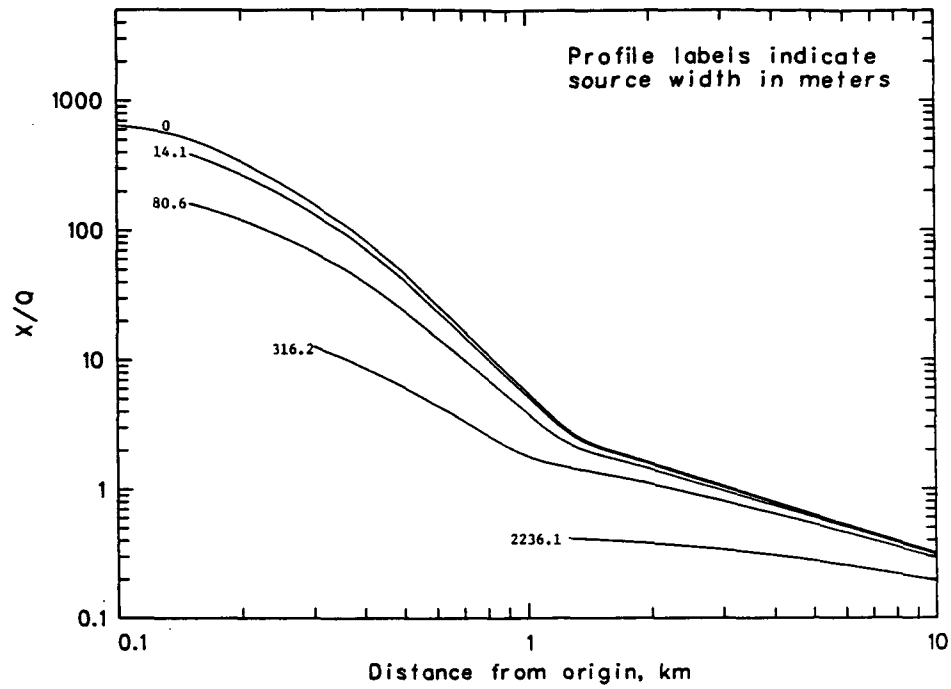

(a) Stability class A

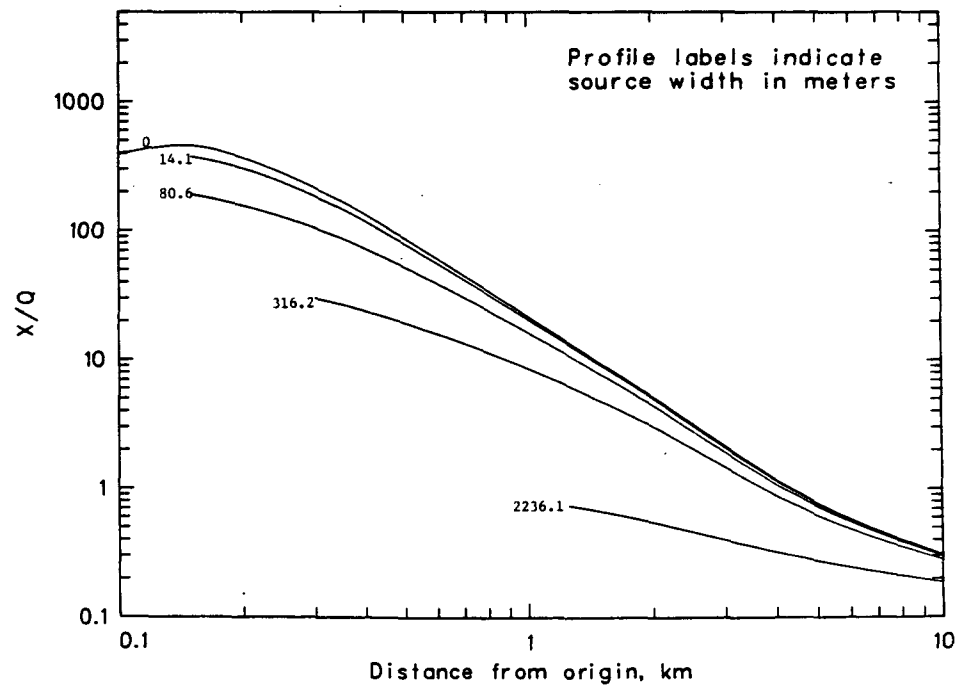

(b) Stability class B

Figure 35. PGPC (X/Q) profiles by source width for each stability class and 20-m-high releases.

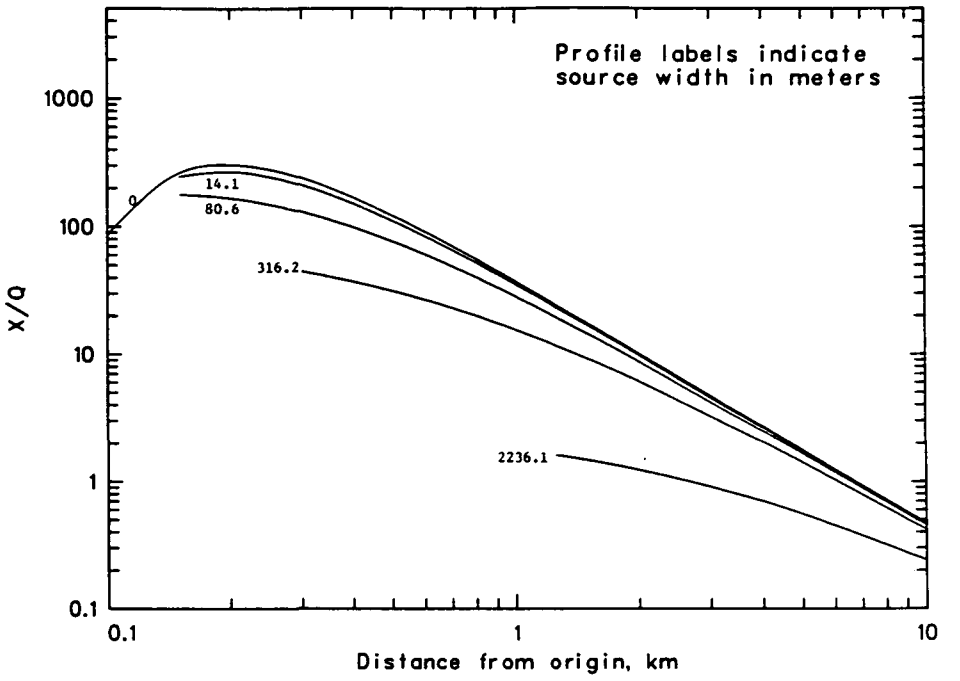

(c) Stability class C

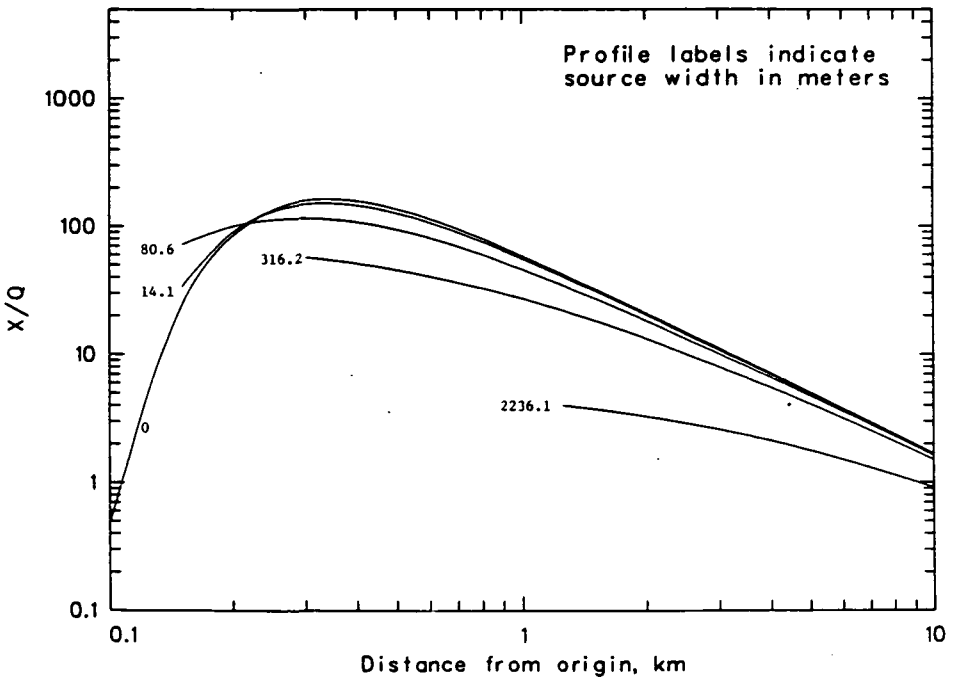

(d) Stability class D

Figure 35. Continued.

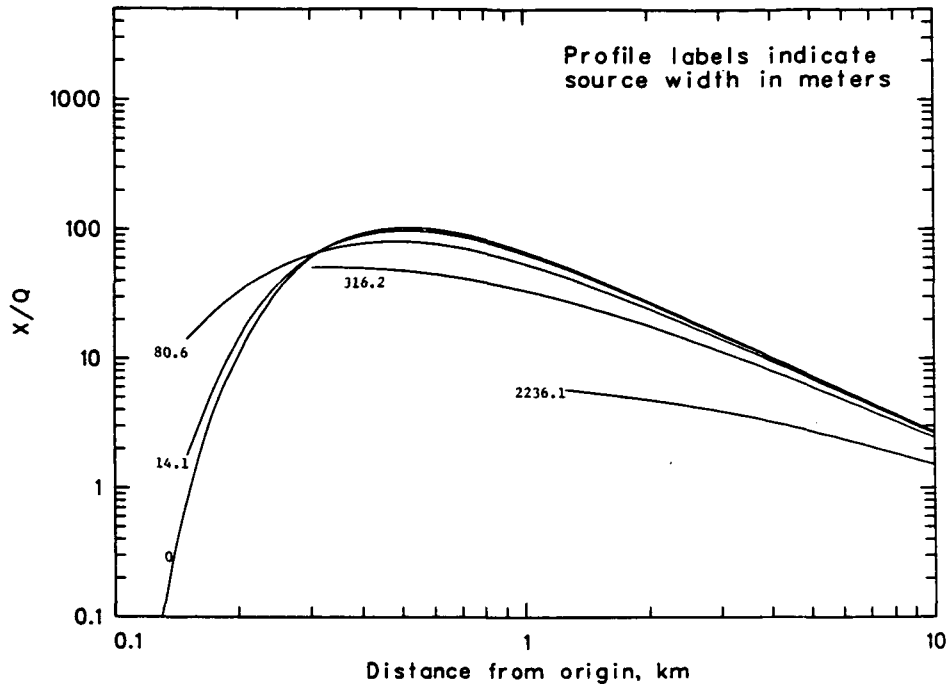

(e) Stability class E

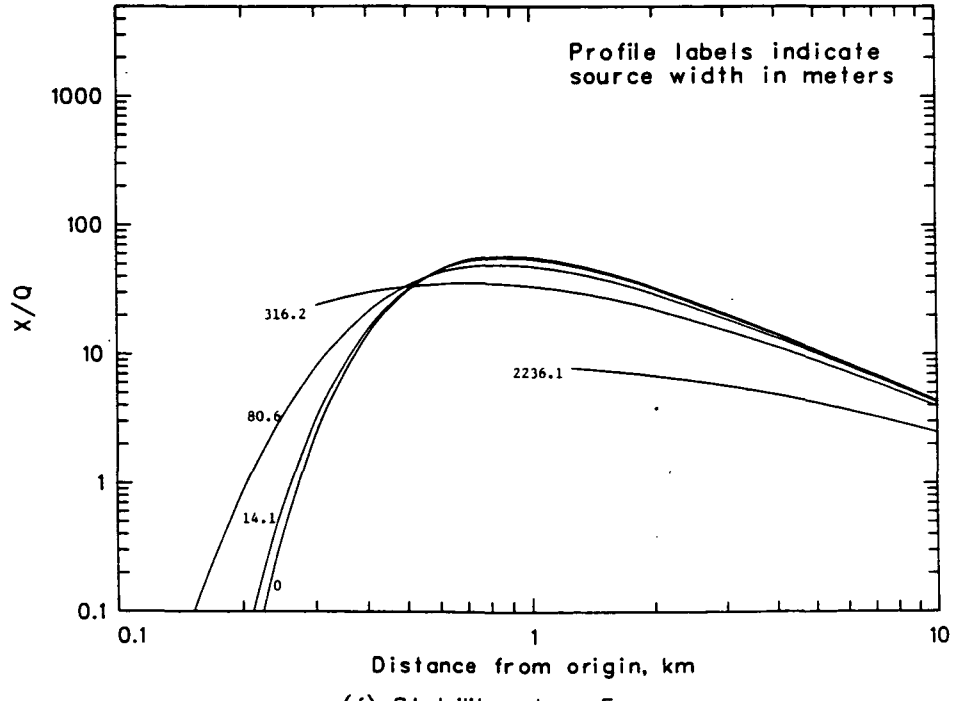

(f) Stability class F

Figure 35. Continued.

APPENDIX F

TGRC (X/Q) PROFILES BY SOURCE WIDTH FOR EACH STABILITY CATEGORY AND RELEASE HEIGHT

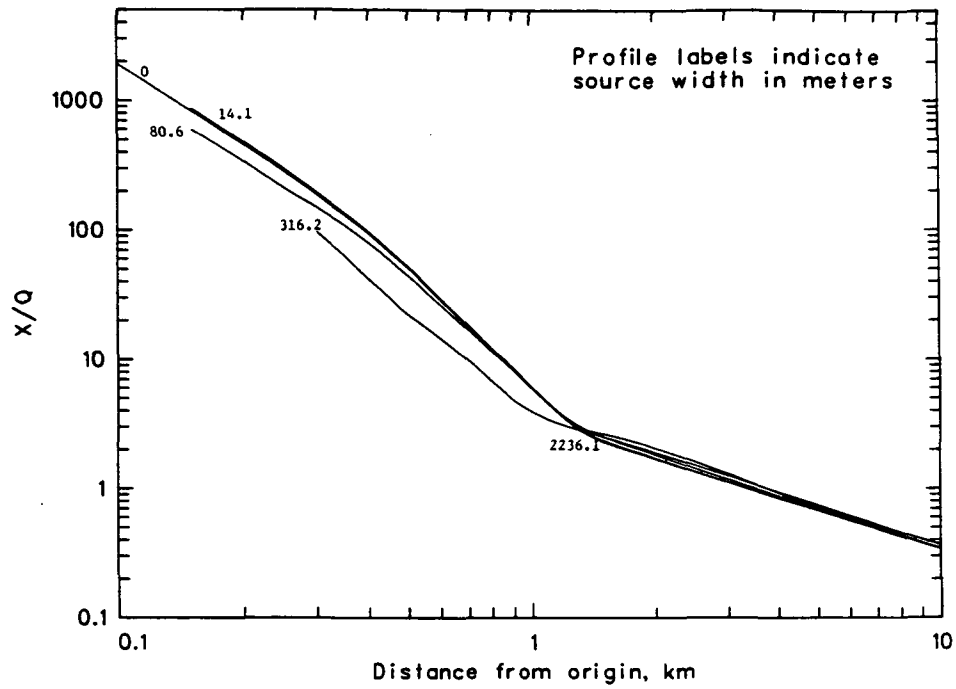

(a) Stability class A

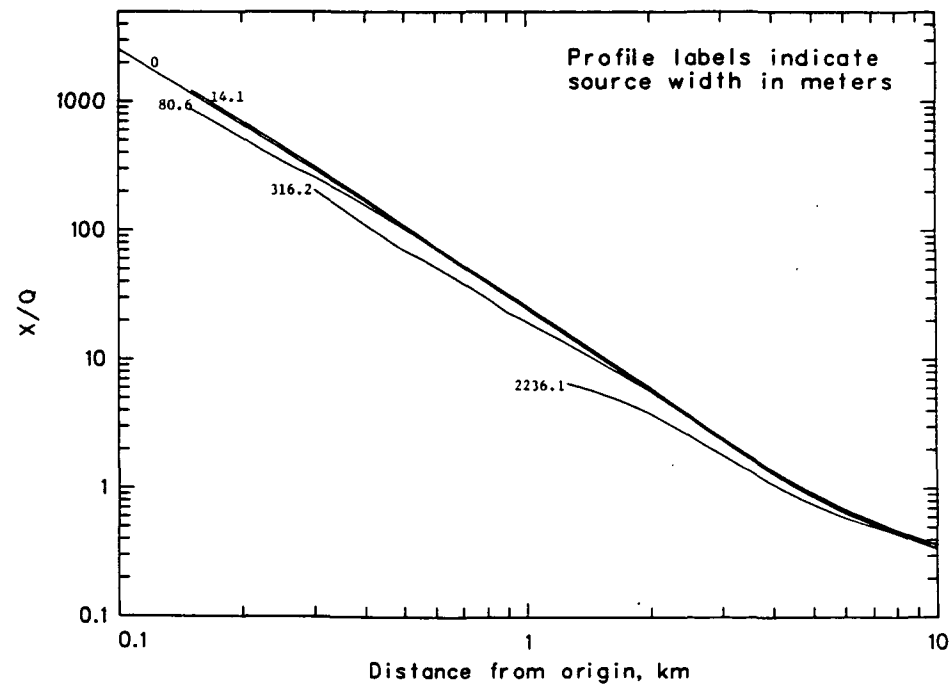

(b) Stability class B

Figure 36. TGRC (X/Q) profiles by source width for each stability class and 0-m-high releases.

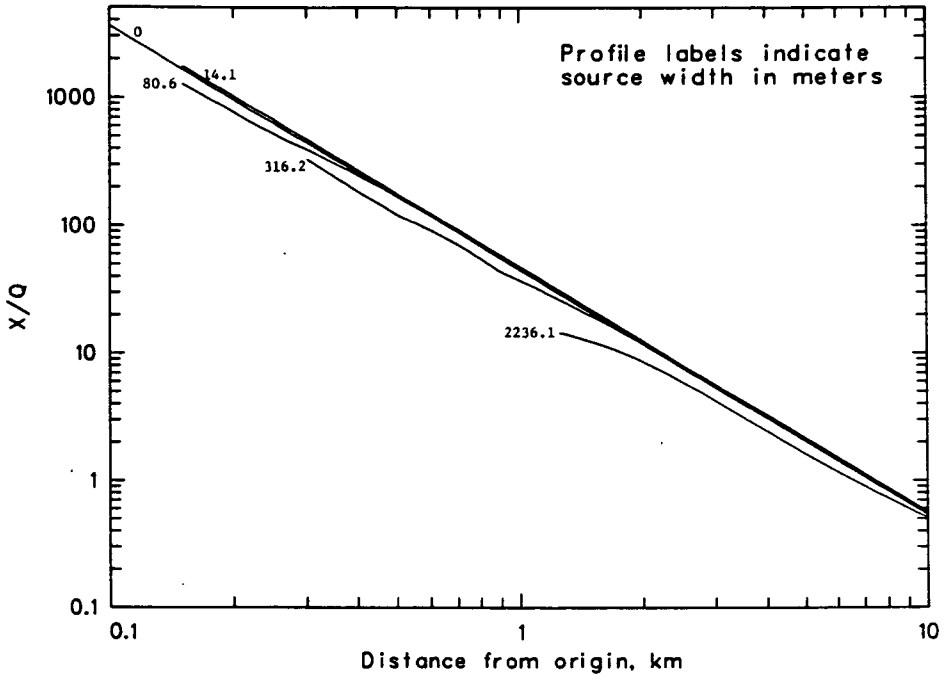

(c) Stability class C

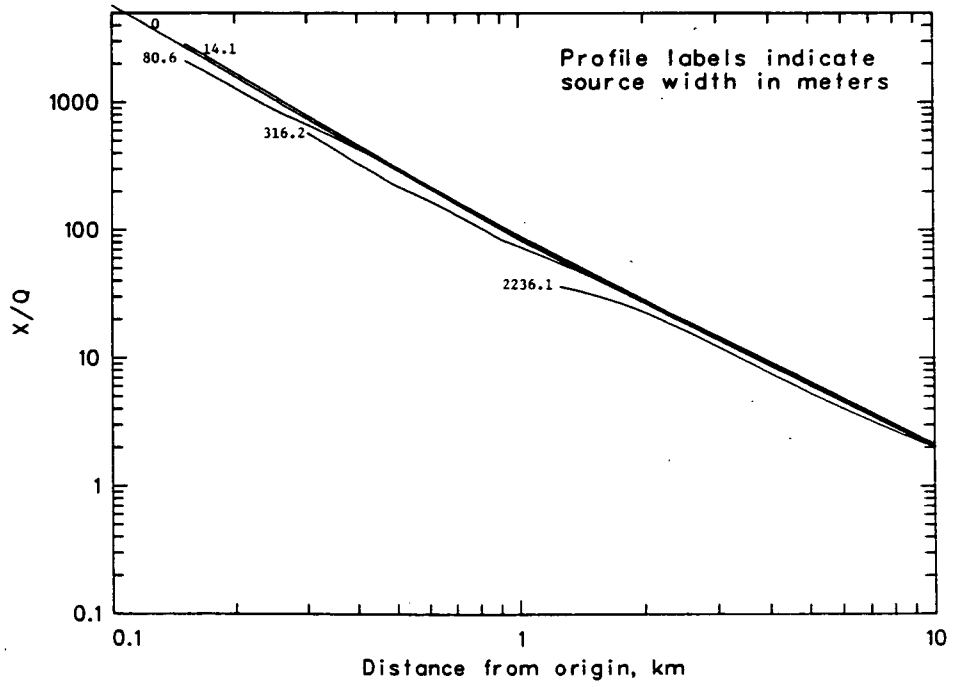

(d) Stability class D

Figure 36. Continued.

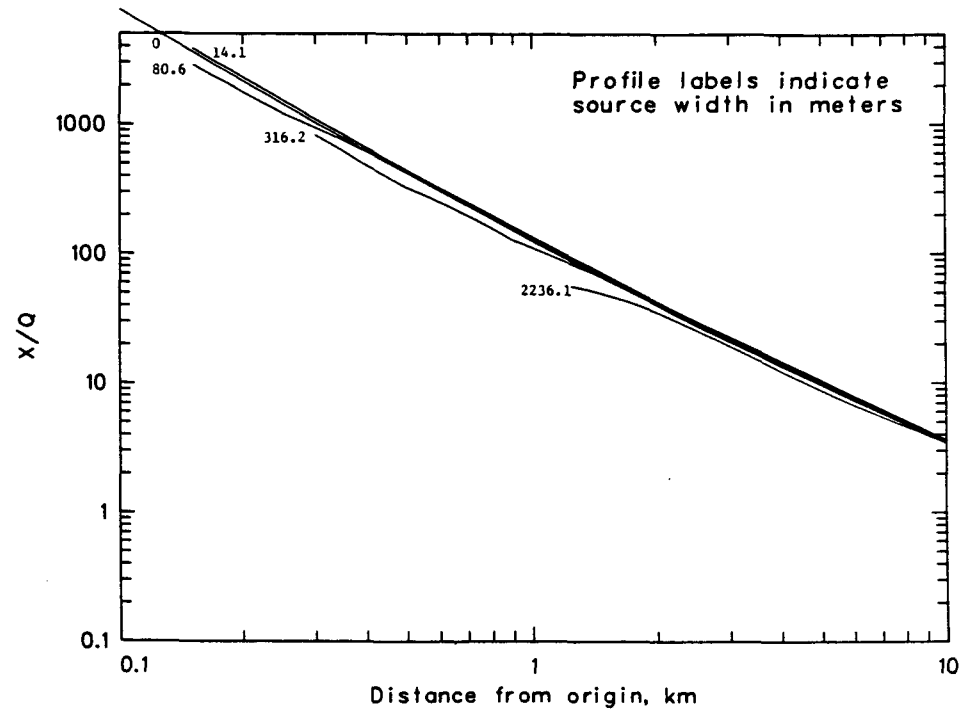

(e) Stability class E

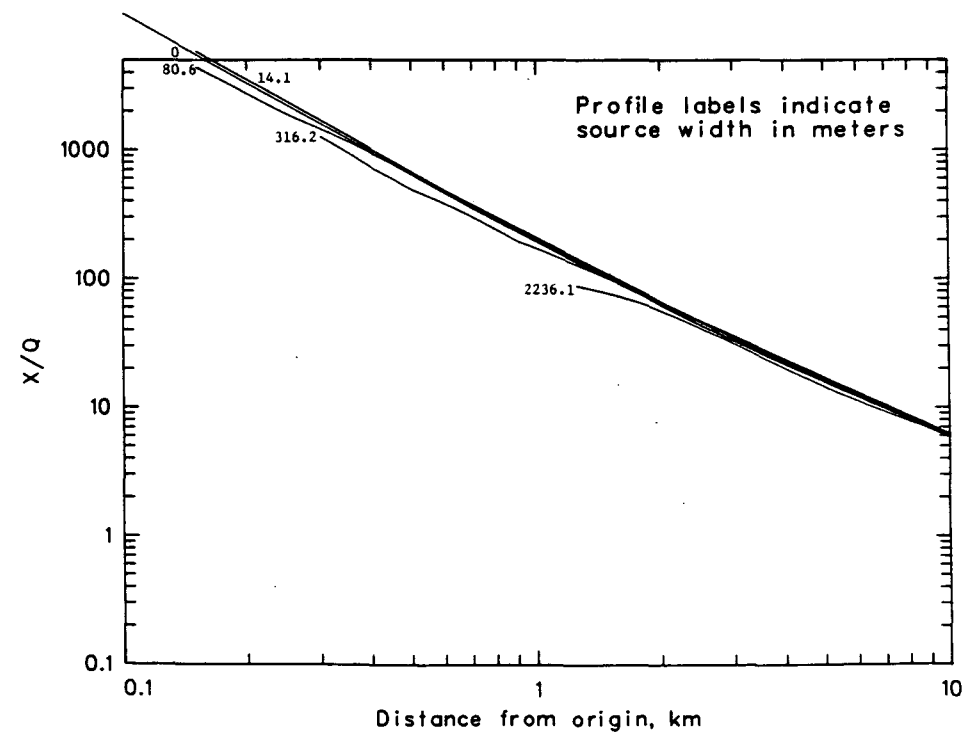

(f) Stability class F

Figure 36. Continued.

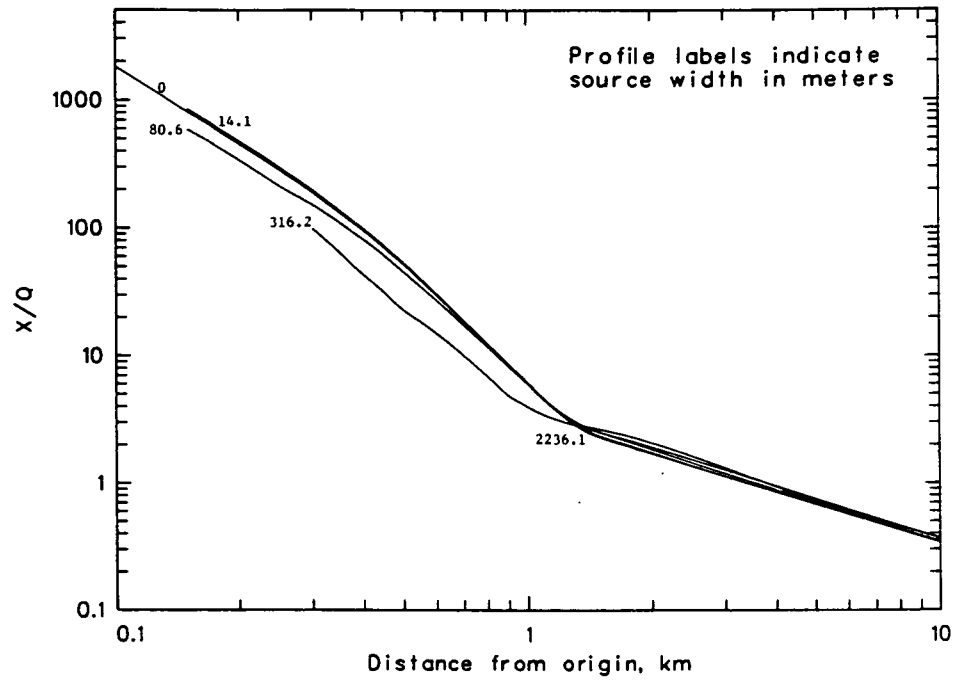

(a) Stability class A

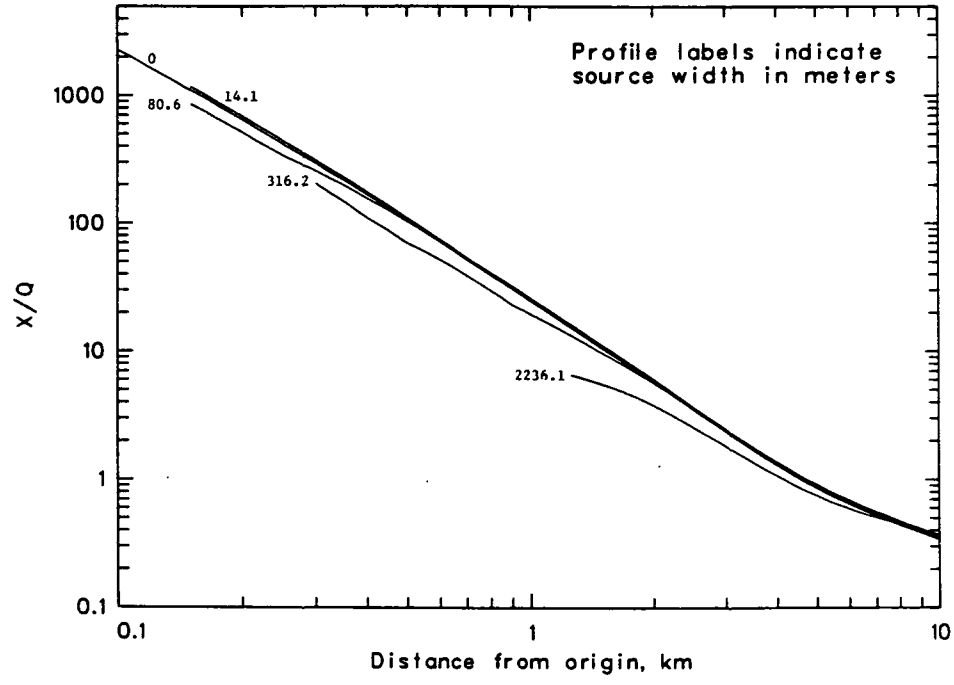

(b) Stability class B

Figure 37. TGRC (X/Q) profiles by source width for each stability class and 5-m-high releases.

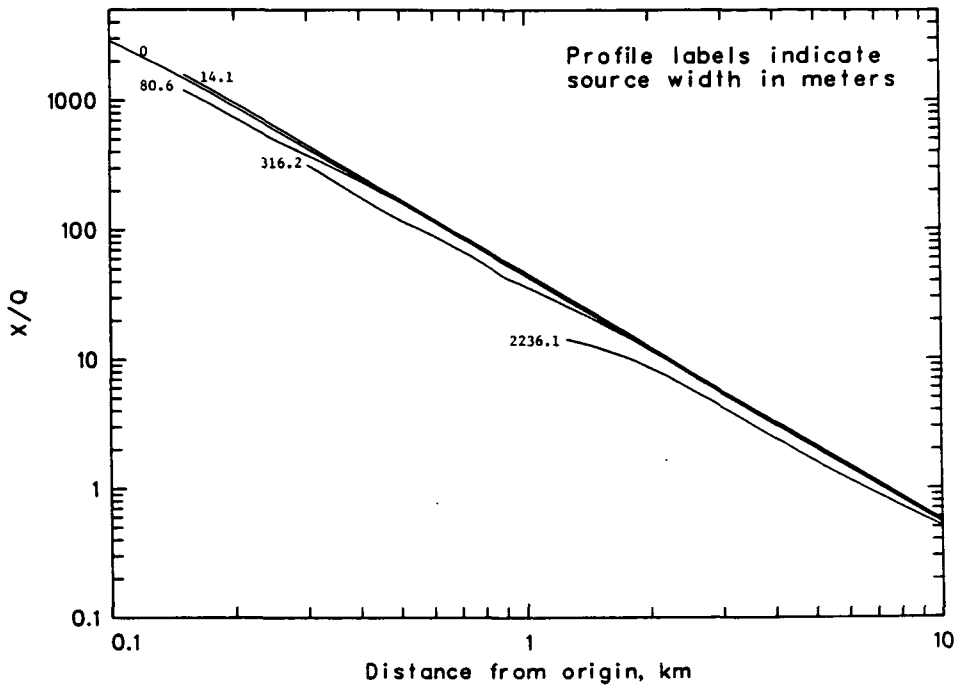

(c) Stability class C

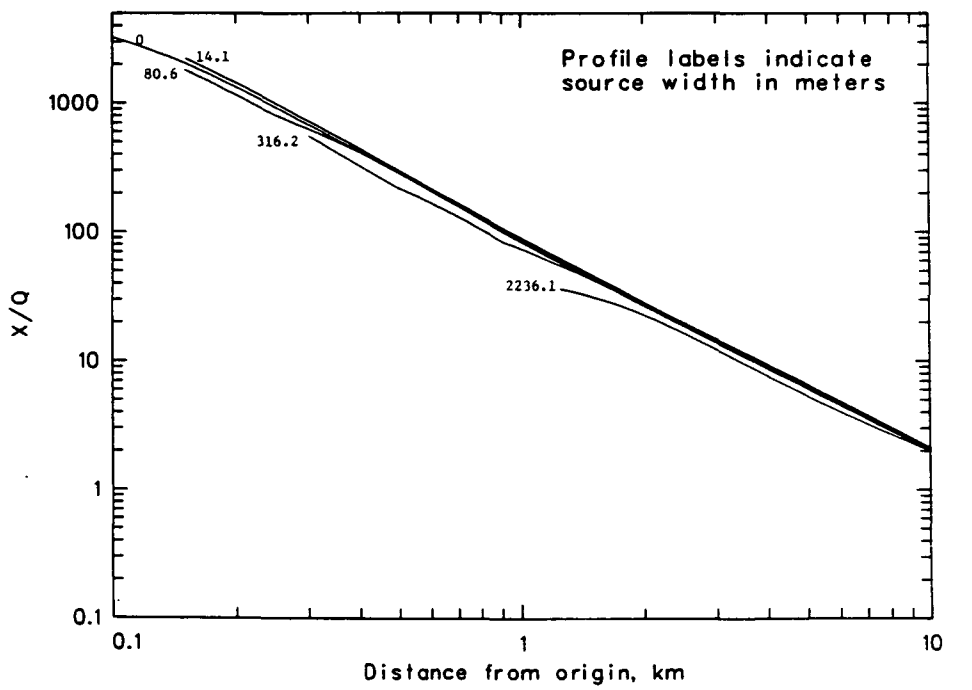

(d) Stability class D

Figure 37. Continued.

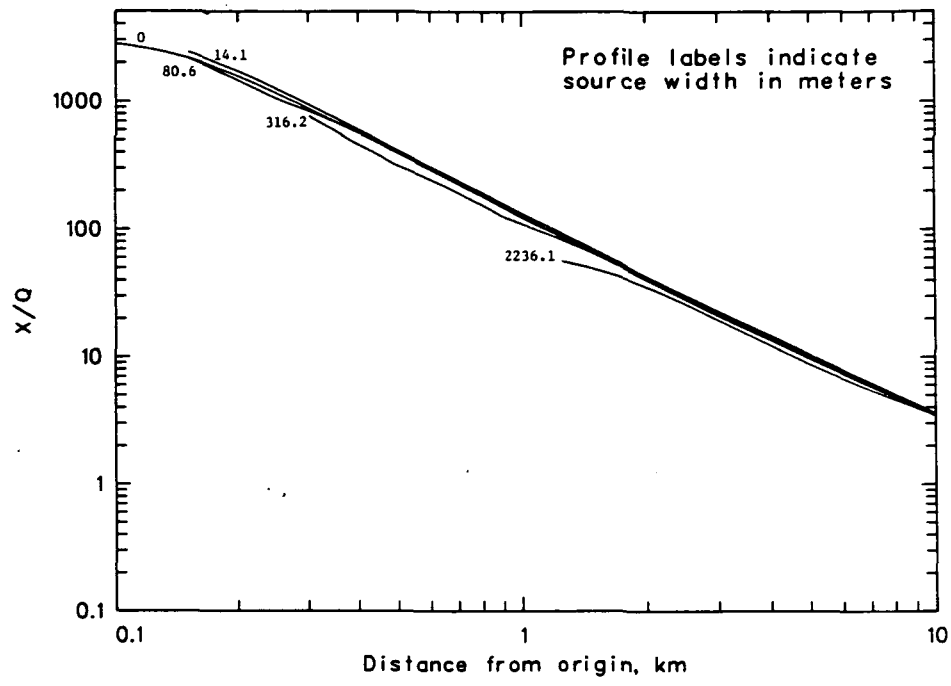

(e) Stability class E

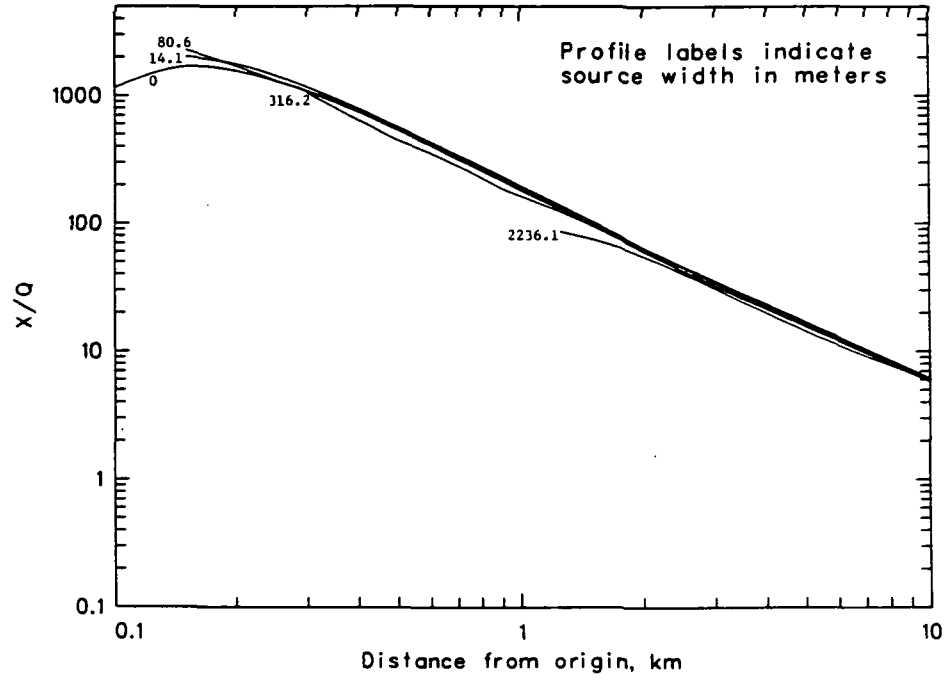

(f) Stability class F

Figure 37. Continued.

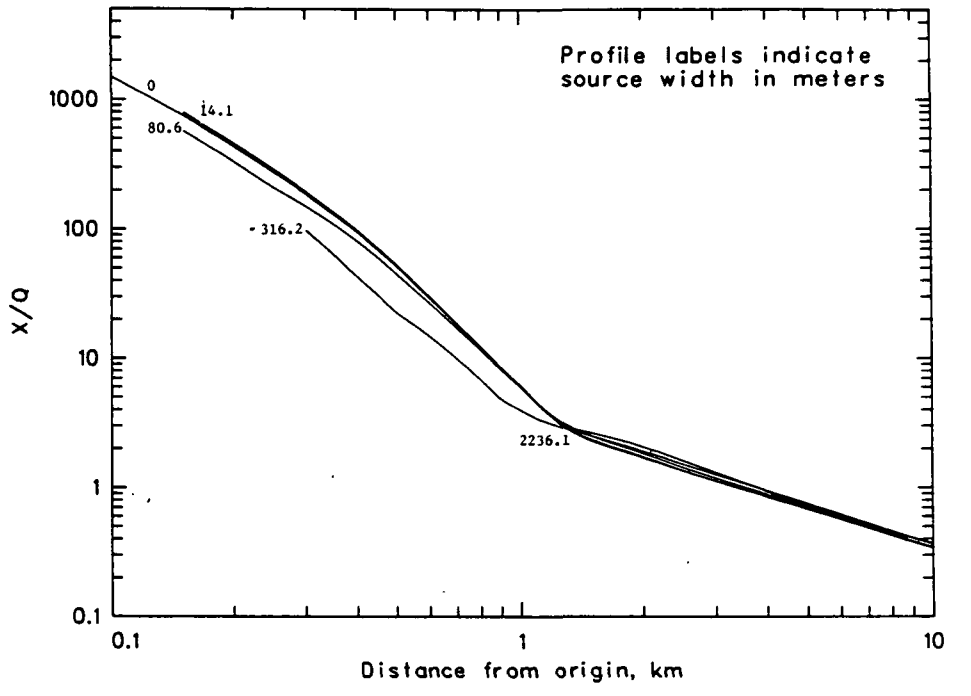

(a) Stability class A

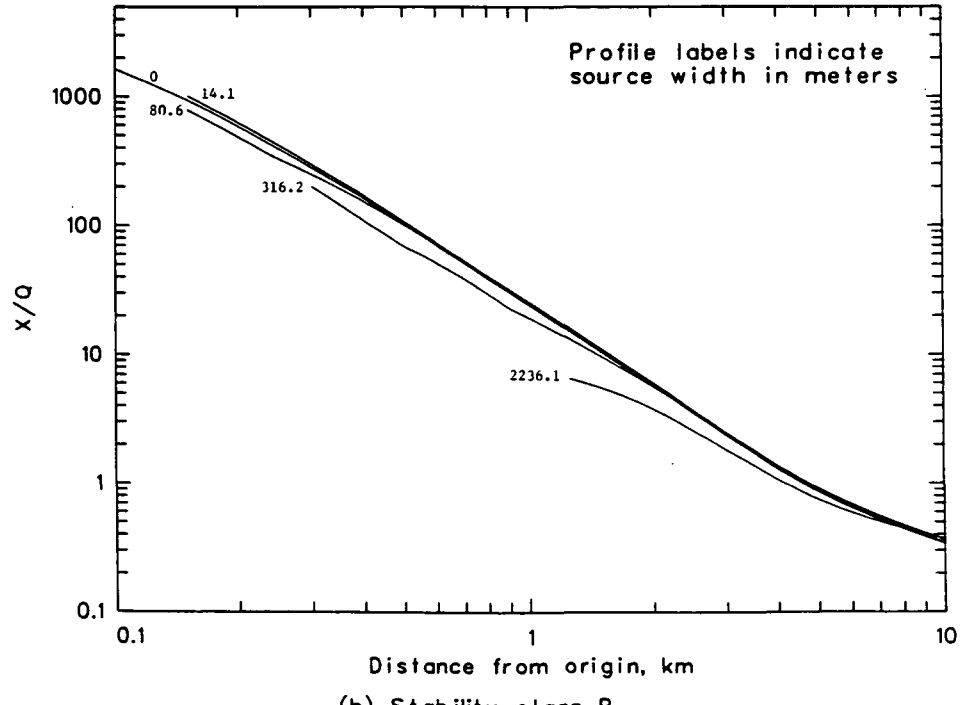

(b) Stability class B

Figure 38. TGRC (X/Q) profiles by source width for each stability class and 10-m-high releases.

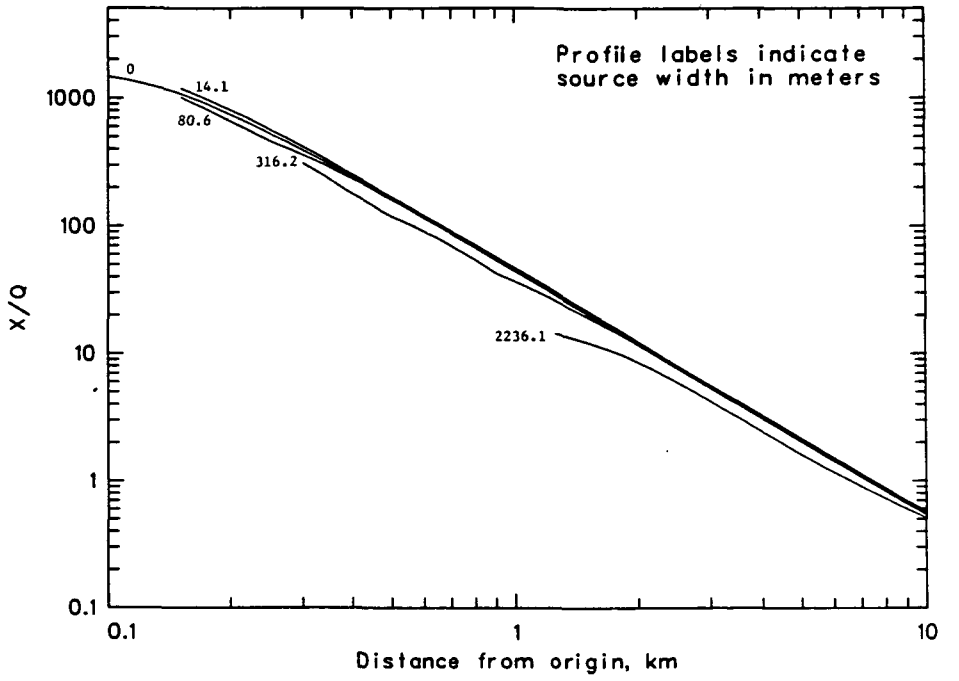

(c) Stability class C

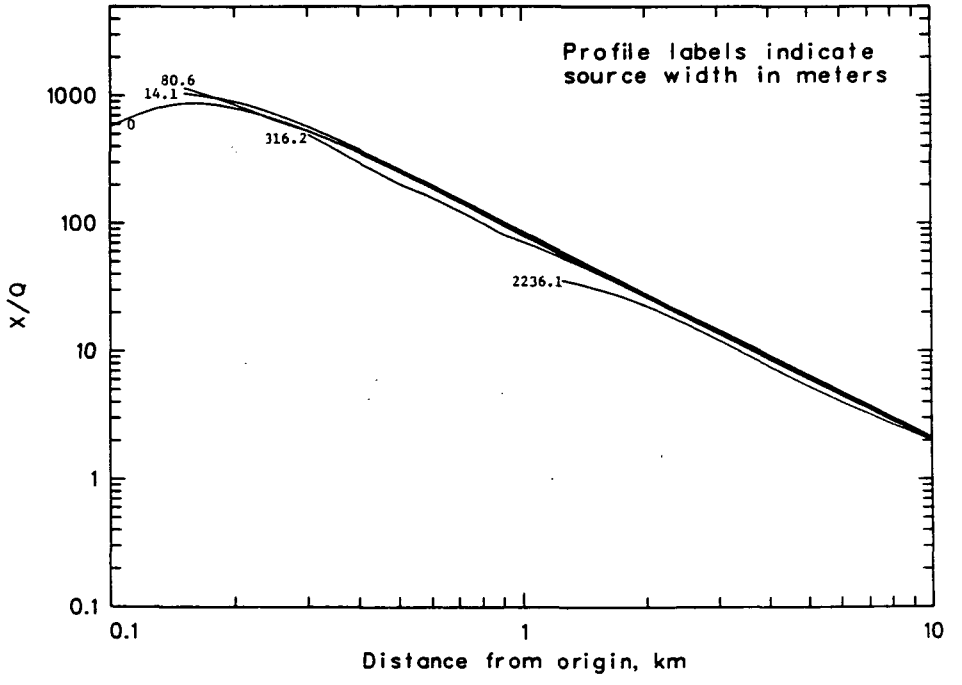

(d) Stability class D

Figure 38. Continued.

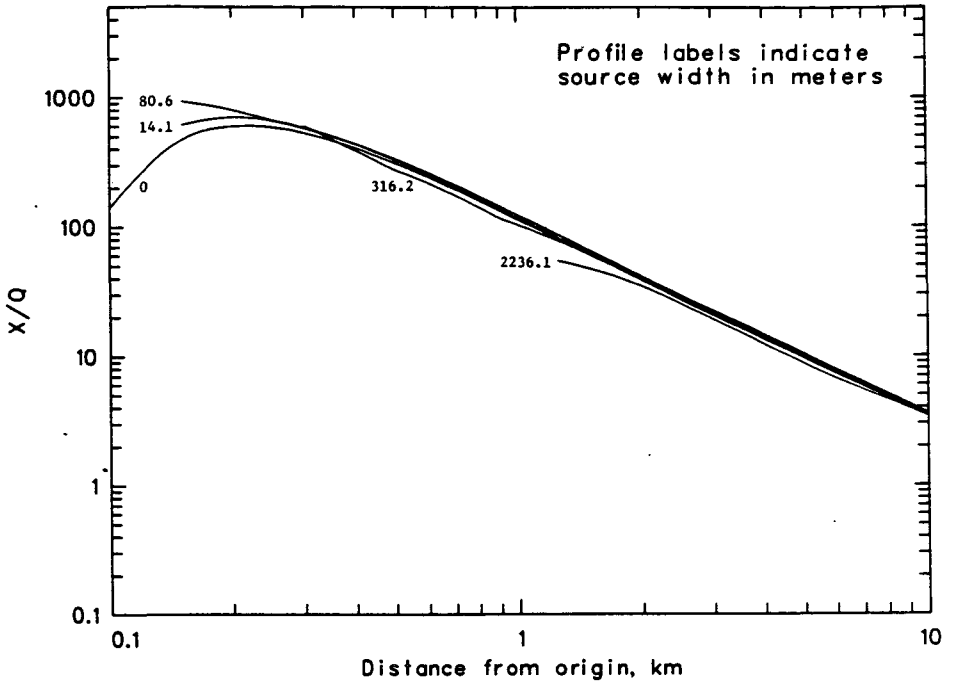

(e) Stability class E

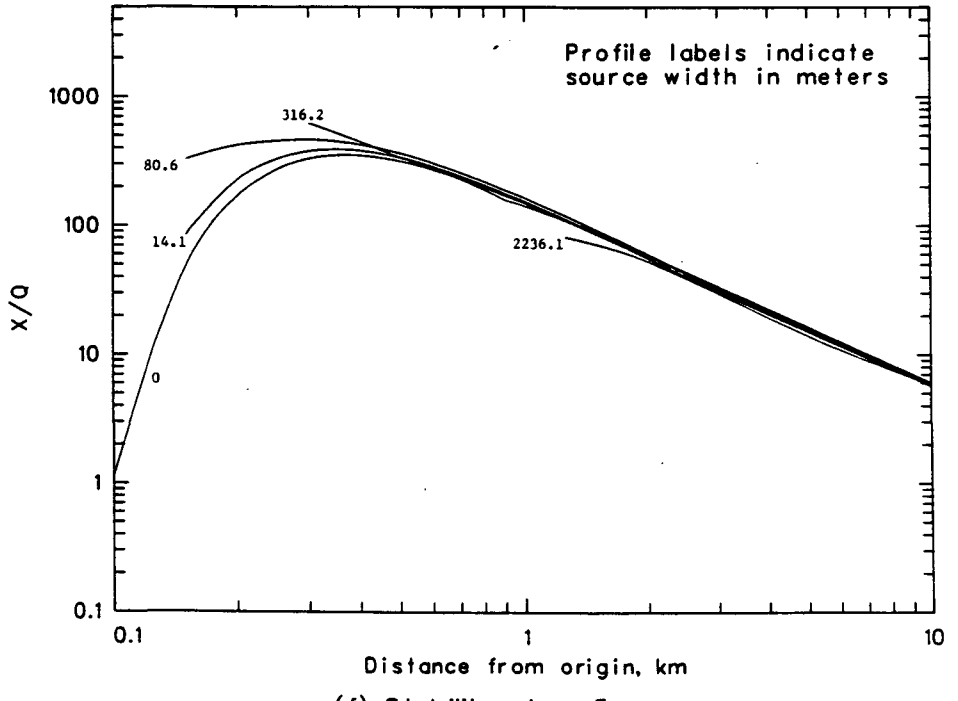

(f) Stability class F

Figure 38. Continued.

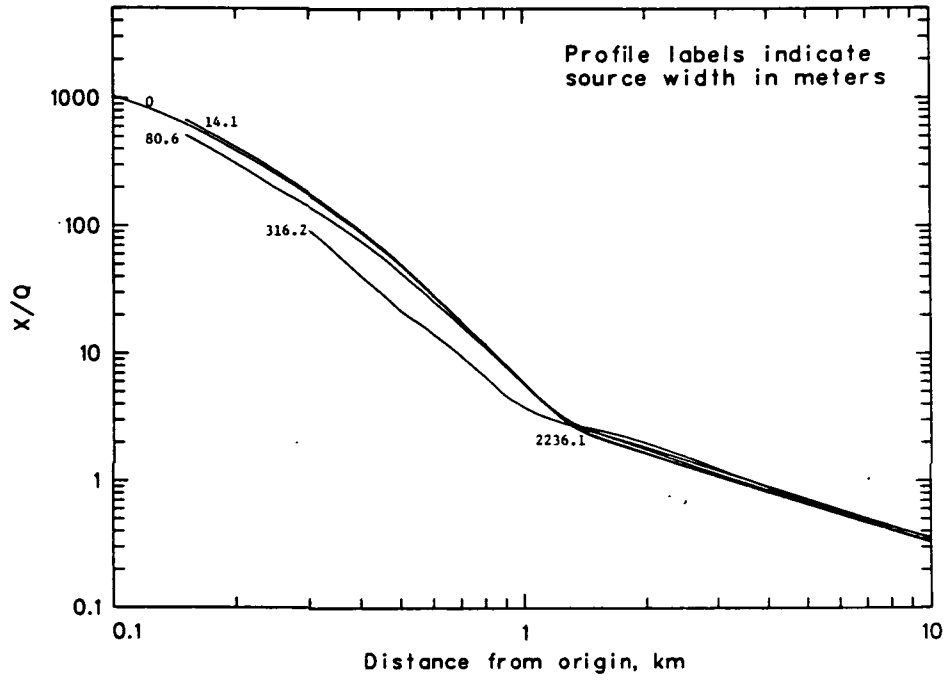

(a) Stability class A

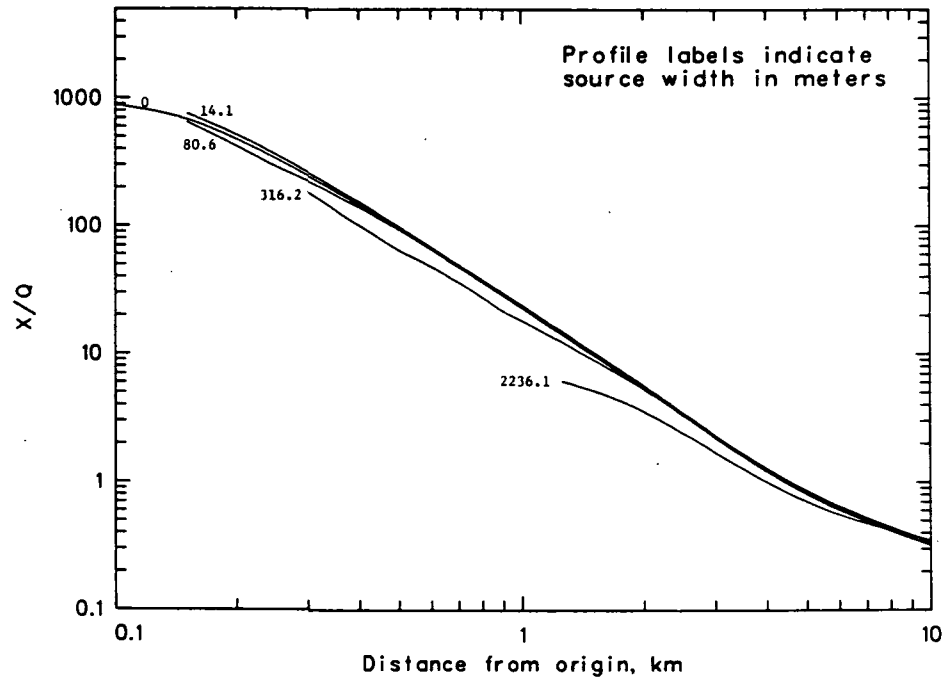

(b) Stability class B

Figure 39. TGRC (X/Q) profiles by source width for each stability class and 15-m-high releases.

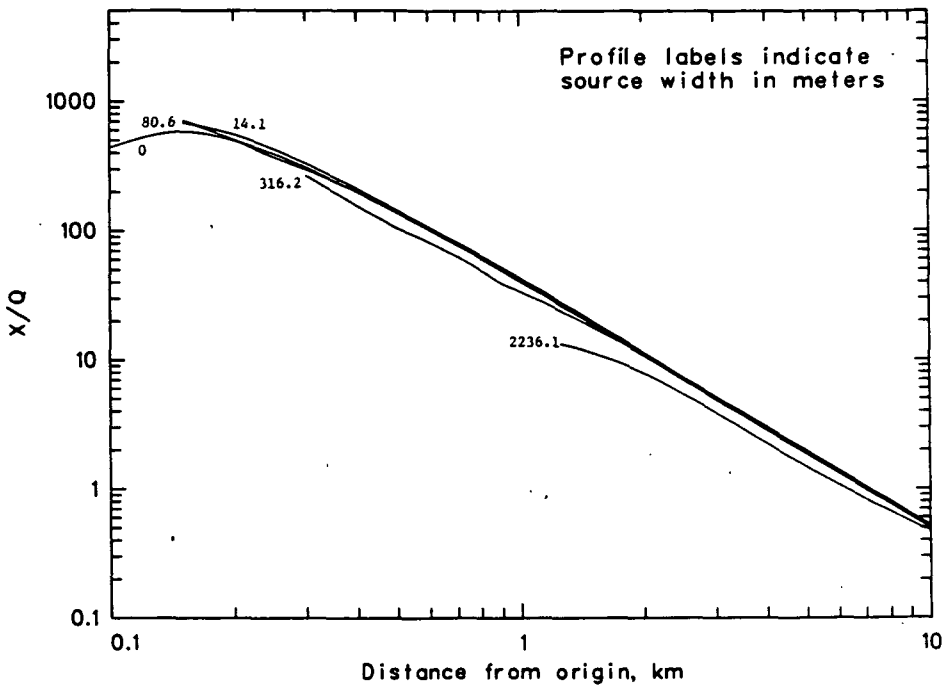

(c) Stability class C

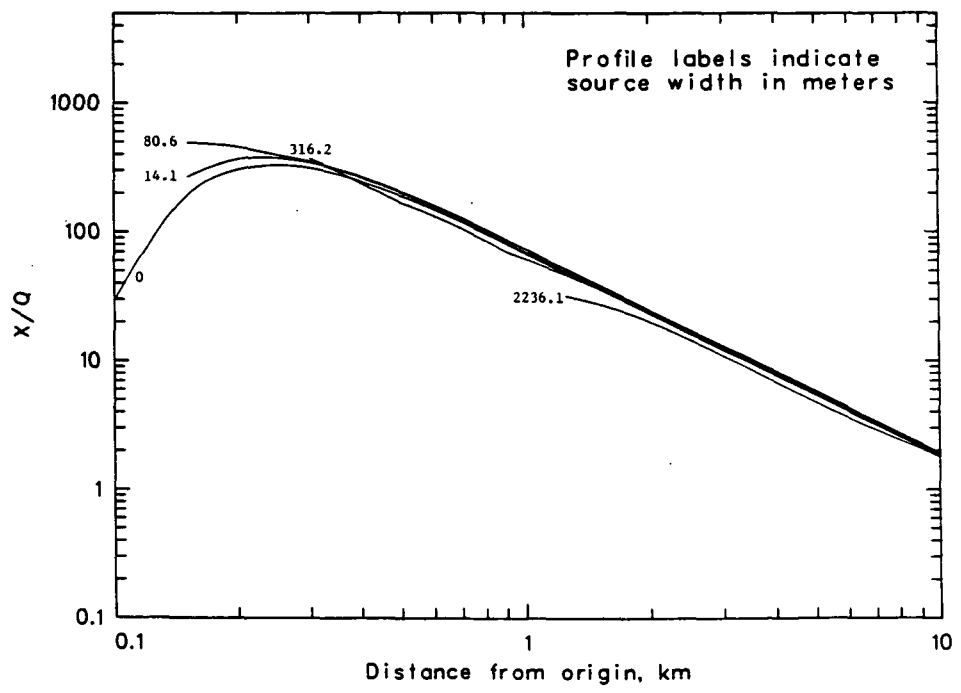

(d) Stability class D

Figure 39. Continued.

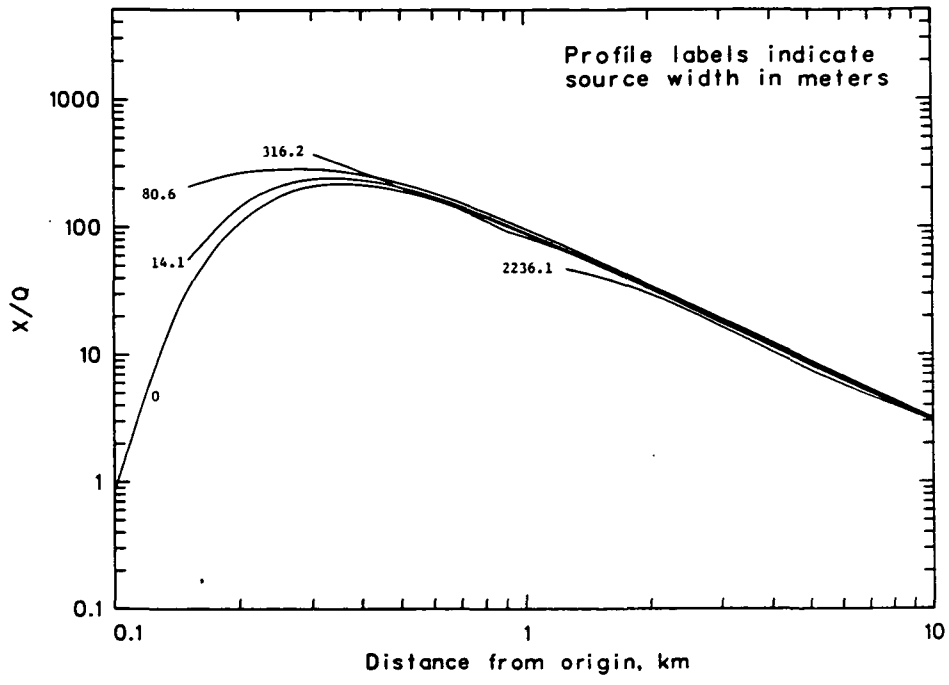

(e) Stability class E

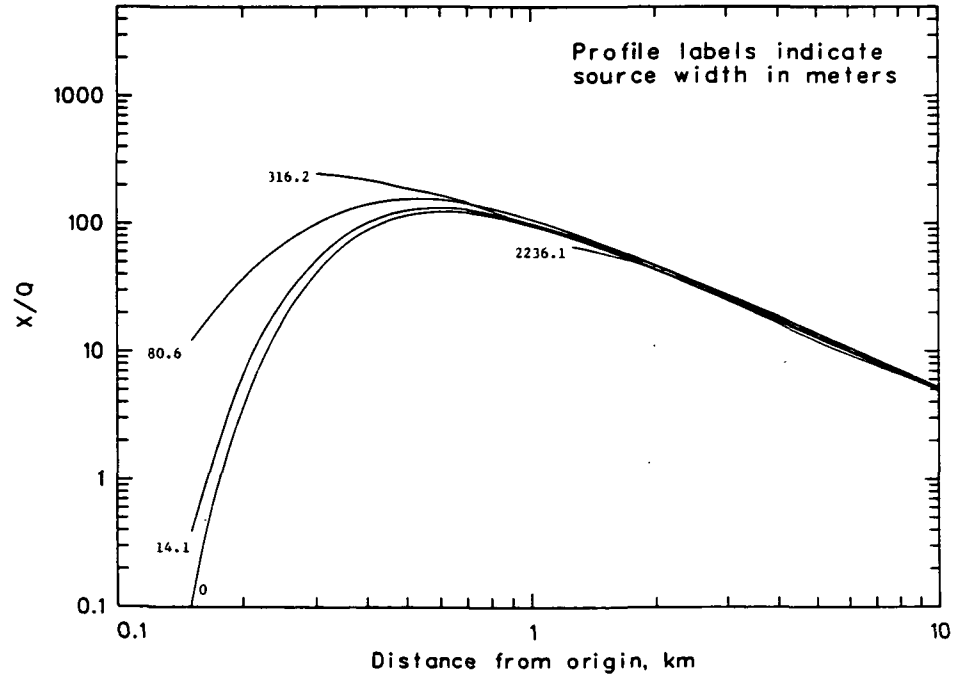

(f) Stability class F

Figure 39. Continued.

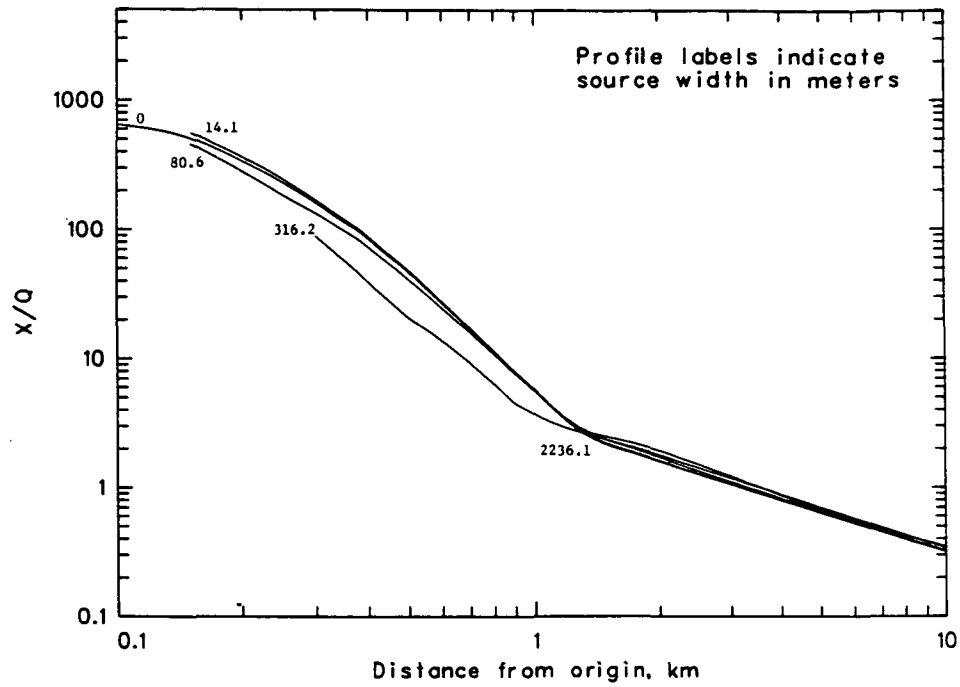

(a) Stability class A

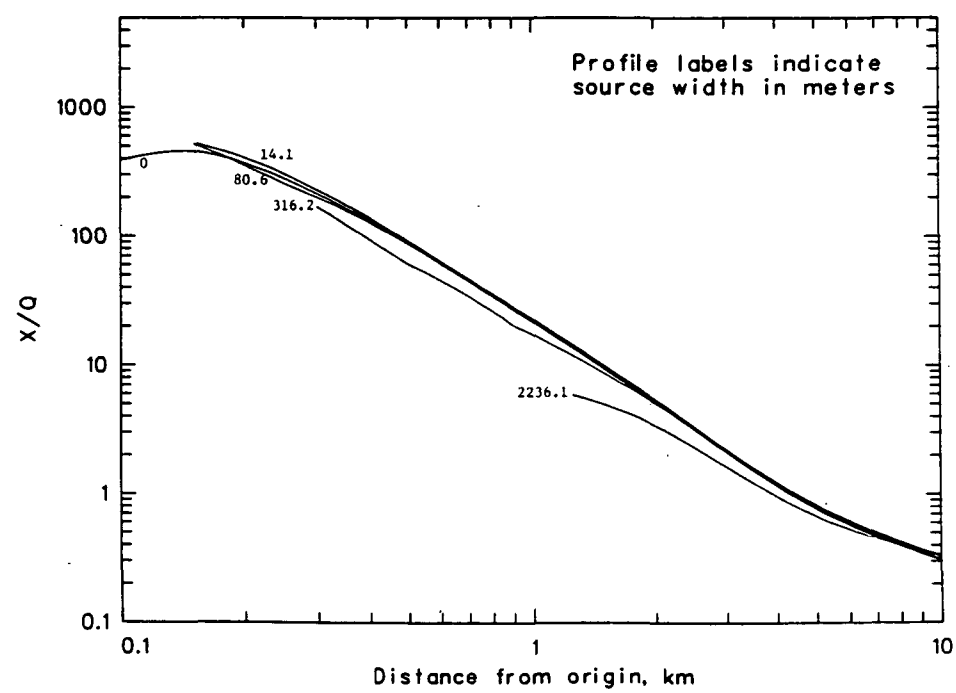

(b) Stability class B

Figure 40. TGRC (X/Q) profiles by source width for each stability class and 20-m-high releases.

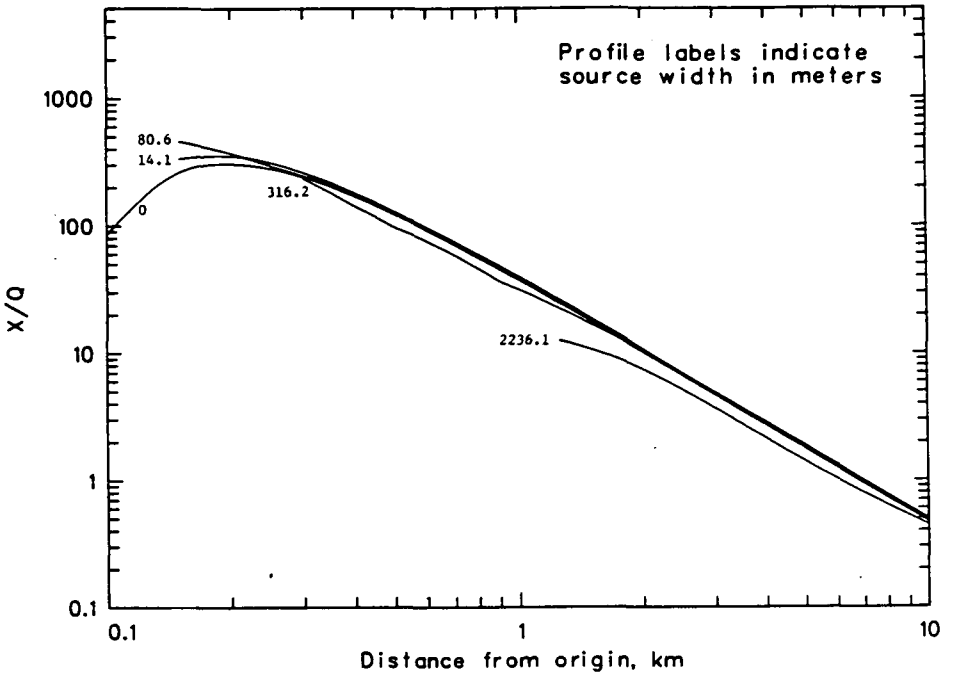

(c) Stability class C

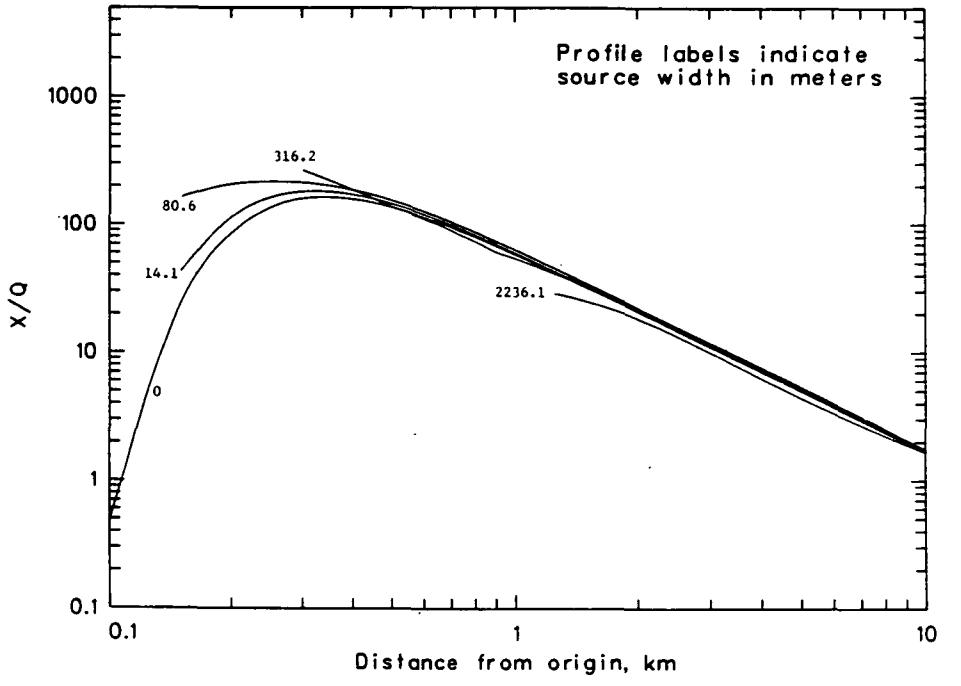

(d) Stability class D

Figure 40. Continued.

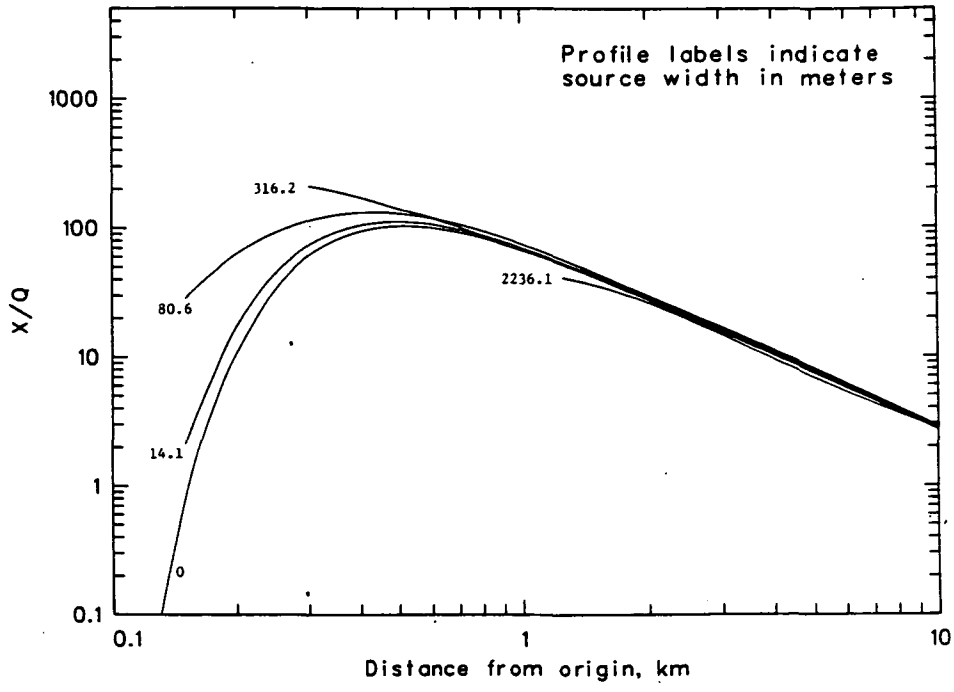

(e) Stability class E

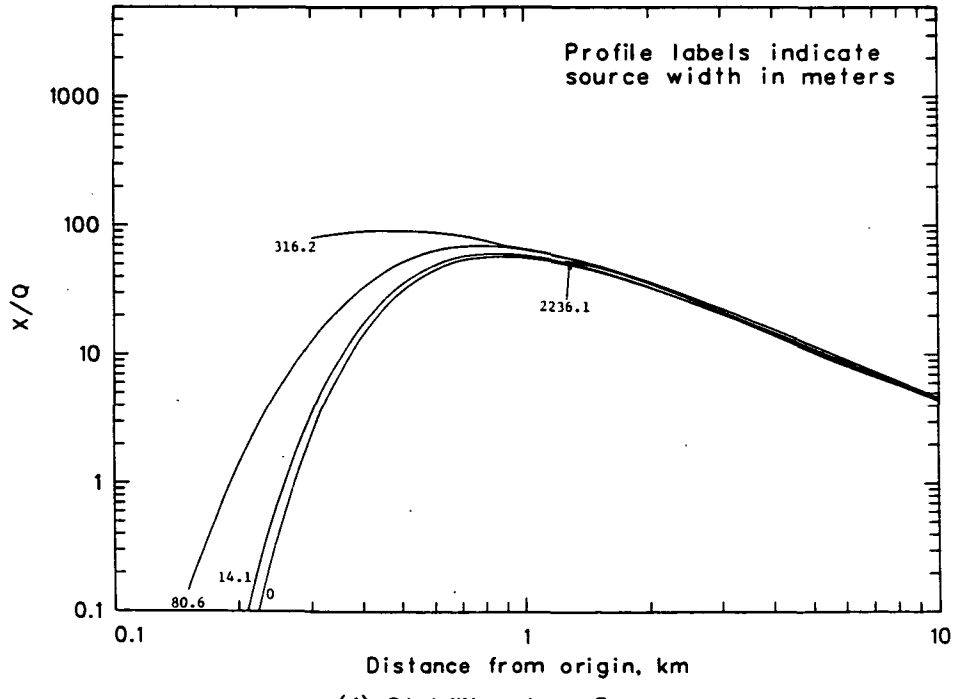

(f) Stability class F

Figure 40. Continued.

GLOSSARY

Centerline: the line that bisects a sector of one of the coordinate systems

Centroid distance, XCk: the distance (m) from the origin to the kth centroid ring

Centroid point, PC(i,k): the intersection of the ith direction vector and the kth centroid ring

Centroid radius: same as centroid distance

Centroid ring, RCk: an imaginary circle of radius XCk drawn about the origin

Centroid system: the polar coordinate system used by CONEX

Direction vector, Di: the ith of 16 imaginary, equally spaced (22.5° apart), radial lines emanating from the origin of both the grid and the centroid systems, where, for example, D1, at 0°, points to the North; D5, at 90°, to the East; D9, at 180°, to the South; D13, at 270°, to the West; and D16, at 337.5°, to the North Northwest

Exposure: the product of a time-averaged airborne pollutant concentration and the number of persons immersed in that concentration over the time averaging interval (person-$\mu g/m^3$)

Exposure potential: an artificial measure of the exposure that would occur if the study area was occupied by a uniformly distributed population with a density of 1 person/m^2.

Grid distance, XGj: the distance (m) from the origin to the jth grid ring

Grid point, PG(i,j): the intersection of the ith direction vector and the jth grid ring

Grid-point concentration, GPC(i,j): the annual-average, sector-averaged, centerline, ground-level, air concentration ($\mu g/m^3$) calculated by ISCLTM at grid point PG(i,j)

Grid radius: same as grid distance

Grid ring, RGj: an imaginary circle of radius XGj drawn about the origin

Grid system: the polar coordinate system used by ISCLTM

Point concentration: same as grid-point concentration

Primary direction: the direction toward which the wind was assumed to blow in this study, D9 or South

Primary grid-point concentration, PGPC(j): the grid-point concentration at grid point PG(9,j), which lies on the primary direction

Primary sector: S(9), the sector centered on the primary direction

Primary sector exposure potential, PSEP: the sum of the sector-segment exposure potentials in the primary sector

Primary sector-segment concentration, PSSC(k): the sector-segment concentration in sector segment SS(9,k)

Sector, S(i): the 22.5° wide sector centered on the ith direction vector

Sector exposure potential, SEP(i): the sum of the sector-segment exposure potentials in sector S(i)

Sector segment, SS(i,k): the area centered on centroid point PC(i,k), which is bounded by grid rings RGj and RGj+1 and imaginary radii that are ±11.25° from the ith direction vector

Sector-segment area, SSA(i,k): the area (m^2) covered by sector segment SS(i,k)

Sector-segment concentration, SSC(i,k): the average concentration ($\mu g/m^3$) over sector segment SS(i,k)

Sector-segment exposure potential, SSEP(i,k): the exposure potential associated with sector segment SS(i,k), defined as SSC(i,k) x SSA(k)

Total exposure potential (TEP) - the sum of all sector-segment exposure potentials

LIST OF ABBREVIATIONS AND SYMBOLS

C1 - ln GPC(i,j)

C2 - ln GPC(i,j+1)

CONEX - Concentration-Exposure Program used in the IEM

Di - ith direction vector

$f_1(i,k)$ - areal fraction of the 1th rectangular population cell that is intersected by sector segment SS(i,k)

GPC(i,j) - grid-point concentration at PG(i,j)

i - direction index for both the grid and centroid coordinate systems

HEM - Human Exposure Model

IEM - Inhalation Exposure Methodology

ISCLT - the long-term version of the Industrial Source Complex Dispersion Model

ISCLTM - the modified version of the ISCLT used in the IEM system; its results are identical to those of the ISCLT

j - distance index for the grid coordinate system

k - distance index for the centroid coordinate system

1 - index for the population cells contained in the population data file

P_1 - total number of persons in the 1th rectangular cell of the population data file

PC(i,k) - centroid point located at the intersection of the ith direction vector and the kth centroid ring

PSSC(k) - primary-sector segment concentration, equal to SSC(9,k)

PGPC(j) - primary grid-point concentration, equal to GPC(9,j)

PG(i,j) - grid point located at the intersection of the ith direction vector and the jth grid ring

PSEP - primary-sector exposure potential

RBE(k) - total exposure in the radial band centered on the kth centroid ring

RCk - kth centroid ring

RGj - jth grid ring

RTEMP - [ln(XCk/XGj)]/[ln(XGj+1/XGj)]

S(i) - 22.5°-wide sector that lies along the ith direction vector

SE(i) - total exposure (person-$\mu g/m^3$) in sector S(i)

SEP(i) - exposure potential in sector S(i)

SS(i,k) - sector segment centered on centroid point PC(i,k)

SSA(k) - area (m^2) of all sector segments centered on the kth centroid ring

SSC(i,k) - average concentration ($\mu g/m^3$) over sector segment SS(i,k)

SSE(i,k) - total exposure (person-$\mu g/m^3$) in sector segment SS(i,k)

SSP(i,k) - number of persons assigned to sector segment SS(i,k)

TE - total exposure in the assessment area

TEP - total exposure potential

TGRC(j) - sum of all grid-point concentrations on the jth grid ring

XCk - distance (m) from the origin to the kth centroid ring

XGj - distance (m) from the origin to the jth grid ring

X/Q - grid-point or sector-segment concentration [($\mu g/m^3$)/(g/s)] due to a unit (1 g/s) pollutant release rate